UNIVERSITEIT VAN PRETORIA
UNIVERSITY OF PRETORIA
YUNIBESITHI YA PRETORIA

BIO-ARTIFICIAL LIVER SUPPORT SYSTEM:
An evaluation of models used in demonstrating or improving metabolic and clinical efficacy

by
MARTIN NIEUWOUDT

UNIVERSITEIT VAN PRETORIA
UNIVERSITY OF PRETORIA
YUNIBESITHI YA PRETORIA

BIO-ARTIFICIAL LIVER SUPPORT SYSTEM:
An evaluation of models used in demonstrating or improving metabolic and clinical efficacy

by Martin Nieuwoudt

Thesis submitted in fulfillment of a PhD in Chemical Technology

in the Department of Chemical Engineering, University of Pretoria, Pretoria, South Africa

Supervisor: Prof. P de Vaal
Co-supervisor: Prof. S van der Merwe

BIO-ARTIFICIAL LIVER SUPPORT SYSTEM: An evaluation of models used in demonstrating or improving metabolic and clinical efficacy

ABSTRACT

Acute liver failure (ALF) is a rare but devastating clinical syndrome with multiple causes and a variable course. The mortality rate is high. Orthotopic liver transplantation is the only therapy of proven survival benefit but the limited supply of donor organs, the rapidity of progression and the variable course of ALF limit its use. A need therefore exists for a method to 'bridge' patients, that is, provide temporary support, to either the spontaneous regeneration of the innate liver or transplantation. One possibility includes bio-artificial liver support systems (BALSS). This technology is composed of an extracorporeal circulation system incorporating a bioreactor that contains parenchymal liver cells (hepatocytes) to perform the detoxifying, transforming and synthetic properties of a liver. However, the development of a BALSS holds particular challenges. Despite approximately four decades of research, bio-artificial liver (BAL) technology globally remains in a pre-commercial stage. The University of Pretoria (UP) and the Council for Scientific and Industrial Research (CSIR) have developed a BALSS with novel characteristics. These include a computationally optimized radial-flow primary porcine hepatocyte bioreactor perfused with blood plasma, and a perfluorocarbon oxygen carrier which replaces hemoglobin. There are also novel design properties in the circulation system itself. Demonstrating the metabolic and clinical efficacy of a BAL device requires implementing, *in vitro* (cell biology), *in vivo* (animal) and mathematical modeling studies. These studies are a formal necessity but are inherently 'models' of the *in vivo* human clinical circumstance. That is, they are limited by their experimentally controlled configuration/s. In investigating these, this thesis firstly provides a foundation by reviewing the clinical and biological context of ALF and BAL technology, then presents and evaluates particular studies/models that have been implemented over several years in the course of the UP-CSIR BAL project. For each section, thoughts and recommendations regarding future work that will facilitate the development of BAL technology are discussed in detail. The thesis is concluded with an evaluation of success and the consensus-agreed requirement of continued research and innovation in the field.

Keywords: acute liver failure, bio-artificial liver, hepatocyte bioreactor cell biology, animal models, compartmental pharmacokinetic models, prognosis modeling, bioprocess monitoring, state estimator.

BIO-KUNSMATIGE LEWER ONDERSTEUNINGSTELSEL: ’n Evaluasie van modelle wat gebruik is in die demonstrasie of verbetering van metaboliese en kliniese doeltreffendheid

SAMEVATTING

Akute lewerversaking (ALV) is ’n seldsame maar vernietigende kliniese sindroom met veelvuldige oorsake en uiteenlopende nagevolge. Die sterftesyfers is hoog. Leweroorplanting is die enigste terapie met bewese oorlewingsvoordele, maar die tekort aan oorplantingsorgane en die verskeie nagevolge van ALV beperk die gebruik daarvan. Daar is dus ’n behoefte aan ’n ‘oorbruggingsmetode’, om pasiënte te ondersteun terwyl spontane regenerasie van die bestaande lewer kan plaasvind, of voordat ’n leweroorplanting gedoen word. Een so ’n moontlikheid is ’n bio-kunsmatige lewerondersteuningstelsel (BKLOS). Hierdie tegnologie is ’n buiteliggaamlike sirkulasiestelsel insluitende ’n bioreaktor wat lewerselle (hepatosiete) bevat wat die suiwering, transformasie en sintese eienskappe van die lewer vervul. Die ontwikkeling van ’n BKL-ontwerp hou definitiewe uitdagings in. Ten spyte van vier dekades se internasionale navorsing, bly bio-kunsmatige lewer tegnologie in ’n pre-kommersiële stadium. Die Universiteit van Pretoria (UP) en die Wetenskaplike en Nywerheidnavorsingsraad (WNNR) het ’n BKLOS met uitsonderlike kenmerke ontwikkel. Dit sluit in ’n rekenaar-geoptimiseerde radiaal-vloei primêre vark-hepatosiet bioreaktor wat deurentyd gevul word met bloedplasma en ’n perfluorostikstof suurstofdraer wat hemoglobien vervang. Die sirkulasiestelsel self het ook unieke ontwerpeienskappe. Die demonstrasie van die metaboliese en kliniese doelteffendheid van ’n BKL-ontwerp vereis die implementering van *in vitro* (selbiologie), *in vivo* (diere) en wiskundige modeleringstudies. Alhoewel sulke studies noodsaaklik is, is hulle inherent ‘modelle’ van die *in vivo* menslike kliniese omstandigheid. In hierdie proefskrif is eerstens ’n basis gebou deur die kliniese en biologiese samehang van ALV en BKL tegnologie te ondersoek. Daarna stel dit voor en evalueer spesifieke studies/modelle wat oor verskeie jare in die loop van die UP-WNNR BKL projek geïmplementeer is. Na elke afdeling is voorstelle bespreek in verband met toekomstige werk wat die ontwikkeling van BKL tegnologie sal vergemaklik. Die proefskrif word afgesluit met ’n evaluering van suksesse tot op datum asook behoeftes aan voortgesette navorsing en ontwikkeling in die veld.

CONTENTS PAGE

LIST OF FIGURES

LIST OF TABLES

LIST OF TERMS AND ABBREVIATIONS

The majority of definitions were taken from the *on-line* medical dictionary of the University of Newcastle Upon Tyne (available at http://cancerweb.ncl.ac.uk/omd/).

Term	Meaning
a priori	previously defined or assumed (facts)
acidosis/ alkalosis	a metabolic condition, characterized by an increase or decrease in hydrogen ion concentration
allocompatibility	immunological compatibility of substance/fluid from another person or organism
average relative accuracy/error region	the product of the measurement range and the standard deviation of the relative error (see below)
bioanalytical/bioprocess monitoring system	a (typically) predictive, *on-line* monitoring system for a contained biological process (normally for commercial purposes)
biochemical	a molecule characterized or produced by chemical reactions in a living organism
bioreactor	a closed device housing cells used for generating/metabolizing biological substances
bioresorbable	a material that may be metabolized/absorbed when inserted into an organism's tissues
biosensor	a sensor for particular biological stimuli in a bioprocess
bio-systems model	a computational representation of a biological system or bioprocess
boolean switching net	a network of switches employing Boolean rules
bootstrapping	a statistical method for generating theoretical data where limited or no measured data is available
cardiac arythmia	an irregular electrical pattern of cardiac activity
cell aggregation/support matrix	a synthetic or biological three dimensional matrix into which aggregation dependent cells are seeded
chemokine	cytokines that are chemotactic for leucocytes (e.g. IL-6)
disseminated intravascular coagulopathy	a complication of septic shock where endotoxin induces systemic blood clotting, depletion of coagulation factors and thrombocytopenia leading to widespread spontaneous bleeding.
chemotactic	the responsiveness of motile cells to concentration gradients of particular dissolved substances
cytokines	small molecules released by cells and having specific effects on cell-cell interaction, communication and behaviour (e.g. IL-1β)
data driven modeling	modeling procedures based on empirically observed (rather than theoretical) trends in measured data
devascularization	surgical occlusion or all or most of the blood vessels to an organ or tissue
endotoxin	toxic membrane lipopolysaccharides of gram negative bacteria
epileptiform activity	brain electrical activity normally associated with epileptic seizures
etiology	a branch of medical science concerned with the

	causes or origins of diseases
flow injection analysis	the analysis of a chemical substance by removing a sample from a flow stream and mixing it with a reagent to produce a measurable reaction for a detector and subsequent data logging device
gluconeogenesis	the synthesis (mainly be the liver) of glucose from non-carbohydrate precursors
genotype	the total genetic constitution of a cell or organism
glomerular filtration	filtration function performed by the glomerular cells of the kidney
glycolysis	the anaerobic conversion of glucose to pyruvate
haemodynamic	relating to physical aspects of the blood circulation
hepatectomy	the surgical removal of the liver
hepatocytes	the epithelial cells composing (approximately) 80% of the liver
hepatotoxic	toxic to the liver
hepatotrophic	causing liver growth or regeneration
hyper/hypocapnia	an excess or deficiency in carbon dioxide in the blood resulting from hypo or hyper ventilation and leading to acidosis or alkalosis respectively
hyper/hypoglycemia	an excess or deficiency of glucose in the blood
hyper/hypokalemia	an excess or deficiency of potassium in the blood
hyper/hypometabolic	an excess or deficiency in metabolic activity
hyper/hyponatremia	an excess or deficiency of sodium in the blood
hyper/hypophosphatemia	an excess or deficiency of phosphate in the blood
hyper/hypotension	persistently high or low arterial blood pressure
hyper/hypovolemia	increased or decreased blood volume
hyperammonemia	a pathologically increased blood ammonia concentration
hypoxic	a lack of oxygen (low pO_2)
immunosuppression	the suppression of T or B lymphocytes with particular drugs
in situ	in a natural or normal bodily compartment without entering any other place
in silico	a computer-based simulation or model of a system
in vitro	observable in an artificial environment (e.g. a laboratory)
in vivo	within a living body
ischemic	a lacking in oxygen supply to the organs commonly due to a decrease in blood perfusion
Kalman filter	a linear bioprocess observer used to reconstruct the state of a system (including the estimation of non-measurable variables) and to decrease measurement noise. It has time varying observer gain and the descriptive equations are a linear combination of ordinary differential equations.
knowledge-based	a system incorporating clinical knowledge
laparotomy	general abdominal surgery
leucocyte	a member of the group of white blood cells
linearization	a mathematical procedure by which a (non-linear) function is estimated in terms of the expansion of its derivatives at a point of interest
lipohylic/phobic	lipid/fat soluble or insoluble

mass transfer	the concentration gradient of a particular substance at a defined interface
metabolic zonation	the ability of tissues within an organ to adapt to different metabolic requirements
microdialysis	very low volume flow injection method for analyzing biological fluids
mitogenic	the ability of a substance to induce mitosis (division) in eukaryotic cells i.e. growth or regeneration
model	an experimentally controlled simulation of an objective system, circumstance or reality.
model standardization	the reduction of a complex system to particular criteria or rules determining its validity or success
monte carlo analysis	a statistical method in which (bound) random data is generated to overcome limitations in the amount of measured data available (see 'bootstrapping')
necrosis	a form of cell death
nephrotoxic	toxic to kidneys
object oriented model	a model in which the functional units of a system are defined as objects having characteristics that are definable using particular computational methods (e.g. the UML)
Occam's razor	The principle, by which particular predictions of a model are excluded, based on their not being observed in reality. Alternately, 'the simplest explanation is the best'
off-line	not measurable at the time at which a process takes place i.e. results are only available subsequently
on-line	measurable at the time at which a process takes place so that results may potentially be input into a control system
parenchymal/non parenchymal	tissues/cells composing (or not composing) the general functional framework or stroma of an organ
perfusate	a body fluid perfusing a particular stream in a system (e.g. a plasma perfused bioreactor)
periportal	surrounding or close to the intrahepatic portal vein branches (i.e. high oxygen content blood at the inlet of the liver)
perivenous	surrounding or close to the central vein (i.e. low oxygen content blood at the outlet of the liver)
petri net	describes a process in terms of places (circles), transitions (rectangles) and arcs (lines). The formal mathematical semantics used to define discrete distributed systems
pharmacokinetic compartmental model	a closed system of physiological compartments between which the mass transfer (production or clearance) of particular substances may be described using ordinary differential equations (i.e. as defined by Michaels-Menten kinetics)
phenotype	the expressed functional characteristics of a cell or organism resulting from the interaction of its genotype to particular environmental conditions
point error	the difference between corresponding predicted to measured values as a fraction of each measured value

prognostic criteria	particular rules or metabolic indices that may be used to forecast the probable outcome of a clinical intervention or disease process
prophylaxis	preventive treatment for a disease
real-time	sinonymous with *on-line* i.e. data measurable during an experiment or procedure
relative error	a percentile value for the point error divided by the standard deviation of the measured population
software sensor	an indirect computational method for estimating a non-measurable process variable
spectrophotometric detection	a method for determining biochemical concentrations in a sample based on the absorbance/transmission of light at particular wavelengths
splanchnic circulation	blood circulation to the internal organs and lower limbs
state estimator	a system which produces estimates of measurable and non-measurable state variables in a bioprocess
state machine/diagram	a UML graphical representation of the behaviour of a system i.e. the total set of states and transitions through which the system may proceed
stellate cell	Star-shaped, non parenchymal cells in the liver facilitating the phenotypic stabilization of hepatocytes during liver regeneration
systemic	pertaining to the integrated functions of the body as a whole
tornado diagram	a diagram displaying the sensitivity of the outputs of a model in term of its inputs
tumorigenic	tendency to cause cancer
vasoconstriction/dilation	the diminution/enlargement of vascular diameters (especially arterioles) leading to a decrease or increase in blood perfusion to tissues/organs downstream
xenogenic	originating from outside and introduced into an organism (i.e. a foreign material)
zoonosis	the transmission of a disease from an animal or non-human species to a human

Abbreviation	**Meaning**
ABG	arterial blood gas
ABP	arterial blood pressure
AHF	acute hepatic failure (synonymous with acute liver failure)
ALF	acute liver failure
AMC-BAL	Amsterdam Medical College bio-artificial liver
ANN	artificial neural network
ANOVA	analysis of variance
ARDS	acute respiratory distress syndrome
BAL	bio-artificial liver
BALSS	bio-artificial liver support system
BLSS	bio-artificial liver support system
CE	cerebral edema

CFD	computational flow dynamics
CPP	cerebral perfusion pressure
CSIR	Council for Scientific and Industrial Research
CVP	central venous pressure
CVVHDF	continuous veno-venous hemodiafiltration
DIC	disseminated intravascular coagulopathy
ECG	electrocardiogram
EEG	electroencephalogram
EGF	epidermal growth factor
ELAD	extracorporeal liver assist device
FDA	US federal drug administration
FHF	fulminant hepatic failure
GCP	good clinical practice
GFR	glomerular filtration rate
GMP	good manufacturing practice
GUI	graphical user interface
HAL	hepatic artery ligation
HBAL	hybrid bio-artificial liver
HBV	hepatitis B virus
HE	hepatic encephalopathy
HGF	hepatocyte growth factor
HIV	human immuno virus
HRS	hepato-renal syndrome
ICP	intracranial pressure
IL-1β	interleukin-1beta
IL-6	interleukin six
INR	international normalized ratio
IVC	inferior vena cava
K_m	Michaelis constant
MAP	mean arterial pressure
MARS	molecular adsorbents recirculation system
MCA	monte carlo analysis
MELS	modular extracorporeal liver support
MEM	minimum essential medium
MOF	multi-organ failure
NAC	N-acetylcysteine
NO	nitric oxide
OLT	orthotopic liver transplantation
OUR	oxygen uptake rate
PCA	porto-caval anastomosis
pCO_2	partial pressure of carbon dioxide
PET	positron emission tomography
PERV	porcine endogenous retrovirus
PFC	perfluorocarbon
PFOB	perfluorooctyl bromide
pO_2	partial pressure of oxygen
PROM	Prometheus artificial liver support system
PT	prothrombin time
PUF	polyurethane foam
RFB	radial flow bioreactor
SFHF	subfulminant hepatic failure
SIRS	systemic inflammatory response syndrome

SOM	self organizing map
TECA-HAL	TECA-hybrid artificial liver support system
TGF-α	transforming growth factor alpha
TNF-α	tumour necrosis factor alpha
UML	unified modeling language
UP	University of Pretoria
UPBRC	University of Pretoria Biomedical Research Centre
V_{max}	Michaelis-Menten kinetics V max value

1. INTRODUCTION

"The map is not the territory"

Alfred Korzybski, circa 1930

1.1 Background

The liver is the largest internal organ in the body, weighing approximately 1.5 kg and accounting for 2% of the weight of an adult. It is of great anatomical and physiological complexity, second only to the brain, and is perfused by 25 % of cardiac output consuming 20-30% of the body's oxygen (O_2) supply. The functional units of the liver are polyhedral hepatic lobules whose corners have portal tracts containing venules, arterioles and bile ductules while the centre is drained by a central vein. The 'hepatocytes' are the parenchymal cell population of the liver, they compose 70-80 % of its mass and are arranged in unicellular plates in the lobule. Each lobule is interspersed with anatomically and functionally separate bile canaliculi and sinusoids. Along the periportal to perivenous axis of the sinusoid there is a polar zonation of metabolic functions which are determined by gradients of oxygen, growth factors and hormones. The remaining non parenchymal cell population includes Kupffer, endothelial, stellate, pit, Ito and bile duct cells [1,2].

At least 500 liver functions have been identified thus far. Examples include the endocrine secretion of albumin and urea into the blood, the exocrine secretion of bile into the intestine and the storage of fuel in the form of glycogen. The liver plays an integral role in maintaining the body's metabolic homeostasis by regulating carbohydrate, fatty acid, amino acid and cholesterol metabolism. It plays an important role in systemic responses to injury through its ability to switch to a hyper-metabolic state and the production of acute phase proteins. Additional to metabolism, the liver has a critical defense function by inactivating toxins and xenobiotics absorbed in the intestines and clearing foreign bodies from the blood [2].

The liver is unique in its ability to regenerate and may restore its original mass even if only as little as 15-20 % of the cells remain undamaged [2]. On a molecular level, liver regeneration is associated with hepatocyte hyperplasia [3]. However, the hepatocyte population may be restored through trans-differentiation from a variety of other cell types, including oval cells, multipotent stem cells and fetal liver cells [4].

Following damage, the liver has an initial orientation to protein synthesis, to restore its mass and manage the increased metabolic load, followed by an increase in lipid and fatty acid synthesis. Under the synchronized expression and control of large scale genetic pathways, many factors impact regeneration. These include for example, insulin and glucagon production by the pancreas, glucose metabolism, portal blood flow, plasma amino acid composition, bile acid concentration, cytokines such as tumor necrosis factor (TNF), interlekin-6 (IL-6), transcription factors such as AP-1 complex and STAT-3, growth factors such as hepatocyte growth factor (HGF), epidermal growth factor (EGF) and transforming growth factor-β (TGF-β). Regeneration also requires complex signaling interactions between hepatocytes and other cell types, particularly Kupffer, endothelial, stellate cells and blood platelets, in view of their secreting growth and transcription factors critical to the process [3].

Acute liver failure (ALF) is a severe form of liver injury. It is associated with an abrupt loss of hepatic cellular function in a patient without pre-existing liver disease with the subsequent development of coagulopathy, jaundice and encephalopathy. It is a rapid and devastating clinical syndrome with significant mortality (60 % - 90 %) despite advances in its clinical management [5-7]. ALF is complex and life threatening, often due to brainstem compression and herniation secondary to intracranial hypertension. Additional to the neurologic complications, multi-organ failure often follows [8].

Presently, orthotopic liver transplantation (OLT) is the only treatment of proven benefit in ALF. However, there is a global shortage of donors and patients are often forced to wait for organs to become available. Thus, a ‘bridging’ treatment to support the ALF patient prior to OLT is highly desirable. Such a treatment might also allow the patient’s innate liver to spontaneously regenerate, in so doing avoiding the need for transplantation [7].

One such bridging treatment is a bio-artificial liver support system (BALSS). This is a 'hybrid' technology composed of an artificial extracorporeal circulation system with an integrated biological component in the form of a hepatocyte-seeded bioreactor. The operation of a BAL device relies on replacing/augmenting as many of the functions of an *in vivo* liver as possible. The most important functions are particularly the detoxifying, transformatory and synthetic properties since these are not reproducible by artificial chemical or mechanical means [9].

The University of Pretoria (UP) and the Council for Scientific and Industrial Research (CSIR) have developed a BALSS. This device has novel characteristics, for example, it contains a radial-flow, plasma-perfused polyurethane foam [PUF] matrix bioreactor loaded with primary hepatocytes and stellate cells. The system is perfused with plasma as opposed to whole blood, to prevent immunological reactions, and a perfluorocarbon (PFC) oxygen carrier is included in the bioreactor sub-circulation to improve O_2 mass transfer to hepatocytes [10]. The UP-CSIR BALSS is currently in a preclinical phase of testing.

Developing a BAL unavoidably necessitates implementing a variety of studies aimed at demonstrating or improving various aspects of the metabolic functionality and clinical efficacy of the system. These inherently employ 'models', which are necessarily abstractions of the *in vivo* human situation. Emulating multitudinous liver functionality and the practicalities of the required experimental and clinical systems present particular challenges. Testament to this fact is that despite approximately four decades of research, BAL technology (globally) remains in a pre-commercial stage. Significant scientific and financial commitments are required. As part of such an endeavor, this thesis aims to present, evaluate and provide thoughts and recommendations for progress in models and technology of this type.

1.2 Defining *Models*

To quote Wikipedia (http://en.wikipedia.org/wiki/Model):
"A model is a pattern, plan, representation (especially in miniature), or description designed to show the main object or workings of an object, system, or concept."

In this thesis the term *model* is used in the generic sense of an 'abstraction', however, the investigations that follow include specifically three types:

1. *In vitro* models, which are miniature or *scaled-down* laboratory versions of the BAL and are designed to demonstrate and/or improve the metabolic functionality of the bioreactor component,
2. *In vivo* animal models, which are used to demonstrate particular aspects of the clinical scenario being studied (i.e. severely liver-compromised circumstances), and,
3. Mathematical mass-balance and bio-process models that are used to demonstrate and/or predict aspects of the combined BAL-patient system's clinical functionality.

The means of evaluation of each type is as per the methods that are normal with respect to the field in which they would be published.

1.3 Problem statement

Demonstrating the metabolic functionality and/or clinical efficacy of BAL technology requires the implementation of a variety of in vitro, in vivo and mathematical studies or systems. As a formal necessity these are 'models', or experimentally controlled configurations of the in vivo circumstance. Bearing this in mind, how can these models be used to facilitate the development of a BAL that meets the human clinical need and what research is underway or necessary in this regard?

1.4 Thesis structure

The thesis is composed of a set of logically progressive studies arranged in technically-related sections. Each section is preceded by an overview introducing the included studies. All the studies and underlying models are evaluated individually, as per the methods that are normal to their respective fields, followed by thoughts and recommendations regarding progress in BAL technology particular to and succeeding each section. In general, all the studies have a composition as required for publication in a scientific journal i.e. an introduction, materials and methods, results and discussion/conclusion. For purposes of efficiency, certain methods and/or verification

results that are only incidental to model definition/evaluation have been truncated in the text and detailed in the appendices.

Briefly,

1. Section 1 (this one) introduces the thesis and provides technical information regarding the manner of its presentation.
2. Section 2 is a literature review that defines the clinical context of ALF and the biological factors involved in the development of BAL devices.
3. Section 3 briefly details the UP-CSIR BAL technology which, together with section 2, lays a foundation for what follows.
4. Section 4 includes 3 *in vitro* cell biology studies: The first details a model for isolating large quantities of liver cells, a formal requirement for creating metabolically functional BAL bioreactors. The second investigates the functionality of these bioreactors and the effect of including a PFC oxygen (O_2) carrier in the system. The third, in response to earlier difficulties, uses improved methods to further investigate bioreactor functionality under conditions simulating the treatment of an ALF patient. In the thoughts and recommendations section concerns regarding cell source models and recent progress in the field are mentioned.
5. Section 5 includes 2 *in vivo* (animal) studies: The first employs a model of liver injury and regeneration in rats to investigate the potential toxicity of the PFC O_2 carrier if leaked intravenously in a BAL treatment. The second describes the standardization of an *in vivo* surgically-induced large animal model of acute liver failure in preparation to clinically testing the BAL device. The thoughts and recommendations detail the impact of the latter model on such tests, the prognostically important metabolism and reduction of blood ammonia and the impact of this on BAL device design.
6. Section 6 includes 2 mathematical modeling studies: The first is a mass-balance pharmacokinetic compartment model of the BAL-patient system using actual clinical and metabolic data to provide useful insights regarding BAL design. The second is a conceptual and numerical model whose purpose is the development of an *on-line* 'in theatre' ALF-bioprocess monitoring system that provides *real-time* prognosis indications [11,12]. Thoughts and recommendations follow regarding

refining biomarker/prognostic models, additional mathematical experiments, 'fusing' model types and the implementation of bioprocess monitoring systems.

7. The thesis is concluded with an evaluation of success, and consensus on what is required for progress in the technology.
8. The references are followed by,
9. The appendices, which provide additional details on methods and verifications incidental to defining the models.

Please note, the University of Pretoria Animal Use and Care Ethics committee (or the Animal Ethics Committee of the Tshwane University of Technology) first granted approval prior to commencement of any animal experiments described in this thesis.

1.5 Copyright and authorship issues

Permission was requested and received from journals for articles in which copyright had been assigned for publication. These include the following:

Nieuwoudt MJ, Kreft E, Olivier B, Malfeld S, Vosloo J, Stegman F, Kunneke R, Van Wyk AJ, Van de Merwe SW. A Large Scale Automated Method for Hepatocyte Isolation: Effects on Proliferation in Culture. *Cell Transplantation* 2005;14(5): 291-299.

Nieuwoudt M, Moolman S, Van Wyk AJ, Kreft E, Olivier B, Laurens JB, Stegman F, Vosloo J, Bond R, van der Merwe SW. Hepatocyte Function in a Radial-flow Bioreactor Using a Perfluorocarbon Oxygen Carrier. *Artif Organs* 2005;29(11): 915-918.

Nieuwoudt M, Kunnike R, Smuts M, Becker J, Stegmann GF, Van der Walt C, Neser J, Van der Merwe S. Standardization criteria for an ischemic surgical model of acute hepatic failure in pigs. *Biomaterials* 2006;27(20):3836-45.

Nieuwoudt MJ, Engelbrecht GHC, Sentle L, Auer R, Kahn D, van der Merwe SW. Non-toxicity of IV injected perfluorocarbon oxygen carrier in an animal model of liver regeneration following injury. *Artificial Cells, Blood substitutes, and Biotechnology* 2009;37(3):117-24.

Nieuwoudt MJ, Wiggett WS, Malfeld S, van der Merwe SW. Imaging glucose metabolism in perfluorocarbon-perfused hepatocyte bioreactors using positron emission tomography. *Journal of Artificial Organs* 2009;12:247-57.

Publications in progress include:

Moolman SF, Nieuwoudt MJ, Shatalov M. A pharmacokinetic compartment model for demonstrating Bioartificial liver performance.

Nieuwoudt MJ, Cilliers P, van der Merwe SW. The development of an *on-line* predictive clinical monitoring system for acute liver failure patients.

2. THE CLINICAL AND BIOLOGICAL BACKGROUND OF ACUTE LIVER FAILURE (ALF) AND LIVER SUPPORT TECHNOLOGY

2.1 Introduction

Acute liver failure (ALF) is a devastating clinical syndrome associated with the sudden loss of a patient's liver function. The course of ALF is rapid, multi-systemic, and variable and the mortality rate is high. Liver support devices are being developed with the intent of 'bridging' ALF patients to the only treatment that has shown statistically significant improvements in survival, namely orthotopic liver transplantation (OLT). The shortage of donor organs and the time taken to OLT validate the use of the technology. This is particularly relevant in Africa in that the only centres conducting transplants are the Groote Schuur and Red Cross hospitals in Cape Town, the Wits Donald Gordon hospital in Johannesburg and an Egyptian Transplant Centre in Cairo. The University of Pretoria (UP) and the Council for Scientific Investigation and Research (CSIR), has collaborated in the development of a Bio-artificial liver support system (BALSS), with which to treat ALF.

Understanding the clinical aspects of ALF and the biological principles underlying BAL devices requires knowledge of several scientific disciplines. For this reason the following section reviews the relevant issues to provide a foundation for the studies and/or models subsequently presented and evaluated.

2.2 Defining ALF

The original definition of fulminant hepatic failure (FHF) by Trey and Davidson (1959) [13] was based on the occurrence of hepatic encephalopathy (HE) as the consequence of severe liver injury developing within 8 weeks of the onset of non-specific symptoms in patients without pre-existing liver disease.

Bernau *et al* (1986) [14] discriminated between fulminant hepatic failure (FHF) and subfulminant hepatic failure (SFHF). In FHF, hepatic encephalopathy (HE) develops within 2 weeks of the onset of jaundice, while in SFHF the HE is delayed beyond 2 weeks, taking up to several months. FHF and SFHF were similar in etiology, i.e. viral hepatitis (A, B, D and E), acetaminophen overdose, idiosyncratic drug reactions, ingestion of toxins (e.g. amanita mushrooms) and metabolic disorders (e.g. Reye's syndrome). However, the prognoses were different and the classification was therefore important. FHF resulted in better long-term prognosis than SFHF.

Subsequently, O'Grady *et al* (2005) [15], introduced the terms hyperacute, acute and subacute to differentiate between ALF in which the onset of HE occurs within 7 days of the onset of jaundice (survival 36%), 7-28 days (survival 7%) and 28 days or more (survival 14%).

ALF is currently defined by the sudden loss of hepatic function in a person without preexisting liver disease. In contrast to the original definition the later classifications allow for the inclusion of cases with previously asymptomatic chronic liver conditions, such as Wilson's disease and the reactivation of an underlying hepatitis B infection [16]. ALF is considered a syndrome rather than a disease due to multiple causes that give rise to variations in course and outcome. Severe acute liver failure is characterized by the presence of coagulopathy resulting in spontaneous bleeding (e.g. epistaxis with international normalized ratio (INR) $\geq$ 1.5), any degree of HE and the duration of illness anywhere $\leq$ 24 weeks. Many patients develop coma within $\leq$ 1 week [17].

2.3 Epidemiology and etiology

ALF is rare and figures are not readily available for global incidence possibly as a result of its multi-systemic presentation leading to spurious diagnoses. ALF has an incidence of about 1 per 150 000 inhabitants yearly. There are approximately 2000 cases per year in the USA (http://www.unos.org 2006/7) with a similar incidence in Western Europe. Patients suffering from chronic liver diseases have been estimated at 250 000 per year with 25 000 deaths [18]. Current South African estimates are approximately 300 ALF, with 30 000 chronic liver disease patients per year [19]. Due

to the shortage of donor livers, a large fraction of patients suffering from FHF will die while on a waiting list for OLT. In the Eurotransplant zone there was a need for 2249 liver transplants in 2006, while only 1277 liver transplantations were actually conducted (http://www.eurotransplant.nl). In the US at the end of 2001, 18 500 patients were awaiting OLT. In 2004, 5250 of 25 750 patients (20 %) received a donor liver, whereas 1978 (8 %) of ALF patients died while on a waiting list [20]. The waiting times for donor livers and consequent deaths on waiting lists have been increasing in recent years [21].

The distribution of ALF etiologies varies geographically. In the US and UK acetaminophen overdose is the most common cause of death in ALF patients. In Africa and Asia, hepatitis A and B followed by E, are the leading causes [12,13]. ALF due to hepatitis C has been described but is very rare [22,23].

Since the liver metabolizes the majority of drugs almost any drug can cause acute hepatitis. Drug toxicities may be dose-dependent and predictable, but are more often idiosyncratic, in that the toxicity results from an immunological reaction triggered by the drug or its metabolite. 50% of all pediatric cases are due to indeterminate causes. Less common causes of ALF include various cancers, lymphoma, Wilson's disease, acute ischemic liver injury, autoimmune hepatitis and Budd-Chiari syndrome [24,25].

The outcomes of ALF have been changing in recent years owing to improvements in intensive care and patient management. Acetaminophen, shock and hepatitis A are more likely to demonstrate spontaneous recovery than drug-induced, autoimmune and indeterminate-cause ALF. However, ALF remains a challenging system with high mortality [17].

2.4 Pathogenesis and the clinical syndrome

ALF develops from either or both of cytotoxic and cytopathic injury to hepatocytes. The two processes of cell death, necrosis and apoptosis form the basis of the liver injury. Apoptosis, due to tumor necrosis factor (TNFα) and Fas ligand activation of the caspase cascade in ischemic liver injury, Wilson's disease and hepatitis B. Necrosis, due to ATP depletion from mitochondrial damage is more common in

acetaminophen overdose patients. Lipid accumulations associated with abnormalities in mitochondrial fatty acid and ammonia metabolism may be present. The degree of the injury is dependent on the balance of activated pro- and anti- inflammatory cascades, on the modulation of the adaptive immune responses and on factors related to the aetiology, such as viral factors. In a significant number of cases (15-30 % in the West) the aetiology is not identifiable (e.g. whether it is an idiosynchratic drug reaction, or autoimmune reaction, without autoimmune markers, or an unrecognized paracetamol hepatotoxicity).

The most common clinical features of ALF are abnormal liver chemistries, jaundice, systemic inflammatory response syndrome (SIRS) and hepatic encephalopathy. Patients normally present with icterus and elevations in liver aminotransferase levels. In patients that are likely to recover, serum bilirubin levels and prothrombin times (PT) normalize, whereas patients in whom the disease progresses have rising bilirubin levels and increasing PTs, even if the aminotransferase levels drop. The mortality of ALF is mainly due to the associated complications, including, cerebral edema, renal failure, sepsis and cardiopulmonary collapse resulting in multi-organ failure [24-26]. The severity and complexity of the disease have resulted in ongoing demands for improvement in treatment methods.

2.4.1 Hepatic encephalopathy (HE)

The presence of HE is a distinguishing prognostic feature of ALF. It is a spectrum of reversible neuropsychiatric abnormalities characterized by a rapid deterioration in consciousness level and increased intracranial pressure that may result in brain herniation and death. It is graded on a scale of 1 to 4 (table 2.1). Generally HE will fluctuate in the early stages but will progress with the severity of the ALF. Prognosis decreases as the grade increases. In acetaminophen overdose HE usually occurs on the 3^{rd} to 4^{th} day after ingestion and will rapidly progress to stage 4 within 24-48 hours. The prognosis will be poor as a result of the alterations in mental status leading to additional complications such as the inability to maintain respiratory functions, including secretion, which results in an increased risk of infections. Raised plasma ammonia levels above 150 μmol/L, the presence of SIRS and infection (with *especially* gram-negative bacteria) are important indicators of HE.

Table 2.1 Grade scale for hepatic encephalopathy [24]

Grade	Clinical features	Asterixis	EEG	Pupillary changes
I	slow mentation, disturbed sleep, reversal of diurnal/nocturnal rhythm	mild	normal	none
II	increasing drowsiness and inappropriate behaviour (agitation and aggression)	present	abnormal with slowing	none to hyperactive
III	stupor	present	abnormal	hyperactive to hippus to slow reactive
IV	coma	lacking	abnormal	slow reactive to fixed and dilated as coma worsens

Although extensive efforts have focused on elucidating the pathophysiology of HE in recent years, it is still only partially understood. For present purposes this complex clinical entity is only briefly summarized, please refer to the recent review of Haussinger *et al* (2009) [27] for additional information. HE originates in the failure of the biotransformation and excretion of toxins normally processed by the liver and is produced by the interplay of ammonia, inflammatory responses and cerebral haemodynamic autoregulation. It is accompanied by large scale pathogenetic changes in brain astrocytes.

Due to the liver injury a disruption in endogenous toxin clearance and the urea cycle occurs, leading to an increase in plasma ammonia and alterations in the ratio of circulating branch-chain to aromatic amino acids (Fischer's ratio). Brain blood-barrier permeability is directly increased by the ammonia, leading to an elevated cerebral metabolic rate, an increase in the production of reactive oxygen and nitrogen species (ROS/NOS), which trigger multiple protein and RNA modifications, and the build-up of glutamine in the astrocytes following ammonia detoxification by means of glutamine synthetase. The actions of ammonia, inflammatory cytokines, benzodiazepines and hyponatremia integrate at the level of astrocyte swelling and oxidative stress.

Mitochondrial dysfunction leads to a build-up in brain lactate in neurons and astrocytes, electrolyte imbalances and alterations in receptor concentrations. An

increase in ammonia (and possibly also glutamine) leads to an increase in osmotic water movement into the brain and a consequent predisposition to cerebral herniation. There is a positive feed-forward regulatory loop between astrocyte swelling and oxidative stress (stress leads to swelling and swelling leads to stress).

A consequence of the production of ROS/NOS is also the induction of protein tyrosine nitration, which may increase circulating inflammatory cytokine levels (TNFα and the interleukins (IL-1β or IL-6)). This leads to the inactivation of glutamine synthetase in both the brain and the liver, further impairing ammonia detoxification. In addition to electrolyte imbalances and receptor concentrations, RNA oxidation also leads to alterations in neurotransmission as a result of the inhibition of synaptic protein synthesis. This plays a role in memory formation, providing a link between oxidative stress and the cognitive defects seen in HE.

Infection, which is detectable in 80 % of ALF patients, gives rise to a proinflammatory cytokine cascade with a synergistic worsening of ammonia-HE as important as the effects of the pathogen itself. The activation of the cytokine cascade subsequently contributes to the development of SIRS in which increased glycolysis leads to an increase in circulating lactate. Other circulating bowel-produced toxins that may also affect the severity of HE include glutamate, zinc, mercaptans, short-chain fatty acids, benzodiazepine-like substances, γ-amino butyric acid and toxic metals [27-42].

2.4.2 Cerebral edema (CE)

Disruptions in blood-brain-barrier permeability, neurotransmission and cerebral circulatory auto-regulation all contribute to CE and an increasing intracranial pressure (ICP) [19]. Patients with grade IV HE have an 80 % chance of developing CE, which is the primary cause of death in paracetamol-induced ALF [43]. The clinical signs include systemic hypertension, bradycardia, papillary abnormalities, decerebrate posturing, epileptiform activity, seizures and brainstem respiratory patterns [25]. Diagnosis of CE is performed by jugular oxymetry or intracranial epidural pressure monitoring [26]. A prolonged cerebral perfusion pressure (CPP) below 50 mmHg or an ICP above 40 mmHg is associated with poor neurological recovery. ICP may

initially be treated with mannitol or thiopentone which reduce brain water. Phenytoin may subsequently be given with mechanical hyperventilation and moderate (32-33 ^{o}C) hypothermia [25,44].

2.4.3 Coagulopathy

ALF is associated with a profound decrease in the synthesis and an increase in the consumption of clotting factors involved in coagulation. This manifests in an increase in the prothrombin time (PT). The disturbance of the coagulation profile in ALF may resemble a disseminated intravascular coagulopathy (DIC), which may make the distinction between the two difficult [25,26].

2.4.4 Metabolic abnormalities

There are several metabolic abnormalities associated with ALF, including, hyponatremia, hyperkalemia, hypophosphatemia, acidosis (with acetaminophen), alkalosis (metabolic and respiratory), lactic acidosis, hypoglycemia and acute pancreatitis. Hypoglycemia is seen in 40 % of patients and is due to the depletion of glycogen stores and impaired gluconeogenesis [24]. With acetaminophen overdose a pH of less than 7.3 carries a poor prognosis. Lactic acidosis, associated with SIRS, causes increasing tissue hypoxia. The management of the abnormalities is achieved through treating the consequent alterations in the systemic circulation [25,26].

Circulatory failure is most likely due to the high levels of circulating endotoxin and tumor necrosis factor. Hypovolemia with a decreased systemic vascular resistance and cardiac arythmias may present as a result of the metabolic abnormalities. Hyperventilation, hypercapnia and respiratory alkalosis occur which exacerbate HE resulting in respiratory depression and apnea. Intrapulmonary shunting occurs with sepsis resulting in respiratory distress and pulmonary edema [24]. Management of the systemic circulation relies on maintaining adequate central venous pressure (CVP), maintaining plasma volume and increasing sodium levels. Hypotension (mean arterial pressure (MAP) below 60 mmHg) is treated with inotropics paired with continuous arterial pressure monitoring. Epinephrine and norepinephrine are commonly provided to increase vasoconstriction. In the US dopexamine (a dopamine analogue) is often

used to increase splanchnic and renal blood flow and to improve oxygen delivery to tissues. It also has an anti-inflammatory effect, which aids in attenuating leucocyte adherence to the splanchnic microvasculature [25].

2.4.5 Renal Failure

Renal failure develops in approximately 55 % of ALF patients. If it is secondary to the liver failure it is known as hepatorenal syndrome (HRS). The renal failure may also be due to an insult that affects both the kidneys and liver (e.g. paracetamol overdose). HRS is characterized by a hyperdynamic circulation and is caused by intense renal vasoconstriction [45]. The MAP is generally low, the cardiac output is high and the patients are hypotensive. There is severe arterial underfilling in the systemic circulation due to pronounced arterial vasodilation in the splanchnic circulation, which is related to portal hypertension.

In the kidney, on the other hand, there is intense vasoconstriction activated by the sympathetic nervous system and the renin-angiotensin and arginine vasopressin systems, as a homeostatic response to improve the under-filling of the arterial circulation. As a result of the increased vasoconstriction, renal perfusion and glomerular filtration are greatly reduced and tubular function is preserved [46]. Data suggests that the arterial under-filling is due to vasodilatation of the splanchnic circulation related to increased splanchnic production of vasodilator substances, particularly nitric oxide (NO) [47].

The renal failure is functional and will always recover when there is a return of liver function, thus, the kidneys are histologically normal in the early stages [48]. In the absence of spontaneous hepatic recovery, OLT will reverse the HRS [45]. There are two types of HRS: Type I is characterized by rapidly progressive renal failure, associated with the ALF, with a serum creatinine above 2.5 mg/dl or a glomerular filtration rate (GFR) below 20 mil/min and is followed by death. Type II is a chronic form, associated with chronic liver disease, characterized by moderate renal failure with a GFR below 40 ml/min or a serum creatinine above 1.5 mg/dl.

HRS may also be precipitated by spontaneous bacterial peritonitis and increased endotoxin levels, or by large volume paracentesis without plasma volume expansion. The increased endotoxin levels are associated with bacterial overgrowth and this correlates with increased serum NO and TNF-α levels [48]. These observations explain the association of HRS with SIRS. The treatment of HRS aims at improving renal perfusion and the GFR. In general systemic vasoconstrictors (e.g. vasopressin analogues) in combination with plasma volume expanders (e.g. colloids) are used to reduce the splanchnic vasodilatation, increase the MAP and to suppress the vasoconstrictors activated in the HRS. Antibiotics are usually also given [25,26,46,48].

2.4.6 Multi-organ failure

A wide range (10 % - 80 %) of ALF patients develop bacterial infection and sepsis as a result of the failure of the hepatic reticuloendothelial system. Staphylococcus and Streptococcus are the common invading organisms. SIRS usually precipitates multi-organ failure and it is the end point of the activation of multiple inflammatory pathways mediated by the chemokine-cytokine responses. It can be measured through the pulse rate, respiratory rate, the leucocyte count and temperature [42].

SIRS is linked to respiratory distress and sepsis. Prolonged hospitalization may also predispose patients to bacterial and fungal infection [49,50]. Once multi-organ failure is present the prognosis is poor. The liver, however, has a unique capacity for regeneration following an acute self-limited injury. Since there is no specific therapy for ALF, treatment generally focuses on supportive measures for the anticipated complications, allowing the liver time to heal [51]. N-acetylcysteine (NAC) is given in all cases of acetaminophen overdose to help in replenishing hepatic glutathione stores, but may also be useful in non-acetaminophen cases [24].

2.5 Prognostic scoring systems

Prognostic criteria aid in determining the likelihood of spontaneous recovery from ALF and therefore aid in decision making regarding OLT. These have been defined using the multivariate analysis of patient data at discrete time points, normally at

admission to the clinical institution. Prognostic criteria are dealt with in greater detail in section 6.2.

Briefly, fulfilling for example the King's criteria carries a poor prognosis for spontaneous recovery. What is apparent is that survival depends on several factors, such as etiology, patient age, severity of hepatic dysfunction, degree of liver necrosis, the number and nature of the complications and the duration of the illness. There is also a strong correlation between the grade of HE and mortality: At grade II mortality is 30 %, at grade III it is 50 % and at grade IV it is over 80 %. Generally survival is better in cases of acute hepatitis A and acetaminophen overdose (40 %) than in idiopathic, toxin related, HBV-hepatitis D co-infection and idiosyncratic drug reactions (80%) (table 2.2) [24].

Table 2.2 Some historically commonly employed prognostic criteria for ALF

System	Criteria	Reference/s
King's College criteria		[52,53]
in acetaminophen overdose	arterial pH < 7.3 despite normal intravascular filling pressures (irrespective of grade of HE), or all three of the following: • PT > 100 secs, • serum creatinine >300 µmol/l, • grade III- IV HE.	
in all other cases of ALF	PT > 100 secs (irrespective of grade of HE), INR > 3.5, or any three of the following (irrespective of grade of HE): • non-A, non-B reaction (cryptogenic), • halothane hepatitis, • or other drug toxicity • jaundice > 7 days before the onset of HE, • age < 10 or > 40 years, • serum bilirubin > 300 µmol/l. • PT > 50 secs	
APACHE II	acute physiology and chronic health evaluation score	[54]
Cliché Criteria	clotting factor V < 20% of normal in a person of < 30 years, or both of the following: • Factor V < 30% and • grade III-IV HE in patients of any age.	[55,56]
serum-globulin [Gc protein] level	scavenger protein bound to actin and released into the circulation by dying hepatocytes	[57]
serum alpha-fetoprotein [AFP] level	an increase from day 1 to day 3 correlates with survival	[58]
severity of SIRS	using various indices of the inflammatory response	[59-61]

liver biopsy	when necrosis > 70% mortality is > 90% without transplantation	[62]

2.6 Orthotopic Liver Transplantation (OLT) for ALF

The first OLT procedure was performed by Starlz *et al* (1963) [63] and it has remained the definitive treatment for ALF patients who meet the criteria for transplantation. Practically speaking, the majority of transplants are full organ grafts from cadaveric donors. Coagulation factors and platelets are replaced prior to surgery and this is usually adequate to reverse clinical coagulopathy and keep blood losses low. Cerebral edema may be problematic during the dissection and reperfusion phases but often dramatically improves during the anhepatic period. Cerebral autoregulation usually returns to normal within 48 hours of successful transplantation. All cases require immunosuppression. The risk of sepsis, including fungal infection, extends into the post-transplant period and is aggravated by immunosuppression. Renal support is often required for several weeks after the procedure. This is due to the use of nephrotoxic immunosuppressives, antimicrobial drugs and potentially hepatorenal syndrome.

Survival rates vary between 60 % and 90 % depending on the centre. The best transplant results are those for Wilson's disease while the worst are for idiosyncratic drug reactions. For paracetamol overdoses the survival is favored if the transplant occurs within four days of the ingestion. Survival also decreases with progression in the grades of HE at the time of transplantation: 90% for grade I, 77% for grade II, 79% for grade III, and 54% for grade IV. Renal function also correlates with outcome, a serum-creatinine > 200 µmol/l is associated with a poorer outcome [15].

In South Africa, OLTs have historically mostly been done at the Groote Schuur and Red Cross children's hospitals. However, since 2005 the Wits Donald Gordon transplant unit in Johannesburg has also been conducting these surgeries. The problem facing all institutions is donor organ shortage (the global waiting list mortality is in the region of 20 %). In the Eurotransplant zone (http://www.eurotransplant.nl) in 2006 there were 2249 patients on the waiting list and only 1277 liver transplantations were conducted. In Africa there is also a reluctance on the part of physicians to refer

patients and the use of 'marginal' (non-ideal) donors, along with the presence of HIV and HBV virus and tuberculosis with associated isoniazid and rifampicin toxicity [64,65].

2.7 Liver support systems

Ideally, complete hepatic support should prevent or halt the acceleration of the cytokine cascade seen in ALF, provide metabolic, synthetic and detoxifying functions and allow time for organ regeneration [25]. This is clearly a tall order. Minimal support lies in 'bridging' patients to transplantation. There are a variety of design configurations for extracorporeal liver support systems, including dialysis-like artificial (non-biological), hybrid (bio-artificial) support systems and purely biological, (hepatocyte transplantation and liver-to-liver, cross-dialytic systems) respectively (table 2.3):

Table 2.3 Summary of non-biological and biological liver support systems (adapted from van de Kerkhove *et al* (2005) [20] with permission from the author)

Liver support	Technique	Basic outcomes
Artificial or dialysis-like:		
Hemodialysis	Exchange diffusion across a semipermeable membrane between blood and a dialysis fluid	Improved coma, no improvement in survival
Hemofiltration	Continuous convective solute removal across a permeable membrane	Limited outcome
High volume plasmapehersis	Exchange of high plasma volumes	Improvement in biochemical parameters and clinical status
Hemodiafiltration	Convection (large molecules) and diffusion (small molecules) removal across a membrane	Case reports, improved biochemical parameters and neurological status
Hemoperfusion	Perfusion of blood/plasma over charcoal, synthetic neutral resins, or anion exchange resins	Removal of toxins, improvement of mental status, no survival benefit
Hemodiabsorption	Dialysis against a combination of charcoal and cation-exchanger	Biochemical improvement and clinical status, no improvement in survival
Molecular Adsorbent Recirculating System (MARS)	Removal of protein-bound and water soluble substances across a specialized albumin impregnated membrane against albumin rich recirculating dialysate	Improvement in biochemical parameters and clinical status, significant survival benefit for subgroup of patients

Albumin dialysis system	Hemodiafiltration using albumin dialysate without recirculation	Improvement in biochemical parameters and clinical status
Artificial liver support system	Combination of plasma exchange, charcoal hemoperfusion, plasma bilirubin absorption, charcoal plasma perfusion, hemofiltration and hemodialysis	Improvement in biochemical parameters and clinical status
PF-Liver Dialysis	Combines hemodiabsorption with push-pull sorbent-based pheresis	Improvement in biochemical parameters and clinical status
Biological and Bio-artificial:		
Blood xeno cross-hemodialysis	Patient's blood dialyzed against blood of a living animal	Beneficial to patient, not suitable for further clinical application
Tissue xeno cross-hemodialysis	Patient's blood dialyzed against animal liver tissue preparations	Beneficial to patient, not suitable for further clinical application
Xenogeneic liver perfusion	Patient's blood perfused through an animal liver	Safe and provides metabolic support to the comatose AHF patient
Human cross-circulation	Shunt between patient's blood and blood of healthy human	Beneficial to patient, but harmful for donor
Exchange transfusion	Replace patient's plasma with healthy human plasma	Reversal of hepatic coma, large amount of normal plasma needed
Hepatocyte transplantation	Transplantation of isolated human hepatocytes in the patient's spleen or peritoneal cavity	Not much known in AHF patients, beneficial to patients with inborn metabolic errors, survival improvement in animal studies
BAL	Patient's blood or plasma perfused through an extracorporeal bioreactor filled with hepatocytes	Significant survival improvement in animals Safe in humans, improvement in clinical and biochemical parameters. Improved survival ALF subpopulations

2.7.1 Non-biological liver support

Renal support technology has been adapted for treating ALF. Water-soluble and protein-bound, low and middleweight toxic substances are thought to cause multiple organ failure, HE and consequently coma and death. It was therefore thought that dialytic filtration systems for detoxifying the patient's blood would be successful. To date no single system has demonstrated statistically significant improvements in patient survival in prospective, randomized controlled clinical trials. Non-biological therapies have routinely demonstrated improvements in HE and patient biochemistry

(such as with the MARS system [66]). However, their limited benefit is thought to be due to their inability to synthesize liver proteins and hepatotrophic factors and the non-specific removal of toxins and mitogens from the blood.

2.7.2 Biological liver support

The biological approach relies on the ability of the parenchymal cells of the liver, i.e. the hepatocytes, to support ALF patients. This is owing to their ability to perform detoxification, metabolism functions and the synthesis of proteins and mitogens critical for liver regeneration.

The two most promising approaches include the transplantation of isolated human hepatocytes into ALF patients and extracorporeal bio-artificial liver circulation systems. Purely biological, animal-to-human and human-to-human, liver to liver or blood, cross-dialytic systems have been discarded due to xenozoonotic or immunological concerns. Portal hepatocyte transplantation has shown some promise in animals but in human patients long-term efficacy has not been demonstrated [67]. This may be due to the susceptibility of hepatocytes to viral infection in hepatitis-virus positive patients, or exposure to toxins and drugs in drug-induced ALF. Research has also been conducted on implanted hepatocytes encapsulated in biocompatible matrices. The two basic designs include vascularized or micro-encapsulated implants, the former involving a biodegradable matrix with direct exposure to the host immune system and the latter a protected but diffusible non-biodegradable matrix. Stimuli responsive and bio-active matrices that (for example) stimulate tissue healing have also been experimented with [68].

Bio-artificial liver support systems (BALSS) are designed for temporary extracorporeal dialysis and contain a bioreactor housing hepatocytes. A large variety of bioartificial liver systems have historically been developed, with the differences mainly in the design of the bioreactor. The most common design has been the hollow-fibre bioreactor in which the cells are incorporated into either the internal or external blood perfusion surfaces. Other designs include for example packed-bed alginate encapsulated or direct-plasma contact radial-flow bioreactors. In all cases, there is a complex trade-off between metabolite and gas mass-transfer gradients, contact with

the host immune system and the degree to which the cellular environment is *in vivo*-like [69-73]. A selection of systems that have been employed in the human clinical setting demonstrated results as follows (table 2.4):

Of the tested devices only two (ELAD [74] and the HepatAssist [75] systems) have progressed to Phase II/III, i.e. clinical efficacy, while all of the others have only been evaluated in Phase I trials, i.e. clinical safety. In the Phase I group an improvement in survival was not viewed as the primary end-point. In the Phase II group only the HepatAssist system showed statistically significant improvements in survival. Specifically, when survival was analyzed accounting for confounding factors, in the entire patient population which included primary (OLT) graft non-function patients there was no difference between the treated and un-treated control patients. However, survival in the fulminant/subfuliminant hepatic failure sub-group of patients was significantly higher in the BAL versus control group (risk ratio = 0.56,P = 0.048). Unfortunately, the trial was terminated by the FDA prior to completion as it was concluded that demonstrating a significant survival benefit using the particular analytical methods was unlikely. This study in particular demonstrated the challenges associated with undertaking multi-centre randomized controlled trials [75].

The majority of the tested devices were well-tolerated and safe, displayed improvements in the patient's neurological status, improvements in blood biochemistry, tested negative for porcine endogenous retrovirus (PERV) (when the cell type in the bioreactor was of porcine origin), no clinical complications as a result of the treatments and several patients could be bridged to OLT. These trials demonstrated that the utility of BAL devices resides in their ability to bridge ALF patients to OLT rather than in completely replacing liver functions. There remains considerable positive expectation that a BAL device will eventually demonstrate significant improvements in survival in all patient sub-groups in the future.

Table 2.4 System characteristics and outcomes of clinical trials (adapted from van de Kerkhove *et al* (2005) [16] and Chamuleau et al (2006) [70] with permission from the authors)

System	ELAD	HepatAssist	TECA	BLSS	RFB	LSS-MELS	AMC-BAL	HBAL
Reference	[74]	[75]	[76]	[77]	[78]	[79]	[80]	[81]
Cell type	C3A-Human tumor	Porcine	Porcine	Porcine	Porcine	Human primary	Porcine	Porcine
Cell source	cultured	cryopreserved	isolated	isolated	isolated	isolated	isolated	isolated
Amount of cells	200-400g	$5\text{-}7*10^9$	$10\text{-}20*10^9$	70-120g	200-300g	600g	$1*10^{10}$	$1*10^{10}$
Membrane pore size	70 kD	0.2 µm		100 kD	1 µm	400 kD	Direct contact	100 kD
Perfusion medium	blood	plasma	plasma	blood	plasma	plasma	plasma	plasma
Exchange rate	150-200 ml/min	50 m l/min		100-250 ml/min	22 ml/min	31 ml/min	50 ml/min	
Bioreactor flow rate	200 ml/min	400 ml/min		250 ml/min	1.5 ml/min/g hepatocytes	200 ml/min	150 ml/min	
Added detox device	no	Activated charcoal	Activated charcoal	no	no	albumin dialysis	no	Activated charcoal
Trial type	clinical	clinical	safety	safety	safety	safety	safety	safety
Total of patients	24	171	6	4	7	8	12	12
Outcomes	6 bridged, 7 died no OLT		atleast 2 survived no OLT		6 bridged, 1 died	6 bridged, 1 survived no OLT 1 died no OLT	11 bridged, 1 died no OLT	9 survived no OLT, 1 died post BAL
Survival improvement	no	only 33% of acetaminophen group	N/A	N/A	N/A	N/A	N/A	N/A
Complications	hypotension, bleeding	hypotension	no	hypotension	no	no	hypotension	no
Neurological improvement	possibly	yes	yes	no	yes	yes	yes	unclear
ammonia elimination	-8%	18%		33%	33%		44%	unclear
bilirubin elimination	-20%	18%		6%	11%		31%	unclear
PERV	N/A	negative		negative	negative	N/A	negative	

Notes: N/A=not applicable. Where data has been omitted none was provided

Subsequent to the above, an additional Phase I trial has been conducted by the US company Vital Therapies with the ELAD system in Beijing, China. The results have not been published as yet, but according to the website (as at June 2009, http://www.vitaltherapies.com) demonstrate significant improvements in transplant-free survival for acute-on-chronic liver failure (in mostly hepatitis-B patients) that has been sufficient to justify a Phase II trial currently underway in the US (http://www.clinicaltrials.gov).

2.7.3 Biological principles in the design of BAL devices

As alluded to above, a variety of design aspects of BAL systems impact their clinical efficacy. Important choices include, the cell type and source, the cell culturing method, the amount of cells in the bioreactor, the means of cellular oxygenation, the type of cell-adhesion matrix in the bioreactor, the bioreactor sub-circulation flow rate (i.e. mass transfer characteristics), the exchange rate between the BAL device and the patient and the presence of an additional (artificial) detoxification device in the BAL circuit [79,82,83]. These factors are briefly reviewed below:

2.7.3.1 Cell type, source and mass

Cell type and source remains an important issue in the design of BAL devices and this subject is consequently returned to subsequently (section 4.4). In the beginning the following questions must be asked: Should the cell type be human or animal and should the cell type be cultured or primary in origin? The advantages and disadvantages of the various BAL appropriate cell types are as follows (table 2.5):

The choice of cell type has an important practical aspect, in that it determines the development of techniques for routinely sourcing large amounts of cells in a sterile manner. The expenses and difficulties faced in establishing these models are significant. For example, transformed and immortalized cells require sterile *in vitro* culturing in large quantities, which is expensive, time consuming and requires extreme vigilance on a technical level. Primary xenogenic (pig) cells, on the other hand, require the establishment of a sterile, numerically large scale isolation method which is usually more feasible than the above (section 4.1). The easy availability,

inexpensiveness, metabolic efficacy of the cells and the physiological and anatomical similarity of pigs to humans has led to many research groups initially working with primary porcine cells. Porcine endogenous retro-virus (PERV) contaminations have also not been demonstrated in clinical tests of BAL systems utilizing these cells. However, concerns regarding zoonoses limit the international applicability of these cells.

Table 2.5 The advantages and disadvantages of cell sources for BAL's [83-86]

Cell Source	Advantages	Disadvantages
primary human hepatocyte-non-parenchymal co-cultures.	functionally active allo-compatible	low availability difficult to stimulate for *in vitro* growth
transformed human hepatocytes, hepatoma cells. e.g. C3A-(HepG2)	allo-compatible highly available	poor functionality potential tumorigenicity must be cultured in sufficient quantity for a BAL
human stem cells- e.g. embryonic stems (ECs)and multipotent adult progenitor cells (MAPCs)	allo-compatible moderate availability	differentiation into hepatocytes cannot be guaranteed in a BAL
reversibly immortalized human hepatocyte-non parenchymal co-cultures. e.g. NKNT3 + TWNT3 cells, OUMS-29 cells	allo-compatible highly available	potential tumorigenicity lower functionality than primary cells logistically difficult to culture in sufficient quantity for a BAL
primary xenogenic hepatocyte-non parenchymal co-cultures. e.g. porcine cells	highly functional physiological similarity to human cells highly available	potential immunogenicity potential transmission of zoonoses [PERVs] questionable biocompatibility

The *in vitro* cell culture model in the bioreactor impacts BAL metabolic functionality; Liver hepatocytes have an epithelial polarity and junctional cell-cell communication structures. These structures are lost in *in vitro* culturing and several studies have established that *in vitro* hepatocytes do not independently perform as effectively as they do *in vivo*. For this reason, non-parenchymal liver cells such as stellate or fibroblast cells may be co-cultured with hepatocytes in a specific ratio, facilitating the phenotypic and functional stabilization of the hepatocyte aggregate structures. The cell culture media that is used to perfuse the bioreactor prior to BAL connection also determines subsequent functionality. Media composition must be carefully attended to and usually involves supplementation with mitogens and hormones.

Interestingly, in Africa many donor livers go to waste simply due to the insurmountable logistical difficulty of getting the livers to transplant facilities within acceptable time frames. This fact validates the development of a liver support system in this context but potentially also presents an opportunity to populate the bioreactor with primary human cells. Primary human cells are obviously preferable for use in a BAL system, for the reasons stated above, but are mostly only available following liver resections from oversize organs used in transplants.

Stem cells of human origin are an attractive potential source of liver cells in view of their greater replicative capacity and immunological *naiveté* relative to adult tissue. There are currently several techniques for *immortalizing* mammalian cells so that they will maintain primary-like properties for as long as possible. For example, simian virus 40 (SV40) T antigen, adenovirus E1A and E1B, human papilomavirus (HPV) E6 and E7 work by inactivating the tumor suppressor genes (such as p53 and Rb). Alternately, the use of recombinant telomerase adenovirus or retroviral vectors results in the expression of the human telomerase reverse transcriptase protein (hTERT) which causes the cells to maintain telomere lengths that will prevent replicative senescence. hTERT immortalized cells often indefinitely retain a stable genotype along with critical phenotypical markers. The Cre-lox system uses Cre recombinase (from the P1 bacteriophage of S. cervisiae) which catalyzes the site-specific recombination between two 34-bp repeats called loxP. When Cre binds to loxP the intervening section is permanently excised. Using this it is possible to *reversibly* immortalize primary cells by transducing an oncogene flanked with loxP sequences, enabling subsequent site specific excision with Cre. Having said this, stem cell research is still in a relatively early stage [83-86]. This subject is returned to subsequently (section 4.4).

An early question in the history of BAL research was what minimal cell mass is required to maintain a patient in ALF? The relevance of this question is three-fold: First, an obvious concern is to source sufficient cells for a metabolically effective device, second, the size of the cell mass is a practical determinant of the employed methods [87] and third, the cellular metabolic requirements determine aspects of BAL design [88].

Early surgical studies attempted to answer this question through resections to determine the minimal liver mass required to maintain survival [89-92]. However, this methodology is misleading in that the resected liver has an existing blood supply and surgical complications may confuse the outcomes. Additionally, hepatocytes in a liver are not all simultaneously maximally functional, thus, the organ may have huge 'metabolic functional reserves' under stress.

Current estimates are that between 10 % and 30 % of the host liver mass is required for effective support of ALF [83,92]. Since an adult liver weighs approximately 1500 grams and is composed of approximately 80 % hepatocytes, the estimated minimal amount of hepatocytes required for a BAL is in the region of 150-300 grams. However, subsequent studies on rats in ALF have shown biochemical improvements with as little as 2 % of the normal liver mass [93] and adult humans are known to survive following even 90 % partial hepatectomy [75]. To maintain a cell mass of 150 g a bioreactor design is required that will facilitate sufficient mass transfer to all or as many of the cells as possible.

2.7.3.2 Cellular oxygenation

For effective hepatocyte function BAL design must focus on an adequate oxygen supply to maintain optimal metabolic properties. Due to the liver's intense metabolic activity, it consumes 20-30% of the body's oxygen (O_2) translating to 30-40 ml/min, in the maintenance of liver functions [94-98].

BAL systems are perfused either by whole blood or by plasma only. In the former case, adequate oxygenation relies on hemoglobin, but then the possibility for an immune foreign-surface-related reaction exists. In the latter case, the relatively low O_2 carrying capacity of plasma may become limiting at high cell densities in the BAL. In treating an ALF patient, in which the plasma may be toxic and/or hypoxic, this may be a real concern.

There are generally two means by which bioreactor oxygenation may be improved: Either the diffusion distance of O_2 to the hepatocytes may be decreased, or the concentration of O_2 entering the bioreactor may be increased [99]. Consequently,

several different whole blood and plasma perfused bioreactor designs have been described, including for example, stackable flat membrane bioreactors [100,101], direct contact bioreactors [102-103], and several different configurations of hollow-fiber bioreactors [104-106]. Each configuration has both advantages and disadvantages. However, an ongoing concern amongst investigators is the presence of domains of low O_2 tension and consequent hypometabolism in their bioreactors [107,108].

2.7.3.3 Cell support matrices

Since hepatocytes are aggregation dependant cells, maintaining normal cell polarity (phenotype) and thus function in a bioreactor requires a biocompatible cell-aggregation matrix to enable 3-D cell spheroid formation. The phenotype is also dependent on the extracellular matrix and cell-cell communication. Possibilities therefore exist to coat matrix surfaces with collagen (or similar) and non-parenchymal cells (such as stellates) may be included in a 'co-culture'. Many culturing configurations have been experimented with, for example: bioresorbable matrices (e.g. hydrogels), non-resorbable open-cell sponge-type matrices (e.g. polyurethane), encapsulated or microcarrier packed-beds (e.g. alginate beads) and many different kinds of microfilament membrane matrices (e.g. polysulfone or cellulose acetate). Each has advantages and disadvantages. For good reviews on this see Tzanakis *et al* (2000)[1], Chan et al (2004)[68], Nahmias *et al* (2006)[2], Streetz *et al* (2008)[82].

The choice of matrix should ideally be preceded by modeling the bioreactor flow configuration and consequent gas and metabolite mass transfer characteristics to the cells. The availability of nutrients to a cell may be expressed quantitatively [108]. Assuming nutrients transfer by diffusion within the hepatocyte compartment with diffusivity D (cm/s). If the cell consumes at a rate R (mol/cm^3/s), dimensional analysis gives a (unit-less) cell lifeline number (S).

$$S = R \cdot L^2 / D \cdot C_0 \qquad (2.1)$$

where C_0 is the source solute concentration and L the distance from the source. In this model the source is the compartment from which the diffusion is taking place

(e.g. either whole blood or plasma depending on the design). For values of $S \approx 1$, L represents the greatest distance from the source of the nutrient. The same formula applies to hepatocyte synthesis, and then S correlates with the supply of hepatocyte synthetic products to the patient. A consequence of equation (2.1), is that the metabolic efficacy of the cellular compartment is determined by the distance (L) from the perfusate, thus, a design trade off must be made between the 3-dimensionality of the cell culture and the diffusion distance to the perfusing compartment. This fact has been borne out by the variable success of the many bioreactor designs proposed to date.

In principle, the more closely the configuration emulates *in vivo* liver structure, the better the metabolic function (table 2.6).

Table 2.6 The relative advantages and disadvantages of culture configurations

Culture Method	Duration and extent of hepatic functionality	Performance as BAL
in vivo liver structure*	long term and enhanced	excellent
3-D co-culture 2-D co-culture collagen sandwich spheroids microencapsulation porous matrices extracellular matrices microcarriers	↑	↑
	short term and poor	limited

* theoretical (not-yet existing) culture configuration.

2.7.3.4 Flow rates, exchange rates and the priming volume

A consequence of equation (2.1) is also that mass transfer to and from the hepatocyte compartment is determined by the rate of flow of the perfusate to that compartment. Similarly, mass transfer between the patient and the bioreactor is determined by the rate of exchange between the two compartments. In principle, the faster the flow rates the greater the mass transfer; however, the fluid shear rate over the cells may then become sufficiently great to have a deleterious effect on cell adhesion. In most BAL devices the bioreactor has a sub-circulation rate that is faster than the rate of exchange between the patient and the BAL. This is for practical reasons in that it is difficult to maintain exchange rates exceeding approximately 200 ml/min.

The priming volume is the amount of fluid (normally either plasma or blood) that is required to fill the BAL prior to enabling the recirculation circuit between the patient and the BAL. This volume creates a blood dilution effect that may temporarily benefit the patient through reducing circulating toxin levels. However, when excessive, the increase in blood volume may result in haemodynamic instability in the patient, which may impact the subsequent clinical course. For example, a loss of hematocrit is known to have deleterious effects on survival. ALF is also associated with haemodynamic instability. Consensus amongst research groups is that a system priming volume of 1 litre or less is ideal. However, achieving this in a complex recirculation system may present an engineering challenge.

2.7.3.5 Detoxification devices and the use of multiple, functionally optimized bioreactors

Despite all efforts it is unlikely that hepatocyte or co-culture bioreactors will replace all the functional abilities of a normal liver. Assuming these hepatocytes express the normal bile-conjugate transporters (such as MRP2 or BSEP) the cells still *physically* lack a biliary system. However, if the hepatocytes in the bioreactor form canaliculi during culturing they will be able to excrete conjugated bilirubin into the circulating blood plasma, which will subsequently be removed by the kineys. Since the liver is compromised in BAL treated ALF patients, protein-bound bile acids and salts are likely to increase in the patient's blood. Bilirubin is toxic to both the patient and the cells in the bioreactor. Similarly, ammonia and other nitrogenous compounds accumulate in ALF patients due to the sub-optimal transformation of these substances into urea. Practically it is impossible to incorporate into a bioreactor the same amount of hepatocytes as found in an innate liver, nor maintain the same blood perfusion rate. Thus, the accumulation of blood borne toxins may be difficult or even impossible to prevent using BAL devices as defined to date.

It may therefore be desirable to include an artificial detoxification module in the BAL circuit since doing so aids both the patient and BAL bioreactor. Various adsorption columns exist and are often composed of a large surface area of activated charcoal. Albumin cross-dialytic renal technology may also be employed for blood protein-bound toxin removal. As stated, a potential disadvantage of artificial detoxification

lies in the non-selective removal of compounds including hepatotrophic substances that may facilitate liver regeneration. The specification of the employed detoxification device is therefore important in terms of BAL clinical operation. This subject is returned to subsequently (in section 5.3.4).

In the *in vivo* liver there is metabolic functional 'zonation'. This zonation is due to factors including, for example, hormone gradients, substrate concentrations and the perfusing O_2 gradient, the latter of which is an important modulator of cellular function [109]. Thus, 'perivenous' and 'periportal' regions exist in which enzymatic activity is different. Cytochrome P450 isoenzymes, which perform much of the biotransformations occurring in the liver, tend to be localized in the perivenous region while urea-synthesizing enzymes tend to occur in the periportal region. Both of these functions are important in terms of an effective BAL device. It has therefore been proposed [68], that potentially several bioreactors, each of which has been metabolically 'primed' for a particular function, may be included in a single BAL treatment. This is a principally sound concept, but would be difficult in practice to implement.

3. THE DESIGN OF THE UP-CSIR BALSS

Although not precisely in the scope of this thesis, the design of the bioreactor and BALSS circulation system underlie some of the studies presented below. For the sake of illustration it is therefore useful to provide information in this regard. However, in view of proprietary issues this is unfortunately only generically possible.

Broadly speaking, both the bioreactor and circulation system have progressed through two design iterations and are in the process of a third. The system design engineer was Mr. AJ van Wyk of the department of Mechanical Engineering of the University of Pretoria [110,111].

3.1 Bioreactor optimization

As part of a Mechanical Engineering project [112] Mr. LJT Ronné of the Department of Mechanical engineering employed particle tracking computational flow dynamics (CFD) to optimize the bioreactor for even flow and mass transport throughout the open-cell polyurethane foam (PUF) cell aggregation matrix in the bioreactor. The attractive biocompatibility characteristics of this matrix resulted in its choice in this case. The PUF had a mean cell volume of approximately 1 mm diameter allowing the formation of large hepatocyte aggregates (this is investigated in section 4.2.3).

The radial flow geometry of the bioreactor (figure 3.1) was chosen to perfuse a maximal possible PUF volume (and thus aggregated cells). However, following both *in vitro* and *in vivo* experiments it became apparent that the overall first-iteration bioreactor shape had areas of flow stagnation, i.e. ‘dead’ spaces, where hypoxic circumstances would inevitably result. CFD modeling of this bioreactor then confirmed what had been observed in practice (figure 3.2)

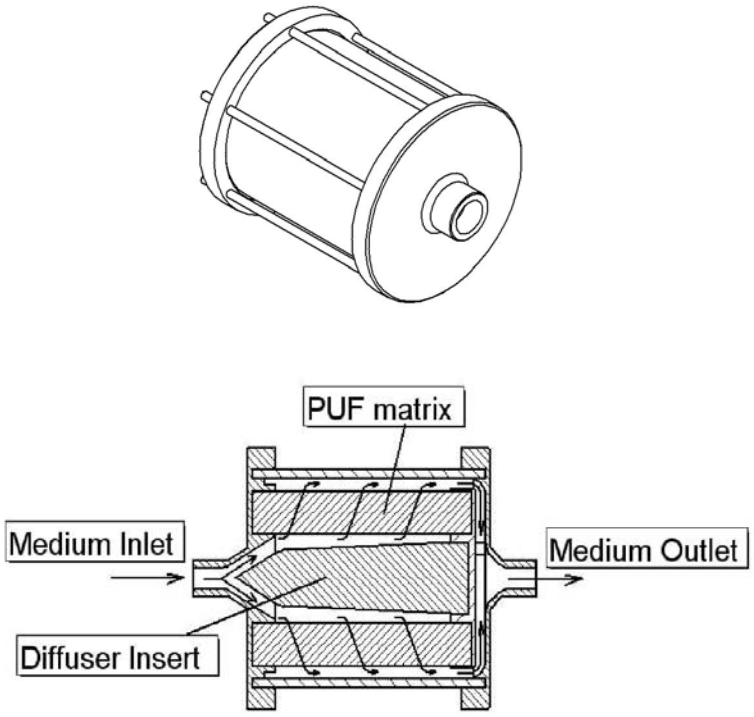

Figure 3.1 First iteration, non-flow optimized bioreactor

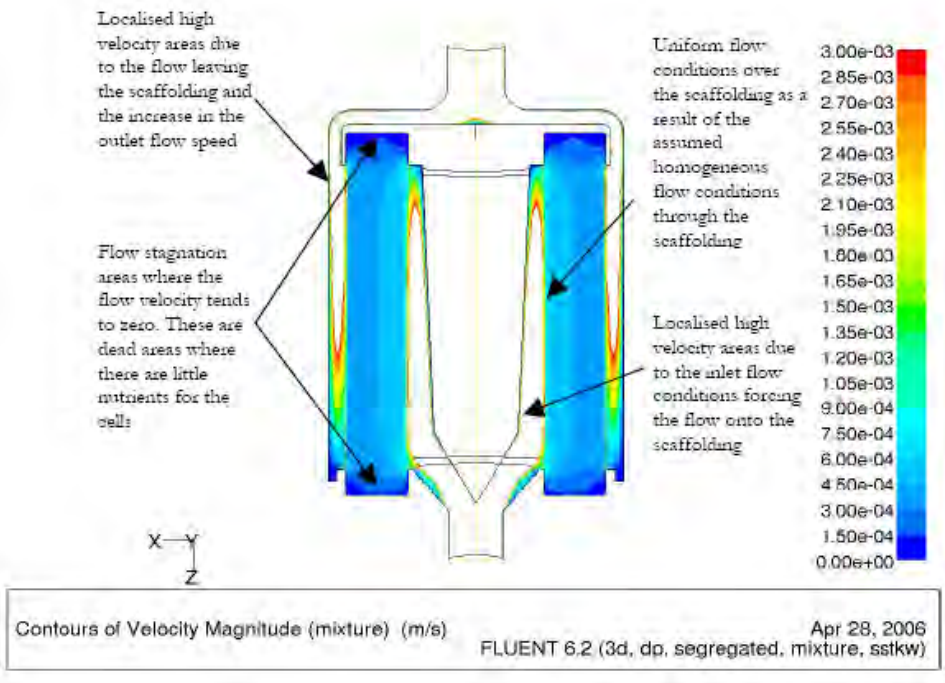

Figure 3.2 CFD model of velocity contours of a plasma-PFC mixture over the PUF cell aggregation matrix in the non-optimized bioreactor configuration (this figure was reprinted with permission of Mr. LJT Ronné [112]).

In response to these problems the bioreactor design was then changed to ensure that the plasma-PFC mixture would perfuse all of the PUF matrix evenly, with no 'dead spaces', ensuring that all aggregated cells received the same oxygenation and mass transfer conditions. To make this possible the bioreactor was basically shortened on the long axis and the foam support was redesigned.

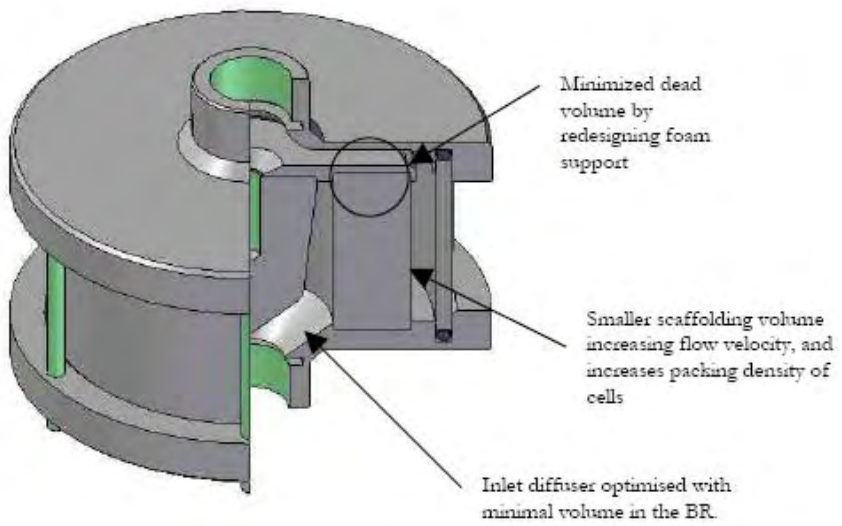

Figure 3.3 Optimized bioreactor design. The dead spaces have all been removed.

As before, the redesigned bioreactor was then simulated using CFD and it was confirmed that there was homogenous flow throughout the matrix (figure 3.4). Having said this, the internal configuration and material composition of the bioreactor, including the aggregation matrix, are currently being reviewed. A third, presumably considerably better, iteration will hopefully result.

As a matter of interest, the first iteration bioreactor was used in the first of the bioreactor-*in vitro* studies (section 4.2) and in the evaluation of the UP-CSIR BALSS in a large animal model (section 5.3). Thereafter, the optimized bioreactor was employed in the second bioreactor-*in vitro* study (section 4.3).

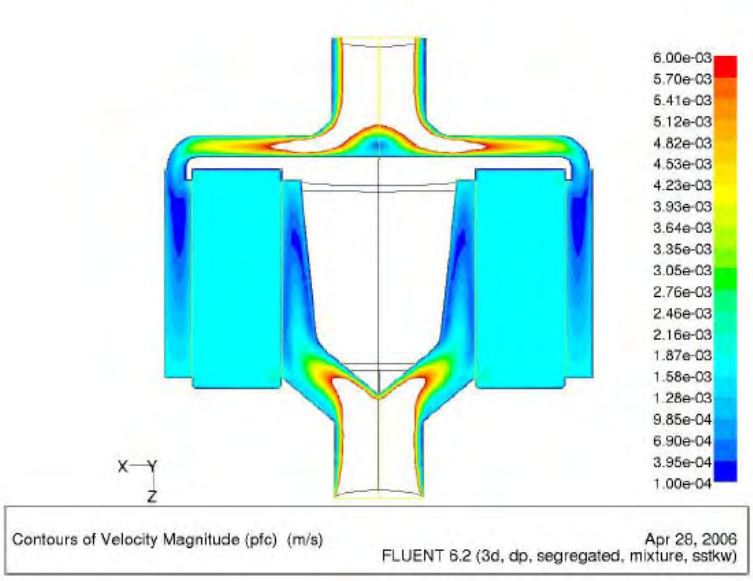

Figure 3.4 CFD model of velocity contours of the plasma-PFC mixture over the PUF cell aggregation matrix in the optimized bioreactor configuration. The removal of 'dead' areas was confirmed (reprinted with permission of Mr. LJT Ronné [112]).

3.2 BALSS circulation system optimization

The design of the BALSS circulation system (figure 3.5) incorporates the following components:

- An intravenous (IV) blood input line, normally from the jugular vein, which proceeds to,
- A plasma separator, as is routinely used in dialysis applications, enabling the input of plasma-only at 70-100 ml/min into the system. The separated cellular component of the blood is passively returned to the patient.
- A reservoir, into which the plasma flows and is mixed with a 40 % v/v PFC emulsion, doubling its volume so that the resulting PFC concentration is 20 % v/v. The resulting PFC-plasma mixture then flows through,
- An in-circuit neonatal oxygenator, fed with an external gas supply, which oxygenates the mixture, followed by,
- A bioreactor as described above, which is perfused with the plasma-PFC mixture. The cells therefore treat oxygen-rich plasma, facilitating their synthetic and toxin clearance functions. The internal bioreactor circulation system circulates more rapidly than the plasma inflow rate in order to further improve mass transfer functions. Thereafter,

- A PFC filter then separates the PFC from the 'treated' plasma, which rejoins the cellular component of the initially separated blood and returns to the patient. The separated PFC, on the other hand, returns to the abovementioned reservoir where it is re-mixed with the incoming plasma as already described.

The specifications of the filters, some sub-circulation flow rates, gas supply and the details regarding control and monitoring are aspects of the proprietary 'know-how' of the system and are therefore not listed.

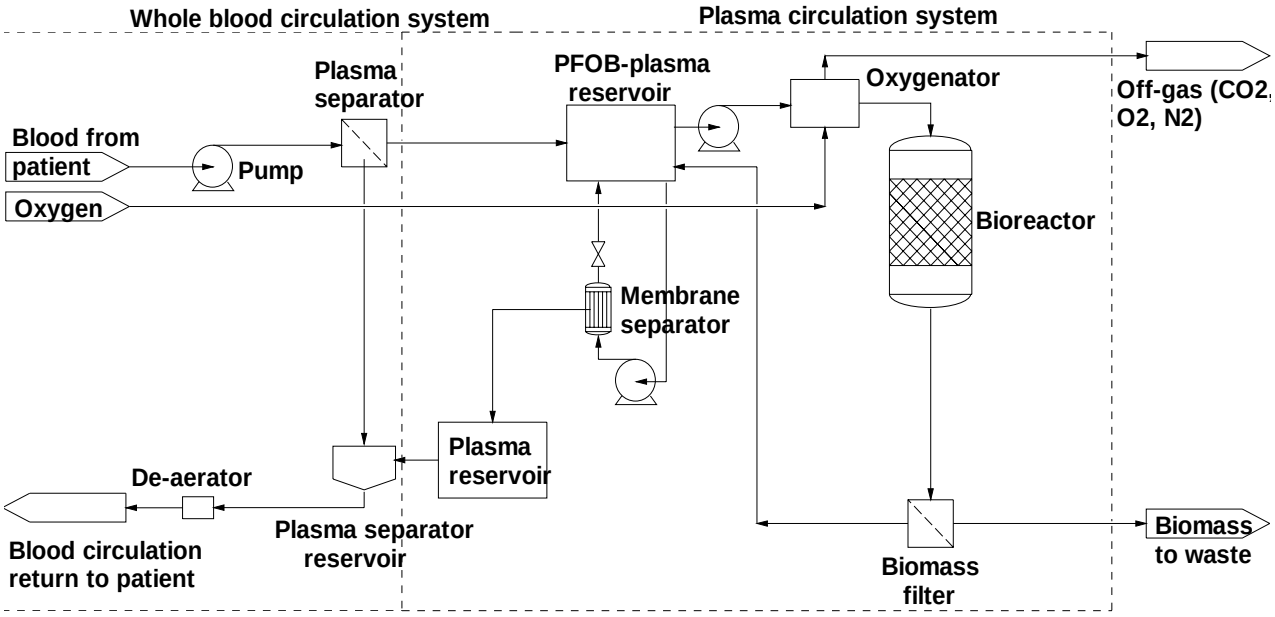

Figure 3.5 Schematic of the UP-CSIR BALSS (reprinted with permission from Mr. K van Wyk, system designer).

The first of the circulation system iterations (the mark I model, figure 3.6) was designed prior to the accumulation of empirical data regarding the behaviour of the system. The system was, visibly, rather complex and used tubing and components normally used in laboratories rather than in the clinical environment.

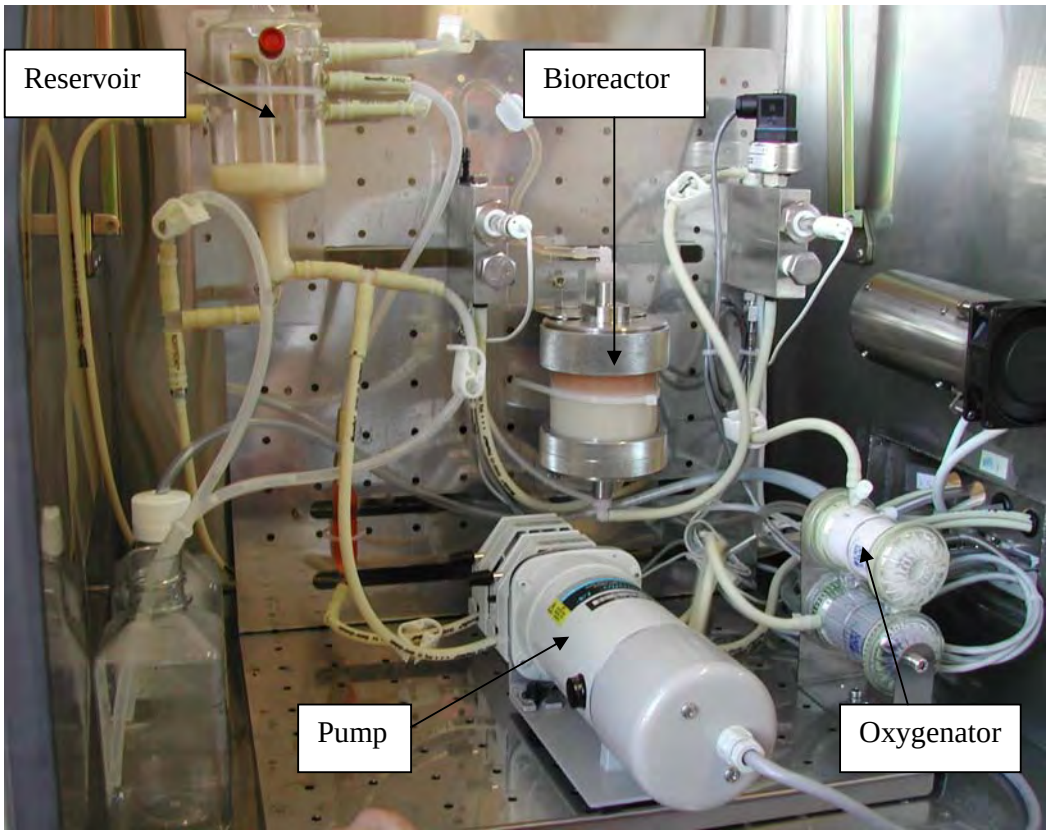

Figure 3.6 The BALSS mark I system. The components were more appropriate to a laboratory than clinical setting.

However, the mark I system was useful for collecting design parameter data in 5 animals. This led to a complete redesign, resulting in the mark II (figure 3.7) which was optimized for subsequent clinical evaluation in large animals (section 5.3.1 below). The mark II, although identical in principle to the mark I, employed as far as possible, tubing and components normally used in the clinical setting. However, the mark II was still understood to be a research device: It contained sensors for flow, pressure and temperature, blood gas and even biochemistry (section 6.3.4) which enabled *on-line* system monitoring and data collection that would be valuable for additional system redesign subsequently. The mark II had a graphical user interface (GUI) enabling the direct control of all system parameters including manual shutdown if necessary. In the event of power outages it was also equipped with a programmable logic controller (PLC) and uninterruptible power supply (UPS), so that system functions would not terminate even following the potential loss of access to the GUI.

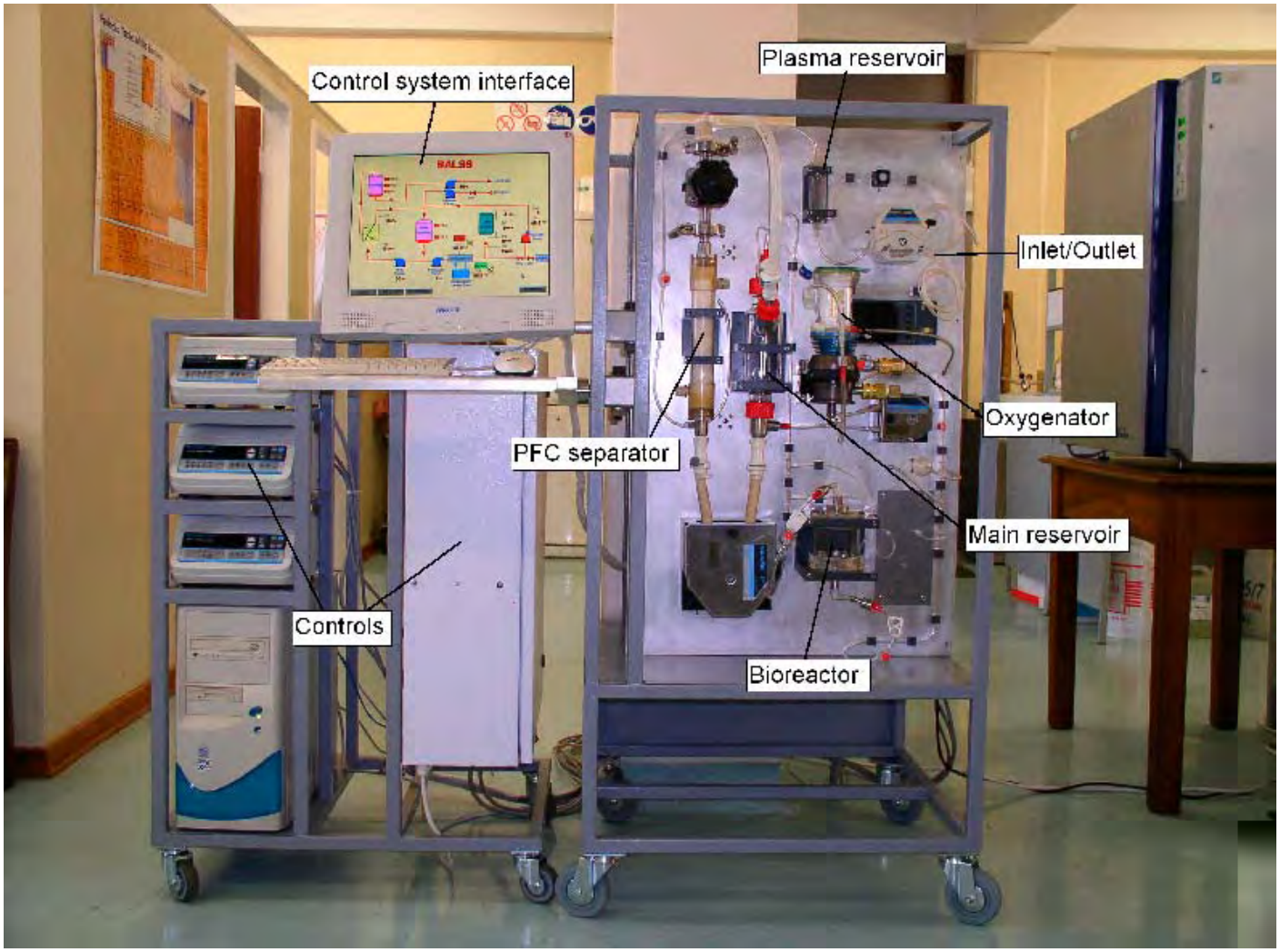

Figure 3.7 Annotated image of the UP-CSIR mark II BALSS

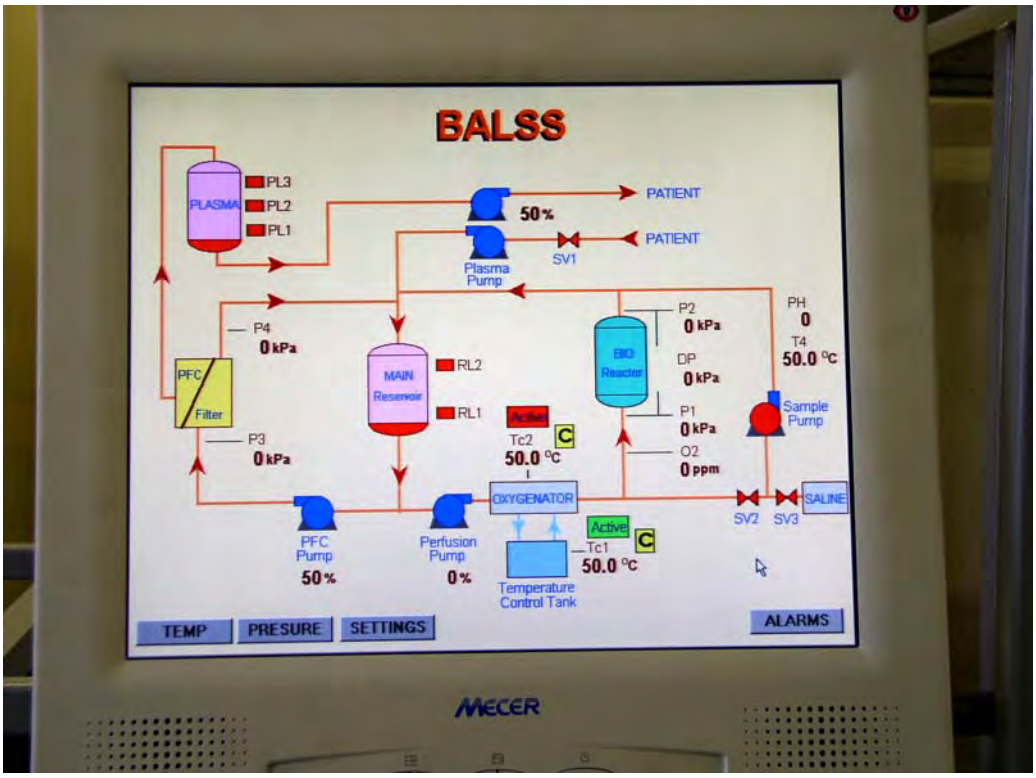

Figure 3.8 Graphical user control interface for the mark II model. Direct control was possible for the system as a whole and all sub-circulation flow rates.

During large animal trials (section 5.2 below) a comprehensive intensive care unit (ICU) was assembled and in which the mark II BALSS was evaluated for clinical efficacy in animals (figures 3.9,10). Simutaneously, a large amount of data was collected regarding the operation of the system itself. Particularly the following became apparent regarding the mark II:

- It was bulky, i.e. required a large amount of space.
- It required excessive attention to the sterile preparation of some of the components prior to treatment, which consequently took long.
- Particular components were not GMP/FDA approved.
- It was complex and required skilled personnel to control it during treatments.
- Its 'behaviour' changed over the course of treatments as a result of coagulation effects in the system.
- Some of the materials used in the system could have been improved for biocompatibility, e.g. the use of steel and glass in the first iteration bioreactor.
- The extracorporeal volume was greater than 1 litre, i.e. rather large, which may have contributed to haemodynamic instability in some of the patients.

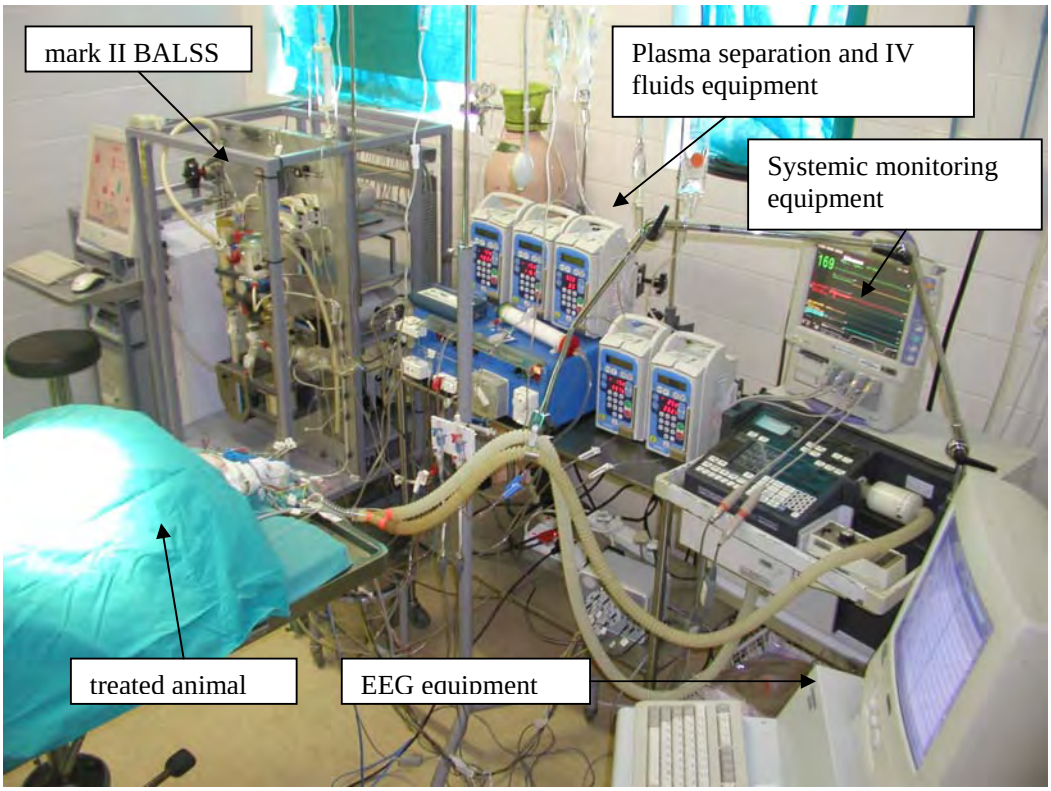

Figure 3.9 Intensive care unit (ICU) in the evaluation of the mark II BALSS.

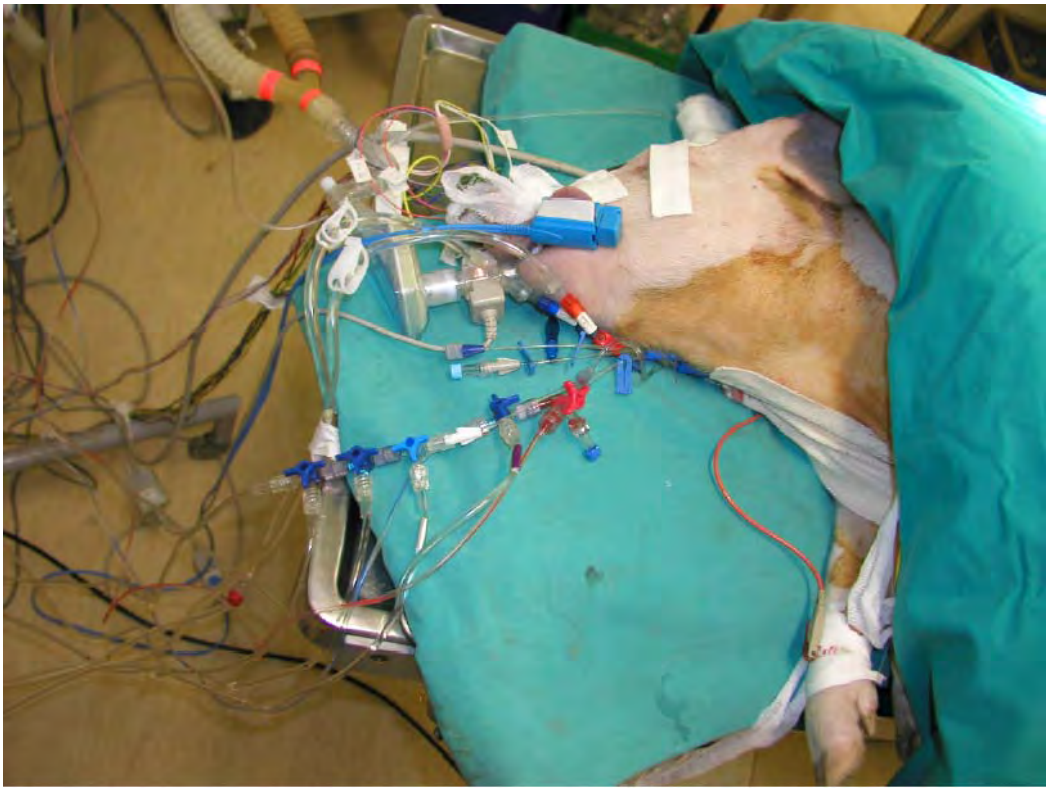

Figure 3.10 Animal undergoing a BALSS treatment. The blood lines configuration was complex.

These findings led to a comprehensive review of the required improvements. These may be summarized as follows:

- The use of more biocompatible materials in all parts of the system with emphasis on preventing coagulation effects.
- Bioreactor and oxygenator redesign.
- Extensive *in silico* system modeling for operational parameter optimization.
- A decrease in the overall size of the system to a bed-side unit.
- A decrease in the internal volume of the system.
- Attention to the ergonomics and aesthetics of the device.
- The operational simplification of the system so that a dialysis technician with minimal training would be able to operate it.
- The compilation of all standard operating procedures, i.e. a system manual.
- The use of, as far as possible, pre-sterilized standard dialysis equipment.
- GMP/FDA approval for all materials, suppliers and operating procedures.

Based on an examination of the history of institutions conducting similar work, these findings and/or requirements are generic for all BAL's. Following the implementation of the above, a mark III version will result, and its purpose will be to conduct additional animal experiments before proceeding to safety and efficacy trials in humans. It is expected that the mark III will be the final version in the design-optimization-redesign cycle that has been underway.

4. *IN VITRO* CELL BIOLOGY STUDIES

Overview

The following section presents three studies in which *in vitro*, biologically-based models of the BAL system have been developed. These models are designed to demonstrate or enable the metabolic functionality of the bioreactor component of the BAL and are *scaled-down* or simplified laboratory versions of the system. The studies are presented in a logically progressive order as determined by the methods or findings consecutively established.

The first of the studies details a sterile method for isolating large quantities of primary cells (hepatocytes), the metabolically active component of a BAL bioreactor of this type. Without cells in requisite quantities, such bioreactors would be insufficiently functional to fulfill the intended clinical need. Thus, such methods (or models) are a formal necessity for BAL systems. In this case the success of the method is evaluated in terms of impacts on cell functionality and the quantities isolated. Comparisons are made with previously published methods and the particular benefits of this one are highlighted.

The second study investigates the metabolic activity of cell-seeded bioreactors in a scaled-down recirculation system (model) of the BAL. This aims to demonstrate the metabolic function of the bioreactors as determined by their design, including the novel application of a perfluorocarbon (PFC) oxygen carrier, relative to controls. A variety of issues determining the relative success of these demonstrations (and thus of the model) are discussed. For example, design and methodological differences between studies, the effect of cell density on bioreactor metabolism and the impact of the oxygenating gas mix concentration when using PFC.

The third study similarly aims to demonstrate bioreactor metabolic functionality while employing PFC in a model version of the BAL, but differs in terms of improvements in the employed methods following knowledge evolution in the field. Specifically, the simultaneous use of radio-transparent small-scale bioreactors with and without PFC, seeding with co-cultures rather than hepatocyte-only monocultures, alteration of the gas mixes to more physiological O_2 levels and the novel use of positron emission tomography for studying primary cell bioreactor metabolism on the same time-scale as would occur in the treatment of a patient with a BAL.

Thereafter, thoughts and recommendations follow regarding alternate potential cell sources that may meet all the requirements of the global BAL device regulatory authorities. As was stated, a sterile large-scale cell source (model) is a formal necessity for the development of an effective BAL device. Examples mentioned include the development of genetically engineered swine and human chimeric animals. The problems surrounding presently existing transformed and primary cell sources are also discussed to provide additional clarity to the above arguments.

4.1 A large scale automated method for hepatocyte isolation: effects on proliferation in culture

Nieuwoudt MJ, Kreft E, Olivier B, Malfeld S, Vosloo J, Stegman F, Kunneke R, Van Wyk AJ, Van de Merwe SW.

Cell Transplantation 2005; 14(5): 291-299.

4.1.1 Introduction

Efficient, non labour-intensive and sterile methods for isolating large quantities of hepatocytes are desirable in the development of artificial liver support systems for the treatment of acute liver failure (ALF) [113]. There is some debate regarding exactly how many cells are required in order to adequately fulfill the needs of treating an adult human being in ALF [83]. However, considering cost and practicality, an increased hepatocyte yield in each procedure is a highly desirable end point. Porcine livers and hepatocytes are useful for establishing isolation methods since they have anatomical and physiological similarities to human livers and hepatocytes and have unlimited availability [114].

The purpose of this study was to evaluate a novel numerically high-yield hepatocyte isolation method as compared to the traditional centrifuge method. We investigated the impact of the isolation procedures on the hepatocytes for 7 days during subsequent in vitro culturing, using trypan blue counting, flow cytometry, phase-contrast microscopy, the lactate to pyruvate ratio, LD and AST leakage, albumin production and lidocaine clearance.

4.1.2 Materials and Methods

Media and Chemicals

All media and chemicals are as defined by Nieuwoudt *et al* [87] and presented in Appendix A.1.

Animals, liver preparation and perfusion

Non-fasted pathogen-free, female, white Landrace pigs of 20 kg average mass were prepared for surgery by intramuscular injection of 0.75mg/kg midazolam (Dormikum, Roche) and 10mg/kg of ketamine (Anaket, Centaur). After intubation, anesthesia was maintained by continuous infusion of propofol (Diprivan, Astra Zeneca) at 2.5 mg/kg/hr with ventilation using medical oxygen.

Briefly, a midline incision was made from xiphisternum to pubis. The portal vein was dissected out to the level of the pancreas and the small pancreatic branches were clamped and divided. Two ligatures were placed around the portal vein and between a small incision was made into which the bubble-end of a size 4.0 (5.6 O.D.) endotracheal (ET) tube was inserted to the level of the bifurcation of the vein. The ET tube was secured into place and gravitational perfusion commenced using 1L of supplemented clinical saline, followed by 1L of University of Wisconsin (UW) solution. After hepatectomy, the liver was placed in a sterile polypropylene dish and gently massaged until complete blanching could be observed, and then transported to the in vitro laboratory.

Upon arrival, the polypropylene dish was placed on a raised grill inside a stainless steel dish that was housed in a laminar flow cabinet. The ET tube was connected to a circulation loop (LS25 Masterflex tubing, Swiss Labs Johannesburg SA), which accessed the various buffers (figure 4.1.1). A Masterflex peristaltic pump was used to circulate the buffers through the liver. Initially 1L of the perfusion buffer containing EDTA was used (Buffer 1), followed by 2L without EDTA (Buffer 2) and then the waste outlet was clamped, enabling recirculation of the collagenase solution at 30 ml/min until the liver became jelly-like in consistency. After 5 recirculations the liver capsule would normally rupture, whereupon flow was terminated and the liver combed to a cellular mass using a broad-toothed steel comb. The same initial procedure was used in either isolation method; thus, the hepatocyte yield per liver was expected to be similar.

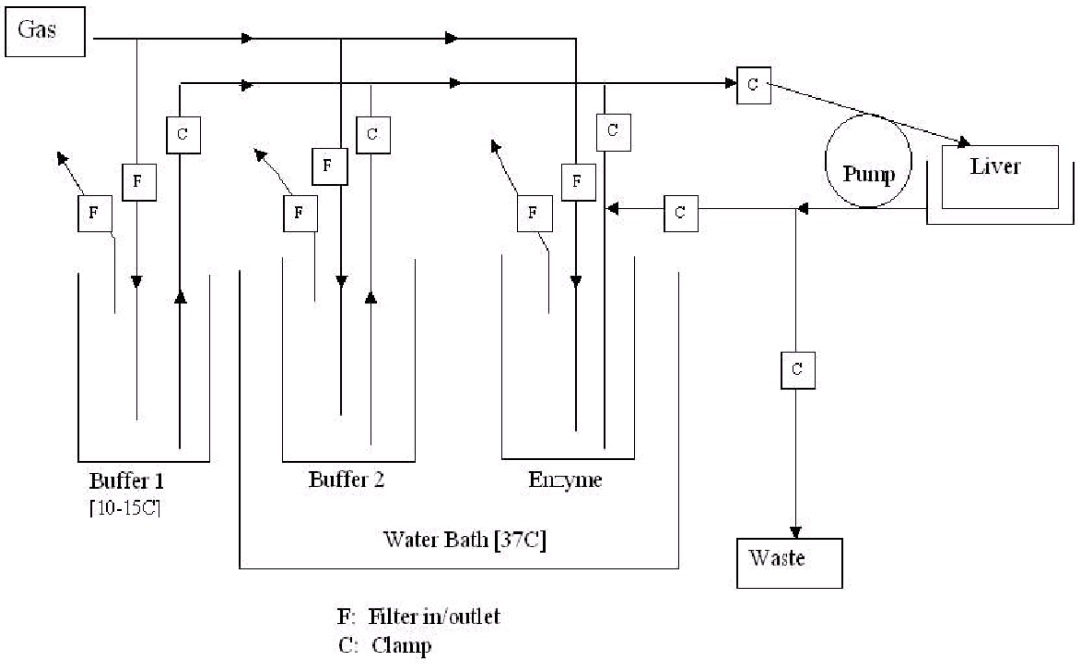

Figure 4.1.1 Schematic of Perfusion Apparatus

Hepatocyte isolation procedures

Using modified minimum essential culture medium (MEM) the cell suspension was washed from the dish into a 250µm nylon mesh that was folded into a filtration funnel. The funnel was mounted on a glass flask that was designed to enable either vacuum filtration or oxygenation (figure 4.1.2). To the vacuum inlet was connected a Sartonet pump, while the oxygenation inlet was clamped, allowing vacuum filtration of the suspension into the flask. During filtration the suspension in the filter was massaged using the round end of a 100ml sterile test tube, while MEM was added as needed. After the initial filtration, the filtrate was agitated then transferred to a 100-µm filter in the funnel of another flask and filtration again followed. Two different isolation procedures were then compared. In the first procedure all of the cell filtrate was decanted into 50 ml centrifuge tubes, normally 12, and a 'manual' isolation protocol was followed as is described below in A. In the second procedure, B, the Baylor Rapid Autologous Transfusion (BRAT) machine was employed in addition to two samples upon which the centrifuge method, A, was employed in parallel.

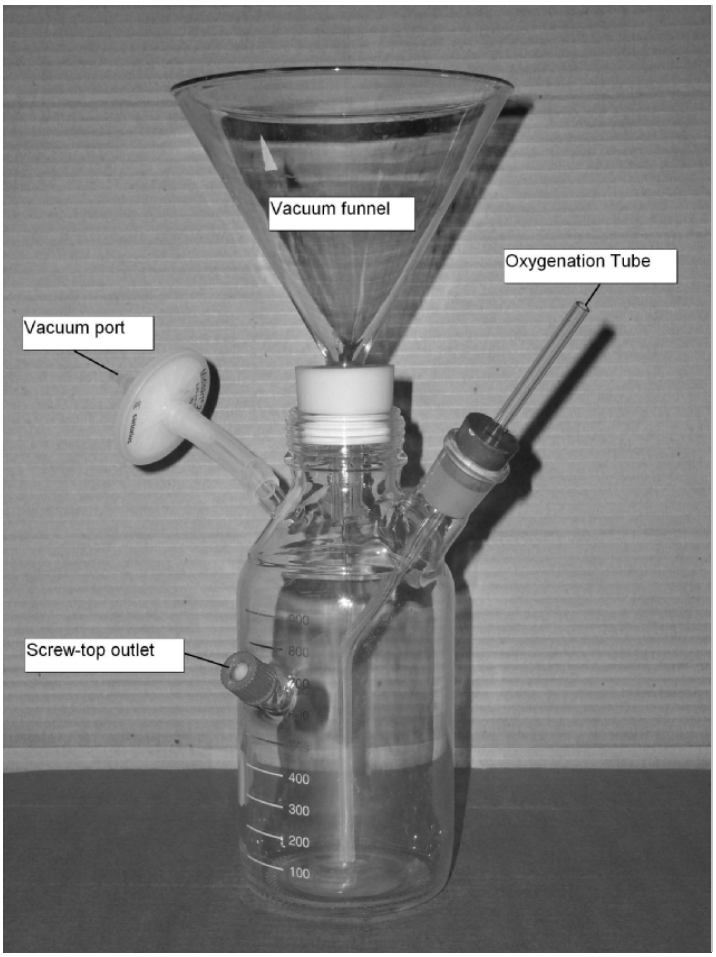

Figure 4.1.2 Oxygenation flask

Procedure A: 40 ml samples of the agitated cell filtrate were poured from the screw-top outlet of the oxygenation flask and used to perform a 'manual' hepatocyte isolation procedure, which in principle is the traditional method described by several authors [115-117]. Briefly, the suspension was centrifuged at 40G for 5 minutes at 4 ^{o}C, then washed with MEM and centrifuged 3 times at 30G for 4 minutes at 4 ^{o}C. Percoll:HBSS solution, as described in Appendix A1 (Percoll solution), was mixed with the cell pellet to achieve a concentration of 1.06 g/ml, that is, 11 ml of the Percoll solution with 20 ml of the cell-pellet suspension in each of the 50 ml tubes. Centrifugation followed for 10 minutes at 50G. Following separation of the hepatocytes from the non-parenchymal cells, 3 MEM washing steps followed for 4 minutes each at 30G. A hepatocyte-only suspension then remained.

Procedure B: While gently oxygenating the cellular filtrate in the oxygenation flask, containers with 2L of Wash buffer, 1L of supplemented MEM and 300 ml of Percoll solution were placed in the laminar flow cabinet. A BRAT machine was placed adjacent to the cabinet (figure 4.1.3]. In essence, the function of this machine is to transfer cells through sterile tubing by means of a peristaltic pump to a centrifuge, where centrifugation achieves cell separation based on density. The apparatus is composed, respectively, of a fixed volume transparent centrifuge bowl (either 250 ml or 165 ml) that clamps into the centrifuge housing, connected to a length of subdivided plastic tubing that is fitted into the peristaltic pump, allowing the alternate filling or emptying of the bowl in the directions of waste, washing or filling solutions (figures 4.1.4,5). The centrifuge bowl (figure 4.1.5) is designed to spin on a rotating ceramic joint, and is composed of an inner and outer wall allowing the cleaning and separation of cell fractions by allowing fluid entry into the bowl during centrifugation.

In these procedures the centrifuge speed was manually set to 50G, in the hardware, and used at that speed throughout the procedure. Using the filling line, cell suspension was sucked out of the oxygenation flask into the centrifuge bowl. Since the volume of the cell suspension was always larger than that of the bowl, to transfer the entire cell suspension required several fill cycles and these were done without stopping the centrifuge. To clean cell debris from the cell suspension after each 3-minute centrifugation cycle, wash buffer was passed down the washing line at the peristaltic pump’s lowest speed, 200 ml/min, until the waste line became clear. After each cycle, to provide the cells in the bowl with a physiologically preferable medium, the wash buffer in the bowl was displaced with oxygenated, supplemented MEM and the cells were allowed to resuspend by stopping the peristaltic pump.

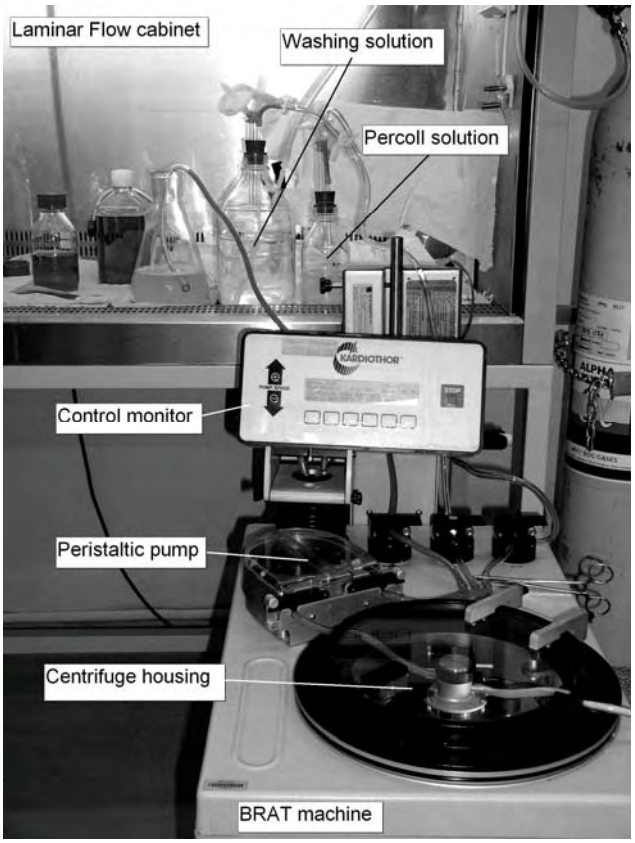

Figure 4.1.3 The BRAT machine

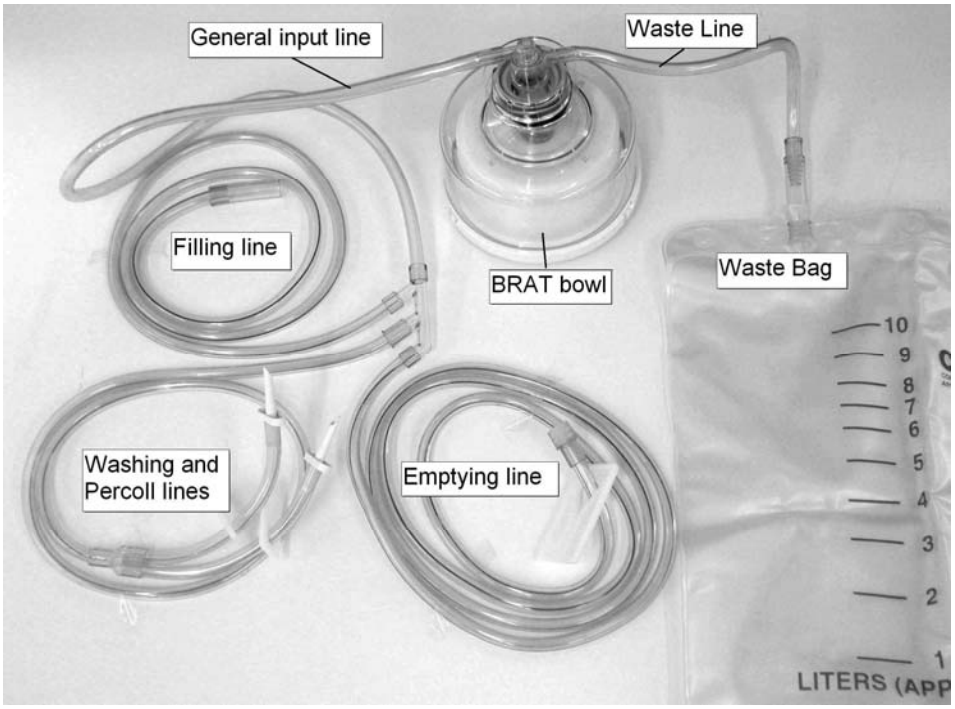

Figure 4.1.4 Disposable BRAT apparatus

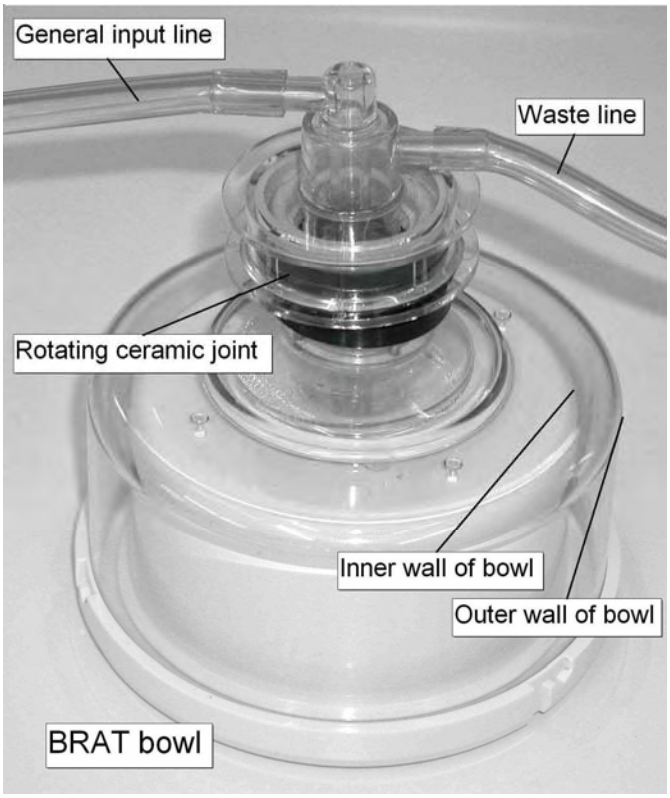

Figure 4.1.5 BRAT bowl

To create a density gradient between the non-parenchymal and hepatocyte cell fractions, the MEM remaining in the bowl after the last cycle was displaced with Percoll solution, followed by centrifugation at 50G for 10 minutes. The volume of the Percoll solution added depended on the volume of the bowl, 137.5 ml for a 250ml bowl and 90.8ml for a 165ml bowl. However, a great benefit of this method is that the addition of Percoll could be terminated during centrifugation, when it was observable that a clear separation had formed between the parenchymal and non-parenchymal cell fractions in the bowl. This is possible since the two cell fractions are different in colour (figures 4.1.6a, 6b) and it was confirmed by comparing the two fractions under light microscopy subsequently. The non-parenchymal cell supernatant was then removed from the hepatocyte fraction using 4 wash buffer-MEM cycles. A hepatocyte-only suspension then remained and it was pumped out of the bowl through the emptying-line into a second oxygenation flask. The final volume of the suspension was noted for hepatocyte yield and viability calculations.

Figure 4.1.6a BRAT Bowl prior to addition of Percoll. Separation has not yet occurred.

Figure 4.1.6b BRAT Bowl after addition of Percoll. Separation has occurred.

Hepatocyte culturing and evaluation methods

All employed methods are as described by Nieuwoudt et al [87] and also presented in Appendix A.2.

Briefly, cell suspensions from the Centrifuge and BRAT procedures were evaluated for viability and cell count. Flow cytometry was conducted on cells immediately after the procedures to determine the effects of oxygenation, and also on cells in 2D culture flasks to determine the impact on the cell cycle 3 and 7 days after seeding. The resulting DNA histograms indicated the relative cell cycle status of the suspension, that is, the proportion of DNA in the G0/G1, S or G2M phases. Daily media sampling evaluated hepatocyte viability by means of LD and AST leakage and to examine the state of cellular oxidation and aerobic metabolism by means of the lactate to pyruvate ratio. On day 2 galactose elimination, on day 3 urea production, on day 4 lidocaine clearance and on day 5 albumin production was measured. Digital micrographs, were taken at day 3 and day 7 after seeding to examine if cell populations were proliferating normally and to confirm the sterility of the procedures.

All values are presented as the mean $\pm$ the standard deviation. Where appropriate P values ($P<0.05$) were calculated using the 2-tailed Mann-Whitney t-test to indicate significant differences.

4.1.3 Results

Isolation procedures

Table 4.1.1 presents cell yield and viabilities produced by the Centrifuge and BRAT procedures. In agreement with Morsiani *et al* (1995) [118], our finding was that two to three people are able to perform the centrifuge procedure in 40-45 minutes. With the BRAT machine one person could perform the procedure in 20-30 minutes. As was expected, the hepatocyte yield per liver was comparable in that the same initial procedure was used. However, differences in hepatocyte viability were apparent: With the centrifuge procedure, viability was 92.5 % $\pm$ 1.29, while with the BRAT procedure, viability was 95.91 % $\pm$ 2.95. The deceased viability of cells from the

centrifuge method was possibly due to cell damage caused by increased contact with plastic centrifuge vials, and an increase in the duration of the isolation procedure. The success of an isolation procedure was determined by media aliquots testing pathogen free.

Table 4.1.1 Yield and viability of hepatocytes per liver, following isolation using Centrifuge and BRAT technology

Mass of pigs	Sample Size	Hepatocyte Yield (Centrifuge)	Hepatocyte Yield (BRAT)	Cell viability % (Centrifuge)	Cell viability % (BRAT)
Mean = 20.1 kg	Centrifuge = 6	Mean = 5.2 $\pm$ 2.1 x 10^9	For **250ml bowls** Mean = 7.3 $\pm$ 5.37 x 10^9	Mean = 92.5 $\pm$ 1.29	Mean = 95.91 $\pm$ 2.95
	BRAT 250 ml = 8 165 ml = 6		For **165ml bowls** Mean = 2.8 $\pm$ 1.0 x 10^9		

Note: *Values are represented as means $\pm$ standard deviation.

The vacuum filtration/oxygenation flask (figure 4.1.2) was found to be very efficient in aiding cell filtration. However, oxygenation prior to and during the BRAT procedures was found to facilitate hepatocyte aggregation, in so doing, hindering accurate cell counting. This observation is in agreement with the findings of previous authors [119-121]. Since it is difficult to accurately count cells when there are clumps present, cell counts are represented in table 4.1.1 as counts excluding aggregates. Thus, the values are minimal amounts relative to those actually present. To decrease aggregation, either manual or magnetic stirring was employed and this was partially successful.

Microscopy

Daily microscopic observation of hepatocyte cultures revealed no discernable differences between cells that originated in either procedure. Both procedures resulted in cytoplasmic vacuolization and granularities that steadily decreased and normally disappeared by the fourth day after seeding. It was observable that all viable cells had attached prior to the first change of culture medium 12 hours after the isolation procedures and no cell debris was visible in the discarded medium every 24 hours

thereafter. During the first 4-5 days the attached hepatocytes grew cytoplasmic extensions and cell spreading was the predominant process. By the 7-th day the culture was usually nearing confluence, although the Flow cytometry results indicated that the cells were still dividing (figure 4.1.8). Digital micrographs taken at day 3 indicated that vacuoles were present in addition to cytoplasmic extensions. By day 7, all granularities and vacuolization had disappeared.

Flow Cytometry.

A comparison of hepatocyte DNA profiles following oxygenation or not during the BRAT procedure (figure 4.1.7) revealed that the G_0/G_1 phase was dramatically increased when oxygenation had not taken place, 74.18%, as opposed to when it had, 40.04%. In addition, the S and G_2M phases were increased when oxygenation had occurred as opposed to when it had not, that is, BRAT + O_2, S = 46.15% and G_2M = 13.82%, while BRAT – O_2, S = 22.36% and G_2M = 3.46%. This result suggests that lack of oxygenation caused G_0/G_1 cell cycle arrest, whilst oxygenation promoted cell cycle progression. However, the benefit must be weighed against the fact that hepatocyte aggregation is also facilitated by oxygenation. Nonetheless, this was an interesting observation that will benefit from further study.

After 7 days following the BRAT procedure 37.59% of the DNA was in the S phase, as opposed to 32.02% at 3 days, while with the Manual procedure at 7 days, 34.57% of the DNA was in the S phase, as opposed to 27.62% at 3 days. Two tailed, Mann-Whitney tests ($P<0.05$) revealed no significant differences when the G_0G_1, S and G_2M phases at Day 3 were compared in the two procedures, while the same was found at Day 7. Additionally, no statistically significant differences were observed when Day 3 was compared to Day 7 (figure 4.1.8). This indicated that cell harvesting using the BRAT system had no negative impacts on cell replication, relative to the Manual method.

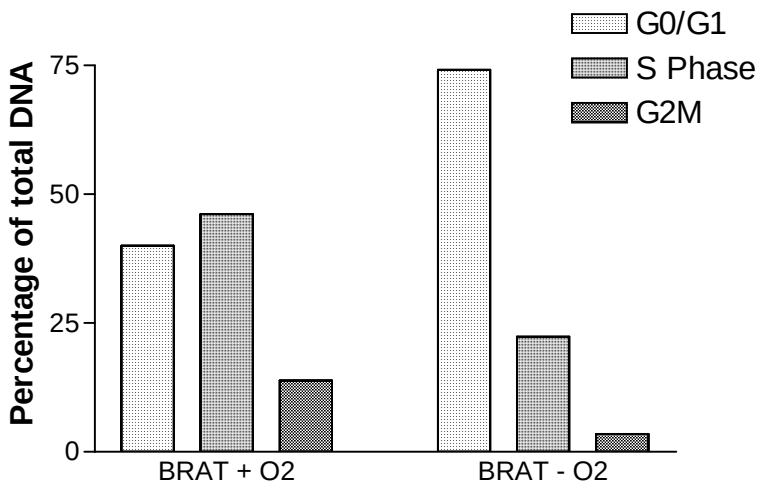

Figure 4.1.7 Flow Cytometry: DNA profile after BRAT procedure with and without oxygenation and prior to culturing

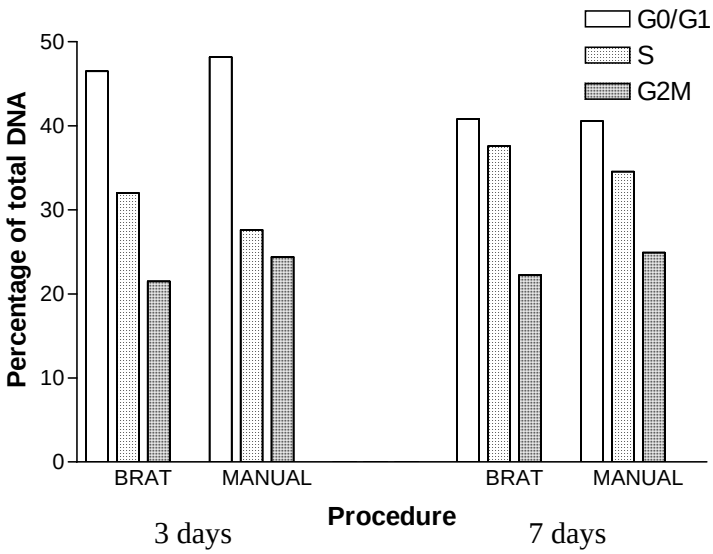

Figure 4.1.8 Flow Cytometry: DNA profile after 3 and 7 days culturing

Biochemical Analyses

In agreement with the microscopic and flow cytometry findings, no significant differences could be determined between the Centrifuge and BRAT methods. The trend was for the lactate to pyruvate ratio to decline towards day 3 after isolation and

then to stabilize for the remainder of the isolation period. The decline in the ratio was due almost entirely to a change in the lactate concentration. LD and AST similarly decreased and stabilized after 3-4 days in culture, indicating a progressive stabilization of the culture towards Day 7. Lidocaine clearance was measurable and found to be a mean of 7.37 ± 4.7 µg/hr/Million cells in experiments conducted at Day 4 after isolation. This result indicates that the cytochrome P450 system was active at that stage. At Day 5, albumin production could be measured and averaged 14.76 ± 0.61 µg/hr/Million cells.

4.1.4 Discussion

The development of effective cell-based bio-artificial liver assist devices relies on the isolation of large quantities of hepatocytes. In this study we describe a largely automated and sterile hepatocyte isolation procedure wherein high cell yield and viability were achieved following surgical removal of the liver. Attention to the composition and utilization of each perfusion step undoubtedly improved cell survival and viability. The centrifuge based isolation method using the modified Seglen protocol is well described [113,115-117]. However, this method is time consuming, which may negatively impact hepatocyte viability. In addition, it is limiting in terms of hepatocyte isolation from large animals since multiple handling steps may decrease viability, as was observable in the results, while increasing the likelihood of bacterial contamination. It should also be noted that while establishing *in vitro* laboratory isolation procedures, repetition is required in order to develop skills. Since only the results of successful experiments are presented, the development of these skills is not apparent. Thus, using a procedure that minimizes potentially un-sterile handling is of obvious benefit.

By using the BRAT machine, isolated cells could be handled in a manner that was guaranteed to be sterile. The historical application of this device was in the cleaning of whole blood products. An advantage of this method is that it is possible to control the addition of the Percoll solution during centrifugation, based on observing the separation of hepatocytes from non-parenchymal cells. Morsiani *et al* (1995)[118], have previously described a high yield isolation procedure using a COBE 2991 Cell Processor as opposed to the BRAT machine. A benefit of the BRAT machine is that,

similar to the COBE 2991, the disposable tubing and centrifugation apparatus is sealed and sterile. The differences between the machines are, firstly, the COBE 2991 uses a flexible donut-shaped bag, while the BRAT uses an inflexible fixed volume bowl, and secondly, while the former has added functionality, the latter is considerably less expensive. In addition, prior to the centrifugation steps we used a novel filtration/oxygenation flask as opposed to an orbitally shaken filtration apparatus: We found vacuum filtration of the post-enzymatic cell suspensions to be very efficient. Advantages of both the oxygenation/filtration flask and the BRAT procedure are that it is possible to oxygenate the cell-suspensions and media during the procedure. The results of flow cytometry suggested that oxygenation facilitated cell division, indicating that it was beneficial to proliferation.

As was to be expected, a comparison of cell yields between the two procedures revealed that they were comparable. The benefits of the application of the BRAT machine lie in convenience and speed, the ability to oxygenate during the procedure and guaranteed sterility. Sterility is of critical importance if the bioreactor is to be employed in a clinical application. The use of the BRAT machine did result in high cell yields (7.3×10^9 for 250ml bowls) and viabilities (95.91%) when compared with previous studies (83,113,115,116,118]. Flow cytometry confirmed that the hepatocytes were progressively recovering after the isolation procedures and tended toward proliferation between Days 3 and 7. No significant difference could be detected between cells from the Centrifuge and BRAT procedures and these observations were confirmed by microscopic and biochemical studies. Our general observation was that isolated hepatocytes only regained their functional polarity after 3-4 days in a culture configuration excluding an extracellular matrix and this appears to be in agreement with the findings of previous studies [113,122-124]. This observation obviously has bearing on the timing of the use of prim**a**ry cells in bioartificial liver devices or in *in vitro* drug testing.

In conclusion, we have established a large-scale, automated, sterile and reproducible procedure whereby large quantities of viable porcine hepatocytes may be isolated, using technology normally available in large-centers.

4.2 A study to determine hepatocyte function in the UP-CSIR radial-flow bioreactor using a perfluorocarbon oxygen carrier

Nieuwoudt M, Moolman S, Van Wyk AJ, Kreft E, Olivier B, Laurens JB, Stegman F, Vosloo J, Bond R, van der Merwe SW.

J Artif Org 2005; 29(11): 915-918.

4.2.1 Introduction

The aim of this study was to determine the effect of bioreactor design and the inclusion of a circulating oxygen carrier on the *in vitro* metabolic activity of hepatocytes in a simplified BALSS circuit. The UP-CSIR BALSS [10,94] incorporates a direct hepatocyte-plasma contact, radial-flow bioreactor with a polyurethane foam (PUF) matrix. The open-cell pore size of the PUF matrix is on average 500 µm, each of which may incorporate an aggregate with 15 000 or more hepatocytes. The internal volume of the PUF matrix is 250 ml, thus, a total of 6×10^{10} cells or 300 g may be seeded, accounting for 20 % of a normal liver's hepatocyte mass. This should be sufficient to maintain the estimated minimal requirements for liver support [83,84].

An ongoing concern amongst investigators is the presence of domains of low O_2 tension and hypometabolism in their bioreactors [83,107]. To overcome potential mass transfer limited domains within the UP-CSI bioreactor a perfluorocarbon (PFC) oxygen carrier that is incorporated in the bioreactor sub-circulation has been developed. Perfluoro-octyl bromide (PFOB) is a synthetic perfluorinated aliphatic compound with high gas solubility. It is chemically and biologically inert and tends to be both hydrophobic and lipophobic. Thus, it requires emulsification (normally with lecithin) prior to use in a recirculating aqueous environment [10,94].

This study investigates, using established indicators of liver function, firstly, the metabolic activity of hepatocytes seeded into the PUF matrix of the radial-flow

bioreactor, and secondly, the performance of the bioreactor is compared, with and without PFC, to monocultures.

4.2.2 Materials and methods

All media and chemicals used in the cell culturing, transport and dissolution of the liver are as described by Nieuwoudt *et al* (2005)[87]. Perfluorocarbon-lecithin emulsions were prepared according to the method of Moolman *et al* (2004) [10,94]. The emulsions were mixed with double concentrated MEM and sterile deionised water, to achieve a 20% v/v PFC emulsion-MEM mixture. The mixture was pH adjusted and used as a culturing medium. For liver perfusion and hepatocyte isolation the method of Nieuwoudt *et al* (2005)[87] was used throughout.

Cell count and viability was assessed with Trypan-blue. The suspension was then seeded into a sealed recirculating system in an incubator, representing a simplified *dynamic* model of the BALSS. Briefly, each system (figure 3.2.1) was composed of LS 25 Masterflex tubing that connected a 500 ml glass reservoir, a 100 ml internal volume bioreactor, with a sampling port, and the reservoir medium was oxygenated using an aquarium bubbler. All was housed in a non-gas incubator at 37 ^{o}C (Scientific 2000, Instrulab, South Africa). To facilitate homogenous seeding throughout the matrix, the bioreactor was designed for even flow using computational fluid dynamics (CFD), see section 3 above. A total of eight, 7-day long metabolic trials were conducted on the *dynamic* and *static* systems. Five studies employed ordinary MEM, (PFC(-)), while 3 used the supplemented PFC-MEM emulsion (PFC(+)).

Cell culturing and metabolic evaluation

All methods are as defined by Nieuwoudt et al [88] and presented in Appendix A3.

Briefly, daily samples were taken for LD, AST, glucose, lactate and pyruvate. Blood gas samples for pH, pO_2, pCO_2 were taken and the oxygen uptake rate (OUR) was calculated.

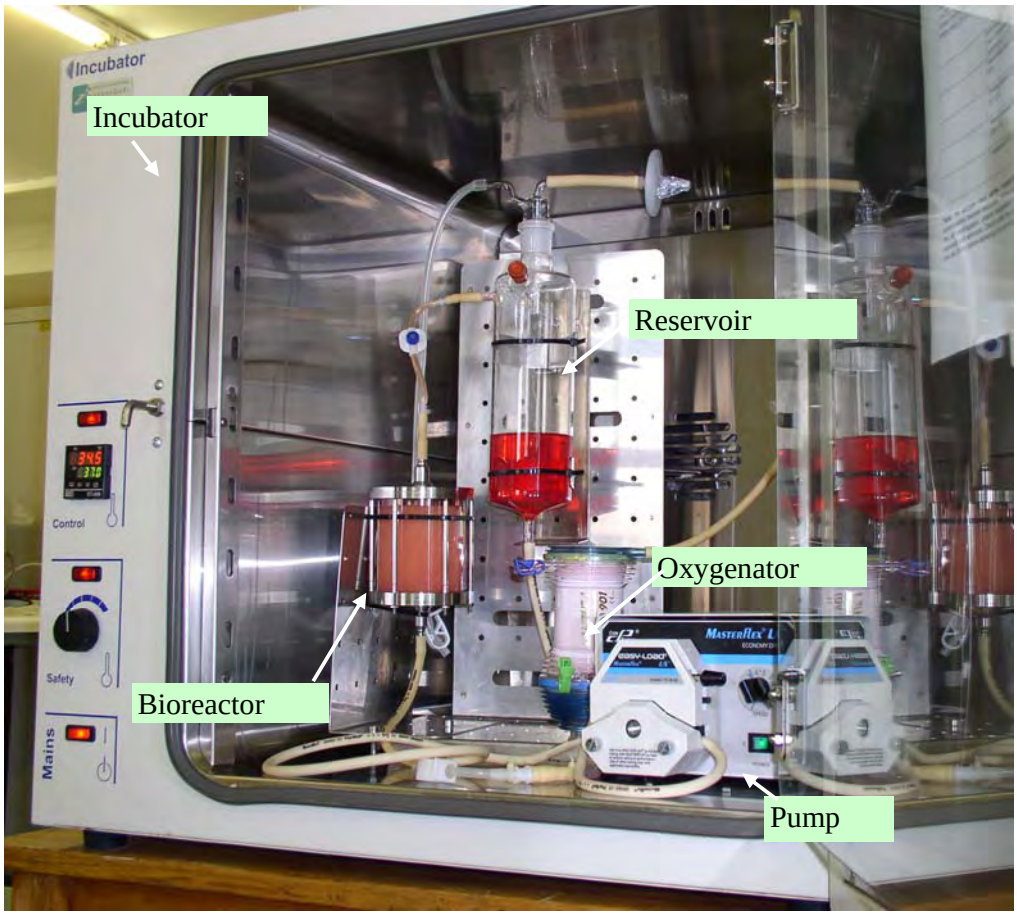

Figure 4.2.1 Simplified *in vitro* dynamic model of the BALSS

Metabolic clearance/production studies were performed in both dynamic and static configurations: on day 2 D(+)galactose elimination, on day 3 ammonia detoxification and urea synthesis, on day 4 lidocaine clearance and on day 5 albumin production. Upon termination on day 7, imaging studies involved either scanning electron microscopy (SEM), to investigate the presence of cells in the foam, or isotopic scanning to examine the seeded-distribution of active hepatocytes in the foam. The latter was performed following the injection of a 300 µCi dose of ^{99m}Tc-labeled-DISIDA N-(2,6-diisopropylacetanilide)-imino-diacetate into the circulating medium. DISIDA is only metabolized by active hepatocytes. After draining and flushing the circuit the cell aggregation foam was removed and cut into radial sections at the inlet, central and outlet portions along the bioreactor axis. These sections scanned for 10 minutes using a gamma camera. All values are presented as the mean $\pm$ standard deviation. Statistical significance was measured using Student's t test.

4.2.3 Results

Cell counts ranged between 6 x10^9 and 2 x10^{10} for all studies, with viability 95.91 % ±3.0%. Daily sampling: pO_2, pCO_2 and pH values averaged 286.5 ±25.5 mmHg, 30.0 ±1.4 mmHg and 7.45 ±0.03 respectively in both PFC(+) and PFC(-) cultures. Within the detection ability of the electrodes no significant drop in pO_2 was measurable when PFC was present. Thus, daily OUR determinations were only possible in PFC(-) cultures, average: 17.8 ±4.0 nmol/hr/10^6 cells. The gas carrying ability of PFC is far greater than that of MEM or plasma (figures 3.2.5,6). Since the majority of all other measurements of the PFC(-) and PFC(+) cultures were similar, OUR was assumed to be equivalent. Lactate values were similar in both cultures, while pyruvate values were slightly decreased in the PFC(+) cultures. Since an increase in the lactate to pyruvate ratio is generally due to an increase in anaerobic metabolism, it is possible that the difference may have been due to PFC interference in pyruvate measurement, rather than by an anaerobic state (although PFC was removed by centrifugation in all determinations). AST and LD concentrations decreased exponentially in the first 3 days of culturing, with initial levels of 217.9 ±60.7 IU/L and 98.4 ±50.8 IU/L respectively, descending to 23.0 ±19.5 IU/L and 48.2 ±22.4 IU/L by day 5. This would serve to indicate the progressive stabilization of the cell culture.

Metabolic clearance/production studies: D(+)galactose elimination on day 2 revealed that PFC(+) and PFC(-) cultures cleared similar amounts, 1.6 ±0.1 and 1.7 ±0.1 µg galactose/hr/10^6cells respectively. Monocultures cleared 0.35 ±0.2 µg/hr/10^6cells. Urea production on day 3 revealed that PFC(+) cultures produced 42.34 ±14.5 µg urea/hr/10^9cells, PFC(-) cultures produced 148.93 ±20.1 µg/hr/10^9cells and flasks produced 20.2 ±8.2 µg/hr/10^9cells. The differences in production may reflect interference with the measurement of urea in PFC(+) cultures. The clearance of ammonia was similar in the 3-D cultures; 8.2 ±3.0 µg ammonia/hr/10^9cells for PFC(+) and 8.6 ±4.4 µg/hr/10^9cells for PFC(-). The clearance of lidocaine on day 4 was 1.6 ±0.1 µg lidocaine/hr/10^6cells for PFC(-) cultures. PFC(+) cultures cleared lidocaine at 2.8 ±0.3 µg/hr/10^6cells which was significantly better than PFC(-) cultures ($p<0.05$). Monocultures cleared 0.6 ±0.4 µg/hr/10^6cells. The production of albumin on day 5 was similar in the 3-D cultures, PFC (-) cultures produced 21.9 ±0.9 µg albumin/hr/10^6cells, while PFC(+) cultures produced 21.9 ±0.5 µg/hr/10^6cells.

Upon termination on day 7, SEM confirmed the presence of hepatocyte aggregations in the open-cell matrix (figures 4.2.2,3). Isotopic imaging demonstrated that the distribution of actively functional hepatocytes in the matrix was determined by the flow of the circulating medium through the foam (figure 4.2.4). While there were irregularities in the foam it was taken that CFD had indeed been useful for bioreactor design.

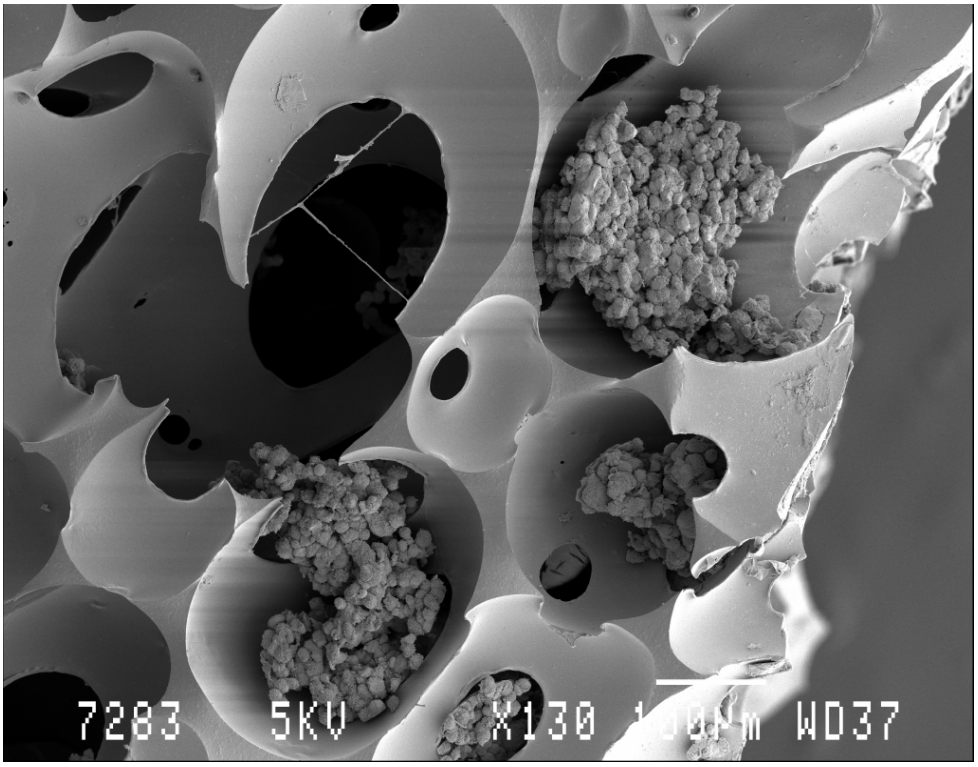

Figure 4.2.2 SEM image of open-cell PUF cell adhesion matrix with cell aggregations. Magnification: 250x.

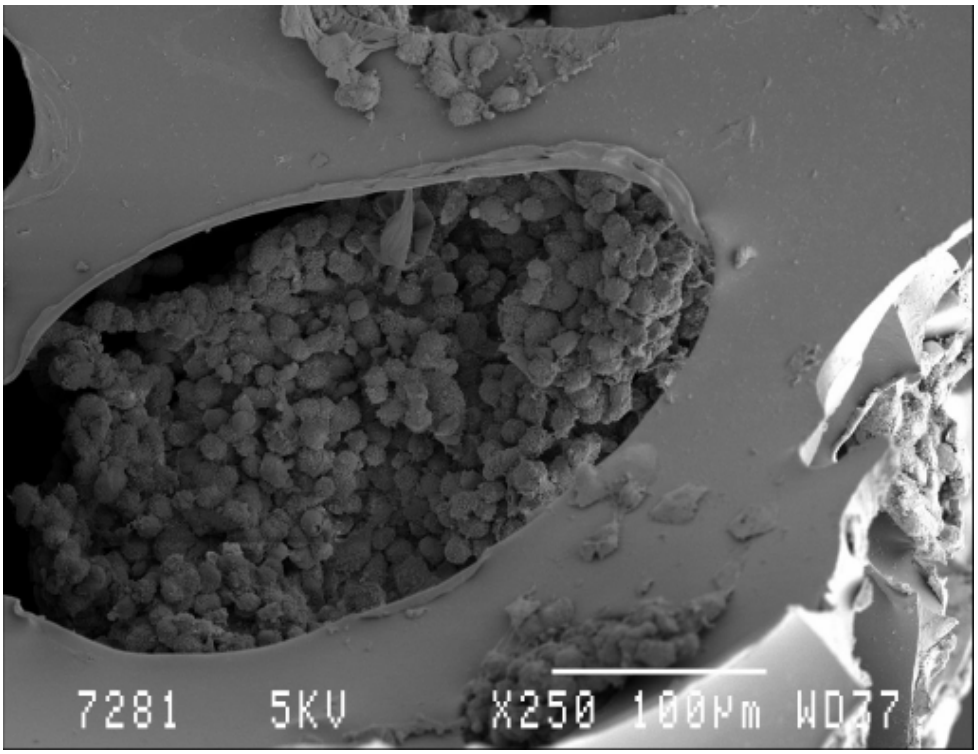

Figure 4.2.3 SEM Image of a single large cell aggregate in the PUF adhesion matrix. Magnification 130 x.

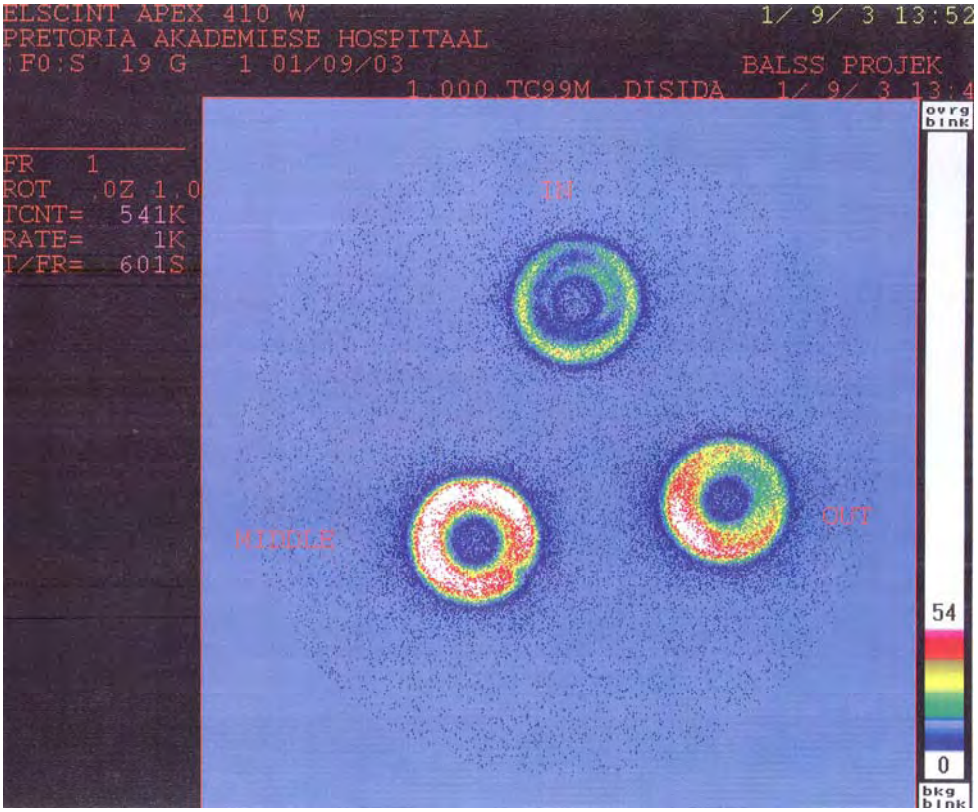

Figure 4.2.4 ^{99m}Tc-DISIDA isotope scan of PUF cell aggregation matrix. The radial-flow foam was sectioned into inlet, middle and outlet portions along the axis of the

bioreactor. White portions indicate large quantities of radio-labeled, actively functioning hepatocytes. Regions that appeared to be inhomogenously seeded were found to be due to irregularities (bubbles) in the foam and to inaccurately sliced sections. The cells aggregated according to the flow of the medium through the matrix.

4.2.4 Discussion

The interpretation and evaluation of the *in vitro* performance of an hepatocyte bioreactor is complicated by especially two factors: Firstly, to quote Hoekstra *et al* (2002) [125], "many researchers do not quantify BAL or cell functions as an absolute figure related to cell quantities functioning during a defined period", and secondly; when figures are available, very large divergences (in the values for various liver functions) are apparent (table 3.2.1). Whether this divergence is due to innate biological variation as a result of differences in the culture configuration, or due to differences in the analysis methods, remains to be answered. Until this is satisfactorily done, the complete confirmation of the metabolic efficacy of bioreactors for BALSS devices may remain impossible.

In this study observations suggested that the OUR of the UP-CSIR bioreactor tends to a limit determined by cell density and the pO_2 of the circulating medium. However, the usefulness of OUR as an indicator of the metabolic state of hepatocytes in a bioreactor is balanced by the challenge of its accurate determination in 3-D cultures. The assumption that the OUR measured for hepatocytes grown in monolayers is constant in 3-D culture configurations at high cell densities may be incorrect [98,107]. Previous investigations of the OUR of a variety of types of hepatocytes have revealed that as cell density and the pO_2 of a perfusing culture medium increases, OUR per unit cell mass decreases [126]. It has been proposed that the release of humoral factors controlling cell-cell communication may enable the cells to manage "crowding" by temporarily suppressing oxidative metabolism [127]. Perhaps the decrease in OUR with increasing cell density follows an allometric relationship such as that first described by Kleiber [128,129]? This relationship represents an evolutionary strategy whereby OUR is diminished with increasing body mass. There is utility in observing such a relationship: OUR may potentially be scaled to large cell numbers, enabling real-time functional quantification of a bioreactor.

Table 4.2.1 Variation in results for porcine hepatocytes

Author/s	Bioreactor Configuration	Clearance/ Production:	Reported as:	Converted to:
Flendrig *et al* [104]	Hollow-fiber with mesh	Urea	1.8±0.2 µg/hr/10^6 cells	1.8±0.2 µg/hr/10^6 cells
Abrahamse *etal* [105]	Hollow-fiber	Urea	5.5±0.4 µg/hr/10^9cells	$5.5x10^{-3}$±$4x10^{-4}$ µg/hr/10^6 cells
de Bartolo *et al* [100]	Flat membrane	Urea	25±5 ng/hr/cell	$25x10^3$±$5x10^3$ µg/hr/10^6 cells
Bader *et al* [101]	Flat membrane	Urea	80±10 pg/hr/cell	80±10 µg/hr/10^6 cells
Gerlach [106]	Multi axial hollow fiber	Urea	38.3 mg/hr/10^{10}cells	3.83 µg/hr/10^6 cells
Yanagi *et al* [103]	Microcarrier packed bed	Urea	$4.4x10^{-13}$±$1.5x10^{-13}$mol/hr/cell	26.4±9.0 µg/hr/10^6 cells
	Monoculture		$7x10^{-13}$±$2x10^{-13}$mol/hr/cell	42.0±13.8 µg/hr/10^6 cells
Nieuwoudt *et al*	**PUF matrix: -PFC**	**Urea**		**0.15±0.02 µg/hr/10^6 cells**
	+PFC			**0.04±0.01 µg/hr/10^6 cells**
	Monoculture			**0.02±0.01 µg/hr/10^6cells**
Abrahamse *etal* [105]	Hollow-fiber	Ammonia	25±10 µmol/hr/10^9cells	25±10 µmol/hr/10^9cells
de Bartolo *et al* [100]	Flat membrane	Ammonia	56±10 pg/hr/cell	$3.3x10^3$±$0.6x10^3$µmol/hr/10^9cells
Bader *et al* [101]	Flat membrane	Ammonia	14±0.5 pg/hr/cell	820±30 µmol/hr/10^9cells
Gerlach [106]	Multi axial hollow fiber	Ammonia	605 µmol/hr/10^{10}cells	60.5 µmol/hr/10^9cells
Nieuwoudt *et al*	**PUF matrix: -PFC**	**Ammonia**		**8.6±4.4 µmol/hr/10^9cells**
	+PFC			**8.2±3.0 µmol/hr/10^9cells**
Morsiani *et al* [102]	Radial flow mesh	Albumin	5.9±0.7 ng/24hr/10^6cells	$2.46x10^{-4}$±$2.92x10^{-5}$ µg/hr/10^6 cells
Gerlach [106]	Multi axial hollow fiber	Albumin	5.33 mg/hr/10^{10}cells	0.533 µg/hr/10^6 cells
de Bartolo *et al* [100]	Flat membrane	Albumin	1.4±0.2 pg/hr/cell	1.4±0.2 µg/hr/10^6 cells
Nieuwoudt *et al*	**PUF matrix: -PFC**	**Albumin**		**21.9±0.9 µg/hr/10^6 cells**
	+PFC			**21.0±0.5 µg/hr/10^6 cells**
Balis *et al* [130]	Monoculture	OUR	0.6±0.15 nmol/sec/10^6cells	$2.16x10^3$±$0.54x10^3$ nmol/hr/10^6cells
Morsiani *et al* [102]	Radial flow mesh	OUR	6±1 nmol/hr/10^6cells	6±1nmol/hr/10^6cells
Morsiani *et al* [102]	*Calculated from human liver	OUR	15 nmol/min/10^6cells	900 nmol/hr/10^6cells
Nieuwoudt *et al*	**PUF matrix: -PFC**	**OUR**		**17.8±4.7 nmol/hr/10^6cells**

Note: The above values are a selection of literature results and not intended as a summary or review. Certain values have been read off graphs and are thus approximate.* Value from *in vivo* human liver for comparative purposes.

In this study ammonia clearance, albumin production and galactose elimination were similar in the dynamic cultures and higher than in monocultures. Increased metabolic activity was therefore observed in dynamic compared to monolayer cultures. Urea production was increased in PFC(-) cultures relative to PFC(+) cultures, while lidocaine clearance was significantly higher in PFC(+) cultures. The increased lidocaine clearance in PFC(+) cultures may indicate that lidocaine metabolism (cytochrome P450) is more dependent on oxidative metabolism and higher O_2 tension than the other metabolic variables studied. Several previous investigators using PFCs in production bioreactors have noted significantly improved metabolic functions [131-133]. It was observed that similar results were obtained for PFC(+) and PFC(-) cultures for most variables studied. It should be borne in mind that there is 0.5 times more CO_2 and 4.5 times more O_2 present in a 20% v/v PFC emulsion relative to normal medium (figure 4.2.5). Thus, the benefit of adding PFC may only be apparent when high cell densities are employed in a bioreactor. If the O_2 carrying ability of plasma is taken to be approximately equal to that of medium it is clear that the emulsion would be far better at preventing hypoxia in high density, stressed cellular environments.

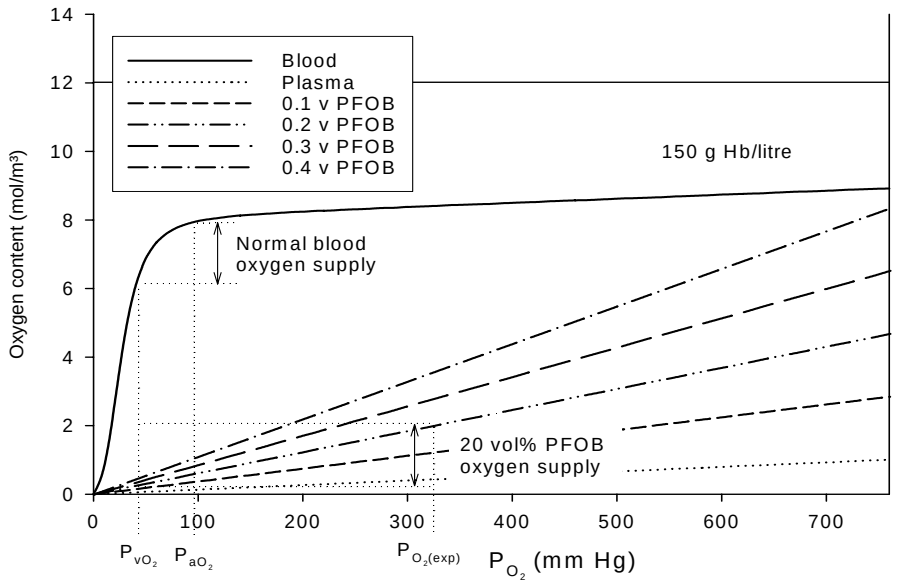

Figure 4.2.5 Increased PFOB volume fraction increases the oxygen carrying capacity of the emulsions. The oxygen solubility in the emulsions follows a linear relationship with partial oxygen pressure. The experimentally measured partial oxygen pressure in the UP-CSIR BALSS is indicated on the graph, showing similar potential oxygen delivery compared to blood (if exposed to normal venous partial oxygen pressure).

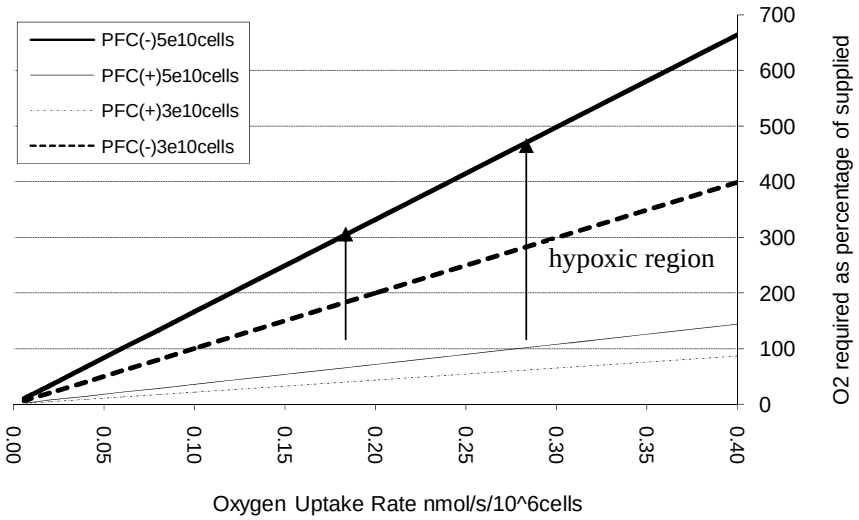

Figure 4.2.6 Simulation of bioreactor O_2 requirements. PFC emulsions provide a significant advantage to high cell densities in a BALSS. The cell densities in this study were insufficient to challenge the O_2 supplied to the bioreactor. The flow rate was 300 ml/min.

Additionally, calculations of bioreactor O_2 requirements, Moolman *et al* (2004) [10,94], indicated that with increasing OUR the demand relative to the supply of O_2 becomes severely limiting when PFC is not used (figure 4.2.6). It was also revealed that the present experiments were conducted at cell densities that were insufficient to challenge the O_2 supply of the bioreactor. This may explain why the metabolic performance was similar.

In conclusion, in this study it was observed that hepatocyte aggregation occurred in the PUF matrix of the bioreactor and metabolic functions were improved relative to flask cultures. The addition of PFC to the medium improved some hepatocyte functions such as lidocaine clearance and no adverse effects were otherwise detectable. Calculations indicated that the cell densities employed were insufficient to challenge the O_2 supplied to the bioreactor and this may explain the similarity in the results. The true benefits of PFCs are more likely to be found in preventing hypoxia when very high cell densities are employed in a bioreactor.

4.3 Imaging glucose metabolism in perfluorocarbon-perfused hepatocyte-stellate co-culture bioreactors using positron emission tomography

Nieuwoudt M, Wiggett S, Malfeld S, van der Merwe SW.

Journal of Artificial Organs, 2009;12:247-57.

4.3.1 Introduction

In vivo hepatic functional zonation, from periportal to perivenous along the sinusoid, is determined by gradients of oxygen (O_2), hormones, nutrients/metabolites, extracellular matrix components, and the non-parenchymal cell distribution [2,134]. This zonal heterogeneity includes energy, carbohydrate, lipid, nitrogen, bile and xenobiotic metabolism and enables the liver to function as a 'glucostat', i.e. to maintain stable blood glucose levels during feeding or fasting states [135-138]. The periportal zone functions optimally at blood pO_2 levels of 60-70 mmHg (13 % v/v), while the perivenous does so at 25-35 mmHg (4 % v/v) [2].

A variety of *in vitro* studies have shown that hepatocytes cultured in 2D and 3D configurations demonstrate metabolic functionality that is dependent on the pO_2 of the oxygenating gas mix [109,120,121,139-143]. In general, physiological O_2 gas mixes lead to gluconeogenesis, while hypoxic gas mixes lead to glycolysis. A glycolytic bioreactor metabolism is not ideal in that a similar pre-existing clinical condition may be exacerbated in treating an acute liver failure (ALF) patient. Maintaining a stable hepatocyte phenotype is also dependent on interactions with non-parenchymal cell populations, which constitute 30-35 % of the liver [86,134,144-147]. Recapturing hepatic functionality in bioreactors designed for bioartificial liver (BAL) devices requires particular attention to these facts.

Some BAL designs perfuse only plasma to avoid the coagulatory and immunological reactions associated with whole-blood exposure to extracorporeal materials. However,

under normal conditions approximately 98 % of the O_2 in whole-blood is carried by haemoglobin (Hb). Thus, atmospheric gas concentrations, metabolically active hepatocytes in plasma-only BALs are likely to become hypoxic and consequently exhibit glycolytic metabolism. Synthetic perfluorocarbons (PFC) are exceptionally inert and have excellent O_2 carrying properties. Their inclusion in the circulating medium or plasma therefore represents an attractive hemoglobin replacement solution without immunological consequences and may be used to emulate the heterogenous gas levels in the liver.

The O_2 carrying benefits of PFCs have been demonstrated in a limited number of *in vitro* studies, including 2D hepatocyte cultures [148-151] in alginate packed-bed 3D configurations and 3D microbial bioreactors [152-154]. However, in dynamically-circulating 3D primary hepatocyte or hepatocyte-stellate co-culture bioreactors this has not been conclusively shown to date. In a prior study we demonstrated that including a (20 % v/v) perfluorooctyl bromide (PFOB)-lecithin emulsion retained the metabolic functionality of hepatocyte bioreactors (section 4.2). Lidocaine clearance was significantly improved relative to PFC(-) controls but all other metabolite measurements were similar. Our calculations indicated that the O_2 level of the oxygenating gas mix (60 %) was likely too high to result in hypoxia in the PFC(-) bioreactors (section 4.2)[88].

A difficulty in demonstrating bioreactor metabolic functionality is limited access to the hepatocytes once they have aggregated in the matrix. Accessing them requires a bioreactor design that enables parts of the cell-containing matrix to be removed *during* operation without disrupting either the sterility or metabolic functionality of the system. Bioreactors are normally autoclaved for sterilization prior to application and subsequently remain sealed units. Flow cytometric or gene expression techniques that require the enzymatic liberation or lysis of cells from the matrix consequently result in the termination of an experiment. Similarly, there is also a lacking in consensus regarding the means of reporting metabolite production or clearance values and highly divergent results have been presented [125] (table 4.2.1 above). Thus, physiologically relevant, *in-situ* methods for demonstrating bioreactor metabolism remain desirable. Owing to its particular benefits, positron emission tomography (PET) may be one such method.

In this study, primary *in vitro* hepatocyte-stellate co-culture bioreactors with and without 20 % v/v perfluorooctyl bromide-lecithin emulsions were compared in terms of their O_2-dependent glucose uptake. The 20 % v/v level was selected based on optimal oxygenation and viscosity characteristics [10,94]. 'Hypoxic' and 'ambient' O_2 gas mixes were used as the oxygenating gas mixes. PET scans, using radioactive glucose (2-[^{18}F]fluoro-2-deoxy-*D*-glucose or ^{18}FDG) as the imaging label, were then conducted on the bioreactors within 24 hours following the primary cell isolation procedure [87], i.e. the same as would occur if a patient was to receive such a BAL treatment. PET is an attractive method for studying bioreactors in that it is well-established in the human clinical environment, provides metabolically relevant information and the results are visual and numerically quantifiable.

4.3.2 Materials and Methods

After gaining approval from the University of Pretoria Animal Use and Care Ethics committee, a total of 8 Landrace pigs were used in these experiments.

Media and chemicals

All media and chemicals used in the perfusion and transport of the livers are as described by Nieuwoudt *et al* (2005)[87]. Perfluorocarbon-lecithin emulsions were prepared according to the method of Moolman *et al* (2004)[10,94]. The emulsions were mixed with double concentrated cell culture medium and sterile deionised water, to achieve a 20 % v/v PFC emulsion-medium mixture. The mixture was adjusted to pH 7.35 – 7.4 and used as a culturing medium. In contrast to our earlier studies 'modified hepatocyte growth medium' (m-HGM)[155-159] was used for all cell culturing purposes. This formulation aimed to provide the best possible milieu for hepatocyte function. Please refer to Appendix A4 for the composition.

Cell isolation procedures

Hepatocyte isolation was performed according to the method of Nieuwoudt *et al* (2005) (section 4.1)[87]. After a clean hepatocyte-only suspension had been produced it was pumped out of the BRAT bowl through the emptying-line into an oxygenation

flask. The final volume of the suspension was noted for yield and viability calculations.

Simultaneous to the hepatocyte isolation procedure, stellate cells were fractionated from the non-parenchymal cell suspensions using the method of Riccalton-Banks *et al* (2003)[144]. Briefly, the cellular collagenase perfusate and discarded supernatant from the hepatocyte washings was pooled in a 1L Schott bottle and gently oxygenated. The cell suspension was poured into 50 ml centrifuge tubes then centrifuged for 5 mins at 50 g. The cell pellets were discarded after transferring the supernatant to new tubes and centrifuged again for 5 min at 50 g. The pellets were then discarded and the supernatant centrifuged for 10 min at 205 g. Thereafter, the supernatant was discarded and the pellet resuspended in 10 ml m-HGM. Two 10 min centrifuge (at 205 g) and pellet DMEM resuspension cycles followed. The remaining cells were confirmed to be stellates using microscopy.

Bioreactor seeding and evaluation methods

After evaluating the cell suspensions from the above procedures for viability and cell count the suspensions (hepatocytes and stellates) were pooled into one container and divided in half to make two volumes of 300 ml m-HGM with an equal number of cells in each. These volumes were transferred to the bioreactor reservoirs and re-circulated into two identical 150 ml radial-flow bioreactors to allow ‘seeding’ in the open-cell polyurethane foam (PUF) cell-aggregation matrices as previously described [79]. The medium was circulated at 50 ml/min in the two identical sterile, sealed circulation systems and driven by a single peristaltic pump. This system represented a two bioreactor *in vitro* dynamic model of the BAL device and was housed in a non-gas non-humidified incubator at 37.5 ^{o}C (figure 4.3.1 below). The medium in the reservoirs was oxygenated using an autoclavable aquarium bubbler using a single high pO_2 gas mix source (60% O_2, 5% CO_2, balance N_2) which facilitated hepatocyte aggregation/seeding in the PUF matrix. Previous studies have demonstrated that high pO_2 levels facilitate hepatocyte aggregation following cell isolation procedures [120,121,126,139].

After 4 hours of circulation and seeding, the medium containing the remaining non-aggregated cells was discarded and replaced with fresh medium. One bioreactor was given normal m-HGM while the other received the PFC-m-HGM mixture as described above. The oxygenating gas was then changed to 'hypoxic' (5% O_2, 5% CO_2, balance N_2) or 'ambient' (20% O_2, 5% CO_2, balance N_2) mixes depending on the experiment in progress. The term 'ambient' was used in view of the similarity of the particular O_2 level to that of air (21 %). These gas mixes were selected based on calculations by ourselves (section 4.2), and the findings of prior studies [109,120,121,139]. They were chosen to discriminate differences in O_2-dependent carbohydrate metabolism, i.e. glucose uptake between PFC(+) and PFC(-) cell-seeded bioreactors.

Steady-state medium sampling

After 24 hours of oxygenation and circulation, sterile 1 ml media samples were taken from the sampling ports of both bioreactors for the electrochemical detection of steady-state pH and gas partial pressures, pO_2 and pCO_2. A Chiron diagnostics Rapidlab 865 clinical blood gas analyzer (Bayer, South Africa) was used for this purpose. At the same time, media samples were also taken in duplicate and immediately frozen for glucose, lactate and pyruvate detections to investigate bioreactor carbohydrate metabolism as represented by the composition of the circulating extra-cellular medium. Standard spectrophotometric laboratory kits were used for this purpose (Sigma-Aldrich kits 472500 for glucose, 445875 for lactate and 726 for pyruvate).

Figure 4.3.1 The dual bioreactor *in vitro* model/s of the BALSS. The PFC reservoir and bioreactor are on the left (pink). The PFC(-) medium reservoir and bioreactor are on the right (red). Compare this configuration with the earlier single version (figure 4.2.1 above).

Bioreactor transport and PET imaging

The bioreactors were then removed from the incubator and transported to the Little Company of Mary hospital PET facility in Pretoria, South Africa. Recirculation was maintained throughout by powering the peristaltic pump with a 12 volt car battery and a 220 volt inverter. The media in the reservoirs was also oxygenated using the particular gas mix being tested in each experiment. The duration of transport was no more than 20 minutes, allowing minimal loss of bioreactor temperature.

At the PET facility the bioreactors were placed on the scanning bed of a Siemens Biograph 6 CT-PET machine and then centralized with respect to the gantry. Media recirculation and oxygenation was continued throughout. The standard brain scan image data acquisition program was loaded.

Independent 2.1 ± 0.01 mCi IV-syringe doses of ^{18}FDG were eluted from the on-site Eclipse RD cyclotron and associated Explora FDG_4 automated chemical synthesis unit. In these instruments deoxyglucose is labeled with ^{18}F ($t_{1/2}$ = 110 min) by nucleophilic displacement of an acetylated sugar derivative (1,3,4,6-tetra-*O*-acetyl-2-*O*-trifluoromethane-sulfonyl-β-*D*-mannopyranose) followed by hydrolysis with hydrochloric acid. The hyrolysate then passes through a C-18 Sep-Pak column and yields ^{18}F-2-fluoro-2-deoxyglucose (^{18}FDG).

Each bioreactor was sequentially subjected to an identical procedure. The ^{18}FDG dose was injected into the respective PFC(+) or PFC(-) bioreactor circuit's sampling port and circulated in the medium for 15 minutes allowing uptake by the resident cells. Thereafter, the radioactive medium was discarded followed by 2 x 5 minute washout cycles using 150 ml of fresh non-radioactive medium after which that was also discarded. This ensured, firstly, that any radioactivity remaining in a given bioreactor accounted for only glucose taken up by cells, and secondly, that a minimal amount of the PFC remained in the cell aggregation matrix. Each bioreactor was scanned with the brain scan program for 20 minutes, first by computed tomography (CT) for positioning, followed by PET for ^{18}FDG absorption. Image slice intervals were set to 4 mm. Since positron-electron extinction reactions result in coincident gamma photons, the selective detection of these photons by the PET machine results in inherently 3-dimensional images.

Image analysis and reporting

CT-corrected PET images were reconstructed using the system's Syngo (Siemens) image processing software. This fuses the anatomical (CT) data with the functional (PET) data and enables the rotation of the reconstructed bioreactor in 3-D. The resulting files were then transferred to a Siemens multimodality workstation (MI applications 2006A). A volume of interest was drawn around *only* the cell aggregation matrix within each bioreactor in 3 axes i.e. the transverse, sagittal and coronal. The ^{18}FDG radioactive 'heat' or count density (in Bq/ml) for the volume of interest was then recorded. Reports were drawn up by slicing each bioreactor through its midline in the above axes and displayed in rows from the top down of the PET images, then the CT images, then the fused CT-PET images (figures 4.3.2,3). The report for each

bioreactor was printed using a HP colour laser printer. 3D-rotatable video reconstructions were also generated and saved to CD-rom.

Following PET scanning the bioreactors were returned to the laboratory and dismantled. The PUF foam from each bioreactor was removed and photographed to confirm that cells were present.

Statistics and calculations

Microsoft Excel (2003) was used as the spreadsheet for all data. Mean and standard deviations were calculated where possible. Statistix 8, (Analytical software, Tallahassee FL, USA) was used when significant differences ($p<0.05$) were calculated with two-sample T tests.

The dissolved gas concentrations in the recirculating medium were calculated using the method of Moolman *et al* (2004)[10,94]. i.e. these were either [theoretical]'s calculated from absolute atmospheric levels compared to [measured]'s calculated from the electrochemical results:

$$C_{CO_2/O_2,total} = \left[\frac{\emptyset_p}{H_{CO_2/O_2-p}} + \frac{1-\emptyset_p}{H_{CO_2/O_2-w}}\right].P_{CO_2/O_2-w}$$

$in\ \frac{mol}{m^3}\ and\ pressure\ in\ bar$

where,

$\emptyset_p = PFOB\ volume\ fraction\ in\ emulsion,$

$P_{CO_2/O_2-w} = partial\ gas\ tension\ for\ CO_2\ or\ O_2$ in acqueous/water/plasma phases, in bar

$H_{CO_2/O_2-p} = Henry's\ constant\ for\ CO_2\ or\ O_2\ in\ PFOB\ at\ 37^oC$

$H_{CO_2/O_2-w} = Henry's\ constant\ for\ CO_2\ or\ O_2\ in\ water\ at\ 37^oC$

with constants:

$H_{O_2-p} = 0.0516\ bar.\frac{m^3}{mol}$

$H_{O_2-w} = 0.95\ bar.\frac{m^3}{mol}\ in\ water$ or $0.988\ bar.\frac{m^3}{mol}\ in\ blood\ plasma$ (taken as ~ equivalent)

$H_{CO_2-p} = 0.0121\ bar.\frac{m^3}{mol}$

$H_{CO_2-w} = 0.0394\ bar.\frac{m^3}{mol}\ in\ blood\ plasma$

and assumptions:

1. The gases were completely equilibrated in all phases, e.g. $pO_{2\ (water)} = pO_{2\ (gas)}$. This is reasonable in that the 0.2 µm droplets have a large surface area for mass transfer and measurements were taken following 24 hours of in-gassing.
2. The medium was maximally gas loaded, ie. pCO_2 and pO_2 were at their maximum when the CO_2 in the gas mix was 5 %.
3. O_2 consumption and CO_2 release by cells was not taken into account in that the medium was in-gassed maximally during the experiments.

4.3.3 Results

Since the BRAT centrifuge bowls used for isolating hepatocytes were all of a fixed volume (165 ml) and the stellate isolation procedures were identical, the total cell quantities remained approximately equivalent, i.e. a mean of 1.852×10^{10} hepatocytes and 1.84×10^8 stellates prior to sub-division for the two bioreactors. The number of PET experiments conducted per experimental group, the mean number of cells seeded per bioreactor (9.26×10^9 hepatocytes and 1.84×10^8 stellates), the calculated gas concentrations, the electrochemically measured media pH and gas partial pressures 24 hours after isolation and the mean radioactive glucose uptake per bioreactor are presented in table 4.3.1. Figures 4.3.2 and 4.3.3 are PFC(-) and PFC(+) bioreactor CT-PET scans respectively.

A total of 16 PET scans were conducted: Four pairs on cell-seeded bioreactors using the ‘hypoxic’ (5 % O_2) gas mix, two pairs on cell-seeded bioreactors using the ‘ambient’ (20 % O_2) gas mix and two control pairs on cell-free bioreactors using each of the above mixes. In all the hypoxic and ambient scans, cell–seeded PFC(-) bioreactors were more radio-active than PFC(+) ones. This was significant in the ‘hypoxic’ experiments, i.e 57 % ($p = 0.01$), not so in the ‘ambient’ i.e. 62 % ($p = 0.3$), but significantly so when they were combined, i.e. a mean of 59.5 % ($p = 0.04$). Thus, more glucose was taken up from the circulating medium by cell-seeded PFC(-) bioreactors than PFC(+) ones, indicating a more glycolytic metabolism in the former. Since the ‘ambient’ PFC(-) experiments were more radio-active than their PFC(+)

counterparts, it suggested that the 20 % O_2 gas mix may also have been slightly *hypoxic* for the cells.

As expected, the cell-free controls scans were similar, although both demonstrated that PFC(-) bioreactors were more radio-active than PFC(+) bioreactors: 23.7 % and 15.4 % respectively, i.e. a mean of 19.6 %, combined p = 0.5. Glucose absorption by binding to the *non*-reactive PFC emulsion may be excluded in that the levels of circulating extracellular glucose in the cell-free PFC(-) and PFC(+) configurations were similar. Thus, the most probable cause of the difference was Compton photonic scattering by the high atomic mass PFC molecules remaining in the cell-aggregation matrix, i.e. the long carbon and fluorine 'backbone' of the PFOB ($C_8F_{17}Br$) and any remaining lecithin protein. Despite the initial PFC concentration of only 20 % v/v and the thorough PFC-free medium washout and discardation cycles, it was apparently not possible to eliminate all of the PFC in the matrix. However, equal initial amounts of PFC were used in all bioreactors. Thus, it was possible to exclude the scattering effect by *normalizing* with the difference between the controls, i.e. by subtracting the mean % difference between the cell-free bioreactors, 19.6 %, from the mean % difference between the cell-seeded bioreactors. This resulted in differences of 36.4 % and 42.4 % for 'hypoxic' and 'ambient' PFC(-) versus PFC(+) configurations respectively. Clearly, PFC(-) cell-seeded configurations remained more glycolytic than their PFC(+) counterparts. Visual examination of the individual scans (figures 4.3.2,3) and the 3D video reconstructions also confirmed this difference in each case.

Table 4.3.1 Seeded cell counts, PET-bioreactor radiation counts (^{18}FDG-uptake) and electrochemical pH and gas results, 24 hours after cell isolation procedures

group	gas mix	[theoretical]	cells/ bioreactor	PET counts/bioreactor	measured media pH and gas partial pressures		[measured]
hypoxic (N=4)	5%O_2, 5%CO_2, balance N_2	PFC(-) O_2 = 0.05 PFC(+) O_2 = 0.24 PFC(-) CO_2 = 1.27 PFC(+) CO_2 = 1.84 **PFC(-) O_2/CO_2 = 0.04** **PFC(+) O_2/CO_2 = 0.13**	9.26x10^9 hepatocytes 1.84x10^8 stellates	PFC(+): 3.29x10^4±2.28x10^3 PFC(-): 7.94 x10^4±1.89 x10^4 **(-) > (+): 57.0 + 9.99 %**	PFC(+) pH: 7.615 ±0.021 pO_2: 108.03 ±5.53 pCO_2: 13.48 ±5.51 **pO_2/pCO_2: 8.02**	PFC(-) pH: 7.664 ±0.299 pO_2: 71.74 ±0.79 pCO_2: 24.603 ±0.32 **pO_2/pCO_2: 2.92**	PFC(-) O_2 = 0.10 PFC(+) O_2 = 0.55 PFC(-) CO_2 = 0.83 PFC(+) CO_2 = 0.86 **PFC(-) O_2/CO_2 = 0.12** **PFC(+) O_2/CO_2 = 0.97**
hypoxic control (N=1)	5%O_2, 5%CO_2, balance N_2	as above	0	PFC(+):1.77 x10^4 PFC(-): 2.32 x10^4 **(-) > (+): 23.7 %**	PFC(+) pH: 7.61 pO_2: 67.8 pCO_2: 21.4 **pO_2/pCO_2: 3.17**	PFC(-) pH: 7.46 pO_2: 67.2 pCO_2: 24.0 **pO_2/pCO_2: 2.80**	
ambient (N=2)	20%O_2, 5%CO_2, balance N_2	PFC(-) O_2 = 0.21 PFC(+) O_2 = 0.94 PFC(-) CO_2 = 1.27 PFC(+) CO_2 = 1.84 **PFC(-) O_2/CO_2 = 0.16** **PFC(+) O_2/CO_2 = 0.51**	9.26x10^9 hepatocytes 1.84x10^9 stellates	PFC(+): 2.05x10^4±1.28x10^4 PFC(-): 5.24x10^4±2.81x10^4 **(-) > (+): 62.0 ± 4.0 %**	PFC(+) pH: 7.797 ±0.117 pO_2: 113.6 ±12.45 pCO_2: 9.72 ±1.67 **pO_2/pCO_2: 11.69**	PFC(-) pH: 7.449 ±0.023 pO_2: 106.96 ±12.67 pCO_2: 22.42 ±1.67 **pO_2/pCO_2: 4.77**	PFC(-) O_2 = 0.15 PFC(+) O_2 = 0.73 PFC(-) CO_2 = 0.79 PFC(+) CO_2 = 0.77 **PFC(-) O_2/CO_2 = 0.19** **PFC(+) O_2/CO_2 = 0.95**
ambient control (N=1)	20%O_2, 5%CO_2, balance N_2	as above	0	PFC(+): 4.65x10^4 PFC(-): 5.49x10^4 **(-) > (+): 15.4 %**	PFC(+) pH: 7.61 pO_2: 117.3 pCO_2: 21.4 **pO_2/pCO_2: 5.48**	PFC(-) pH: 7.445 pO_2: 116.0 pCO_2: 24.1 **pO_2/pCO_2: 4.81**	
prior studies	60%O_2 90%O_2	PFC(-) O_2 = 0.63 PFC(+) O_2 = 2.83 PFC(-) O_2 = 0.96 PFC(+) O_2 = 4.29					

Footnotes:

1. All values given as mean ± std dev.
2. Units of ^{18}FDG radiation count density in bioreactor matrices is in Bq/ml
3. Units of measured pO_2 and pCO_2 is mmHg.
4. [ ] = gas concentration in mol/m^3
5. [theoretical] and [measured] was calculated as per the method of Moolman *et al.* [10,94]. See Methods for details.
6. The mean difference in the PET counts for the cell-free controls: PFC(-) vs. PFC(+) was 19.6 %.
7. There was a significant difference between the FDG radioactivity counts of hypoxic cell-seeded PFC(-) vs. PFC(+) bioreactors (57 %, p = 0.01). Not so in the ambient cell-seeded bioreactors (62 %, p = 0.3), but significant when combined (59.5 %, p = 0.04).

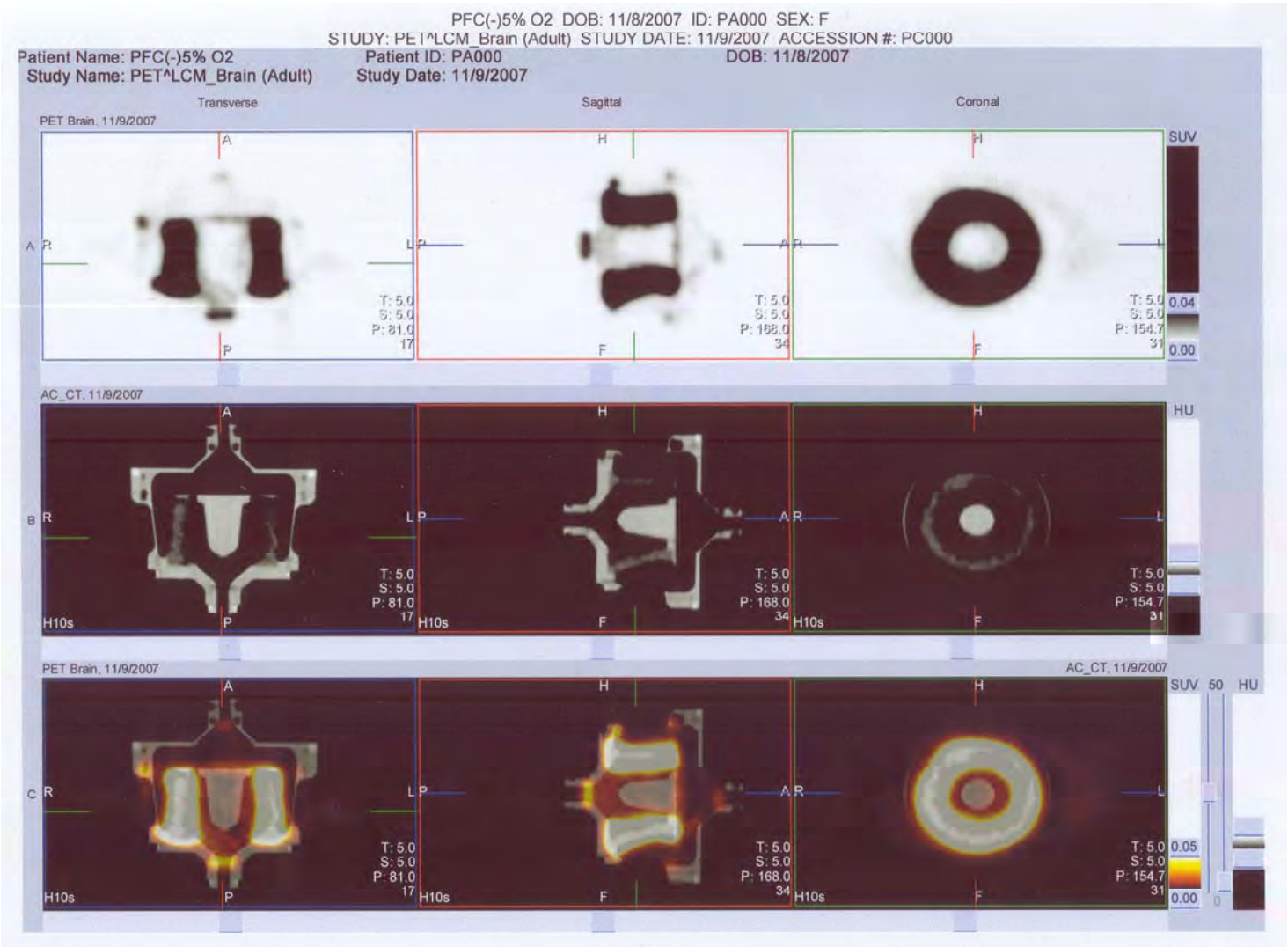

Figure 4.3.2 CT and PET scan of hypoxic gas mix cell-seeded bioreactor *without* PFC. The first row of images are PET only, the second CT only, the third is the combined CT (in black and white) and PET (in colour) images. The columns represent the transverse, sagittal and coronal planes respectively. The PET images of PFC(-) bioreactors were more radioactive or 'hotter', following greater glucose uptake, i.e. with a more glycolytic metabolism than the PFC(+) bioreactors.

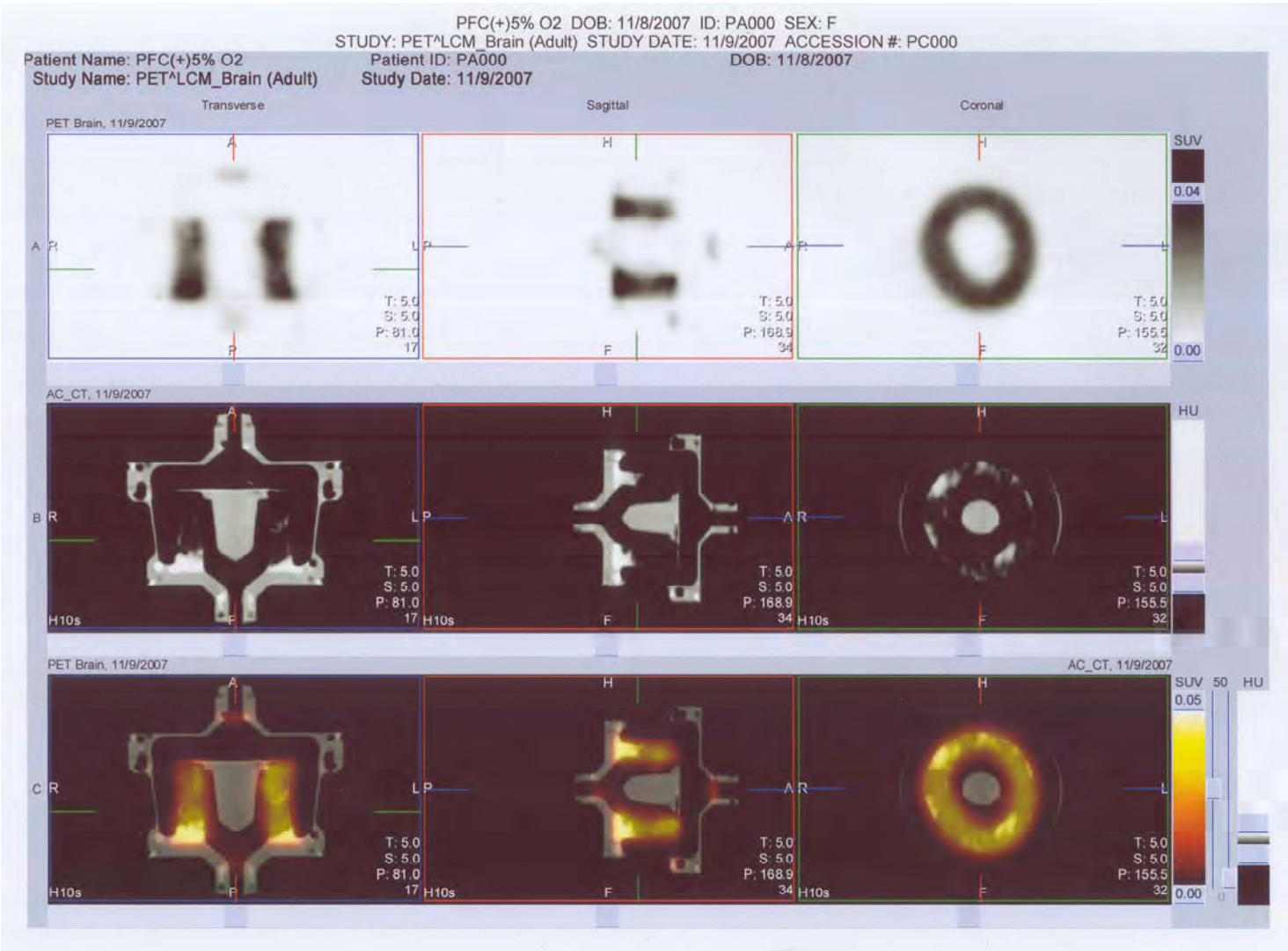

Figure 4.3.3 CT and PET scan of hypoxic gas mix cell-seeded bioreactor *with* PFC. PFC(+) bioreactors were all 'cooler' having absorbed less glucose, i.e. less a glycolytic metabolism than PFC(-) bioreactors.

The metabolic 'steady state' biochemistry (table 4.3.2), as represented by the composition of the extracellular medium 24 hours after isolation demonstrated in both hypoxic and ambient situations that glucose levels were higher and lactate levels were lower in cell-seeded PFC(+) versus PFC(-) bioreactors. This was significant for glucose in the hypoxic situation ($p < 0.01$) but not so in the ambient ($p = 0.5$). No other significant differences were detectable, although measurement variation and the small sample sizes must be considered. These results were in agreement with the PET results in that the PFC(-) bioreactors were more glycolytic than the PFC(+) ones. Interestingly, pyruvate levels were higher in the PFC(-) cell-seeded circumstances, which was unexpected from a glycolytic versus gluconeogenic perspective. From these and prior experiments (section 4.2) it would suggest that either the phospholipidic lecithin PFC emulsifier or the PFC itself interfered with the pyruvate detection method.

Table 4.3.2 Steady state biochemistry at 24 hours post isolation

Group		glucose	lactate	pyruvate
hypoxic	PFC(+):	28.08 ±2.94	2.60 ±0.16	58.63 ±16.98
	PFC(-):	26.44 ±0.73	2.71 ±0.14	89.25 ±27.99
Hcontrol	PFC(+):	33.13 ±0.96	2.21 ±0.36	70.00 ±11.83
	PFC(-):	27.20 ±0.14	1.64 ±0.14	65.50 +16.26
normoxic	PFC(+):	23.58 ±1.76	2.33 ±0.14	39.25 ±7.63
	PFC(-):	22.26 ±1.87	2.40 ±0.28	126.0 ±47.29
Ncontrol	PFC(+):	25.10 ±5.00	2.20 ±0.87	97.50 ±4.04
	PFC(-):	25.68 ±1.22	2.28 ±0.67	100.0 +10.39

Footnotes:

1. There was a significant difference between the glucose levels of hypoxic cell-seeded PFC(-) vs. PFC(+) bioreactors ($p < 0.1$), but not so in the ambient levels ($p = 0.5$). No other significant differences were detectable.
2. Units of glucose and lactate are in mmol/l, pyruvate in µmol/l

The absolute gas concentrations in the medium that were calculated from atmospheric pressures, i.e. the [theoretical]'s, demonstrated greater O_2/CO_2 ratios in PFC(+) versus PFC(-) bioreactors in both hypoxic and ambient circumstances (table 4.3.1). There is little doubt that these differences would have impacted O_2–dependent metabolism in the bioreactors. In the electrochemically measured results, greater pO_2/pCO_2 ratios were apparent in all PFC(+) cases, more so when there were cells than not. However, we have repeatedly found that Clarke–type electrodes, as are found in blood gas machines, produce highly divergent measurements for dissolved O_2 or CO_2 in PFC emulsions. This was visible in the difference between the [theoretical]'s and that calculated from

the measured (pCO_2, pO_2) results, i.e. the [measured]'s and the apparent alkalosis, associated with low pCO_2 levels, in the PFC(+) circumstances. However, in all ratios for PFC(+) experiments a trend was visible. The raised (calculated and measured) O_2/CO_2 and pO_2/pCO_2 values relative to the PFC(-) experiments suggested that O_2 provision to the cells had been improved by PFC in all cases.

4.3.4 Discussion

Several techniques have historically been employed to overcome O_2 limitations in hepatocyte cultures and bioreactors, including for example, optimizing the porosity of the extra cellular matrix (ECM) [160], the incorporation of perfluorocarbon-based O_2 carriers in the ECM [161], the use of bovine hemoglobin O_2 carriers in the circulating medium [162] and increasing the number and diameter of gas carrying hollow fibres (HF) in bioreactors [163]. A simplistic approach is to increase the pO_2 of the oxygenating gas mix. However, this is potentially hazardous in that large hepatocyte aggregates may be exposed to hyperoxic conditions externally, while remaining hypoxic in their internal regions and resulting in an increase in cell mortality [161]. Including a 20 % v/v PFOB-lecithin emulsion in the circulating medium is a feasible method, without immunological impacts, for replacing circulating hemoglobin and attaining a milieu similar to the metabolic zonation found in the *in vivo* liver.

The gas mixes used in this study to represent either hypoxic or ambient/normal situations were based on prior examples [109,120,121,139] and calculated estimates by ourselves (section 4.2). However, some uncertainty remained since bioreactor oxygenation characteristics vary according to design and are therefore different in each case. The bioreactors used in this study were an improved form of an earlier version [79] (figures 3.1,2 and 4.2.1). Extensive flow optimization, mass transport improvement and the minimization of dead-space had subsequently occurred [112]. Thus, flow dynamics in this case would obviously differ from that in 2D culture flasks or 3D HF-bioreactors. Our results suggest that the ambient (20 % O_2) gas mix may also have been slightly hypoxic to the cells. This was despite findings to the contrary in a previous 2D *in vitro* study employing the same gas mix [120].

Mareels *et al* (2006) [163], found by numerical modeling and experimentation that a large majority of the cells in an earlier iteration of the AMC hollow-fiber bioreactor were hypoxic using a 60 % O_2 gas mix. As a result, the AMC bioreactor's internal configuration and oxygenating gas was altered to a 95 % O_2 mix. We have reservations regarding this approach. Our results suggest an ideal O_2 level > 20 %, but certainly < 60 % as was previously employed by us. Additional numerical modeling and experimentation will aid in resolving this figure in the future.

In agreement with a prior study [164], we have found that electrochemical methods, e.g. blood gas machines, are not ideal for measuring the O_2 dissolved in PFC emulsions. This was evident in the difference between the [theoretical]'s calculated from atmospheric pressure and the [measured]'s calculated from the electrochemical results. The measured pO_2 and pCO_2 values (table 4.3.1) represent that in predominantly the aqueous phase and do not accurately account for the substantially more gas dissolved in the micellar-organic phase. Unfortunately, aqueous pO_2 and pCO_2 levels can only indirectly be compared with that measured in whole blood or the organic phase of PFC. However, our results did indicate improved theoretical O_2/CO_2 and measured $pO2/pCO_2$ ratios associated with PFC in all cases. This would suggest that PFC had improved the delivery of O_2 to cells in all cases.

Clinical imaging technologies have previously been employed in studying hepatocyte bioreactors. This has been done using magnetic resonance imaging (MRI), [112,165-169], once by ourselves using single photon emission tomography (SPET) with ^{99m}Tc-DISIDA (figure 4.2.4 above), but apparently never with PET. Two studies used PET to image bioartificial myocardial grafts in a solid matrix [170,171] and one for a tissue engineered trachea [172]. In general, MRI provides anatomical and/or flow information, while SPET and PET provide physiological information. In ^{18}FDG-PET the oxygen in glucose is replaced with Fluorine-18 and owing to its short half life ($t_{1/2}$ = 110 mins) *non-invasive in vivo* studies of carbohydrate metabolism are possible [173]. PET scan data is inherently 3-dimensional owing to the electronic scintillation detection of 180-degree coincident photons originating in a positron-electron extinction reaction. The resolution of the images is high owing to the coincidence detection methodology. PET scans of *in situ* hepatocytes in bioreactors require the latter to be constructed of materials that are sterilizable and radio-transparent to 511 keV gamma photons. In this

case the bioreactors were machined out of polycarbonate, which is autoclavable at 121 ^{o}C and provides no obstruction to such photons.

All the PET scans in this study indicated more glycolytic metabolism in cell-seeded bioreactors without PFC.The extracellular 'steady state' glucose and lactate levels were in agreement with this but also with another study using a similar rationale and which investigated the incorporation of PFC into the ECM [162]. Taken together, this may be accepted as confirmation of the success of our procedures. Bearing in mind the normal clinical purpose of ^{18}FDG-PET, namely to examine glycolytic lesions such as cancer in human patients, [173], it is perhaps unsurprising that it was successful in this case. Having said that, maintaining *exactly* the same experimental conditions was necessary throughout and success must partly be owing to this.

Since the application of PET in this case was novel it was necessary to estimate the radioactive doses. In view of the necessity of discarding the washout media, to maximally control the experimental conditions and decrease radiation exposure to personnel, and the fact that the employed bioreactors were sealed units following their autoclaving prior to cell-seeding, it was not possible to gather information using methods that would require cell liberation or lysis from the cell aggregation matrix. This study was 'short term', i.e. on the same time-scale following cell isolation as would occur in BAL treatments using primary cells. However, hepatocyte metabolism is diverse and may change with the duration of culturing. In the future, the use of lower ^{18}FDG doses may allow longer term, e.g. 5-10 day bioreactor investigations *after* PET scans. It will then be interesting to additionally investigate the effect of improved O_2 provision by PFC on nitrogenous and/or xenobiotic hepatocyte metabolism. No studies thus far have investigated the effects of PFC on bioreactor longevity.

In conclusion, this study demonstrated that ^{18}FDG-PET was an effective imaging modality for investigating the *in-situ* O_2-dependent metabolism of hepatocyte bioreactors in conditions simulating those likely to be found in plasma-only BAL treatments. Agreement for the PET results was found in the circulating extracellular metabolites. In the future longer term metabolic studies will provide complimentary information to the above.

4.4 Thoughts and recommendations

The above *in vitro* cell biology and bioreactor studies presented a large scale, sterile primary cell isolation procedure, an investigation of hepatocyte metabolism over 7-days in a direct plasma-contact hepatocyte bioreactor and the novel use of PET to discriminate between O_2 challenged PFC versus non-PFC flow optimized bioreactors.

From a simple statistical perspective the primary cell isolation method has been very successful: In 40 procedures over a 3 year period, a mean of $2.14 \times 10^{10} \pm 8.60 \times 10^{8}$ hepatocytes and $2.43 \times 10^{9} \pm 1.82 \times 10^{8}$ stellate cells were isolated from the livers of 30 kg pigs with liver masses of approximately 1.5 kg each. Bacterial or fungal contaminations were not found in any of these, which verified the sterility of the procedures.

Of interest, assuming an adult liver has between 1.0 and 1.5×10^{11} hepatocytes, 2.14×10^{10} equates to approximately 15 – 20 % of the total amount, or assuming the liver is composed of 70 % hepatocytes and has a mass of 1.5 kg, the isolated hepatocyte mass weighs 158 – 210 g. These values are within the amount often quoted to be sufficient for an effective bioartificial liver support device [70,83,92]. Having said that, it is ideal to have as large a cell mass as possible, assuming the conditions in the bioreactor are sufficient to maintain them. The disposable BRAT bowls used in the above method were of a fixed volume (either 250 or 165 ml) which limited the total amount of cells that could be isolated. There are consequently efforts underway to use other larger volume apparatus which will increase the isolatable quantity.

The second study successfully demonstrated that there was metabolic activity in both PFC and non-PFC bioreactors over a 7 day period, but presumably due to the employed gas mix was unable to show a difference between them. During the course of this study and in unpublished efforts subsequently, some of the difficulties involved in successfully demonstrating the efficacy of such bioreactors was further highlighted. For example, the mentioned lack of consensus regarding reporting methods, the great variations in reported results and the difficulty of measuring *in situ* cell functions due to a lack of non invasive methods enabling direct access to them. In specifically the latter,

we found that the PFC and fragments of the PUF matrix were difficult to remove from cell aggregate samples taken from dismantled bioreactors after termination. Gene expression and flow cytometry experiments were consequently unreliable.

The subsequent novel use of PET was an attempt to solve the above problems and to conclusively demonstrate that the PFC facilitated cell function under hypoxic conditions, as may be found in the treatment of an acute liver failure patient. They were also performed on the same duration following a primary cell isolation procedure that would occur if such cells were employed in the BAL device. The success of the experiments was partly owing to the use of radio-transparent bioreactor material and attention to maintaining exactly the same experimental conditions.

4.4.1 Developments in cell sources

The obstacle which is arguably solely responsible for preventing the entrance of bioartificial liver technology into the commercial arena is the establishment of a renewable source of sterile, metabolically effective, immunologically safe and affordable cells in sufficient quantities.

Primary human hepatocytes are the obvious ideal choice owing to minimal immunological concerns. However, their low availability and the difficulty of maintaining metabolically effective cells in *in vitro* cultures have prevented their widespread use [174]. Primary porcine hepatocytes are an attractive alternative owing to their easy availability, low cost and their maintenance of metabolic functionality in culture. Ongoing concerns regarding xenozoonoses have prevented their use. European law forbids the use of xenogenic tissue in any human treatments [70].

4.4.1.1 Genetically engineered swine

Despite EU law, no porcine endogenous retrovirus (PERV types A,B and C) infection has been recorded in *in vivo* human cells, neither has any disease resulting from this family of viruses been found in either humans or pigs [175,176]. PERVs also appear to be susceptible to currently available antiviral therapies [177,178]. Thus, assuming the immunological differences between pigs and humans are overcome and animals are

raised in *guaranteed* pathogen-free conditions, the attractiveness of porcine tissues as a cell or organ source remains.

There have been significant advances in genetic engineering: α-1,3 galactosyltransferase gene-knockout (GT-KO) pigs have been developed that no longer express the Galα1,3Gal(Gal) oligosachiride and thus avoid responses from the natural antibodies for this in humans [179]. The PERV infectivity of porcine tissue has been inhibited by the introduction of an RNA interference silences gene (siRNA) [180]. Several of the coagulation-anticoagulation incompatibilities between humans and pigs have also been recognized [181]. Animals transgenic for human anticoagulation genes, such as CD39 [182], tissue factor pathway inhibitor [183] and human complement regulatory proteins (CRP) such as CD46 and CD55 are currently being developed [184,185]. Several other genes such as TFPI, DAF, CD59, HLA-E, ULBP-1 and CD47, are also believed to be important [176]. Thus, while the ideal would be a pig transgenic for all of the above, it does not yet exist. Judging by the pace of progress in this field (and there being no associated physiological complications) it seems reasonable to expect such an animal within the next 10-15 years.

The above developments are indeed auspicious in terms of the establishment of a cell source for a BAL device. However, the focus of the above research has been to develop an animal appropriate for xenotransplantation rather than for simply a hepatocyte source. Assuming success, the fact that the only therapy of proven survival benefit for ALF is OLT, the need for developing an extracorporeal BAL device may be negated. Naturally, unforeseeable developments in the future preclude drawing this conclusion at this time it simply remains an interesting possibility.

4.4.1.2 Chimeric animals

The *in vitro* propagation of human hepatocytes is difficult. For this reason researchers have begun engrafting and expanding human hepatocytes in animals. Two systems are being studied: Urokinase-type plasminogen activator-transgenic severe combined immunodeficiency mice express uroplasminogen activator (uPA/SKID mice) under the transcriptional control of a hepatotoxic albumin promoter. These immunodeficient knockout mice do not reject infused human hepatocytes. As the murine hepatocytes die

they are replaced with unaffected human cells, yielding chimeric human/mouse livers with engraftment levels up to 92 % [186]. Drawbacks to this system include difficulties in animal husbandry, predisposition to renal disease in the immunodeficient animals and difficulties in controlling the mutant hepatocyte phenotype enabling only a narrow time window for engraftment [187,188].

An alternate system developed in response to the above is as follows: Immunodeficient fumarylacetoacetate hydrolase gene/recombination activation gene/interleukin-2 receptor gamma gene ($Fah^{-/-}/Rag^{2-/-}/Il2rg^{-/-}$) 'triple knockout' mice develop an essential hepatocyte deficit due to tyrosemia induced by the omission of the fumarylacetoacetate hydrolase gene. Following pre-treatment with a urokinase expressing adenovirus these animals allow human cell engraftment from many sources including liver biopsies. Serial hepatectomy with human hepatocyte repopulation has been possible up to four times and the expanded cells demonstrate typical human drug metabolism. These animals are easy to breed, do not develop renal disease and are transplantable several times [188,189].

The above *in vivo* systems are still in early development and only limited testing of the metabolic functionality of the mutant cells has occurred. Assuming these approaches are found reliable, the system may be adapted to a large animal such as the (ever reliable) pig to overcome the limitation in expanded cell numbers present in the murine model [174]. From hepatectomized animals such as the latter, a large scale sterile hepatocyte isolation procedure as presented above can then be performed.

4.4.1.3 Concerns regarding other cell types

Stem, tumorigenic and transformed cell types replicate extensively in *in vitro* culture. However, growing sufficient cells in a sterile manner is a significantly more costly undertaking than isolating primary cells. For example, assuming one needs to generate a quantity of 400 g of cells to seed into 1 or 2 bioreactors for a single BAL treatment. (This amount equates to approximately 40 % of the hepatocyte mass of an innate liver):

Table 4.4.1 Simple accounting of expense differences (in South African Rand) between primary and transformed cells for a quantity of 400 g of hepatocytes

Item (primary)	Quantity	Expense	Item (transformed)	Quantity	Expense
Animal (pig)	2	3000			
Surgery + husbandry	2	6000			
Perfusion fluids	2	1600			
Isolation media (collagenase + density gradient)	2	3000	Cell liberation enzyme (trypsin)	10 x100 ml	2000
BRAT disposables	2	1800			
Centrifuge tubes	100	4000	Cell culture flasks	400 x 75cm^2	12000
Media	10 L	800	Media	60 L	24000
Salary (2 people)	1 day	2500	Salary (1 person)	1.5 months	30000
TOTAL		**22700**			**68000**
DIFFERENCE					**factor 3**

Note: These costs exclude research into developing the cell type (e.g. a transgenic animal or a transformed embryonic stem cell) and the overhead laboratory costs.

The difference in the two cell sources amounts to a 3-fold increase in costs associated with the 2-D culturing of the transformed cell type. Additionally, there are significant implications in terms of the time it takes to generate these quantities. Assuming the consistent clinical availability of BAL bioreactors, a GMP-certified laboratory must be growing the requisite large quantities of the cells *in parallel and at all times* [communication with Mr Greg Dane, ex-CEO of the US company Circe]. The cost differences then escalate a factor of 6 to 9 times that of a primary cell source.

Transformed cells are also potentially problematic in view of 'metabolic inappropriateness', in ALF. The question is, since their genotype and/or phenotype is different to a mature primary hepatocyte, are their expressed metabolic paths synthesizing or transforming metabolites in the same way as a healthy liver? For example,

The immortalized human hepatoblastoma C3A cell line, derived from a parental HepG2 lineage, has extensively been grown *in vitro* and clinically employed in the ELAD hollow fibre bioreactor [74]. However, despite reported improvements in HE, these cells synthesize urea by non-urea cycle (arginase II dependent) pathways and therefore do not detoxify ammonia [190]. HepG2 and possibly also C3A cells incorporate ammonia into glutamine via glutamine synthetase [191]. Although glutamine is not inherently toxic to the brain, this strategy is of questionable safety due to its astrocytic build-up in HE. The above underlies the multi-systemic syndrome of ALF (and HE),

but in addition to concerns regarding tumorigenicity, the non-ideal metabolic properties of this particular cell type are indicated. It therefore seems surprising that the US company Vital Therapies using ELAD (http://www.vitaltherpies.com), were successful in Beijing and consequently granted FDA approval to proceed with the ongoing Phase II trial in the US.

A large variety of stem cells are being researched as cell sources for BAL devices, but difficulties with the control of proliferation and differentiation to a mature phenotype remain [69,192]. Unfortunately, proliferation and differentiation in hepatocytes are usually diametrically opposed [82]. For example, cBAL111, a human telomerase reverse transcriptase (hTERT) immortalized human fetal hepatocyte cell line with a good proliferative capacity was recently developed [193,194]. However, this cell has a limited capacity for ammonia detoxification through urea production or to perform cytochrome P450 detoxification. Glycolytic lactate production in the bioreactor may also exacerbate this condition in a patient. Whether the immortalizing gene can truly be turned-off has also not been confirmed. Thus, while efforts at developing cell lines are justified (indeed important), the associated difficulties have prevented their wide acceptance to date.

Hepalife, a US based company, have found in *in vitro* trials that their patented PICM-19 pig epiblast cells [195,196] are able to retain ammonia detoxification, urea synthesis and cytochrome P450 functions at near porcine primary hepatocyte levels for an extended period (14 days) when exposed to human plasma [197]. The bioreactor employed in their system is that originally developed by Gerlach *et al* [198]. Hepalife has also recently purchased the patents, FDA approved IND and intellectual property of the company Arbios which owned the HepatAssist technology [199]. Historically, HepatAssist arguably progressed the furthest, in phase II/III BAL human trials, on the path towards device commercialisation [75]. HepaLife intends conducting large animal trials in the near future. However, despite all of these promising indications, the immunological considerations in employing cells of porcine origin remain.

5. *IN VIVO* ANIMAL STUDIES

Overview

The following section presents two *in vivo*, clinically based animal studies that have been required in the development of the UP-CSIR BAL. The employed models are experimentally controlled versions of the severe liver injury scenarios that are likely to be encountered in the clinical application of BAL devices.

The first of these studies investigates the potential toxicity of IV injected PFC in a rat model of severe liver injury. Despite a lacking in human clinical evidence demonstrating PFC toxicity, the same has not previously been shown in a liver failure scenario. Since PFC is used in a sub-circulation of the UP-CSIR BAL and due to the (unlikely) possibility of its entrance into a patient, the necessity therefore exists to confirm its non-toxicity in a similar scenario. For this purpose a highly reproducible ¾ partial liver resection rat model is employed. No PFC toxicity or any impact on the rate of liver regeneration results. The success of this study is attributed to the employed methods and the study design.

The second study details the establishment and standardization of an ischemic surgical model of irreversible ALF in pigs. Such a model is required in the pre-clinical verification of the efficacy of a BAL. Although similar surgical models have previously been described, the statistical methods used in standardizing this one are unique. Briefly, criteria are defined based on the analysis of trends in the collected clinical data. These criteria are designed to discriminate between animals that do or do not represent a valid model of ALF. However, it is clear that induced animal models of ALF are inherently limited in the degree to which they are comparable to the human clinical scenario.

In the thoughts and recommendations that follow the impact of the chosen ischemic ALF model on the clinical testing of the UP-CSIR is examined. The many difficulties in the model are highlighted, suggesting research into alternate models, design alterations in the BAL device and the exclusion or inclusion of variables based on their newly established clinical value/s. Adding detail to this, arguments are raised regarding the choice of alternate animal models. The prognostic and clinical importance, strategies for measurement and reduction of blood ammonia in ALF and the inclusion of artificial toxin clearance devices into BAL devices are discussed.

5.1 Non-toxicity of an IV injected perfluorocarbon oxygen carrier in an animal model of liver regeneration following surgical injury

Nieuwoudt M, Engelbrecht GHC, Sentle L, Auer R, Kahn D, van der Merwe SW.

Artificial Cells, Blood substitutes, and Biotechnology 2009;37(3):117-24.

5.1.1 Introduction

Perfluorocarbon (PFC) polymers have the properties of exceptional chemical and biological inertness. PFCs also have very high dissolving capacities for oxygen (O_2) and carbon dioxide (CO_2), making them attractive candidates as artificial O_2 carriers in erythrocyte replacement applications, including for example, plasma perfused bioartificial livers [10,88,94]. The intravascular (IV) administration of a PFC requires the development of a heat sterilizable, sub-micron droplet size emulsion that is stable in non-frozen conditions for at least two years [200,201].

In mammals the *in vivo* distribution and elimination of PFC is characterized by its half lives in the circulation and in the reticulo-endothelial system (RES). In the first 24 hours the PFC is cleared from the circulation by the mononuclear phagocyte system accumulating in the liver, spleen and bone marrow. In the second phase, lasting days to weeks, it is cleared from the RES via lipid compartments in the blood into the lungs. Thus, PFC is not metabolized; it is excreted from the respiratory system into the air. During this phase, flu-like symptoms with myalgia and light fever have been reported in clinical studies [201]. Factors affecting the clearance half lives of PFC are emulsion droplet size, molecular weight, surfactant-type, complement activation, animal species and in humans, racial differences [202-204].

In second generation PFC emulsions the toxicity problems associated with earlier attempts [205] have been overcome. Oxygent (Alliance pharmaceuticals, San Diego, USA), a PFC composed of (predominantly) perfluorooctyl bromide (PFOB) ($C_8F_{17}Br$)

emulsified in egg yolk phospholipid (lecithin) as a surfactant, has successfully progressed through both stage II and III clinical trials. In the above trials Oxygent was not found to significantly initiate either immunological or coagulative reactions in healthy volunteers. Furthermore, no subsequent perturbation of normal blood hemostatic or viscosity behaviour could be found (in fact, viscosity improved); there was no reduction in clot formation or strength and no increase in red cell hemolysis [206,207].

Lethal dose experiments in animals have shown that the value for PFOB is 41g/kg, which is remarkably non-toxic [208-212]. However, the non-toxicity of PFCs has not previously been demonstrated in a liver failure scenario. The clinical progress of acute liver failure (ALF) involves the development of a hyperdynamic circulation, a disseminated intravascular coagulopathy (DIC), renal, and eventually, multi-organ failure [213]. Since the IV administration of a toxin may produce a similar profile to the above, experiments such as these must discriminate between the two potential clinical syndromes. In this study a highly reproducible model of reversible liver failure in the form of a ¾ partial liver resection in rats was selected. This model emulates a seriously compromised liver, with failure in the beginning followed by progressive regeneration. Several previous studies have established that 100 % of such animals will recover [214-219]. Thus, the purpose of these experiments was, by using an animal model; to investigate the effects of IV administered PFOB on the recovery of a liver failure patient. They also served to preclude institutional manufacturing differences as the formulation of the UP-CSIR PFOB is similar to that of Oxygent.

5.1.2 Materials and methods

Animals

The experiments were conducted on 56 healthy female Sprague-Dawley rats of approximately 200 g each. These were housed under temperature controlled conditions in Macrolon type 3 cages with a 12 hour light-dark cycle, with sterilized wood shavings for bedding, access to standard rat food pellets and water with 10 % glucose at the University of Pretoria biomedical research center.

Experimental design (table 5.1.1)

The experimental groups were composed of 16 sub-groups in a cross-tabulated design aimed at discriminating between the effects of the surgery and the test substance (PFC). Half the animals received surgery (LI: liver injury) and the other half did not. In turn, half of each of the above received IV injections of either the test substance (PFC) in high (3 ml, 5 g/kg) or low doses (1 ml, 2 g/kg), or saline controls (3 ml). Acute and sub-acute toxicity effects were investigated by terminating experiments at either short (2-day) or longer (4-day) durations.

Table 5.1.1 The experimental sub-groups

		PFC		Saline	
Doses (day1)		LI (+)	LI (-)	LI (+)	LI (-)
Low	2 g/kg	6	6	6	6
High	5 g/kg	6	6	6	6
Durations	Terminations (3 of each dose group above)				
Short	Day 2	6	6	6	6
Long	Day 4	6	6	6	6
	Total surgery	12		12	
	TOTAL				48

Perfluorocarbon composition and dosing

Perfluorooctylbromide-lecithin emulsions were prepared according to the method of Moolman *et al*, as previously described by our group [10,88,94]. Sterile, deionized, autoclaved water was used to make up the PFOB-lecithin emulsion to 20% v/v concentration. pH was adjusted to 7.35 prior to drawing up the IV injections.

PFC doses were provided as either ‘high’ or ‘low’. The high dose (5 g/kg) was 3 ml of 20 % PFC in a 200 g rat, which was calculated to simulate exposure to the IV entry of one liter of 20 % PFC into an adult human. Hypervolumia was prevented in the animals by prior blood sampling of an equivalent volume. The low dose (2 g/kg) was chosen as 1 ml, i.e. 1/3 of the high dose. Saline dose controls (3 ml) were used as controls for the test substance. Surgical controls, i.e. surgeries without any additional treatments were also performed. All doses were introduced through the tail vein.

Liver injury (LI) model

As per the protocol first described by Higgins and Andersen in 1931 [214-219], 3/4 liver resections were carried out (on day 0) on one half (N = 24) of the animals. Briefly, while the animals were under isoflurane anesthesia, a midline incision was made, followed by complete liberation of all liver ligaments to allow the ligation of the pedicles of the median and left lateral lobes i.e. they were scissor clamped, tied off with suturing line and resected. Thereafter, the midline was sutured shut and the animals were allowed to recover. Each procedure took approximately 10 minutes. Prior to the above, 8 rats were used for perfecting the surgical procedure and their organ weights and blood indices were included as healthy controls (baselines) relative to the experimental groups.

For the anesthesia, recovery, pain and toxicity scoring protocols please refer to Appendix B.1.

Analyses

On days 0, 2 and 4, 1 ml blood samples were taken from the tail vein of all animals for blood biochemistry and haematology (tables 5.1.2,3). Upon termination of the 2 and 4 day groups, body, liver, left kidney, lungs and spleen weights were measured. The organs were first examined for macroscopic pathology and hematoxylin and eosin histology.

Statistical methods are as presented in Appendix B.1. No differences could be detected between the high-dose and low-dose PFC groups in the raw data and these were consequently included as one group in subsequent comparisons. The following sub-groups were compared for each of the measured variables to discriminate between the effects of the surgery and the PFC:

1. The surgical versus non-surgical groups at 2 and 4 days (PFC + saline).
2. The 2 versus 4 day surgical groups (PFC + saline).
3. The PFC versus saline non-surgical groups.
4. The PFC versus baseline (no interventions) non-surgical groups.
5. The saline versus baseline non-surgical groups.
6. The 2 and 4 day surgical groups versus the baselines.
7. The 2 and 4 day non-surgical groups versus the baselines.

Only significant ($p \leq 0.05$) or marginal ($p > 0.05 \leq 0.1$) differences between groups are mentioned below.

5.1.3 Results

Table 5.1.2 provides an explanation of the measured variables and their units. Table 5.1.3 provides the mean ± standard deviation of the relevant organ and body weights, blood biochemistry and haematological indicators.

Table 5.1.2 Measured variables and units

Variable	Explanation	Unit
LI	liver injury	
PFC	perfluorocarbon	
SAL	saline	
BW	mean body weight	g
+ and -	with and without	
ΔBW	change in mean body weight	g
spleen	mean spleen weight	g
spleen/BW	mean percentage spleen to body weight ratio	%
Δspleen/BW	mean change in percentage spleen to body weight ratio	%
liver	mean liver weight	g
liver/BW	mean percentage liver to body weight ratio	%
Δliver/BW	mean change in percentage liver to body weight ratio	%
Alb	mean plasma albumin concentration	g/l
ALT	plasma alanine amino transferase concentration	U/l at 37 ^{o}C
AST	plasma aspartate amino transferase concentration	U/l at 37 ^{o}C
Urea	plasma urea concentration	mmol/l
Bili-T	plasma total bilirubin concentration	µmol/l
Ammo	plasma ammonia concentration	µmol/l
RCC	blood red cell count	x 10^{12}/ l
Hkt	hematocrit	% l/l
WCC	blood white cell count	x 10^{9}/ l
Ab-Neutr	absolute neutrophil count	x 10^{9}/ l
Ab-Lymp	absolute lymphocyte count	x 10^{9}/ l
Ab-Mono	absolute monocyte count	x 10^{9}/ l
Plt-C	platelet count	x 10^{9}/ l

Table 5.1.3 Weight changes, biochechemistry and haematology

		Groups							
Variable	**Baseline (N = 24)**	**2-days +LI+PFC (N=6)**	**2-days +LI +SAL (N=3)**	**2-days -LI +PFC (N=6)**	**2-days -LI +SAL (N=3)**	**4-days +LI +PFC (N=6)**	**4-days +LI +SAL (N=3)**	**4-days -LI +PFC (N=6)**	**4-days -LI +SAL (N=3)**
BW	210.97±27.91	215.62 ±9.01	204.73 ±13.68	207.13 ±29.13	222.60 ±8.28	211.82 ±6.58	183.30 ±21.71	225.50 ±7.40	232.70 ±8.62
ΔBW		-29.45 ±16.28	-13.97 ±9.16	-3.42 ±2.56	0.40 ±3.40	-25.60 ±5.30	-18.63 ±5.08	-5.20 ±7.78	0.70 ±4.59
spleen	0.688±0.269	0.637 ±0.142	0.542 ±0.305	0.652 ±0.059	0.540 ±0.023	0.756 ±0.286	0.472 ±0.033	1.02 ±0.38	0.56 ±0.11
spleen/BW	0.326 ±0.111	0.262 ±0.068	0.246 ±0.138	0.314 ±0.050	0.243 ±0.003	0.318 ±0.118	0.235 ±0.020	0.44 ±0.15	0.24 ±0.04
Δspleen/BW		0.064 ±0.068	0.080 ±0.138	0.012 ±0.050	0.083 ±0.003	0.008 ±0.118	0.091 ±0.020	-0.114±0.146	0.085 ±0.04
liver	7.364±1.008	5.107 ±0.528	4.307 ±0.673	8.008 ±0.738	6.818 ±0.634	6.090 ±0.724	5.147 ±0.713	8.311 ±0.596	6.662 ±0.764
liver/BW	3.523 +0.457	2.104 ±0.351	1.966 ±0.269	3.842 ±0.399	3.078 ±0.394	2.566 ±0.300	2.559 ±0.352	3.605 ±0.228	2.874 +0.342
Δliver/BW		1.419 ±0.351	1.557 ±0.269	-0.319 ±0.399	0.445 ±0.394	0.957 ±0.300	0.964 ±0.352	-0.082 ±0.228	0.649 ±0.342
Alb	43.8 ±2.1	33.1 ±1.8	36.17 ±2.23	38.07 ±2.27	47.70 ±3.25	31.20 ±2.80	33.13 ±2.27	35.48 ±2.08	41.70 ±0.95
ALT	44 ±6	338 ±202	450 ±223	53 ±19	62 ± 33	66 ±12	56 ±5	39 ±8	41 ±9
AST	65 ±9	541 ±180	891 ±723	80 ±27	66 ±15	123 ±29	81 ±9	48 ±6	50.7 ±4.9
Urea	7.4 ±0.9	6.2 ±1.3	6.9 ±3.2	5.2 ±1.2	6.1 ±1.7	5.2 ±1.4	5.5 ±1.5	6.3 ±0.9	5.8 ±4.9
Bili-T	4.1 ±0.8	23.8 ±4.7	14.3 ±2.7	4.2 ±1.2	5.2 ±1.5	6. 9 ±1.9	5.6 ±1.4	5.5 ±2.9	5.6 ±2.8
Ammo	52.1 ±20.8	76.2 ±32.5	123.3 ±136.7	31.6±5.3	32.8 ±15.7	53.8 ±16.5	44.2 ±17.4	29.2 ±9.03	49.6 ±15.2
RCC	8.63 ±0.95	7.34 ±0.78	6.25 ±2.30	8.65 ±0.64	8.24 ±0.18	7.46 ±0.70	8.17 ±0.24	8.54 ±0.47	8.70 ±0.23
Hkt	43.5 ±1.4	36.2 ±0.04	30.7 ±11.0	42.5 ±1.9	40.0 ±1.7	38.2 ±3.1	41.7 ±1.5	42.0 ±1.80	42.7 ±0.06
WCC	7.90 ±1.29	10.35 ±3.75	13.58 ±6.45	5.72 ±1.17	4.94 ±1.31	5.98 ±0.92	12.99 ±1.67	6.08 ±1.78	7.53 ±1.36
Ab-Neutr	0.76 ±0.41	4.64 ±1.77	8.26 ±3.47	1.12 ±0.41	1.15 ±0.72	2.70 ±1.18	4.32 ±0.84	0.65 ±0.61	0.58 ±0.23
Ab-Lymp	6.82 ±1.35	5.20 ±2.33	3.82 ±2.76	4.35 ±0.90	3.23 ±1.37	3.34 ±1.10	7.05 ±1.27	5.14 ±1.52	6.48 ±1.36
Ab-Mono	0.24 ±0.21	0.33 ±0.20	1.27 ±0.99	0.14 ±0.08	0.50 ±0.4	0.27 ±0.20	1.53 ±0.92	0.20 ±0.12	0.34 ±0.04
Plt-C	491 ±387	783 ±145	803 ±209	686 ±130	555 ±425	425 ±207	550 ±109	366 ±158	1051 ±112

Notes:

1. In this table the high-dose and low-dose PFC groups were summed as no difference could be detected between them in the raw data.
2. All values are presented as mean ± std deviation.
3. Δ = change in value.

General observations

All animals in the control and experimental sub-groups survived for the duration of the trial. In the first two days all surgical animals demonstrated signs of trauma in the form of hunched postures, pilo-erection (ruffeled coats), red circles around their eyes and gnawing at the wood-shaving bedding material (pain). These signs decreased from 2 to 4 days. In the non-surgical sub-groups (baselines, PFC or saline) this behaviour was not present. One animal was lost from the trial due to disembowlment following the gnawing off its abdominal sutures. This loss did not impact the results as the animal was of the surgical control group.

Body weight loss was found in all groups save the non-surgical saline injected sub-group. This was greatest in the surgical groups, but did not significantly differ in the PFC or saline, 2 or 4 day sub-groups. No increases in the spleen to body weight ratios were found in the PFC versus saline sub-groups. Although kidney and lung weights were measured, no differences between the sub-groups and the baseline animals were detectable and this data was consequently excluded from Table 3. A significant increase in the liver to body weight ratios was found in all surgical versus non-surgical groups at 2 days ($p < 0.001$) and at 4 days ($p = 0.003$). In the surgical PFC or salines at 2 days and 4 days there was no difference in the liver to body weight ratios. The rate of regeneration of the livers of the surgical PFC or saline sub-groups was also not different. Thus, the PFC did not impact liver re-generation following severe injury (figure 5.1.1).

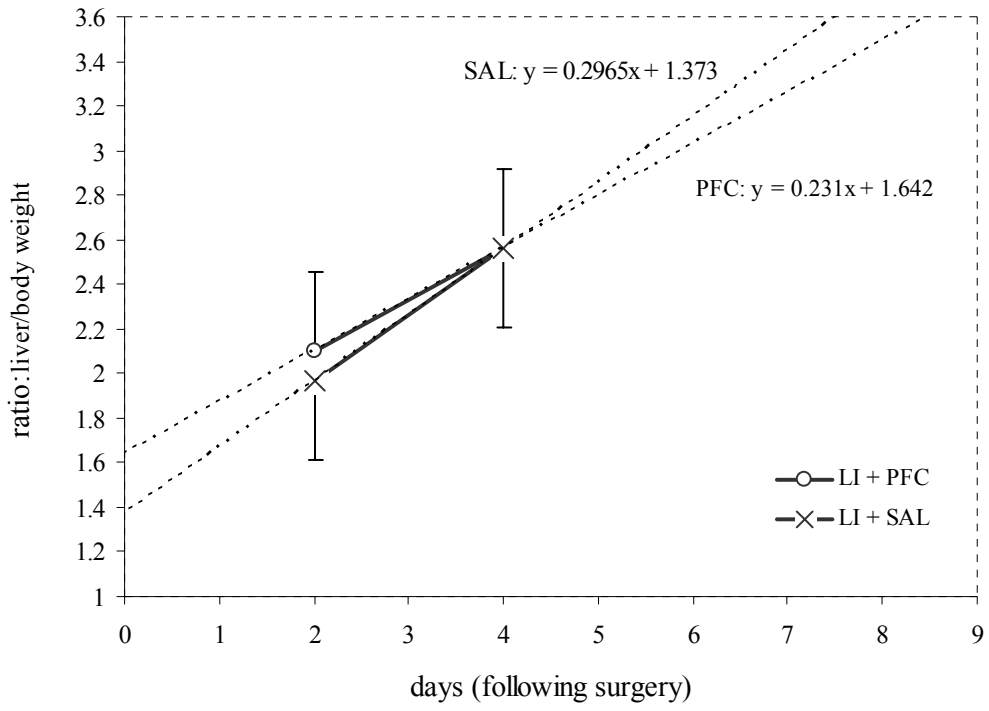

Figure 5.1.1 Liver regeneration projections, assuming linear re-growth.
The rate of regeneration after liver injury and IV dosing of PFC or saline is not significantly different. The y-intercept indicates the amount of liver initially resected. A liver/BW value of 1.5 equates to approximately a 60 % liver weight resection. The projected time to complete liver weight regeneration, i.e. to a liver/BW ratio of 3.5, is 7-8 days. This duration is in agreement with prior experience with this surgical model [214-219].

Biochemistry

Blood albumin in the surgical versus non-surgical groups (PFC + saline) was significantly decreased at 2 days ($p = 0.005$) and 4 days ($p = 0.003$). The non-surgical PFC sub-groups had significantly lower levels than both the salines and the baselines ($p = 0.001$ and $p < 0.001$ respectively). Thus, both the surgeries and the PFC decreased albumin production by the liver.

The liver enzymes ALT and AST, reflecting liver damage, were significantly increased in all surgical versus non-surgical groups, at 2 days (ALT $p = 0.001$, AST $p = 0.001$) and at 4 days (ALT $p = 0.001$, AST $p < 0.001$). At 4 days, levels were significantly higher in the surgical groups (PFC + saline) versus the baselines (ALT p

= 0.001, AST $p < 0.001$). Therefore, the surgeries rather than the PFC caused liver damage.

Bilirubin, reflecting hepatic bile removal, was significantly increased in the 2 versus 4 day surgical groups ($p = 0.001$) and also increased in the (PFC + saline) surgical versus non-surgical sub-groups at 2 ($p = 0.001$), but not at 4 days. The (PFC + saline) 4 day surgical group was significantly increased relative to the baselines ($p = 0.003$), but not the non-surgical group. Thus, surgery immediately decreased bilirubin clearance, followed by a return to normal by day 4. PFC had no effect.

Urea, reflecting hepatic (nitrogenous-waste) metabolism, was significantly lower in the non-surgical PFC and saline groups versus the baselines (PFC $p = 0.009$ and SAL $p = 0.024$ respectively). It was also significantly lower in the (PFC + saline) surgical and non-surgical 4 day sub-groups versus the baselines (+LI $p = 0.005$ and –LI $p = 0.008$ respectively). Interestingly, urea was slightly higher in the 2 versus 4 day surgical groups. It appears that neither the surgeries nor the PFC had any effect on urea production.

Ammonia, reflecting blood nitrogenous toxin levels, was increased in the 2 day versus 4 day surgical groups (but not significantly). The (PFC + saline) surgical groups at 2 days were significantly increased relative to the non-surgicals ($p = 0.002$), but only marginally increased at 4 days ($p = 0.064$). The non-surgical PFC groups (2 + 4 days) were marginally lower than the salines ($p = 0.068$) and significantly lower than the baselines ($p = 0.006$). Thus, similar to bilirubin, surgery decreased ammonia clearance with recovery to normal by day 4. Of interest, the presence of the PFC was associated with decreased ammonia levels.

Haematology

Red cell count (and hematocrit) were significantly decreased in both the (PFC + saline) 2 and 4 day surgical versus non-surgical groups (for RCC $p = 0.005$ and $p = 0.004$ respectively). The 4 day surgical group was significantly lower than the baselines ($p < 0.001$) but not so in the non-surgical group. The non-surgical saline group was marginally lower than the baselines ($p = 0.055$). RCC and Hkt were therefore decreased by the surgeries rather than the PFC.

White cell counts were increased in surgical versus non surgical groups, significantly so at 2 days ($p = 0.011$) but not at 4 days. The baselines were significantly increased relative to the non-surgical PFC groups ($p = 0.005$) but not the salines. Ab-Neutr was significantly increased in the surgical versus non-surgical groups at both 2 days ($p < 0.001$) and 4 days ($p < 0.001$). In the 2 day group this was significantly larger than in the 4 day surgical group ($p = 0.031$) and at 4 days the surgical groups had significantly larger values than the baselines ($p < 0.001$). In Plt-C the surgical 2 day groups had significantly higher counts than 4 days groups ($p = 0.004$). The surgery therefore substantially increased the WCC (especially the neutrophils) while the PFC had no apparent effect.

Macroscopic observations and histology

White droplets were macroscopically noted in the spleens and to a lesser extent in the kidneys and livers in the PFC injected 2-day animals, both surgical and non-surgical. In the 2-day surgical groups (PFC + saline) the liver remnants were blanched and tough relative to healthy livers. In the 4-day surgical groups the livers had grown back to approximately ¾ their original size and were more similar in color and texture to the (healthy) livers of the baselines, than the 2-day group. In the 4-day PFC injected groups, no white droplets could be discerned in any of the organs.

H and E histology of the livers revealed vacuolar swelling with cytoplasmic droplets and an increase in mitosis and apoptosis that correlated with the surgeries. This was more severe in the 2 versus 4 day groups. Vacuolated Kupffer cells, associated with the PFC, were especially detected in the 2-day high-dose animals in the non-surgical groups. Low-dose animals did not demonstrate this. Micro-granulomas were noted in the Kupffer cells in the 4 day PFC injected animals. In the spleens of the PFC injected animals vacuolated reticulo-endothelial cells in the blood sinuses of the red pulp were visible. Kidney sections demonstrated no specific findings. In the lungs, atelectasis presumably associated with anesthetic euthanisation, was found in the majority of the animals. Leucocyte aggregations and alveolar macrophage hypertrophy was observed in several of the PFC injected surgical and non-surgical animals in the 2 day and 4 day groups.

5.1.4 Discussion

The surgical method employed in this study was selected to model the potentially reversible acute liver failure syndrome seen in human patients. However, animal models make extension to the human clinical scenario difficult due to, amongst other reasons, species differences in response to test substances, the degree of reversibility, the disease process duration and the degree of involvement of other organ systems [220,221]. The ¾-partial liver resection in rats is an attractive model in that it is well-described, technically feasible, highly reproducible, non-toxic yet severe, but reversible within a time period sufficient to enable study. Although species differences must obviously exist, extension to the human scenario is reasonable in view of prior findings of PFOB non-toxicity in clinical studies [202,206,207].

The lack of PFOB toxicity was evident in the absence of differences between the control and experimental sub-groups for the parameters studied. Specifically, no changes in the haematological indices as markers of systemic toxicity were apparent in the PFC versus saline injected groups. Similarly, the biochemical indices including bilirubin clearance, urea production and liver enzymes levels were also not impacted by the PFC. Bearing in mind the findings it is therefore safe to assume that this study was successful in meeting its aims. That is, PFC non-toxicity may be extended to include the liver failure case. This was possible owing to the non-toxic surgical model not complicating the effects of the test substance, the cross-tabular design, the measurement of a large number of variables and the given ability to investigate the impact of the PFOB on the rate of liver regeneration following the injury.

The finding that PFOB did not impact the rate of liver regeneration following damage is of particular interest in view of the severity of liver failure in patients undergoing bioartificial liver treatments. In compromised livers, metabolic hypoxia may be significant. We found that PFOB actually decreased blood ammonia levels, possibly owing to improvements in blood oxygenation facilitating liver toxin clearance. A potential benefit may therefore lie in ameliorating the deleterious effects of ammonia. Of additional physiological interest: The decrease in albumin production associated with the PFC may have been due to the presence of the phospholipid lecithin surfactant in the emulsion. This may have activated a negative feedback mechanism

regulating blood albumin levels and thereby, blood viscosity. As previously stated, prior clinical studies [206,207] have demonstrated improvements in blood viscosity following PFOB injection. The 2nd phase flu-like symptoms post-operatively found [202] may also be correlated with the macrophage hypertrophic changes and leucocyte aggregations found in our 4-day lung histology specimens.

To conclude, this study did not provide any indication that IV injected PFOB was toxic at the concentrations employed in either healthy or severe liver injury scenarios. PFOB also had no impact on the rate of liver regeneration following the surgically induced damage. Bearing in mind the results of prior human clinical studies it is reasonable to assume the safety of using a PFOB emulsion in bioartificial liver support system treatments.

5.2 Standardization criteria for an ischemic surgical model of acute hepatic failure in pigs

Nieuwoudt M, Kunnike R, Smuts M, Becker J, Stegmann GF, Van der Walt C, Neser J, Van der Merwe S.

Biomaterials 2006: 27(20);3836-45.

5.2.1 Introduction

The verification of the efficacy of a supportive therapy for acute hepatic failure (AHF), such as a BALSS, requires the establishment of a reliable large animal model of AHF. Two categories of models have been identified as potentially useful in this regard: Firstly, toxic models involve inducing hepatotoxicity with substances such as galactosamine [222,223] and acetaminophen [224,225], and secondly, surgically induced AHF models involve either rendering the animal anhepatic [5,226] or devascularizing the liver by means of temporary [227] or permanent [228,229] hepatic artery ligation with portocaval anastomosis (PCA).

In this study a surgical ischemic model of AHF was investigated for the following reasons: First, total hepatectomy models lack the *in vivo* biochemical effects of a failing liver while devascularization models do not. Second, the total devascularization model used in this study is irreversible, without the potential for liver regeneration as may be present in certain toxic models, and culminates in the animal's demise. Having said this, surgical models are prone to instability and require the development of considerable surgical skill prior to standardization [230]. Several different species have been used in the development of these models; however, there is considerable difficulty involved in scaling a BALSS from a small animal to a large animal [220]. Thus, the porcine model is often used as these animals are available in large numbers and are metabolically and physiologically similar to humans [220,230]. While the model described in this study is not unique, the methods that have been used in standardizing it are.

The statistical analysis of the acquired data in this study, together with clinical experience, was used to determine trends in clinical change and to define model standardization criteria. The purpose of the criteria is to enable the exclusion of animals that present with systemic or biochemical characteristics other than that of AHF as defined by the findings of this study. The expectations were that several prognostic factors would simultaneously determine survival.

Historically, the criteria of Hickman and Terblanche (1991) [231], have been used to establish the characteristics that an ideal model of AHF should satisfy, including reversibility, reproducibility, death by liver failure, sufficient duration for clinical intervention, a large animal model and minimal risk to personnel. Although these criteria have helped direct the development of animal models in the recent past, they are not specific in terms of defining clinical or biochemical characteristics of AHF in any model. No prior studies have attempted to do this. In the human scenario the King's college criteria were defined to provide an estimation of prognosis in AHF, and thereby to aid decision making in terms of potential transplantation. The multivariate analysis of large quantities of hospital patient statistical data was used to establish these criteria [52,53]. No similar criteria exist for animal models.

The availability of specific criteria for each animal model of AHF is highly desirable since these will aid in the establishment of more reliable prognostic indices than have previously been available. Since animal AHF models are inherently complex, invariably use small groups, and are predisposed to inter-individual variation, the establishment of such criteria will also be useful for establishing uniform control and treatments arms in the evaluation of supportive therapies. Thus, more accurate comparisons will result and spurious conclusions may be prevented regarding benefits that occurred by chance. Additionally, clinical interventions are likely to improve and expenses may be limited through the earlier exclusion of non-ideal subjects.

5.2.2 Materials and methods

Study protocol

Experiments were conducted on 15 female Landrace pigs with a mean body weight of 29.2 kg. Each experiment started at a baseline preceding surgery, with T = 0

immediately following surgery and continued until each animal expired. Systemic measurements were made continuously (electroencephalogram (EEG), electrocardiogram (ECG) and arterial blood pressure (ABP)). Arterial blood-gas (ABG) and electrolyte analysis was performed hourly, while metabolic/biochemical sampling was performed every four hours using mixed venous blood, for the duration of each experiment.

Animal preparation, anaesthesia and catheter placement

Acclimated pathogen-free pigs living under environmentally controlled conditions were used in all experiments. These were anesthetized during the surgeries and kept sedated subsequently. Ventilation and volumetric management was as for human ICU patients. Carotid, jugular and urinary catheters were inserted for monitoring. For a complete description of these protocols refer to Nieuwoudt *et al* [213] and Appendix B.2.

Liver devascularization

A midline xyphopubic laparotomy was performed (Diathermy/Coagulator 2000, Electromedical systems). The portal vein was isolated and cleared from the bifurcation in the porta hepatus to the splenic vein and all other connecting veins were ligated and divided. All connecting ligaments and peritoneal attachments were transected. The lesser omentum was opened. The intestines were left inside the animal's abdomen. All structures in the hepatoduodenal ligament except the portal vein were ligated with number 2/0 Silk and divided. The hepatic artery and accessory branches to the liver were also ligated and divided. The infra-hepatic inferior vena cava (IVC) was isolated and cleared to the level of the renal veins. The infra hepatic supra renal IVC was then completely clamped with 2 vascular exclusion clamps $\pm$ 40 mm apart and a $\pm$ 15 mm by $\pm$ 7.5 mm window was made in a lengthwise direction by excising part of the wall of the IVC. The portal vein was cross-clamped with two vascular clamps $\pm$ 40 mm apart then transected. An end-to-side anastomosis of the extra-hepatic portal vein onto the IVC was performed and the period of portal occlusion (Ischemic_time] was recorded. A bolus dose of heparin (3-5 units/kg) was infused with 1000 ml Ringers lactate to prevent clotting at the anastomotic site. The perfusion of the intestinal organs was evaluated by observing capillary filling. A return to pink was regarded as normal. In the event of splanchnic congestion the pig was sacrificed. The abdomen was flushed with 1L of warmed Ringers lactate. The

linea alba was sutured with a simple continuous number 0 nylon. The skin and subcutaneous tissue was closed in one layer with number 2/0 nylon in a simple continuous suture pattern.

Note: In this study the data of animals that had only undergone a laparotomy with subsequent sedation is not presented. Although these 'sham-operated controls' have been claimed as a necessity for the establishment of surgical models of AHF [232,233], the animals in question demonstrated no significant alterations in the systemic or biochemical variables of interest. This is in apparent agreement with the findings of similar studies [227,229]. Thus, this data does not contribute to the definition of standardization criteria. It is also useful to bear in mind that the intensive care regimen aimed at actively maintaining cardiovascular and hemodynamic stability. This study was viewed as the standardization of surgical control data prior to the evaluation of a BALSS.

Intensive care and clinical measurements

Following surgery the animal was transferred to an intensive care unit (ICU) where continuous ventilation, sedation and hydrodynamic stability was maintained until the cessation of cardiac function, which was defined as the point of death in this study. Systemic and biochemical indices (table 5.2.1) were also measured for the total duration as described in Appendix B2.

Post Mortem

After termination complete necropsies were performed to establish the positioning of the catheters, the patency and integrity of the PCA as well as the macroscopic and histopathological changes induced by the procedure. Aerobic bacterial cultures were performed on the intestines and a wide range of other organs.

Statistical analyses

Microsoft Excel was used for general processing while Statistix 8 was used for data analysis. All values are presented as the mean $\pm$ the standard deviation. Linear trends were fitted to each data set, revealing a rate of increase or decrease in that variable. For homeostatic systemic variables, a mean value (average) was calculated. Mean and standard deviations were also calculated for all rates or averages. Since the purpose was to define standardization criteria derived from statistical trends and clinical

experience, only the analysed data is presented. Extensive raw data from the ischemic model has previously been reported [227,229] and for this reason only the absolute and homeostatic mean values and rates of change are provided.

Non-parametric (distribution-free) Spearman correlation coefficients (appropriate for small data sets) were calculated for each variable's rate of change or static mean with the animal's duration of survival. An average coefficient was then calculated from these, with a perfect correlation showing a magnitude of one. The quality of the linear fit, in the form of a coefficient of regression (R^2), is not presented below. These values are the numerical square of the (parametric) Pearson correlation coefficient, which bears some relation to the Spearman correlation coefficient. In general, Spearman correlations return more conservative values than those of Pearson. Paired t-tests ($p<0.05$) were calculated to indicate the significance of change of each variable from the mean T = 0 value until termination.

5.2.3 Results

Table 5.2.1 provides an explanation of the systemic and biochemical variables and their units, while table 5.2.2 presents absolute values, mean rates of change and significance of change. In the surgical period ($T<0$), systemic variables that were measurable *on-line* were correlated with the duration of survival (figure 5.2.1). These variables were useful at this time for three reasons: 1. the initial model was healthy, 2. Systemic indices change rapidly and 3. Only those animals that were stable were able to progress beyond the surgery. Thus, the experiment could potentially be terminated at this point.

Table 5.2.1 Measured variables

Variable name/s	Description	Units
Survival	survival duration from T=0	hours
Mass	animal body weight at baseline	kg
Ischemic_time	portal vein clamp duration	minutes
Bl.loss_Tot	total blood loss in experiment	ml
Urine, _Tot	volume of urine in experiment	ml
MAP, _pre, _isch, _post, r	mean arterial pressure	mmHg
Pulse, _pre, _isch, _post	pulse	beats/min
Temp, _post	temperature	^{o}C
pH, _I, ave_	pH	
pO_2, ave_, r	partial pressure of O_2.	mmHg
pCO_2, ave_, r	partial pressure of CO_2.	mmHg
HCO_3act, ave_	[activated bicarbonate]	mmol/l
Glu, ave_	[glucose]	mmol/l
EEG_Ff_a/d, T=0, r EEG_Fc_a/d, T=0, r	ratio of mean alpha to delta frequencies in frontal or central brain regions	
EEG_Pf_a/d, T=0, r EEG_Pc_a/d, T=0, r	ratio of relative power of alpha to delta spectra in frontal or central brain regions	
Lactate, r	[lactate]	mmol/l
Pyruvate, ave_, r	[pyruvate]	mmol/l
Lac/Pyr, r	lactate to pyruvate ratio	
Ammonia, r	[ammonia]	µmol/l
BilirubinTOT, r	[total Bilirubin]	µmol/l
Glutamine, r	[glutamine] in plasma	µmol/l
BcAA, r	[branch-chain amino acid]	µmol/l
AroAA, r	[aromatic amino acid]	µmol/l
BcAA/AroAA, r	ratio of above	
Total AA, r	[total amino acid]	µmol/l
LD, r	[lactate dehydrogenase]	IU/l
ALT, r	[alanine aminotransferase]	IU/l
AST, r	[aspartate aminotransferase]	IU/l
ALP, r	[alkaline phosphatase]	IU/l
GGT	[gamma glutamyl transferase]	IU/l
Na+, r	[sodium ion]	mmol/l
K+, r	[potassium ion]	mmol/l
Creatinine, r	[creatinine]	µmol/l
Urea, r	[urea]	mmol/l
Fluids_Tot	total volume of fluids provided IV	ml
Hb, r	[hemoglobin]	g/dl
Hkt, r	hematokrit	%
PT, r	prothrombin time	sec
APTT, r	activated thromboplastin time	sec
D-dimers	[D-dimer]	µg/l
Fibrinogen, r	[fibrinogen]	g/l
PLT, r	platelet count	10^9/l
WBC, r	white blood cell count	10^9/l
Factor II, r	percentage of normal factor II	%
Factor V	percentage of nomal factor V	%
Factor VII, r	percentage of normal factor VII	%
Factor IX	percentage of normal factor IX	%
Factor X, r	percentage of normal factor X	%
AntiThrombin, r	percentage of normal antithrombin	%

Notes: 1. Variables with suffices and prefixes: ***_pre*** = baseline, e.g. MAP_pre. ***_isch*** = during ischemic time in surgery, e.g. MAP_isch. ***_post*** = value at T=0, e.g. MAP_post. ***r*** = rate of change, e.g. rAmmonia. ***ave_*** = static mean, e.g. ave_Pulse. ***_I*** = initial value, e.g. K^+_I. ***_Tot*** = total, e.g. Bl loss_Tot. ***T=0*** = value mmediately after surgery.2. Square brackets [ ] indicate the concentration of the enclosed variable in blood.

Table 5.2.2 Values of measured variables

Variable name	Initial Values			*Terminal value*	Mean value (ave_)	Mean rate of change/hour (r)	Significance (p < 0.05)
	Baseline	Ischemic time	T=0				
Survival			17.1 ± 8.3	20.5 ±5.1			
Mass [weight]	29.2 ±6.2						
Ischemic time		18.6 ±8.2					
Bl.loss_Tot				174.4 ±243.2			
Pulse	83.8 ±16.1	160.3 ±29.3	139.2±34.3	128.5±48.1	117.7 ±23.1		0.839
MAP	83.8 ±15.9	43.5 ±14.0	72.4±17.5	45.18±11.66		-1.83 ±0.62	0.000
Urine			102.7 ±95.1	29.2±52.5		-7.86±6.65	0.003
Urine_Tot				927.3 ±533.8			
Fluids			893.58±714.9	627.08±384.36			
Fluids_Tot				3439.7±1136.5			
EEG_Ff_a/d	5.07±0.71		4.91±1.08	6.53±1.84		*-0.13±0.27	0.004
EEG_Fc_a/d	4.68±0.23		4.69±0.70	5.28±0.81		*-0.03±0.16	0.035
EEG_Pf_a/d	1.05±0.68		1.24±1.26	0.74±0.71		*-0.05±0.03	0.439
EEG_Pc_a/d	0.60±0.26		0.74±0.74	2.65±3.95		*-0.06±0.05	0.276
Hb			9.33±1.71	6.33±1.43		-0.18±0.11	0.001
Hkt			32.85±8.01	20.10±5.79		-0.70±0.32	0.002
Temp			35.6±0.5	37.61±1.3	37.41±1.3	0.09±0.06	0.000
pH			7.31±0.10	7.40±0.15	7.41±0.07	nd	0.160
pO_2			138.6±38.3	92.3±26.8	115.6±20.4	-2.1±2.1	0.012
pCO_2			61.1±21.7	47.7±17.9	47.6±5.2	-0.9±0.9	0.033
HCO_3act			27.6±3.6	23.4±6.0	26.9±3.1	nd	0.064
Glucose			8.4±5.5	6.4±4.0	7.2±1.8	nd	0.295
Lactate			1.95±1.48	6.61±6.33		0.21±0.53	0.024
Pyruvate			0.13±0.05	0.28±0.19	0.22±0.09	0.005±0.009	0.027
Lac/Pyr			16.36±11.31	18.30±5.63	16.15±5.04	0.04±0.3	0.056
Ammonia			86.6±41.8	1402.7±506.8		64.2±31.9	0.000
BilirubinTOT			4.53±1.86	43.25±43.25		1.76±1.61	0.009
Glutamine			152.1±34.4	314.5±122.3		9.03±5.3	0.000
BcAA			381.2±62.2	246.6±45.8		-5.80±4.0	0.000
AroAA			111.2±26.2	182.8±37.9		3.86±2.0	0.000
BcAA/AroAA			3.58±1.05	1.37±0.25		-0.10+0.06	0.000
Total AA			2344.0±430.2	2967.3±815.3		31.4±48.2	0.064
LD			330.0±163.3	4890.4±5286.3		281.0±273.5	0.017
ALP			107.3±44.8	544.7±276.4		24.6±12.5	0.000
ALT			39.7±16.6	281.5±210.6		14.07±11.77	0.002
AST			64.4±67.2	4821.6±4593.8		329.9±262.6	0.007
GGT			18.9±6.8	23.67±11.2		nd	0.031
Na+			138.07±6.03	133.81±7.63		-0.28+0.40	0.015
K+			4.09±0.52	6.59±2.31		0.13±0.13	0.003
Creatinine			86.92±31.45	237.78±106.66		7.99±7.21	0.000
Urea			3.03±1.16	2.23±0.99		-0.05±0.07	0.025
PT			10.28±0.75	44.21±43.81		0.88±0.47	0.049
APTT			79.90±57.86	93.87±61.39		3.04±2.23	0.140
D-dimers			65.22±20.7	52.2±5.0		nd	0.146
Fibrinogen			2.47±0.65	0.55±0.36		-0.11±0.03	0.002
PLT			302.00±207.25	168.25±65.36		-14.05±7.23	0.215
WBC			7.72±5.79	24.63±8.89		0.46±0.19	0.119
Factor II			51.65±11.31	15.78±4.09		-1.75±0.60	0.000
Factor V			196±0	171.61±50.5		nd	0.161
Factor VII			57.64±13.47	12.28±6.18		-2.19±0.75	0.000
Factor IX			254.8±0	169.96±62.4		nd	0.002
Factor X			74.59±24.67	6.10±3.16		-3.19±1.17	0.000
AntiThrombin			91.43±14.48	44.35±12.50		-2.19±0.82	0.000

Notes. 1. * Trends calculated toward the lowest value, 2-4 hours prior to death. 2. nd = not discernable. 3. Baseline and T=0 values were taken to be equivalent for slow changing biochemical variables. 4. If the (r) value was (+) the variable increased over time. If (–) then the variable decreased over time.

The sign of the correlations indicates whether survival is benefited or disadvantaged by the absolute value of each variable. For example, the coefficient of Ischemic_time with survival is negative, thus, as the portal clamping time increases, survival decreases. A multivariate picture of survival was revealed. Variables that strongly correlated with survival included the pulse rate during portal occlusion (Pulse_ischemic = –0.65) and the mean arterial pressure following surgery (MAP_post = +0.48). Thus, the maintenance of cardiovascular and hemodynamic stability through fluid and inotropic provision was important in terms of survival. The duration of portal clamping prior to anastomosis (Ischemic_time = -0.31) was important presumably as a result of splanchnic congestion. Since only successful experiments were included, it was felt that the importance of this variable was underestimated in the results. The intactness of the anastomosis was of importance in that it determined the amount of blood lost, as was subsequently measured (Blood loss_Tot = -0.37). Body weight was found to bear some relation to survival possibly due to greater hemodynamic or thermal sensitivity in smaller pigs and an increase in the requisite surgical skill. However, this result may be misleading in that unsuccessful experiments were eliminated. Initially, the finding was that there was some difficulty in maintaining body temperature. Thus, the abdominal organs were not subsequently exposed during surgery. The temperature value provided at T=0 (table 4.2) is reflective of that immediately after surgery, rather than the subsequent thermal baseline measured following stabilization in the ICU.

The ratio of the frequency and relative power of the alpha to delta spectra of the EEG measurements in the frontal and central regions of the brain during surgery did indicate some correlation with survival (EEG_Pf_ad_T0 = +0.62), (EEG_Ff_ad_T0 = –0.41). However, since isoflurane and pentobarbitone were used as anaesthetics in this study it was assumed that a degree of suppression of frontal activity had occurred. Electrodes placed in the temporal and occipital regions were also prone to artefacts (results excluded) presumably due to animal positioning. Using the exclusion criteria (table 4.2.3) the data from three animals was excluded after the surgical period. The criteria that were violated included a case of excessive blood loss (Blood loss_Tot), two of excessively long ischemic times and in all three, survivals of less than 6 hours respectively.

Thus, in the period following surgery (T>0), the animal data that was used for analysis reduced from 15 to 12. In this period correlating absolute values with survival became impossible due to the extended duration of the experiments. The rates of change in the predominantly *off-line* biochemical indices then improved in terms of prognostic value (figure 4.2.2). That is, the sign and magnitude of each coefficient indicates the impact of an increasing or decreasing trend in that variable on the duration of survival. For example, the higher the rate at which ammonia accumulated (rAmmonia), the shorter survival. Significant correlations included those of accumulating plasma branch chain amino acids (rBcAA= +0.89), ammonia (rAmmonia = -0.77), Total urinary excretion (Urine_tot = +0.80), mean blood pH (ave_pH = +0.65), the rate of change of body temperature (rTemp = -0.62) and the losses of Hemoglobin (rHb = + 0.60) and Hematocrit (Hkt = + 0.54). In other variables of interest in AHF lower correlations were noted: Prothrombin time (rPT = +0.30), potassium (rK^+= -0.49), the liver enzymes (rALP = -0.28, rAST = -0.22, rLD = -0.21), total bilirubin (rBilirubinTot = +0.01), the clotting factors (Factors X = +0.35, VII = +0.34, II = +0.21), creatinine (rCreat = +0.46) and lactate (rLactate = +0.22). All of these variables indicated significant changes over the duration of the experiments (table 4.2). Each variable indicates a different aspect of AHF, thus, all were considered useful. There were also significant correlations between survival and variables that may be monitored *on-line*. Thus, prognosis may potentially be evaluated in *real-time* as opposed to after-the-fact. It was apparent in the trends that there was considerable inter-individual variation and this validated the need for the establishment of standardization criteria (table 5.2.3).

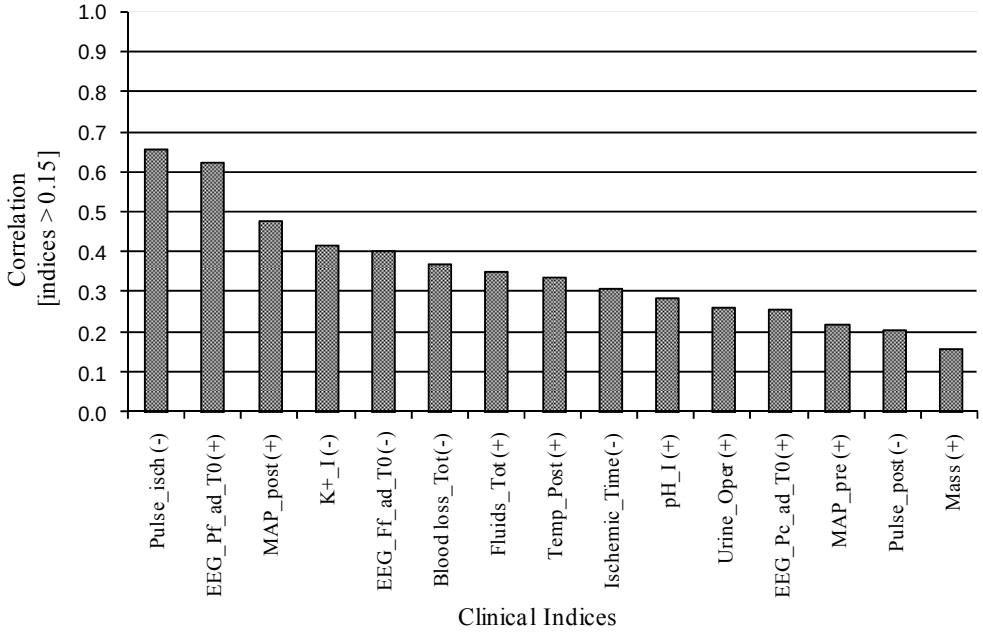

Figure 5.2.1 Magnitude of correlations of absolute values of systemic indices during surgery [T≤0] with duration of survival, N=15. Sign of correlation follows variable name, e.g. as ischemic pulse increases, survival decreases. Prognosis was multivariate

Post Mortem examinations:

A variable volume (60-200 ml) of serosanguinous abdominal effusion was present in most animals. In each case the PCA was found to be intact and patent with suspected complete ischemic necrosis of the liver extending from the edges and diaphragmatic surfaces to the hilus. There were smaller amounts of similar effusions within the thoracic cavity as well as a moderate to severe congestion and oedema in the lungs. The spleen, kidneys, and mesenteric lymph nodes showed variable congestion, while severe diffuse congestion and haemorrhage was observed in the small intestines in 7 of 12 animals. Histopathology revealed moderate to severe diffuse ischemic necrosis of hepatocytes characterised by cytoplasmic eosinophilia and nuclear pycnosis as well as nuclear dissolution in the severely affected foci. There was marked congestion and nephrosis in the kidneys with moderate to severe degeneration and necrosis of tubular epithelial cells. These findings are compatible with a severe functional renal failure of extended duration. No indications of DIC were found. Histopathological changes in the brain were characterised by moderate to severe congestion and oedema. Bacteriology: No unusual (significant) pathogens could be isolated from any of the cases.

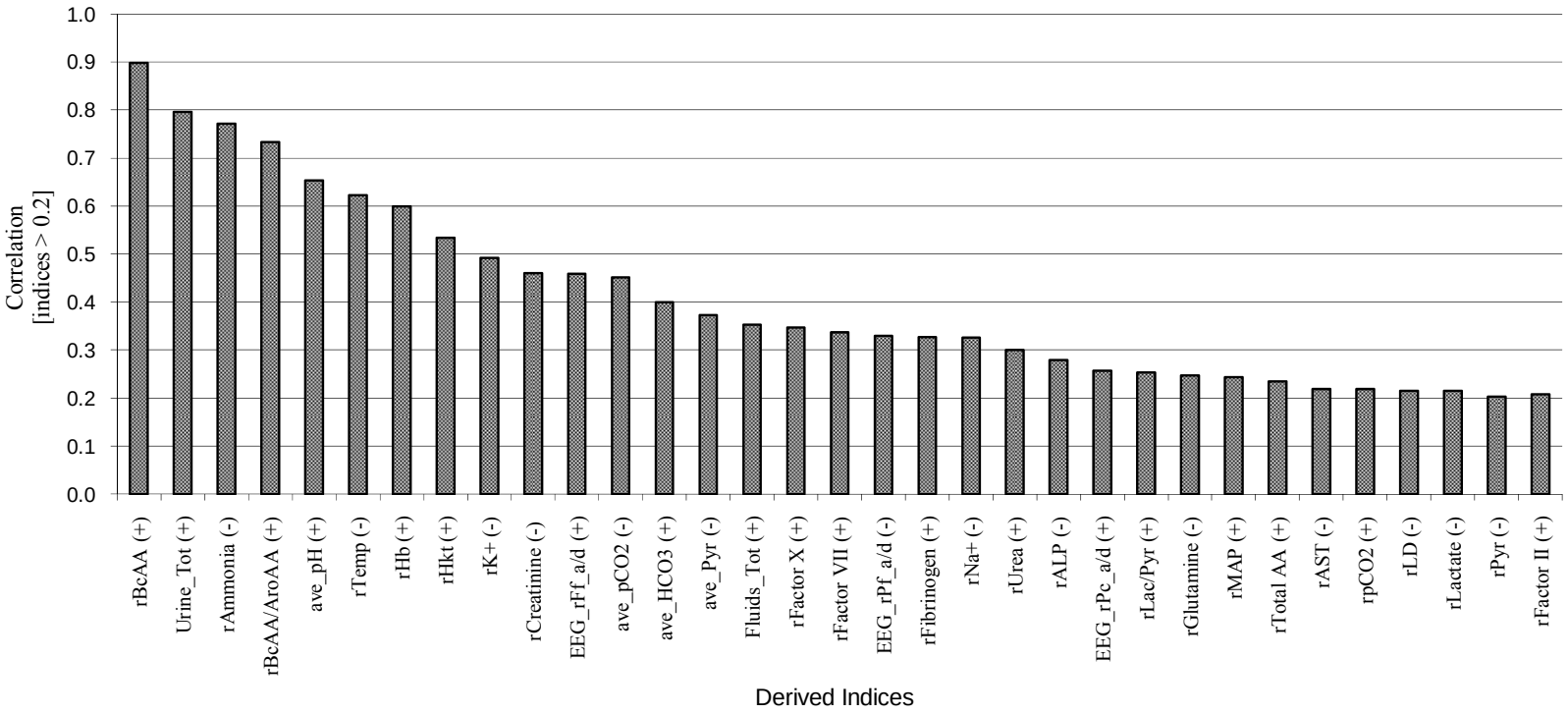

Figure 5.2.2 Magnitude of correlations of biochemical trends following surgery (T>0) with duration of animal survival, N=12. Sign of correlation follows variable name, e.g. As rAmmonia increases, survival decreases. A multivariate prognosis is apparent.

5.2.4 Discussion

Animal models that resemble the entire clinical syndrome of AHF in humans have not been successfully developed as yet [220]. Surgical or toxic animal models are often chosen to evaluate the efficacy of BALSS. Historically, two of the criteria of Hickman and Terblanche (1991) [231] that have proven the most difficult to meet include reversibility and reproducibility. Irreversible surgical models represent an attractive model for BALSS testing owing to the fact that they always end in death. However, AHF is intrinsically complex and the evaluation of support systems often relies on small sample sizes in experimental treatment or control arms. Thus, conclusively evaluating the benefit of the treatment may be difficult. This study describes systemic and biochemical parameters that may be used to define outcomes for an ischemic surgical model of AHF. These parameters facilitate the early detection and exclusion of compromised animals, whilst also allowing the identification of animals demonstrating characteristics predictive of longer survival, prior to BALSS connection.

The following clinical pattern was reproducibly observed in the above model: There was an initial hyperdynamic circulation followed by progressive anuria associated with rising serum creatinine values. EEG tracings revealed an initial slow decline in the ratio of alpha to delta activity, especially in the frontal part of the brain, succeeded by excitation towards the end. The increase in EEG activity was associated with muscular twitching, rigidity and finally gasping and convulsions. Hyperammonemia and lactic acidosis developed within 8 hours of the surgery. Clotting factors II, VII and X, antithrombin, prothrombin time and fibrinogen all declined significantly. On the other hand, the liver enzymes AST, ALP, ALT and LD, bilirubin and potassium all increased significantly. Finally, there was severe cardiovascular decompensation leading to hypotension, refractory shock and cardio-respiratory collapse. The clinical progress was multivariate, with renal failure, hyperammonemia and cardiovascular collapse all contributing to eventual death in these animals.

Since prognosis in this model was found to be dependent on surgical skill and since the disease etiology was complex, it was not desirable to further complicate the clinical

progress. For example, although routinely performed in human AHF treatment, intracranial pressure (ICP) was not monitored as complications have previously been recorded [234]. Similarly, hepatic encephalopathy was not treated with mannitol since it was desirable to gather data in a pure manner. Future studies may include these interventions.

In table 5.2.3 is summarized the systemic indices that are representative of clinical interventions during the surgical interval ($T \leq 0$) and in the blood biochemistry following that ($T > 0$). When these indices were present the animals demonstrated impaired survival. Important criteria that predicted survival during surgery ($T \leq 0$) were, amongst others, the ischemic clamping time (criterion 1), the presence of tachycardia (criterion 2), a loss of systolic blood pressure and the need for inotropic support. Fluid administration prior to portal clamping was shown to improve survival. Thus, by ensuring that the systemic indices reflected an adequate volume status, it was possible to avoid subsequent non-hepatic complications.

In the period following surgery ($T > 0$) the reasoning behind the criteria was as follows: Consensus indicates that AHF is unlikely to present in less than 6 hours following the surgical insult (criterion 8). The mean duration of survival in this study was 20.5 hours, which is in keeping with that observed in similar studies [227,229]. It seems reasonable to define the onset of AHF in terms of minimal or maximal limits in biochemical variables observed at 8 hours following the surgery (criteria 9-17). Animals failing to demonstrate these values (for whatever reason) can thereby be excluded. Fischer's ratio (criterion 9) and a raised ammonia concentration (criterion 10) confirm the onset of hepatic encephalopathy with hyperammonemia. The loss of clotting factors and the increased prothrombin time confirm coagulopathic effects (criteria 11 and 12) while the raised liver enzyme concentrations confirm increasing cellular membrane permeability and thus progressive hepatic necrosis (criterion 13). Loss of hepatic function is confirmed by an increased bilirubin concentration (criterion 14) while and renal failure by an increased creatinine concentration (criterion 15). Since the disease etiology was multifactorial it was felt that the relative importance of several biochemical indicators required definition in the criteria.

Table 5.2.3 Standardization criteria for a porcine surgical (ischemic) model of AHF

Interval	Limit	Criteria
During surgery $T \leq 0$	1. Ischemic clamping time > 15 mins. 2. Pulse > 200 bts/min during ischemic time. 3. Systolic Press. < 40 mmHg during ischemic time. 4. Metabolic acidosis pH < 7.2 following surgery. 5. If there was a small initial urinary volume [< 1 ml/kg body mass]. Alternately, total < 50 ml during the surgery. 6. Temperature < 35.0 ^{o}C immediately following surgery. 7. Total blood loss > 200 ml during surgery.	if affirmative to both 1 and 2, terminate after surgery. if affirmative to 1 or 2 and any two of 3-7, terminate after surgery.
After surgery $T > 0$	8. Duration of survival following surgery < 6 hours 9. Ratio BcAA / AroAA > 1.6 10. [Ammonia] < 500 µmol/L 11. Clotting factors:[Factor X] > 25 % [Factor VII] > 28 % [Factor II] > 30 % 12. PT < 15 secs 13. Liver Enzymes:[ALP] < 260 IU/L [AST] < 800 IU/L [LD] < 800 IU/L 14. [Total Bilirubin] < 12 µmol/L 15. [Creatinine] < 130 µmol/L 16. [Potassium] < 4.4 mmol/L 17. [Lactate] < 3.0 mmol/L	if affirmative to 8, exclude data. if affirmative to both 9 and 10, exclude data. if affirmative to either 9 or 10 and any one or more of 11-17, exclude data.

Notes:
1.T = 0 starts at the completion of surgery.
2. Criteria 9-17 are presented as limit values at 8 hours following the surgery, that is, the particular biochemical variable must be above or below that value at that time. These values are based on the mean values of the particular variables measured at 8 hours, and are in apparent agreement with similar studies [228,229].

Valuable procedural information was revealed by the data analysis in this study. For example, both haemoglobin and hematocrit declined significantly and this correlated

strongly with survival. Thus, it is reasonable to assume that the accumulated effects of loss of blood due to ABG and biochemical sampling, bleeding at surgical wounds and loss of hematocrit through continuous fluid provision, would contribute to the eventual hemodynamic instability and cardiovascular collapse that was observed. The data analysis also identified the variables that were of interest and allowed more selective sampling, improving prognosis and experimental reproducibility. Of interest was the high correlation of the rate of decline of branched chain amino acids (and by implication the branch chain to aromatic ratio), along with the rise in ammonia concentration, with the duration of survival. This finding serves to confirm the validity of Fischer's ratio as an indicator of HE [52,70]. This is the molar ratio of plasma concentrations of leucine, isoleucine and valine as numerator and tyrosine, phenylalanine and tryptophan as denominator. Changes in this ratio correlate with alterations in brain amino acid metabolism aided by an excess of plasma nitrogen in the form of ammonia. The synthesis of brain neurotransmitters is then affected, leading to HE. Alterations in this ratio also serve to confirm the value of providing antibiotics and fasting the animals prior to the surgery. Gut intestinal flora and protein content aid in the over-production of plasma nitrogen, thereby exacerbating HE and complicating the model of AHF.

Most of the biochemical indices are not measurable *on-line*, thus, their utility lies in confirming AHF after-the-fact. It is important to bear in mind that the initial model was healthy and that the biochemical indices started from a normal value. This was illustrated by clotting factor V; it started from a normal value and only declined at the end of the study period. Thus, these experiments were likely of insufficient duration to demonstrate large changes in this factor. In effect, the above criteria are the converse of the King's college criteria. The latter criteria are exercised on human patients already presenting with AHF [52,53] in which clotting factor V would have diminished *a priori*. In this study the criteria are designed to exclude experiments wherein the prognosis is insufficiently bleak, or due to factors other than AHF. Thus, while clotting factor V is of prognostic value in the human scenario, it was not useful in this model. Additionally, although our finding was that the mean arterial pH during an experiment displayed a strong positive correlation with survival, it was excluded as a criterion for two reasons: The animals were ventilated, thus, their pH could be controlled in this manner and due to

its measurement being complicated by the continuous provision of fluids. Since pH in AHF is strongly determined by the presence of lactate, it was felt that the latter would be a better index of AHF (criterion 17), despite the fact that lactate demonstrated a low correlation with survival.

In conclusion, the statistical analysis used in this study produced useful results in the following respects: Procedural information was generated that aided in the establishment of experimental reproducibility. Unnecessary determinations were identified, enabling the limiting of blood sampling, thereby improving prognosis and cutting laboratory costs. Specific standardization/exclusion criteria for discriminating between experiments that did or did not present a valid model of AHF, as defined by the settings of this study, were defined. These criteria are likely to allow more accurate comparisons between small treatment and control groups in evaluating supportive therapies for AHF. Variables were identified that may allow the evaluation of prognosis either in *real-time,* or after each experiment. Finally, the method of analysis and criteria presented in this study may be useful for standardizing AHF animal models prior to evaluating supportive therapies for AHF in the future.

5.3 Thoughts and recommendations

The above studies investigated two animal models to emulate respectively, the potential toxicity of PFC in a rat model of severe liver injury followed by recovery, and a surgically-induced ischemic liver failure model in pigs. These models were selected to determine if PFC would have a toxic effect and an impact on liver regeneration, and the efficacy in improving survival and biochemistry in severe irreversible ALF in a potential BALSS treatment scenario. The difficulty in these models obviously lies in the degree to which they emulate the intended disease process and this is exacerbated by the fact that controlled experiments require initially healthy animals. By comparison, human patients are often in the latter phase of a chronic liver failure or have abruptly progressed to ALF through, for example, drug or viral etiologies.

The rat model of liver regeneration following surgical injury was selected (effectively) by default. It was not possible to use a toxic model of ALF (e.g. CCl_4, galactoseamine, acetaminophen or lipopolysachiride) in that this would complicate the effects of an injected foreign substance, in this case PFC. Additionally, it was desirable to model the regenerative ability of an *in vivo* liver and to determine if the PFC would impact this or not. In both respects the study was successful, owing in all likelihood to the well-controlled study design.

The pig surgically-induced ischemic model of ALF was complex and haemodynamically unstable. Following the standardization experiments our group proceeded to evaluate the clinical efficacy of the BALSS in this model. It rapidly became apparent that the choice of animal ALF model may play a determining role in demonstrating the clinical efficacy of an experimental treatment system.

5.3.1 Clinical evaluation of the UP-CSIR BALSS using the ischemic model

In the course of the subsequent BALSS treatment experiments a large amount of knowledge was gained regarding the ischemic ALF model, the impact of the treatment on

the animal and consequently indicated BALSS-machine design alterations. Unfortunately, after embarking on this course the necessity of maintaining controlled circumstances precluded alterations in any part of the experimental design despite it becoming apparent that such changes may have resulted in improvements in the treatments. For these (and financial deadline) reasons the experiments were terminated prior to conducting the full planned number: 50 pigs were requested of which 29 were used.

As an example of the difficulties involved examine table 5.3.1 below. What was particularly noteworthy was the large range in duration of survival and the variety of causes of death, many of which were due to reasons unrelated to the treatments. Clearly, not all of the data was acceptable for inclusion into a subsequent analysis investigating BALSS clinical efficacy. A subset of the group was consequently selected. Table 5.3.2 below provides a summary and definitions of the variables used to make a comparison between the BALSS treatment group, the cell-free BALSS controls and the Surgical control group (the 'standardization data'). Table 5.3.3 provides the statistical results themselves.

Table 5.3.1 Record of large animal experiments

N	Comments	Survival (hrs)
1	Validation of surgical protocol changes. Ischemic time 13 mins.	36
2	Validation of surgical protocol changes. Ischemic time 12 mins.	32
3	BALSS treatment. Ischemic time 14 mins. High blood loss in surgery animal not connected to BALSS.	-
4	BALSS treatment. Ischemic time 11 mins. BALSS initiated 10hrs post operative. Pig died due to shock 45 mins after connection	11
5	BALSS treatment. Ischemic time 19 mins. Connected to BALSS 8 hours post operative.	20
6	BALSS treatment. Ischemic time 12 mins. Connected to BALSS 8 hours post operative.	29
7	BALSS treatment. Extended ischemic time, 30 mins.	26
8	BALSS treatment. Liver + multi organ failure	30
9	Exercise. Changes recommended by Prof R Hickman	terminated 6
10	BALSS treatment. Epidural omitted. Unsuccessful.	10
11	Haemodynamic instability. Not connected to BALSS	1
12	BALSS treatment. BALSS system unstable	24.5
13	Haemodynamic instability – Heart failure. Not connected to BALSS	9
14	Haemodynamic instability – Porcine circo virus detected– Not connected to BALSS	12
15	Control (-) cells. Haemodynamic instability after BALSS connection	16
16	Control (-) cells. Haemodynamic instability after BALSS connection	12
17	BALSS treatment. Haemodynamic instability after BALSS connection	10.2
18	Terminated prior to BALSS connection - extended ischemic time + blood loss	-
19	Haemodynamic instability after BALSS connection	8.5
20	Experiment without PFC in system. animal stable after connecting to BALSS	18.3
21	Control (-) cells. Haemodynamic instability after BALSS connection	7.5
22	Not connected to BALSS - heart failure	-
23	Control (-) PFC and (-) cells	18
24	Control (-) PFC and (-) cells. Tachicardia	6.5
25	Control (-) PFC and (-) cells Different perfusion circuits connected at different time intervals.	8.5
26	Control. BALSS not connected due to renal failure	-
27	Cardiac arrest in surgery	-
28	Machine failure (Air in plasma separator – machine disconnected after 8.5 h)	16.5
29	Machine failure due to excessive clotting (BALSS connected for 5h)	10

Table 5.3.2 Definition of variables and units

Variable	Definition	Units
Survival	duration from end of surgery to cardiac arrest	hours (hrs)
Treatment	duration of BALSS connection	hrs
Body weight	animal weight prior to surgery	kilogram (kg)
Ischemic time	duration of portal clamp	minutes (min)
Pulse_isch	mean pulse during ischemic time	beats/min
Pulse_post	mean pulse after release of portal clamp	beats/min
MAP_isch	mean arterial pressure during ischemic time	mmHg
MAP_post	mean arterial pressure after release of portal clamp	mmHg
Bl_loss	blood in peritoneal cavity following surgical procedure	milliliters (ml)
Urine_oper	urine volume measured following surgery	ml
pH_post	blood pH after surgery	
Temp_post	body temperature following surgery	degrees Celsius (^{o}C)
rMAP	rate of descent of mean arterial pressure for the duration of survival (i.e. in the ICU following surgery)	mmHg/hr
ave_pH	mean blood pH for the duration of survival	
ave_Lact	mean blood lactate concentration	mmol/l
rK+	rate of increase of blood potassium	mmol/l/hr
rHct	rate of descent of blood hematocrit	percentage (%)/hr
rAmmonia	rate of increase of blood ammonia concentration	µmol/l/hr
rBilirubin	rate of increase of blood total bilirubin concentration	µmol/l/hr
rCreatinine	rate of increase of blood creatinine concentration	µmol/l/hr
hrsFibrinogen > baseline	number of hours taken for fibrinogen to reach its lowest detectable limit (i.e < 0.5 g/l)	hrs and %
hrsPT < limit	number of hours taken for the prothrombin time to reach its detection limit (i.e > 150 seconds)	hrs and %
hrsClot II > baseline	number of hours taken for clotting factor II to reach its lowest detectable limit (i.e < 5 IU/dl)	hrs and %
hrsClot VII > baseline	number of hours taken for clotting factor VII to reach its lowest detectable limit (i.e < 5 IU/dl)	hrs and %
hrsClot X > baseline	number of hours taken for clotting factor X to reach its lowest detectable limit (i.e < 5 IU/dl)	hrs and %
hrsALP < max	number of hours taken for ALP to reach the maximum value for each animal	hrs and %
hrsALT < max	number of hours taken for ALT to reach the maximum value for each animal	hrs and %
hrsAST < max	number of hours taken for AST to reach the maximum value for each animal	hrs and %
hrsLD < max	number of hours taken for LD to reach the maximum value for each animal	hrs and %

Table 5.3.3 Comparison between BALSS treated and non-treated animals

Time period	Variable	†BALSS treatment group (E)	†Cell-free Control group (C)	∂Surgical control group (S)	#p value between E and C	#p value between E and S
Global	Number	6	3	12		
	Survival	23.5 ± 4.3	14.4 ± 3.5	20.5 ± 5.1	**0.018**	
	Treatment	13.8 ± 2.5	7.0 ± 4.6	none		
	Body weight	30.3 ± 3.2	29.7 ± 2.0	30.4 ± 5.1		
Surgery	Ischemic time	13.4 ± 3.2	11.3 ± 1.5	16.8 ± 4.1		**0.020**
	Pulse_isch	131.6 ± 28.5	149.7 ± 19.6	156.8 ± 29.9		
	Pulse_post	125.5 ± 16.3	120.7 ± 21.9	131.5 ± 30.0		
	MAP_isch	55.3 ± 4.1	56.5 ± 4.7	47.1 ± 11.8		
	MAP_post	99.9 ± 21.3	85.0 ± 8.0	78.3 ± 13.6		
	Bl_loss	96.0 ± 41.6	66.7 ± 28.9	96.3 ± 68.6		
	Urine_oper	402.2 ± 336.6	233.3 ± 231.8	122.9 ± 96.0		
	pH_post	7.40 ± 0.05	7.45 ± 0.03	7.32 ± 0.10		
	Temp_post	37.0 ± 1.4	35.8 ± 1.1	36.3 ± 1.6		
ICU	rMAP	-2.1 ± 1.1	-4.3 ± 2.4	-1.8 ± 0.6		
	ave_pH	7.35 ± 0.05	7.36 ± 0.04	7.41 ± 0.07		**0.020**
	ave_Lact	4.51 ± 2.33	4.85 ± 2.32	4.22 ± 3.25		
	rK+	0.11 ± 0.06	0.05 ± 0.04	0.13 ± 0.13		
	rHct	-0.73 ± 0.33	-1.08 ± 0.63	-0.70 ± 0.32		
	rAmmonia	85.8 ± 60.1	70.3 ± 35.4	64.1 ± 31.9		
	rBilirubin	0.55 ± 0.36	0.41 ± 0.43	1.76 ± 1.61		0.052
	rCreatinine	5.71 ± 3.59	6.80 ± 2.24	7.99 ± 7.21		
	hrsFibrinogen > baseline*	9.6 ± 3.3 41%	8.7 ± 2.5 60%	10.3 ± 4.5 50.2%		
	hrsPT < limit*	10.8 ± 2.7 46%	8.7 ± 2.5 60%	20.5 ± 5.1 100%	0.071	**0.0002**
	hrsClot II > baseline*	13.5 ± 5.7 57%	8.7 ± 2.5 60%	19.5 ± 4.7 95%		**0.035**
	hrsClot VII > baseline*	16.5 ± 3.0 70%	7.0 ± 1.0 49%	20.5 ± 5.1 100%	**0.029**	0.069
	hrsClot X > baseline*	10.5 ± 3.0 45%	7.0 ± 1.7 49%	20.5 ± 5.1 100%		**0.0005**
	hrsALP < max*	19.6 ± 6.4 83%	10.0 ± 6.9 69%	20.5 ± 5.1 100%	0.054	
	hrsALT < max*	19.6 ± 6.4 83%	8.0 ± 9.2 56%	20.5 ± 5.1 100%	0.054	
	hrsAST < max*	21.4 ± 3.1 91%	12.0 ± 6.0 83%	20.5 ± 5.1 100%		
	hrsLD < max*	18.8 ± 7.1 80%	12.0 ± 6.0 83%	20.5 ± 5.1 100%		

All values expressed as Mean ± standard deviation, and in all * as percentage of survival duration.
[#] Exact p values, only for significant differences (0.95 in **bold**, 0.90 in normal text), using the Wilcoxon Rank Sum test for non-parametric small populations.
[†] Only for those that survived the surgery (> 6 hrs) and were treated successfully for ≥ 3 hours starting > 6 hrs after the surgery.
[∂] Only for those that survived the surgery (> 6 hrs).

What was clear from the results was that, within the limited number of experiments, there was a significant difference ($p < 0.05$) in the duration of survival between the cell-free controls and the BALSS treated group. However, there was no significant difference in the duration of survival between the BALSS treatment group and the surgical control group, even though the treated group did survive for a longer period. The cell free controls also survived for a shorter period than the surgical group. This implied the following:

1. Adding cells to the bioreactor in the BALSS treatments did significantly improve survival.
2. Adding an extracorporeal circulation system to the surgical model hindered survival. This was to be expected if the haemodynamic instability that is intrinsic to this model of ALF is considered.
3. These results cannot be accepted as a conclusive demonstration of the efficacy of the BALSS mostly in view of the fact that more experiments are required.
4. The difference in the ischemic times reflected an improvement in the surgical technique over time. This was mirrored by differences in the Pulse and MAP after the procedures.
5. Although there was a significant difference in ave_pH between the BALSS and surgical control groups this was not due to lactate accumulation. It was likely as a result of non-lactic metabolic acidosis.
6. Since the rate at which ammonia and potassium accumulated similarly in the various groups, it indicated that an additional artificial clearance device should ideally be incorporated in the BALSS, assuming the use of an acutely toxic model.
7. Since the rate at which the MAP fell during the ICU period was insignificantly different between groups, it suggested that although the ALF model was associated with haemodynamic instability, it was not as a result of the BAL.
8. An impact of connecting the system can be seen in the various coagulation indices. Coagulation (as measured by increasing PT and coagulation factor losses) was increased in the treated groups when the period to coagulation failure was compared to the duration of survival (percentages in table 5.3.2). While these

figures are as expected, a re-evaluation in terms of coagulation of the mark II BALSS (as was used in these experiments) was indicated.

9. The difference between the liver enzymes in the BALSS and cell free groups was not a conclusive indication of differences between the interventions. Liver enzymes (ALP, ALT, AST, LD) are progressively released into the circulation by the ischemic damaged liver and are thus not impacted by the treatment. The differences highlighted the requirement of larger numbers of experiments.

In order to gain the maximum possible information, the unsuccessful experiments were also examined. Thus, a summary of *all* experiments are as follows:

A total of 29 experiments were performed. Of these, 8 were completely successful and 6 were used as controls, either of the surgical procedures (3) or of parts of the circulation system (3). Of the remaining 15, 8 were not connected to the BALSS owing to instability in the surgical model (4 died of cardiac arrest, 1 of renal failure, 1 of a detected circo virus, 1 of renal failure and 1 of instability as a result of the omission of the epidural in the anesthetic protocol). This result was taken as an indication of the many procedural and clinical difficulties associated with the employed model of ALF. 5 animals became haemodynamically unstable 30-45 minutes after connection to the BALSS and these survived a mean of 9.7 $\pm$ 1.4 hours. In the two remaining cases the circulation system failed due to complete coagulation, this resulted in survivals of 16.5 and 10 hours respectively. In these last two animals and in 3 of the 5 that became unstable following BALSS connection it was revealed that the epidural procedure had been omitted from the anesthetic protocol. Thus, the success rate for experiments was 8 out of a total of 15, i.e. 53 %, when only those animals that became unstable following connection or where the BALSS completely coagulated were taken to be failed experiments. This validated the stated clinical difficulty/instability of the ischemic surgical model and indicated the use of a more stable model in the future that will hopefully demonstrate greater differences between experimental and control groups.

As a consequence of the above:

1. Various improvements to the design of the mark II BALSS were planned, including: A simplification of the circulation system, an improvement of the operating methods, a minimization of coagulation effects in the system, the design of a new bioreactor (with better flow characteristics and more biocompatible substances) and the inclusion of an additional artificial toxin clearance device into the system.
2. Several coagulatory, immunological and cerebral variables, not measured in the ischemic experiments, were subsequently identified to have prognostic value in ALF. These new variables will require inclusion in any future experiments (and this issue is mentioned in greater detail in the mathematical modeling section 6.2 below).
3. Research into other animal models of ALF was indicated (see below). The above experiments demonstrated that the ischemic model is both highly acute and inherently toxic, potentially to the extent of 'clouding' any potential the benefit of the BALSS. The return to large animal clinical treatments would occur only once all of the above machine-design issues had been attended to.

5.3.2 Alternate animal models of ALF

Unfortunately, in that liver failure has remained the same, the possibilities for modeling it in animals have done so too. Thus, the issues identified in the second of the above two studies remains valid. Specifically, in evaluating a BALSS:

1. The porcine model should still be used as these animals are available in large quantities and are metabolically and physiologically similar to humans.
2. It is preferable to use surgical models as opposed to toxic ones due to inter-animal variations in response to the toxin/s.
3. Surgical models are prone to instability and require the development of considerable surgical skill prior to standardization.
4. Total hepatectomy models lack the *in vivo* biochemical effects of a failing liver while devascularization models do not.

However, having said the above, anhepatic models may be less *aggressive* than the ischemic model in that the rate of accumulation of endogenous toxins is less pronounced. That is, since there is no *in vivo* ischemic liver, accumulating ammonia and endotoxin in the blood are due only to *non-hepatic* causes. However, the pathophysiological course followed is then related to the absence of a liver, i.e. ammonia and endotoxins from the bowel may play a more important role in the outcomes. In a sense, the anhepatic is a 'control' for the ischemic: Subtracting the rates of accumulations, of the former from the latter, will indicate the contribution/extent of hepatic necrosis. For this reason, should anhepatic trials follow ischemic ones; the former acquired data will to some degree complement the latter. This is useful information in examining prognostic variables.

Other attractive aspects of the anhepatic model lie in its relative procedural simplicity and a decrease in the costs of the experiments. A considerable amount of prior studies have focused on standardizing the anhepatic model [5,220,221,226,230-238]. This, together with the historical experience gained by our group will hopefully function to decrease the experimental failure rate as previously demonstrated (table 5.3.1).

One variant of the anhepatic model seems particularly interesting: Engelbrecht *et al* (1999) [238] describe performing a side-to-side mesocaval shunt distal to the renal veins, followed by total hepatectomy with ligation of the portal vein, hepatic arteries and the bile duct. Their method was performed on rats and required the sacrifice of a donor animal to provide a section of vena cava for subsequent caval reconstruction. In a porcine model this may be performed using sterilizable tubing (e.g. silicon). The benefit of this surgical method lies in the absence of complete portal clamping and consequent splanchnic congestion. The duration of this clamping (ischemic time) was found to correlate strongly with survival in the ischemic model, most likely due to presumed endotoxin build up and then release from the splanchnic circulation.

Unlike in the ischemic model in which a donor animal is required for hepatocyte isolation procedures (to populate the BAL bioreactor), the liver of the anhepatic animal may autologously be used, decreasing the total cost of the experiments. On the other hand, assuming the inclusion of an artificial toxin clearance device into the BAL circulation

system, the experimental design must then control for the additional sub-group/s. Table 5.3.4 below provides an example:

Table 5.3.4 Control and experimental groups in animal trials

Group	Size (N)
Surgical control (no treatment)	5
System control (empty BR, no AL)	5
Experimental 1 (empty BR, with AL)	8
Experimental 2 (cells-BR, no AL)	8
Experimental 3 (cells-BR, with AL)	8
Unpredictables (assuming 30 % rejection rate)	12
TOTAL	46

Abbreviations: BR = bioreactor with or without cells.
AL = artificial toxin clearance system (e.g. dialysis and adsorption column)

5.3.3 Ammonia metabolism, measurement and reduction strategies

Accumulating blood ammonia levels in the ischemic surgical model were found to strongly correlate with the duration of survival of the animals. Additionally, while ammonia is clearly not the only variable of interest in ALF, there has been a growing consensus regarding its importance as an indicator of prognosis in human patients most likely owing to its causative role in hepatic encephalopathy (section 2.4.1, and returned to in section 6.2) [30-33,239-241]. There is consequently an incentive to find fast, convenient, accurate and inexpensive methods for its bedside detection and novel strategies for its reduction/minimization in the patient. A brief summary of ammonia metabolism is instructive,

1. Ammonia metabolism

Ammonia is produced mostly in the gut followed by the kidneys and muscle. The gut contribution is due to ammonia produced by protein catabolism and bacterial metabolism (i.e. from glycine and glutamine). The kidneys employ ammonia to buffer acids, i.e. ammonium is synthesized from glutamine in the proximal tubule then either released into the systemic circulation or used to facilitate proton excretion. Skeletal muscle produces ammonia during seizures or in intense exercise.

Ammonia degradation occurs primarily in the liver. Ammonia originating in the splanchnic circulation and in the muscle is metabolized to urea by means of the urea cycle. The enzymes participating in the urea cycle include carbamyl phosphate synthetase (CPS), ornithine transcarbamylase (OTC), argininosuccinate synthetase (ASS), argininosuccinate lyase and arginase. Arginine is a necessary raw material for the urea cycle. Owing to the healthy liver's efficiency in clearing ammonia, arterial and venous ammonia levels usually do not equate [31-36].

When the liver ceases effective functioning, the elimination of ammonia depends on the kidneys, muscle and brain. The kidneys decrease ammonia production and increase its urinary excretion. The muscle and brain metabolize ammonia to glutamine. Astrocytes normally support neurons with adenosine triphosphate (ATP), glutamine and cholesterol. The neuron metabolizes glutamine to glutamate which participates in neurotransmission by activating N-methyl-D-aspartate (NMDA) receptors. After release in the synapse glutamate is recycled to glutamine by the astrocyte. When ammonia levels rise acutely the astrocytes overproduce glutamine and this interrupts neurotransmission. Intracellular osmolytic changes also cause the astrocytes to swell and die [37].

Astrocytes release inflammatory cytokines (TNF-α, IL-1, IL-6 and interferon) and owing to ongoing oxidative and nitrosative stress additional astrocytes are lost due to apoptosis. In the remaining astrocytes ammonia inhibits alpha-ketoglutarate dehydrogenase and the depletion of carboxylic acids for glutamine synthesis causes the Kreb's cycle to shut down. ATP and reduced-nicotinamide adenine dinucleotide (NAD) production falls. As NADH levels rise in relation to NAD, the production of lactate from pyruvate is favoured (i.e. glycolysis). Thus, there is altered oxidative metabolism associated with mitochondrial dysfunction. With the loss of astrocytes, less receptors are available for glutamate and glutamate overload occurs resulting in seizures. Cerebral blood flow increases, cerebral autoregulation is lost and cerebral edema and intracranial hypertension develop [30-38].

2. Measurement

Historically the most common method of blood ammonia measurement has been routine enzymatic spectrophotometric laboratory approaches. However, this is problematic for a number of reasons. Firstly, the elapsed duration in awaiting results delays clinical decision making and this may be important in critically ill HE patients. Secondly, ammonia is unstable at room (and body) temperature. In the blood it exists in equilibrium between the ionic liquid ammonium (NH_4^+) and gaseous ammonia (NH_3) forms [31]. When blood samples are taken it is critical that they are frozen without delay in order to prevent the escape of the gas. Finally, the enzymatic kits used in the laboratory are exceedingly sensitive to atmospheric ammonia. Since detergents that are used to wash laboratory surfaces may contain ammonia, the blood results are at risk of spurious elevation [personal experience!].

Recently a portable device has become available, the PocketChem BA analyser (Arkay, Kyoto, Japan) which has demonstrated accuracy at least as high as that of the laboratory methods. However, blood samples should ideally be collected onto ice and analysed immediately. The sampling site is also important, levels in for example, the jugular vein or femoral artery are usually different due to the generation or uptake of ammonia by different tissues. Only arterial ammonia has been found to correlate with brain glutamine levels, the severity of HE and thus prognosis in ALF [32,241] and jugular levels were found to have a higher correlation with arterial ammonia than femoral levels [26].

3. Ammonia reduction strategies

In ALF interventions are usually aimed at treating brain edema, decreased cerebral metabolism, and raised cerebral blood flow and ICP rather than specifically the reduction of ammonia. However, ammonia is a critical part of this pathogenesis. Thus, current strategies, both conventional and not yet conclusively proven, are listed below in non-specific order (this is not intended as a review). The approaches fall into two groups [31,33]:

a. Biochemical strategies,

N-acetylcysteine infusion to improve cerebral edema and O_2 delivery and utilisation.
Mannitol to reduce cerebral edema.
Phenytoin to reduce cerebral edema and seizures.
Hypertonic saline to create a blood-brain osmotic (sodium) balance in opposition to that resulting from raised ammonia levels. This reduces the severity of ICP.
Indomethacin to prevent cerebral hyperemia and intracranial hypertension.
Propofol to prevent intracranial hypertension.
Dilantin or Phenobarbital to reduce seizures.
Lactulose to decrease ammonia.
L-ornithine-L-aspartate to enhance the muscular metabolism of ammonia.
Arginine administration to prevent protein catabolism.
Protein intake prevention to reduce ammonia production.
Sodium phenylacetate or benzoate to improve ammonia degradation through alternate metabolic paths.

b. Physical strategies, including,
Mild hypothermia to decrease the cerebral uptake of ammonia, to reduce CBF, to reduce the synthesis of lactate and to rectify alterations in brain osmolarity.
Blood purification/filtration approaches including bioartificial livers, high-volume plasmapheresis (e.g. continuous veno-venous or arterio-venous hemofiltration or hemodiafiltration) and albumin dialysis (MARS and Prometheus) to respectively provide hepatic synthesis/transformation functions, to remove water soluble and protein-bond toxins.

An appropriate combination of biochemical and physical approaches can successfully reduce blood ammonia levels to normal [33].

5.3.4 Which artificial toxin clearance system?

The complex tasks of regulation and synthesis have yet to adressed by the use of liver cells. For detoxification, e.g. the removal of bilirubin, bile acids and toxins, simple dialysis-like artificial detoxification technologies have been shown to be efficient [242]. As will become apparent in section 6.1 artificial toxin clearance devices have a greater capacity to remove blood-borne toxins than any current bioreactor/s. Since many different artificial systems have historically been developed (table 2.3) a difficulty lies in deciding which is most appropriate.

It should be stated that artificial liver support has been developed to a relatively advanced state and it is assumed that 'off-the-shelf' technology will be selected for inclusion into a bio-artificial liver system rather than development from scratch. The following discussion aims simply to identify trends in the literature and the factors that may affect the choice of technology.

Cell-free extracorporeal liver support technology can be divided into 'closed-loop' and 'open-loop' technologies. Closed-loop technology includes the molecular adsorbents recirculation system (MARS) and the Prometheus albumin dialysis system in which a minimal amount of exchanged treated plasma is discarded. Open-loop technology includes single-pass albumin dialysis and a variety of plasma exchange technologies in which large quantities of treated plasma are discarded. Both approaches have drawbacks including limited toxin removal rates, the non-selective removal of molecules (both *good* and *bad*) with open-loop systems, and limitations in perfusion time and thus total quantity removed with closed loop systems [243].

MARS works by an albumin diffusion gradient principle. The albumin is placed on the dialysate side of a high-flux membrane which maximizes the diffusive transport of albumin-bound toxins. The used dialysate is then regenerated in a secondary circuit by passage over adsorption cartridges (anion exchanger and activated charcoal) to remove the concentrated albumin-bound toxins and a low-flux dialyzer cartridge to remove water-dissolved toxins. The Prometheus (PROM) system works on the principle of

fractionated plasma separation and adsorption. A 100 kD cut-off polysulphone membrane allows partial filtration into a secondary circuit which then also cleans using sorbents, as above. Water-dissolved toxins are subsequently removed with a high-flux dialyser [244].

A clinical study comparing the above two systems demonstrated that the PROM system more efficiently removed blood borne toxins than MARS. Both systems caused increases in prothrombin time associated with loss of coagulation factors, however, both systems were well-tolerated and safe [245]. As yet, neither system has shown statistically significant benefits to patient survival in prospective randomized trials [246].

Single-pass albumin dialysis (SPAD) is a simple method of albumin dialysis using a standard renal dialysis machine and a high-flux hollow fiber hemodiafilter identical to that of the MARS system. On the outer side of the membrane (i.e. in respect of the patient's plasma) an albumin solution flows in the opposite direction and this is discarded after use. Continuous veno-venous or arterio-venous hemodiafiltration (CVVDHF or CAVDHF) also uses conventional dialysis equipment (e.g. a 35 kDa pulysulphone membrane) with a cross dialytic current of plasma, and potentially also the inclusion of ion-exchange and adsorption columns. The used dialysate is discarded after use [233]. In general, high-flow hemodialysis systems are superior to albumin dialysis (MARS) at removing (especially water soluble) toxins [247]. From a technical point of view this may suggest that CVVHDF is preferable for inclusion into a system with a biological component.

There are also selective plasma filtration technologies that have progressed through preclinical trials [248,249]. In these systems a high cutoff 100 kDa polysulphone membrane selectively filters toxins from mitogenic proteins in a continuous veno-venous configuration. The toxic ultrafiltrate is discarded followed by replacement with an equivalent volume of plasma. However, the authors believe this technology is superior to the albumin, sorbent and CVVHDF systems owing to the specificity of the toxin removal membrane. These systems are apparently also easy to use.

At present no particular system is ideal under all circumstances and developments in the technology are ongoing. The loss of coagulation factors (and beneficial mitogens) and the challenge of maintaining haemodynamic stability associated with an increase in the circulating extracorporeal volume is relevant to all systems. It would seem that the factors limiting the choice of system reduce to cost, ease of use, safety (haemodynamic stability) and obviously toxin clearance ability. Since CVVHDF and selective plasma filtration use conventional renal dialysis equipment and procedures, and are less costly, than for example MARS, it seems that at this point these may be the better choices. In terms of conducting animal trials a *well-known* and inexpensive control would also be preferable. It remains to be seen what will emerge as the best choice.

6. MATHEMATICAL MODELING STUDIES

Overview

The following section presents two mathematical modeling studies that have been developed with BAL system design-optimization and improvement in mind. These models are abstractions of a numerical rather than biological nature and differ in this respect to the preceding sections. The models presented are to some extent functionally complimentary and one logically leads to the next.

The first study details a pharmacokinetic compartment 'mass balance' model of the BAL-patient system. The value of models of this type include determining the effect of system parameters (such as for example the minimal hepatocyte mass, blood exchange rates, internal circulation rates and the system volume) on the accumulation of endogenous toxin by the patient. The minimal requirements for an effective BAL design are consequently provided by the findings of this model. A discussion follows regarding the limitations of models of this type, including measurement variations and their units, the type of variables that may be employed and the off-line nature of the predictions.

The second study describes a data-driven statistical model of ALF. This model is defined following conceptual UML modeling of the disease syndrome and the analysis of clinical data generated in the ischemic animal model experiments as described in the *in vivo* section preceding this one. This model functions as an on-line prognosis indicator and is designed for patient monitoring and parallel use during BAL clinical treatments. The findings are presented along with comparison to BAL treatment data on which the model had not previously been trained. A discussion details the merits and limitations of presently existing ALF prognosis systems, the conceptual and mathematical methods employed in this study and the practicalities of implementing the proposed on-line system.

The thoughts and recommendations that follow reviews the value/success of the above models then discusses the requirement of refining existing prognostic systems, additional mathematical experiments conducted on the above data, a means of combining the models of the above two studies and additional practical considerations in implementing on-line bioprocess monitoring systems.

6.1 A pharmacokinetic compartment model of the UP-CSIR BALSS

Moolman FS, Nieuwoudt MJ, Shatalov MY.

Manuscript in preparation.

6.1.1 Introduction

Pharmacokinetics has historically been employed in quantitatively evaluating the functions of absorption, production and elimination of drugs or metabolites by BALSS bioreactors [250,251]. Pharmacokinetic compartment models employ the principle of the conservation of mass within a closed system. Ordinary differential equations (ODEs) are used to describe the molar concentration changes or flows of the substance/s between the compartments of the modeled system.

The value of such models includes comparing endogenous toxin production rates by the patient with bioreactor clearance rates and the effect on the above of system parameters such as circulation rates and reservoir volumes. Indications of the requirements of an effective BALSS design are also provided, such as the minimal hepatocyte mass in the bioreactor and the system's blood exchange and internal circulation rates.

The *in-principle* results of models of this type have been well elucidated [251-254]; however, few authors have provided actual quantitative results in prior studies [255-257]. This may be due to: Difficulties in obtaining reliable and comparable *in vitro* data on drug or metabolite clearance/production rates. The fact that the ideal functions of a BALSS bioreactor are incompletely defined [1,68], and possibly due to unappealing predictions of efficacy from the models themselves. For example, *in-principle* models have demonstrated that a BALS's clearance/production ability is directly proportional, to a first order, to the amount of cells in the bioreactor. Since the majority of researchers have used only between 2 and 5 % of the total mass of hepatocytes in a liver, the

expected metabolic capacity of the bioreactor cannot significantly exceed that range [251]. The limiting effects of the cell isolation procedures on hepatocyte phenotype and function can also not be ignored.

The results provided in this study are instructive in indicating innate limitations in BALSS clinical efficacy imposed by design factors. The findings of other authors and limitations in pharmacokinetic modeling methods are also examined.

6.1.2 Materials and methods

A simplified compartmental pharmacokinetic model of the UP-CSIR BALSS was built in Mathcad[1]. The diagram below (figure 6.1.1) is a simplified compartmental representation of the BALSS, with each part of the circuit numbered (compare with figure 2.5). For the model's derivation, nomenclature, units and parameters used, please refer to Appendix C.

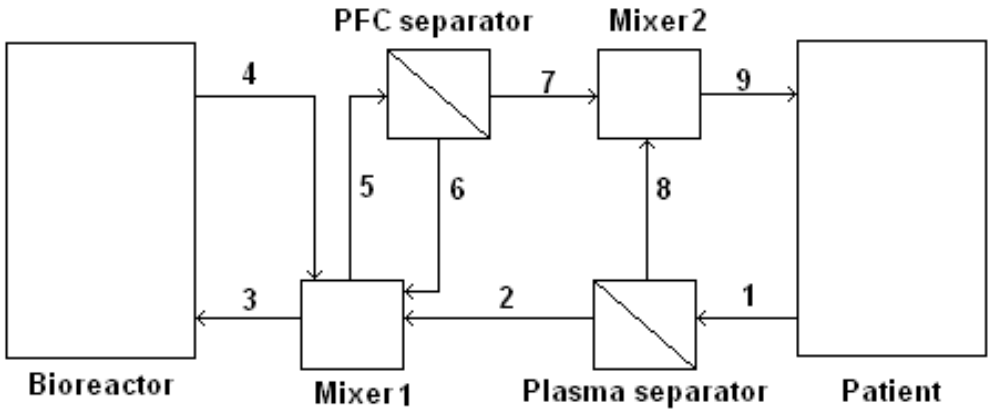

Figure 6.1.1 Compartmental diagram of the BALSS system connected to a patient

6.1.3 Data

The type of input data for such models is limited to drugs or metabolites that are alternately cleared and/or produced by the bioreactor and patient respectively. This

[1] The conceptual model was originated by Dr S Moolman of the M&Mtek [CSIR] and the author. All *in vitro* data was generated by the author. The numerical Mathcad modeling was performed by Dr M Shatalov of Materials and Manufacturing [CSIR]. Model derivation is in Appendix C.

allows the quantification of the conserved molar flow of the input variable between the compartments of the system, in terms of volume and concentration units per time. Since few drugs/metabolites other than arterial ammonia (which is endogenously produced in ALF) fit this characteristic, ammonia data was collected in two sets of experiments: Specifically, hepatocyte bioreactor clearance values measured in *in vitro* configurations of the BALSS (section 4.2) and *in vivo* endogenous ammonia production rates in animals that had surgically-induced ischemic ALF as previously described (section 5.2).
Additional reasons for selecting ammonia data included:

1. The existence of a readily accessible clinical laboratory measurement method with accuracy on the µmol/l level.
2. The fact that ammonia is the predominant substrate for the production of urea by hepatocytes, and is therefore a measure of liver function.
3. Several research groups have reported ammonia clearance values for porcine primary hepatocytes.
4. The overproduction of ammonia in ALF is considered to be an important cause of HE, and thus prognosis for survival.
5. It was approximately linearly endogenously produced in the ischemic ALF model previously described (section 5.2).
6. The possibility that the output of the pharmacokinetic model could be used as the input of another model subsequently investigated (section 6.2 below)

6.1.4 Results

The effect of adjusting particular system parameters on the model's outputs are as follows (figures 6.1.2-5):

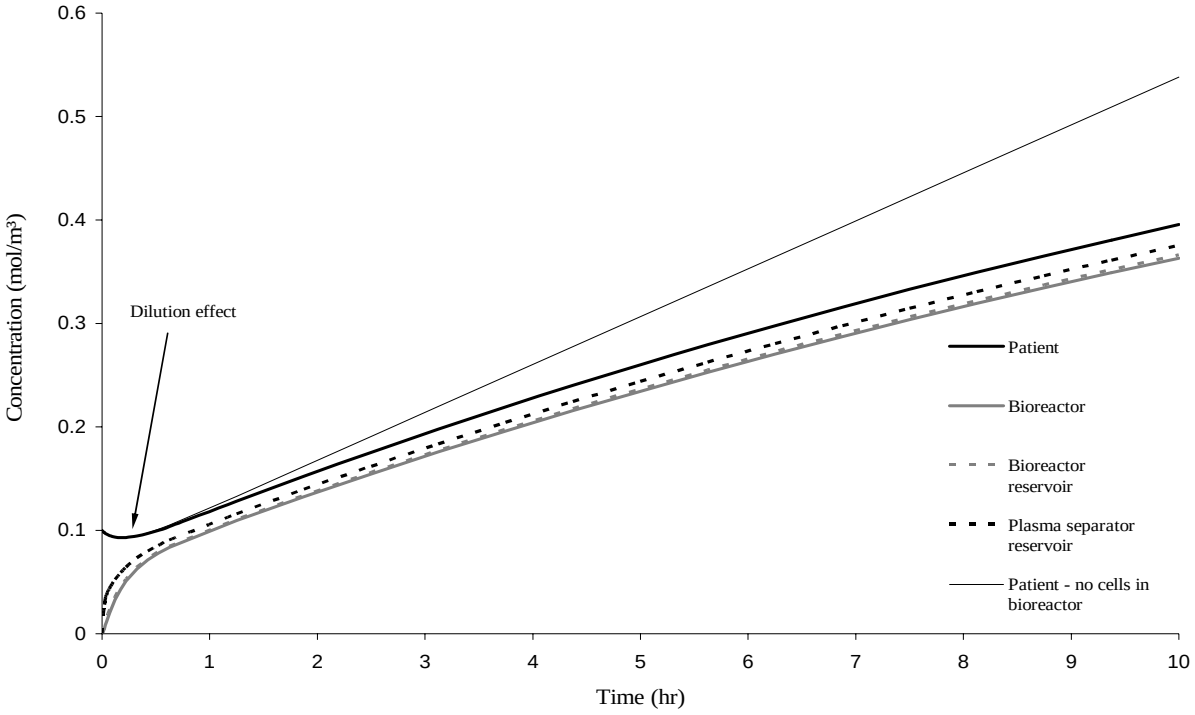

Figure 6.1.2 BALSS sub-circulation concentration profiles for ammonia.
Parameters: 1.5 x 10^{10} cells, V_{max} = 2.2 x 10^{-17} mol/s/cell, r_p = 4.2 x 10^{-8} mol/s, 120 ml/min blood exchange rate

1. The effect of including/excluding cells in a bioreactor (figure 6.1.2). Ammonia concentrations in the various parts of the BALS system can be seen to follow similar *rising* trends regardless of the presence of a cell-loaded bioreactor or not. However, the presence of cells (in this case 1.5 x 10^{10} or approximately 10 % of liver hepatocyte mass) will function to decrease the rate of accumulation. i.e. ammonia will always accumulate in an ischemic model of ALF due to the presence of a non-functional and progressively necrotizing liver, but treating with a cell loaded bioreactor will decrease the rate. A dilution effect in the system, caused by the saline priming volume of the BALSS, is observable in the first 30 minutes of the treatment. This effect has been indicated as a possible cause of improvements in patient survival in human clinical tests [251]. However, this is a limited perspective in that prognosis in ALF is multifactorial. i.e. it is not limited to blood toxin accumulation or artificial ALF treatment methods would historically have demonstrated improvements in survival.

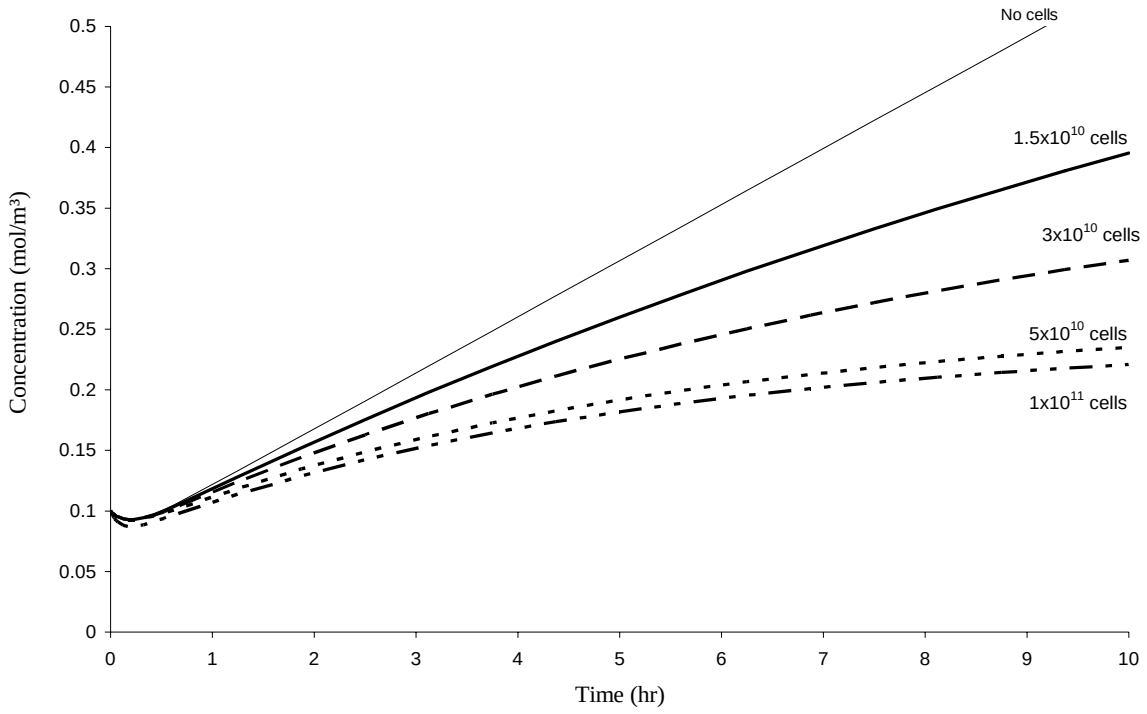

Figure 6.1.3 The influence of bioreactor cell loading on ammonia accumulation
Parameters: V_{max} = 2.2 x 10^{-17} mol/s/cell, r_p = 4.2 x 10^{-8} mol/s 120 ml/min blood exchange rate

2. The effect of cell numbers in the bioreactor (figure 6.1.3). As cell numbers increase, the equilibrium concentration tends to a limit that is higher than the starting (or normal) blood ammonia concentration. A human adult liver contains approximately 1- 2 x 10^{11} hepatocytes. Thus, adding cells even to the point of replacing the entire hepatocyte mass is insufficient to replace a liver's function. This is due to the fact that a BAL is an extracorporeal circulation system with a lower blood exchange/perfusion rate than an *in vivo* liver. Since the bioreactor is intrinsically unable to clear all of the ammonia, the above observation validates the use of adding an additional artificial detoxification device in the BAL circuit. Of interest, an increase in the bioreactor's cellular ability to metabolize ammonia, i.e. the V_{max}, would also result in a decrease in equilibrium blood ammonia levels. This demonstrates the desirability of improving cell functionality.

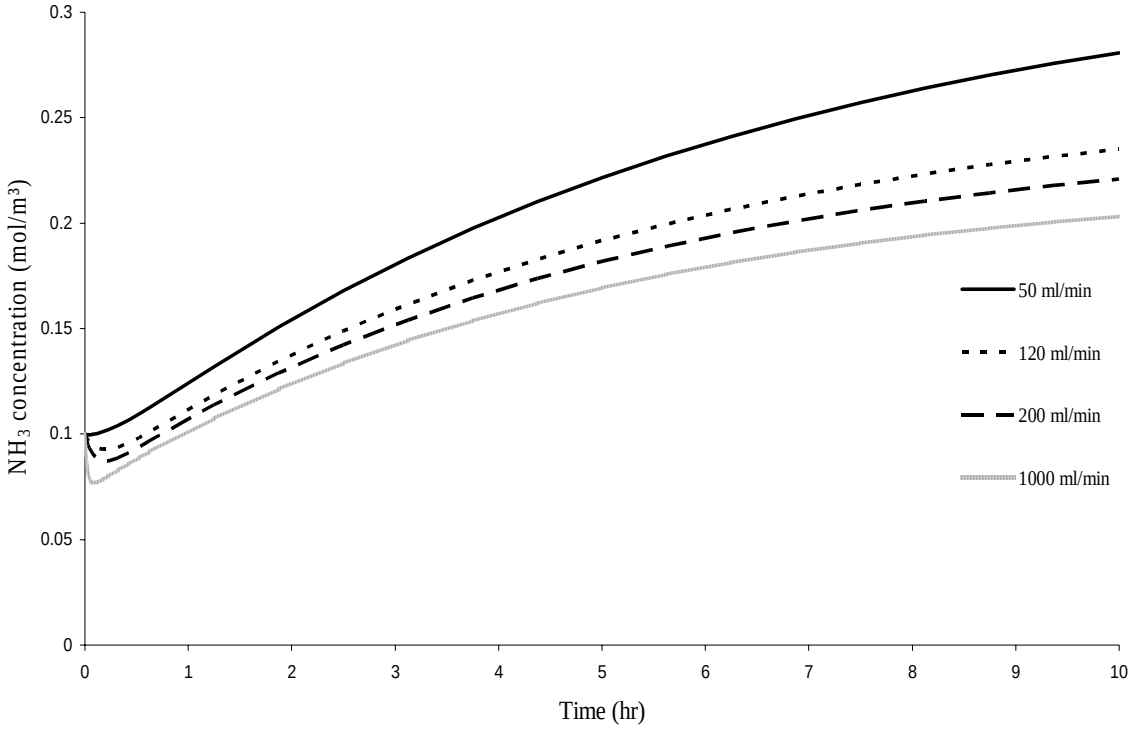

Figure 6.1.4 Influence of blood exchange rate on ammonia accumulation in the patient Parameters: 5 x 10^{10} cells, V_{max} = 2.2 x 10^{-17} mol/s/cell, r_p = 4.2 x 10-8 mo/s

3. The effect of the patient's blood exchange rate with the BALSS (figure 6.1.4). Lower exchange rates between the patient and the BALSS lead to higher ammonia concentrations in the patient. As the exchange rate increases the dilution effect becomes more pronounced, but compresses into progressively shorter time periods. A limit in ammonia concentration is reached at very high exchange rates, e.g. above 1000 ml/min. However, rates above approximately 200 ml/min are difficult to reach, due to e.g. the plasma separator pressure rating. Thus, it is clear that BAL toxin clearance is inherently limited in terms of replacing liver function.

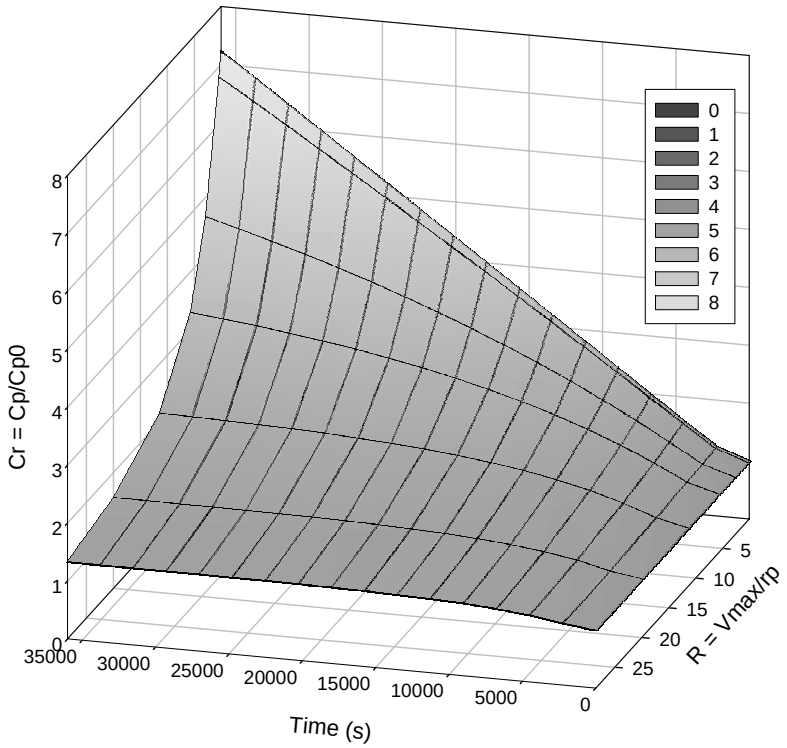

Figure 6.1.5 The influence of the clearance to production ratio on blood ammonia concentration. Graph key: Cr = ratio of actual to initial (normal) concentration, R = ratio of maximum to actual generation rates

4. The effect of the clearance rate (indirectly 'cell functionality') (figure 6.1.5). At low clearance rates ammonia concentration continues to rise and even after 10 hours of treatment, an equilibrium concentration (between actual and starting) may not be reached. At high ratios of clearance to production, an equilibrium may be reached within as little as an hour and at a low starting concentrations. This illustrates the importance of examining actual cell numbers and cell functionality when designing a BALSS. Interestingly, the initial ammonia concentration (C_{p0}) influences the shape of the surface, but not the ultimate equilibrium value.

6.1.5 Discussion

Hepatocytes are the cells accounting for the majority of liver toxin clearance functions and the synthesis of hepatotrophic (liver regenerative) substances. However, artificial blood toxin clearance devices, such as for example activated charcoal filters, are known to be better at clearing toxins than most bioreactors [251]. It is presumably for these reasons that cell-based biological systems have shown improvements in survival (of treated animals), while purely artificial liver support technologies have not (despite the extensive use of the latter in human treatments).

Iwata *et al* (2004) [251] clearly elucidated the results of BAL modeling efforts. Our simulations confirmed these findings. In summary,

1. The clearance value of a BALSS is proportional, to a first approximation, to the number of hepatocytes in the system. i.e. the blood toxin concentration of a patient treated with a device containing a small number of hepatocytes will stabilize at a concentration that is several times higher than the normal (starting) concentration, even after long-term assistance.
2. If an adult is treated with a BAL containing, say, 10 % the hepatocyte mass of an innate liver, the patient's blood toxin concentration will stabilize at a concentration that is approximately 10 times higher than that of the normal (starting) concentration, even after long-term assistance. There is an approximately inverse linear relationship between the hepatocyte mass and the eventual toxin concentration. A liver weighs approximately 1500 g, of which 80 % or 1200 g are hepatocytes. The majority of current BAL bioreactors employ in the region of 50-100 g of hepatocytes.
3. The clearance value of a bioreactor cannot exceed the perfusate flow rate, thus, the plasma exchange rate provides the upper limit for the clearance of toxins. However, the clearance values of most artificial detoxification modules is between 10 and 15 times greater than that of existing bioreactors, thus, the use of these modules is attractive in terms of blood toxin removal in liver support. No existing BAL design can eliminate toxins, such as ammonia, as rapidly from the

systemic circulation as an adult liver. However, should an artificial clearance device be added to a BAL system care should be taken to ensure that filtration does not exclude desirable low molecular weight substances, such as growth factors, from entering the patient and providing regenerative benefits.

4. Since a bioreactor contains, say, only 10 % the hepatocytes of a normal liver, it can only produce a maximum of 10 % of the plasma proteins of a healthy person, even if the patient is treated for an extended period. Thus, supporting a patient by means of plasma exchange is likely to be more efficient than with a BAL alone. However, large amounts of plasma are expensive and animal sources for the treatment of human patients are unacceptable due to concerns regarding xenogenicity. Difficulties also reside in isolating and culturing the very large quantities of metabolically functional cells required.
5. Only a BALSS that has an exchange rate that is capable of matching the blood inflow rate of an innate liver will match the functionality of a normal liver. The blood inflow rate of an adult *in vivo* liver is in the region of 1500 ml/min, while blood exchange rates to a BALSS lie in the 100 - 300 ml/min region. Thus, in terms of treatment, only OLT is able to meet this objective, which may explain why existing systems that have undergone human clinical trials have not shown significant survival benefits. It also explains why the benefit of BAL treatments is expressed as a ‘bridging’ therapy to OLT.

However, there are limitations to pharmacokinetic modeling methods:

1. Measurement variations. As was evidenced in section 4.2, the pharmacokinetic clearance/production values reported for porcine hepatocytes are exceptionally variable. Accurately simulating clearance or production ability of a bioreactor may consequently be difficult. A basic review indicates an excess of a 10 000-fold divergence across reported values (table 4.2.1 and figure 6.1.6).

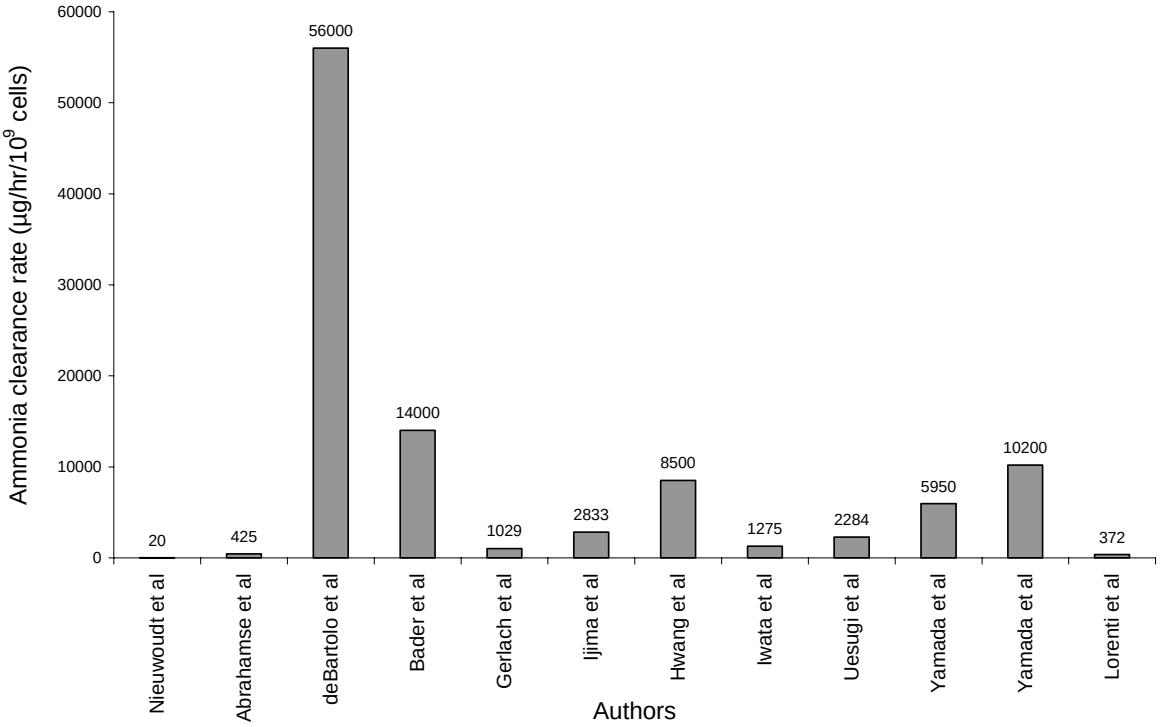

Figure 6.1.6 Variation in reported values of ammonia clearance

2. Measurement units. The means by which clearance values are reported may prevent the direct comparison of values. Data is often reported in units of µg/hr/10^9 cells, which is normally calculated directly from the slope of, e.g. the graph of ammonia, concentration against time and the number of hepatocytes in the system. However, this does not indicate the inherent ability of the cells in the system to clear ammonia. Other factors may affect the results, for example, the starting concentration of ammonia in the system and the ratio of the number of cells to the reactor volume. It would seem highly unlikely that primary porcine hepatocytes would exhibit 10 000 fold variations in ammonia clearance rates based on relatively small changes in reactor size, flow rates or scaffold materials. In an attempt to enable more accurate comparisons between reported values we calculated the parameters Vmax and Km from the raw data (as described in Appendix C). In this case a reduced Vmax (Vrmax) was used, taking into account the cell loading per reactor volume ratio.

3. Measurable variety of liver functions. Pharmacokinetic modeling is limited to only the clearance of toxins and/or synthesis of plasma proteins or metabolites. These must also be readily measurable. While these functions are necessary, there are also other important liver functions in the context of ALF, for example, regeneration. In this process numerous cytokines, chemokines and growth factors participate in complex cell-signaling cascades that initiate and control each step. Hepatocyte growth factor (HGF), epidermal growth factor (EGF) and transforming growth factor alpha (TGF-α) are viewed as the primary stimuli, which are potently mitogenic, but require that hepatocytes first be primed by other soluble factors, including tumour necrosis factor (TNF) and interleukin-6 (IL-6) [258,259]. In ALF, the concentrations of HGF and EGF in the plasma may rise to a maximum of only10 ng/ml, yet this is sufficient to initiate regeneration. This may be viewed as a complex non-linear *on-off* switch, rather than a linear response to the extent of liver damage.
4. *Off-line, after-the-fact*, single metabolite per simulation methodology. Although pharmacokinetic models are a necessary and desirable part of finalizing BAL design they provide predictions regarding the clearance or production of only single substances at a time and only after rates of production and or clearance have been measured in *in vitro* and *in vivo* experiments. However, once this data is available and if one assumes they will remain the same in a treatment, the model can be adapted for an *on-line* application in which, say ammonia is measured on a constant basis.

In summary, while compartmental pharmacokinetic models provide information of value in especially the design of a BALSS, they are limited to describing only the clearance and or production of individual biochemicals. ALF is a complex; multisystemic process that is incompletely understood and consequently the full range of BAL functions are not precisely defined. Other analysis and modeling methods are additionally required.

6.2 Developing an *on-line* predictive clinical monitoring system for acute liver failure patients

Nieuwoudt M, Bond R, van der Merwe SW, Cilliers P.

Manuscript in preparation.

6.2.1 Introduction

A variety of prognostic criteria have historically been proposed for the early identification of acute liver failure (ALF) patients that are likely to die and therefore require orthotopic liver transplantation (OLT), the only treatment of proven benefit. These criteria have, without exception, been defined based on the multivariate analysis of clinical variables measured on patient admission to the clinic [52-56,239-241,260-269]. Owing to the multiplicity of etiologies and pathogenesis in ALF [24-26,72] a large range of variables with prognostic value have been identified, and studies of new/additional variables have subsequently continued [239-241,267,268].

The rate at which a clinician is able to update a patient's prognostic score is based on the regularity at which the involved clinical variables are sampled. For example, blood indices are typically measured 12 or 24 hourly. However, the progress of ALF is rapid with a high mortality rate within 5-10 days following diagnosis. Thus, a pressing need remains for prognostic criteria which are able to provide early and repetitively accurate estimates of prognosis in ALF. Clinical microdialysis (www.microdialysis.se**)** has recently become an attractive addition to the ICU in that bedside systems are able to provide *on-line* indications of physiologically interesting 'biomarkers' using sterile probes and low volume sampling techniques [270,271]. Thus, a possibility exists to combine high-frequency systemic and biochemical monitoring in the ICU with one or more prognostic models. This would be a 'dynamic' prognostic system which would be of value to critically ill ALF patients in whom rapid clinical decision-making is necessary. Predicting outcomes in (expensive) animal experiments may also allow earlier terminations and thus benefit researchers investigating, for example, bio-artificial liver (BALSS) devices.

This study proposes a variety of modeling and hardware implementation methods for the development of a combined *on-line* biochemical and prognosis monitoring system. The underlying models include a conceptual part defined using the Unified Modeling Language (UML) followed by a numerical part employing a multivariate statistical approach. The UML is a graphical systems engineering tool that specifies systems structure (composition) and behaviour (function). It is often used to define software architectures [272-278] and has been proposed as an ideal method for integrating biological data into *in silico* models and meta-models in hierarchical levels of complexity [276-278]. Both the UML and subsequent statistical models aim to represent the multi-systemic pathogenesis of ALF. Technically, the resulting model is a *state estimator* [11,279-283] of ALF and is *data-driven* [284] in that it is based on trends in raw clinical data collected in irreversible (i.e. resulting in death) surgically-induced ALF experiments in pigs, as previously described by our group [213]. It is understood that the proposed model/s are currently relevant to the animal circumstance. Future efforts combining additional animal and human data may subsequently facilitate the implementation of an *on-line* system in the human clinical scenario.

6.2.2 Methods

6.2.2.1 Data processing

The data of a large number of systemic and biochemical variables was collected in the course of experiments aimed at standardizing an ischemic surgical model of ALF in pigs as previously described [213] (tables 5.2.1,2). Of this, 8 cases were selected as ideally representative of future experiments and were used as the training subset in defining the numerical models described below. Thereafter, the *un-trained* data of 8 animals, which were involved in subsequent clinical evaluations of the UP-CSIR BALSS, was used in testing the accuracy of the model. Excel 2003 was used as the spreadsheet for all data, including linearity testing, a macro for Tornado sensitivity diagrams [285], Monte Carlo analysis [286,287] using the random number generator facility and analysis of variance (ANOVA-single factor without replication, 0.05 confidence level). Statistix 8 (Analytical

software, Tallahassee, FL, USA) was used to calculate parametric and non-parametric correlation coefficients and Shapiro-Wilks normality tests.

6.2.2.2 Conceptual (system) modeling

The UML diagrams were made using an IBM-Rational Rose UML modeling tool. The class diagram (figure 6.2.1) provides a hypothetical structural framework for the data attributes of the objects (organs-systems) of the ALF patient-system as a whole. Each class contains the measurable attributes (variables) for the *minimally* involved organs or organ-systems. The associations (arrows) between classes indicate the 'inheritance' of each sub-system, i.e. the composition of each class. Some associations are necessarily bi-directional in that the components (organs) of a physiological system are inter-related. Not all of the variables listed in the class diagram were measured in the pig experiments. The list of attributes (table 6.2.1) is composed of those variables identified in a range of studies [24-26] (and by speakers at the European association for the study of the liver (EASL), Acute Liver Failure congress of 2007 [288,289]) as useful in indicating particular stages in the pathogenesis of ALF in a patient. Naturally, more data attributes may be added or subtracted as knowledge of their prognostic utility develops.

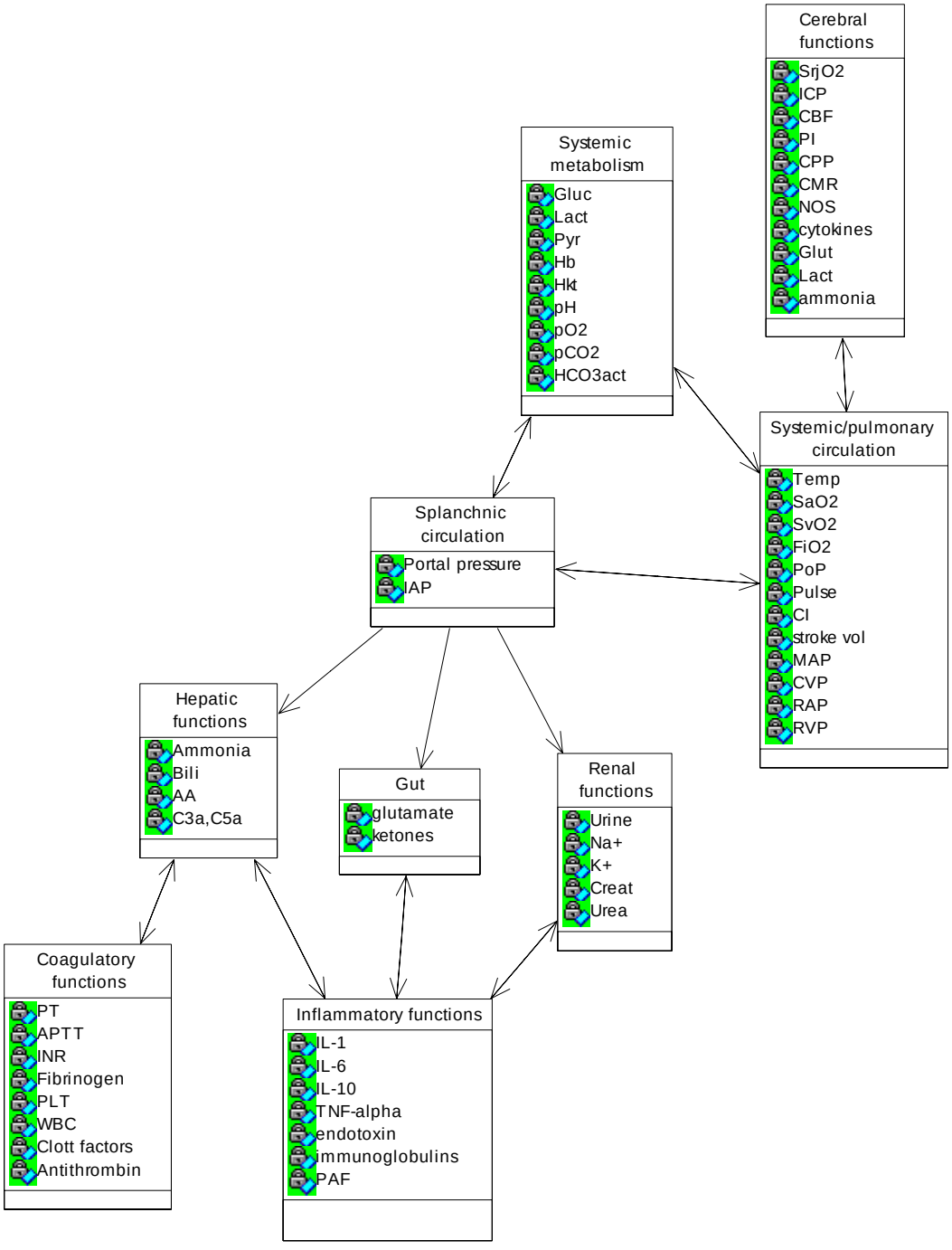

Figure 6.2.1 Class diagram for data attributes (clinical variables) of the patient-ALF-system. Each class represents an organ-system where the measured variables provide information of prognostic value in ALF. Not all the variables were measured in the animal experiments. These may be incorporated into subsequent numerical modeling instances.

Table 6.2.1 Attributes (clinical variables) for the class diagram.
The highlighted variables were not measured in the animal experiments (section 5.2).

Class	Attribute (variable)	Description	Units	Behaviour over time
Systemic metabolism	Gluc	blood glucose	mmol/L	homeostatic
	Lact	blood lactate	mmol/L	increasing
	Pyr	blood pyruvate	mmol/L	homeostatic
	Hb	blood hemoglobin	g/dL/hr	decreasing
	Hkt	blood hematokrit	%	decreasing
	pH	blood pH	pH	homeostatic
	pO2	partial pressure of O_2	mmHg	homeostatic
	pCO2	partial pressure of CO_2	mmHg	homeostatic
	HCO3act	blood activated bicarbonate	mmol/L	homeostatic
Systemic/ pulmonary circulation	Temp	temperature	^oC	increasing
	SaO_2, SvO_2	central arterial and venous O_2 saturation	ml/dl	decreasing
	FiO_2	% inspiratory O_2 concentration	%	
	PoP	pulmonary occlusion pressure	mmHg	
	Pulse	pulse rate	beats/min	homeostatic
	CI	cardiac index	ratio	
	Stroke vol	left ventricular stroke volume	ml	
	MAP	mean arterial pressure.	mmHg	decreasing
	CVP	central venous pressure	mmHg	
	RAP	right atrial pressure	mmHg	
	RVP	right ventricular pressure	mmHg	
Cerebral Functions	$SrjO_2$	reverse jugular venous O_2 saturation	ml/dl	decreasing
	ICP	intracranial pressure	mmHg	increasing
	CBF	cerebral blood flow velocity	ml/min	
	PI	Pulsatile index	ratio	
	CPP	cerebral perfusion pressure	mmHg	
	CMR	cerebral metabolic rate	µmol/g/min	
	NOS	nitric oxide synthase	µmol/L	
	cytokines	see IL and TNF below	µmol/L	
	Glut	glutamine	µmol/L	
	Lact	lactate	mmol/L	
	ammonia	ammonia	µmol/L	
Splanchnic circulation	portal pressure	hepato-portal pressure	mmHg	
	IAP	intra abdominal pressure	mmHg	
Hepatic Functions	ammonia	ammonia in blood	µmol/L	increasing
	bilirubin	bilirubin in blood	µmol/L	increasing
	amino acids	ratio of branched-chains to aromatic	ratio	decreasing
	complement	C3-a and C5-a in blood	µmol/L	
Gut	glutamate	glutamate in blood	µmol/L	
	ketones	ketones in blood	µmol/L	
Renal Functions	Urine	urine volume	mL	constant
	Na+	change of [sodium]	mmol/L	decreasing
	K+	rate of change of [potassium]	mmol/L	increasing
	Creat	rate of change of [creatinine]	µmol/L	increasing
	Urea	rate of change of [urea]	mmol/L	decreasing

Class	Attribute (variable)	Description	Units	Behaviour over time
Coagulatory Functions	PT	rate of change of prothrombin time	secs	increasing
	APTT	rate of change of activated partial thromboplastin time	secs	increasing
	Fibrinogen	rate of change of [Fibrinogen]	g/L	decreasing
	PLT	rate of change of platelet count	10^9/L	decreasing
	WBC	rate of change of white blood cell count	10^9/L	increasing
	Clott Factors II	percentage of normal clotting factors II, V, VII, IX, X in blood	%	decreasing
	AntiThrombin	rate of change of percentage of normal anti thrombin in blood	%	decreasing
Inflammatory functions	IL-1,6,10,	interleukins 1,6,10	µmol/L	
	TNF-alpha	tumour necrosis factor-alpha	µmol/L	
	endotoxin	endotoxin	pmol/L	increasing
	immunoglobulins	immunoglobulins	µmol/L	
	PAF	platelet activating factor	µmol/L	

Note: In the surgical ischemic experiments all biochemicals/metabolites were measured in whole blood or plasma. Where behaviour over time is not included the trend must still be determined.

The purpose of a state transition diagram (figure 6.2.2) is to describe the behaviour of a system. In this case specifically the pathogenesis of ALF, albeit in a simplified way. In general the state of an object changes over time and transitions may be reversible. For example, in the human clinical scenario early ALF may revert to health (the initial state) owing to the innate regenerative ability of the liver. However, the degree of disease progression determines the likelihood of reversion (i.e. the further down in the diagram the worse the prognosis). In the ischemic surgical animal model, on the other hand, state transitions were irreversible in that death (the terminal state) was always the end-point. For this reason the resulting models are dependent on the particular data employed at this stage. Each state or sub-state may be defined based on a set of numerical values of the attributes (variables) of the organ-systems of the patient at any given time (table 6.2.2).

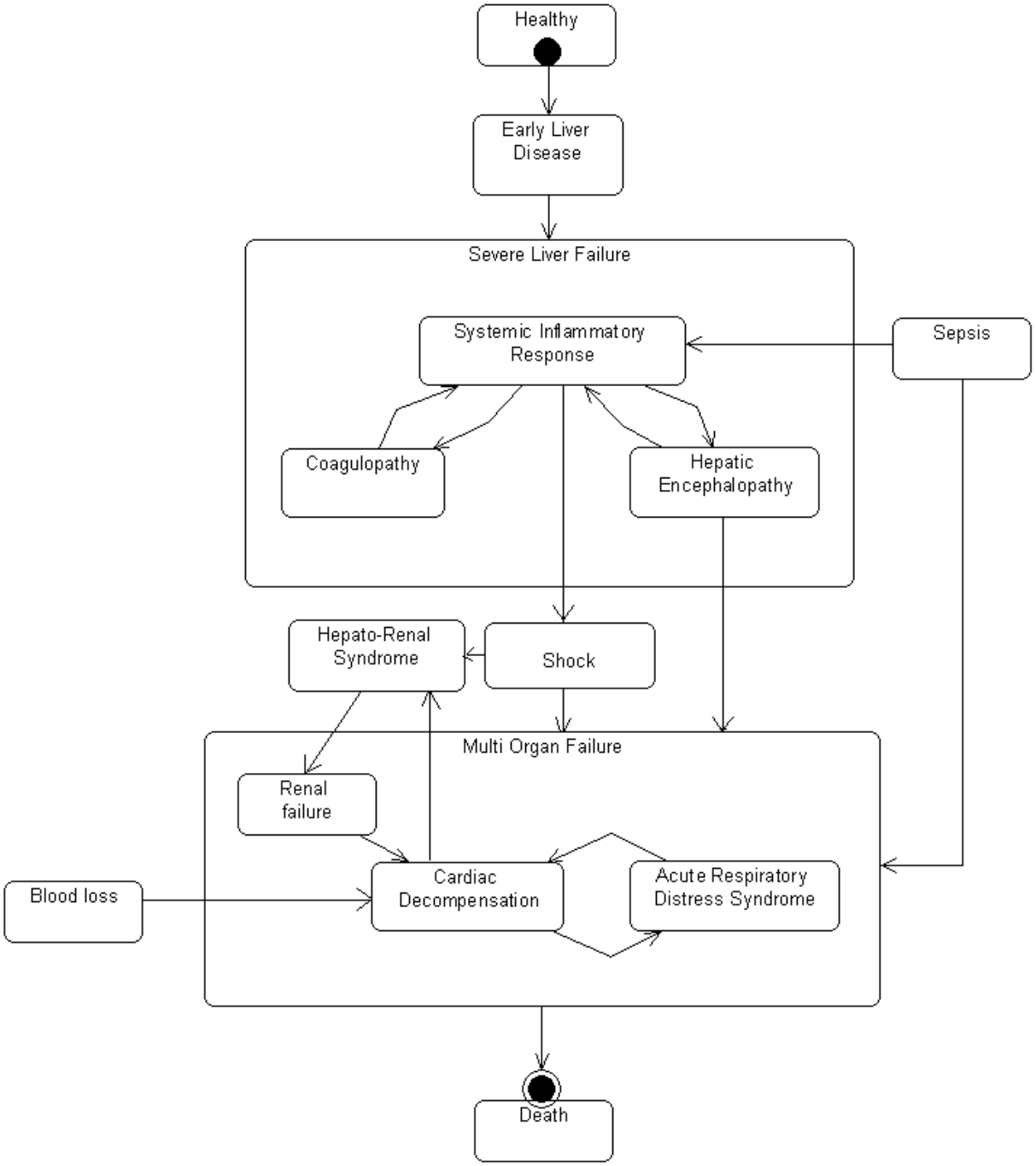

Figure 6.2.2 A system state transition diagram for the ALF-patient system in the ischemic surgical model. Defining state diagrams requires collaborative agreement between researchers and clinicians. Since ALF is only partially understood at present the above is understood as an iterative instance.

6.2.2.3 Numerical modeling

This was based on clinical variables that were found to have prognostic value in the porcine surgical model of ALF. Analysis of the data revealed that prognosis was intrinsically multivariate, with many variables simultaneously determining survival and none predominating [213].

Briefly, the 'raw data' was divided into two depending on the period in which it was acquired. In the initial surgical period (T < 0) in each experiment, the impact of the surgically-induced ALF intervention/s was measured in terms of predominantly systemic absolute-valued indices. In the latter intensive care (ICU) stage (T > 0), the progress of the disease was measured in terms of the rates of change (first derivatives) of predominantly biochemical variables. These rates were the mean gradients of the *best-fit* linear equations derived for each of the animals in each of the biochemical variables as a function of time and were considered the 'derived data'. Non-parametric (Spearman) correlation coefficients, for small data sets, were calculated between the durations of survival, the raw data from the surgical period and the derived data from the ICU respectively. Multivariate linear equations (internally weighted by their correlations) were then derived between the durations of survival (dependent variable), the surgical systemic data and the ICU biochemical trends (independent variables).

The method used was as follows: The dependent variable,

$$Y = \sum_{i=1}^{N} f(x_i) \cdot w_i \qquad (6.1)$$

where N = the total number of equations used to determine the dependent variable Y, $f(x_i)$, is the linear function between each independent variable x_i, and the dependent variable in question. The percentile weight, w_i is the following ratio:

w_i = (the specific weight between the $f(x_i)$ and Y) / (the sum of specific weights to N), (6.2)

where the 'specific weight' is the Spearman correlation coefficient between each independent and dependent variable. Thus, the sum of percentile weights would be equal to one. i.e.

$$\sum_{i=1}^{N} w_i = 1 \qquad (6.3)$$

The independent variables for the model were selected based on their satisfying the following criteria:

1. As high a correlation, or 'weight', with the dependent variable as possible (i.e. a clinical association of relevance in the animal ALF model).
2. As linear over time as possible, and
3. The existence of sensors and equipment for their o*n-line* measurement during experiments.

This method aimed to model the multi-systemic nature of ALF with a multivariate numerical approach. This *stabilized* the model's predictive ability by proportionally assigning weight to variables according to their prognostic value. This method is akin to estimating a multivariate non-linear function at any particular time by the Taylor expansion of its composing derivatives [286,290].

Two instances of the numerical model were created: a Prognostic indicator (PI) and a Biochemical Indicator (BI). These were designed to provide on-line predictions of, respectively, the duration of survival as a primary end-point measure of prognosis, and the numerical value of normally *off-line* biochemicals as secondary 'biomarker' end-points. i.e. the BI provides values for biochemicals normally requiring *off-line* laboratory analysis. Future iterations of such a model may have different end-points.

6.2.3 Results

For purposes of efficiency much of the model sensitivity and verification results have been moved to Appendix D. Only the results critical to demonstrating the accuracy of the model are presented below. For more information please refer (to Appendix D) as accordingly referenced.

6.2.3.1 Class associations

A simple physiological reasoning was initially applied to identify numerical associations of biological interest for potential quantification at a later stage. Correlational statistical analyses investigated the presence of numerical associations (arrows) within classes (i.e *internal* associations) and between classes (i.e. *external* associations) as shown in the class diagram (figure 6.2.1). A clearly multi-variate profile, as was found in section 5.2 was apparent. Since not all pairs of the associated variables are measurable *on-line*, these associations were of a theoretical interest at this point. Please refer to table D.1.1 in Appendix D.

6.2.3.2 Quantification of states

Thereafter, the states/sub-states of the state transition diagram (figure 6.2.2) using the attributes (variables) of the class diagram (figure 6.2.1) were numerically quantified (table 6.2.2). The value in quantifying these states is that an appropriately programmed *on line* monitoring system will be able to provide real time indications of changes in the patient's clinical state. This will facilitate more rapid clinical decision-making than has previously been possible.

Table 6.2.2 Examples of state and sub-state definitions (for reference see section 2.4)

State	Sub-state	Definition
Healthy		Mean values of all variables at start of experiments
Early liver disease		Values < 6 hrs after start
Severe liver failure		Values > 8 hrs after start
	Systemic Inflammatory Response (SIR)	2 or more of: a) fever (Temp > 38 ^{o}C) or hypothermia (Temp < 36 ^{o}C) b) tachypnoea (Respiration rate >24 breaths/min) c) tachycardia (Pulse > 90 beats/min) d) leukocytosis (>12000/µl), leukopenia (< 4000/µl), or >10% bands which may have a non-infectious aetiology
	Coagulopathy	International Normalized Ratio >1.5
	Hepatic Encephalopathy (HE)	I. Behaviour changes with minimal change in level of consciousness II. Gross disorientation , drowsiness, possible asterixis, inappropriate behaviour III. Marked confusion, incoherent speech, sleeping most of the time but arousable to vocal stimuli IV. Comatose, unresponsive to pain, decorticate or decerebrate posturing
Sepsis		Inflammatory response to a proven / suspected infectious etiology
Hypovolemic Shock		hypotension (arterial blood pressure < 90mmHg systolic, or 40mmHg less than normal) for > 1 hr despite adequate fluid resuscitation OR Need for vasopressors to maintain systolic blood pressure $\geq$ 90mmHg or MAP $\geq$ 70mmHg
Hepato-Renal Syndrome (HRS)		a. creatinine level > 220 µmol/L with portal hypertension b) no sustained improvement in renal function after volume expansion with isotonic saline solution Urine – a) volume < 500ml/d, b) Na < 10mEq/L, c) osmolality greater than plasma osmolality, d) red cell count < 50 per high power field, e) serum Na < 130mEq/L
Blood loss		Loss > 20% of total blood volume
Multi Organ Failure (MOF)		Dysfunction of more than 1 organ, requiring intervention to maintain homeostasis
	Renal failure	Renal urine output < 0,5ml/kg/hr for 1 hr despite adequate fluid resuscitation;
	Cardiac Decompensation	Adequate fluid resuscitation – pulmonary artery wedge pressure $\geq$ 12mmHg or central venous pressure $\geq$ 8mmHg
	Acute Respiratory Distress Syndrome	Respiratory $PaO_2/FIO_2 \leq 250$ or, if the lung is the only dysfunctional organ, ≤ 200
Death		Mean values at termination of experiments

Note:

1. The above are definitions arising from the human scenario; each state may be further numerically resolved in terms of limits in measured variables at particular time points.

6.2.3.3 The PI equations

Using the numerical method described above the PI was defined as follows:

Table 6.2.3 Model equations and weights for the PI

Independent Variable [x]	Time period	Survival Y = f(x) (hours)	Weight [Spearman correlation]	Percentile Weight Used	Survival data used for training
Body weight		y = -0.003x + 26	0.103	0.045	
Ischemic time		y = -1.16x + 43	0.805	0.354	
MAP_isch		y = 0.06x +22.2	0.012	0.005	
MAP_post		y = -0.083x + 32.2	0.417	0.183	
Pulse_isch	**T<0**	y = 0.072x + 14.3	0.196	0.086	
Pulse_post		y = 0.006x + 25	0.258	0.113	
Temp_post		y = -0.87x + 57.4	0.264	0.116	
Urine_oper		y = 0.021x + 23	0.218	0.096	
Range					20-36 hrs
Mean					*24.875 hrs
TOTAL			2.274	1.0	8 cases
rAmmonia		y = -0.2218x + 36.412	0.485	0.25	
ave_pH		y = -75.627x + 589.2	0.256	0.15	
rHb		y = -6.6337x + 32.459	0.400	0.20	
rHkt	**T>0**	y = 10.415x + 32.459	0.412	0.23	
rK+		y = -19.914x + 28.019	0.230	0.10	
rMAP		y = 5.5301x + 34.909	0.679	0.08	
Range					20-36 hrs
Mean					*26.625 hrs
TOTAL			2.463	1.0	8 cases

Notes:
1. The above variables were chosen as indicators of survival due to their availability for *on-line* measurement, linearity with time and clinical relevance in ALF. Subsequent modeling iterations may employ different variables.
2. In the initial period (T<0), the independent variables were chosen so as to indicate the impact of the surgical interventions. They were composed of absolute values, e.g. the suffix ' _isch' was the mean value of the particular variable during the ischemic clamping time. The suffix '_post' was the mean value after the ischemic time was over.
2. In the latter ICU period (T>0) the independent variables were for the rates at which the listed variables changed over time.

The underlying assumptions of the numerical model were tested as follows:

6.2.3.4 First-order assumptions

The predictive ability of the numerical model relies on the degree to which the independent variables of its composing first-order equations approximate either linear appreciation or depreciation over time. This assumption was investigated by determining the best-fit linear equation for each data set of all variables according to time. A mean R^2 value, the numerical square of the Pearson coefficient was calculated for all variables. The majority of all variables had R^2 values above 0.5 (i.e. Pearson coefficients > 0.7) indicating that variables did linearly change over time and justified the numerical design of the model.

In general, the variables used for prediction during the surgical interval (T<0) had lower R^2 values (were less linear) than those used during the ICU period (T>0). This validated the use of a larger number of variables in the T<0 period, each with relatively less weight than in the T>0 period. It was also expected that the T<0 part would be less accurate than the T>0 part. For more details on these results refer to Appendix D.2.

6.2.3.5 The BI equations

The linearity of the variables in the T>0 part was intrinsic to defining the BI part of the model (tables 6.2.4,5). In this case, highly linear derived variables that were of prognostic value in ALF (and which could be monitored *on-line*) were chosen as independent variables. Firstly, best-fit linear equations were determined for the dependent variables according to time. Then first-order equations were derived that related the derivatives of the independent variables to the derivatives of the dependent variables.

The purpose was to determine the absolute value of a biochemical (that cannot be monitored *on-line*) at any particular time in an experiment using the rate at which a highly linear, independent variable (that can be monitored) was changing in real-time. The difference with the PI is that the absolute value of an *off-line* variable may be determined through the relationship of its first derivative with the derivative of another independent *on-line* variable.

Table 6.2.4 Variable candidates for the BI

Independent variables	**Ranked survival correlation**	**Linearity with time (R^2)**	**Dependant variables**	**Ranked survival correlation**	**Linearity with time (R^2)**
Ammonia	0.772	0.912	BcAA/AroAA	0.734	0.733
K+	0.492	0.569	Glutamine	0.248	0.608
Hb	0.599	0.872	Bilirubin	0.010	0.805
Hkt	0.535	0.808	Fibrinogen	0.327	0.880
			PT	0.370	0.922
			Antithrombin	0.120	0.878
			Factor II	0.208	0.882
			Factor VII	0.337	0.821
			Factor X.	0.347	0.785
			ALP	0.280	0.904
			AST	0.220	0.832
			LD	0.216	0.823
			ALT	0.010	0.781
			Creatinine	0.460	0.632
			Urea	0.301	0.508

Notes:1. The inclusion criteria for the independent variables were:
a. The variables had to be of interest in ALF.
b. The R^2 value, indicating linearity, should be ≥ 0.5.
c. The Spearman (ranked) correlation coefficient, indicating correlation with the duration of survival, must be ≥ 0.5. (K^+ was judged sufficiently close to this value for inclusion).
2. The inclusion criteria of the dependant variables were the same as for a. and b. above. However, as can be seen, the dependant variables demonstrated less correlation with survival than the independent variables. The weighted structure of the model was used to 'stabilize' predictions.

Table 6.2.5 BI model equations

		Independent variables (x)							
Function of initial variable (y) with time (t)	**Dependant variables (y')**	**rAmmonia**	weight	**rK+**	weight	**rHb**	weight	**rHkt**	weight
BcAA/AroAA = y't +3.58	rBcAA/AroAA	y' = -0.0016x + 0.0004	0.387	y' = -0.4736x - 0.0521	0.460	y' = 0.2276x - 0.051	0.407	y' = 0.0556x - 0.0489	0.339
Glutamine = y't +152.10	rGlutamine	y' = 0.0832x + 3.6009	0.317	y' = 22.124x + 6.4388	0.400				
Bilirubin = y't +4.53	rBilirubinTOT					y' = -3.8422x + 1.1073	0.564		
Fibrinogen = y't +2.47	rFibrinogen	y' = -0.0004x - 0.077	0.464	y' = -0.1245x - 0.0895	0.536	y' = 0.1973x - 0.0692	0.429	y' = 0.0561x - 0.064	0.657
PT = y't + 10.28	rPT			y' = 1.2325x + 0.7003	0.400				
Antithrombin = y't +91.43	rAntiThrombin					y' = 4.4269x - 1.4852	0.250	y' = 0.9887x - 1.5065	0.267
Factor II = y't +51.65	rFactor II			y' = 2.2772x - 2.0043	0.446				
Factor VII = y't +57.64	rFactor VII			y' = 1.9639x - 2.4117	0.436				
Factor X = y't +74.59	rFactor X							y' = 2.275x - 1.6933	0.479
ALP = y't + 107.3	rALP			y' = 57.521x + 16.998	0.525	y' = -49.387x + 15.048	0.291	y' = -16.927x + 12.141	0.264
AST = y't + 64.4	rAST	y' = 4.4629x + 59.621	0.555						
LD = y't + 330.0	rLD	y' = 6.6529x - 135.8	0.373	y' = 1049.2x + 141.74	0.427				
ALT = y't + 39.7	rALT	y' = 0.1495x + 5.3928	0.282						
Creatinine = y't +86.92	rCreat	y' = 0.1556x - 3.1144	0.355	y' = 49.361x + 1.4321	0.643	y' = -35.25x + 0.1292	0.346	y' = -8.6656x + 0.4563	0.273
Urea = y't + 3.03	rUrea					y' = 0.2484x - 0.0129	0.618		

Notes:

1. The arbitrary inclusion criterion for any particular equation was that there must be a Spearman correlation coefficient of magnitude no less than 0.25 between the dependant (y') and independent variables (x) in question. The empty parts of the table represent those equations that did not meet the inclusion criterion. Some of the outputs are described by only a single input; consequently, these predictions are likely to be less accurate than those predicted by several inputs.
2. The Spearman correlation coefficients were used as weights in determining a summated product for the particular biochemical rate in question.
3. Once a dependant variable's summated value was determined, an absolute value for the biochemical could be calculated from the function of the biochemical raw data with time (first column).
4. The above statistical trends were determined from the data of a total of 12 animals. These were animals that successfully met the criteria of inclusion (table 5.3).
5. The shaded dependant variables (rGlutamine, rCreat and rUrea) were considered for subsequent omission from the model, due to the divergence of predicted values from those measured.

6.2.3.6 Model sensitivity

This was tested using Tornado diagrams and Monte Carlo numerical simulation methods. A selection of the resulting graphs are presented in Appendix D.3.

1. Tornado diagrams [285].
These diagrams display the sensitivity of the output of a model in terms of the numerical range of its input variables. This method assumes Gaussian normality in the input populations. As was expected in this case, the weight appropriated to each of the input variables strongly influenced their effect on the model's output. This was true in both the PI and BI parts of the model and further validated the weighted numerical design of the model.

2. Monte Carlo (MC) simulation [286,287].
Populations of random numbers, either normal on uniformly-distributed, were also used as input to the model. This was done both individually and in combination, i.e. either one variable was randomized independently while retaining all other variables on their mean values, or all variables were randomized simultaneously, followed by the summation of the results and graphical projection. In all cases, each of and a combination of the input variables very closely approximated the measured mean values (i.e. < 10 %). However, there was consistently less variation in the predicted values than in the measured population. This may have been due to the limited size of the training population. The effect of using uniform distributions was to slightly under-estimate the output. The model would therefore tend to produce more conservative estimates with non-normally distributed data.

5.2.3.7 Assumptions of normality

The predictive ability of the numerical model is also dependent on the degree to which its input popoultions are normally distributed. To investigate this assumption the measured raw input data was tested for normality using Shapiro-Wilk tests. Despite the small size of the population from which the model's equations had been derived, normality was only

excluded in the derived variables rHb and rAmmo (PI model). Similar to the above, the effect of uniformly distributed populations was to marginally underestimate the measured results. Thus, prediction error would tend to be conservative. In practice therefore, the requirement of clinical interventions would be indicated earlier rather than later (a good thing!).

The above results are presented in Table D.4.1 in Appendix D.

6.2.3.8 Factors affecting BI accuracy

The following four factors potentially determining the prediction accuracy of the BI were identified:

1. The number of independents used to determine each dependent variable (see table D.5.1 in Appendix D).
2. The accuracy of measurement of the independent variable/s. Specifically, the large measurement deviation in the biochemical variables (section 5.2), and
3. The strength of correlation between the variables.

It was consequently expected that the BI would not be as accurate as the PI.

6.2.4 Model Verification

This was performed using a variety of statistical techniques, including analysis of variance (ANOVA), 'relative error' calculation and direct comparison with prospectively acquired, *un-trained* data. For more detail on these techniques refer to Appendix D.6. Briefly,

6.2.4.1 ANOVA

After calculating mean and standard deviations and percentage deviations between all measured and predicted populations it was found that the predicted means very closely approximated the measured means, i.e. < 1%. In certain biochemical variables, such as

Factor X, urea, creatinine and glutamine the percentage error was unacceptably large, indicating their potential exclusion from the BI part of the model.

An ANOVA comparison was drawn between all predicted and measured populations. It was found that the variances were similar although that in the predicted populations tended to be greater. In summary, it was not possible to detect significant differences between the populations in any of the parts of the model. These results were taken as a positive indication of the accuracy of the model.

6.2.4.2 Relative error

For visual and statistical indications of prediction error-range and magnitude the following was done:

The *point error* error (i.e. the deviation of each predicted to corresponding measured value as a fraction of each measured value) was calculated. This was then divided by the standard deviation (std dev) of the measured population to give *relative error (re)*. As *re* approaches zero, the greater the model's prediction accuracy. These results were graphically projected. Significant differences were taken to be where the *point error* exceeded 100 % of the std dev of the measured population. The std dev of the *re* (SD*re*) indicates the predicted *error range*. To overcome potential weaknesses in this method associated with variables demonstrating large measurement variations the measurement range was multiplied with the standard deviation of the relative error (SD*re*) for a quantitative comparison. The larger the returned value, the larger the prediction *error region*. For details of these results please refer to Appendix D.6.2.

In the surgical period (T<0) the PI's point errors all fell within $\pm$ 8 %, and in the post-surgical period (T>0) it fell within $\pm$ 3.5 %. In the BI, only in urea did the relative error fall outside of the 100 % mark. These findings agreed with that previously found. Specifically, the PI was more accurate than the BI. In the latter case this was not

considered critical since its purpose (the BI's) was to have *on-line* estimations for biochemical variables for which there were no sensors.

6.2.4.3 Comparison with prospectively acquired *un-trained* BALSS treatment data

Following the definition of the model, data was subsequently collected during 8 BALSS treatment experiments, including with-cells versus without-cells (control) bioreactor configurations (table 6.2.6). (The evaluation of this data was also previously described in section 5.3)

The PI, based on the rate of change of biochemical variables in the ICU (T>0), was accurate to within less than 10 % in all cases. As expected, the PI was less accurate in the T < 0 period than in the T >0 period and also more accurate in the BALSS with-cells versus without-cells configurations. In the first instance this was likely due to the greater number of absolute-valued, less 'weighted' (i.e. in total, less linear first-order) variables used in the surgical versus ICU periods. In the second instance, the lower accuracy, specifically the survival over-estimation in the cell-free configurations, would seem to indicate that the model was *missing something*, i.e. there were changes in variables that the model was not designed to register. As per our prior evaluation (section 5.3), the likely explanation lay in the observed coagulation problems in those experiments. Indeed, in this model's instance, neither part (T < or > 0) was designed to predict prognosis based on coagulatory variables. This was as a result of the fact that there were no *on-line* sensors for any coagulatory variables at the time. This circumstance has subsequently changed. Since ALF is multi-systemic, a prognosis model should employ (ideally *on-line*) independent variables representing as many of the involved organ-systems as possible.

Importantly, the ischemic animal trials were terminated prior to completion (due to financial deadlines) limiting the amount of data available for the prospective verification of the model. Despite the observed accuracy, a larger data set would obviously have been preferable.

Table 6.2.6 Comparison of predicted to measured *un-trained* BALSS test data with the PI

	Measured survival (hrs)	**Predicted survival**		**Percentage Difference**	
Group		**T<0**	**T>0**	**T<0**	**T>0**
BALSS + cells	20.5	23.7	21.7	+ 15.6	+ 5.9
	29	29.3	28.1	+ 1.0	- 3.1
	30	29.6	32.3	- 1.3	+ 7.7
	24.5	27.3	22.1	+ 11.4	- 9.8
	21	26.9	19.0	+ 28.1	- 9.5
absolute mean	N = 5			11.5	7.2
BALSS – cells	14.5	25.9	25.3	+ 78.6	+ 74.8
	10.6	26.8	18.1	+152.8	+ 70.8
	17.5	26.9	18.7	+ 53.7	+ 6.8
absolute mean	N = 3			95.03	50.8

Note: The sensitivity of the numerical scale should be considered, e.g. one hour is 5 % of 20 hours (the mean survival). The time of death was often measured to only an accuracy of 30 minutes. Thus, predicting to within less than 2 hours in these (rather difficult) experiments qualifies as accurate and validates the prognostic value of the variables used in the model.

6.2.5 Discussion

The prognosis of surviving ALF has steadily globally improved over the last 4 decades. This has been as a result of improvements in the molecular understanding of the disease and intensive care methods [24-26]. As yet, no BAL device has demonstrated sufficient efficacy in the human clinical scenario to lead to a commercially available product. This is despite great efforts in this respect. Artificial liver systems have also not shown improvements in patient survival in randomized clinical trials although improvements in patient biochemistry have often been demonstrated [72,82]. A picture that appears to have emerged is that improving patient biomarkers does not translate to improvements in survival. However, the value of an *on-line* biomarker system is obvious: Knowledge of the degree of progression of a highly acute disease will almost certainly provide a benefit to the clinician and therefore the patient.

In the above regard, a recent study investigating the clinical efficacy of the MARS artificial liver support system employed the MELD score (and the SOFA score, Glasgow coma scale and APACHE II criteria) on ALF patients at admission and at 3 months follow up after a treatment series [269]. It was discovered that the treatments resulted in improvements in the MELD score, but that improvements in survival were not calculable based on the small patient cohort. Importantly, the MELD score is defined in terms of biomarkers and fundamentally assumes a correlation between mortality and the resulting score. By implication, an improvement in biomarkers was associated with an improvement in survival.

A basic review of existing prognostic systems [52-55,239-241,261-269], independent of etiology, reveals that the extensive range of variables that have been employed are mostly of a biochemical nature (table 6.2.7). i.e. they are metabolic biomarkers. Despite extensive historical efforts no single prognostic criteria system has achieved worldwide use (although the MELD score appears to be becoming progressively more universally applied). This circumstance may be due to regional demographic

and etiological differences in ALF, with consequently varying pathogenesis. In general, first world countries have more cases resulting from self harm attempts (e.g. acetaminophen), while third world countries present with more of a viral origin (e.g. HBV). This fact may limit the accuracy and specificity of prognostic criteria employed on different patient groups to those on which they were defined. Investigations into the prognostic value of new/additional clinical variables are ongoing [239-241,267].

Without exception, the *historical* biomarkers of ALF have been identified using multivariate statistical analysis of patient data on admission to the hospital/clinic. An underlying principle seems apparent, namely that several variables representing the multi-systemic nature of ALF should ideally be incorporated into any particular prognostic system. Such an approach would ensure the representation of all physiological systems, even if any one variable failed to demonstrate a routinely high correlation with survival. For example, using variables from the following possible organ-systems may result in a more molecularly representative prognostic model than has been available to date:

1. coagulatory system variables, e.g. INR, PT , clotting factor 5.
2. immunological variables, e.g. IL-6, TNF-α.
3. liver toxin clearance variables, e.g. ammonia, bilirubin.
4. liver synthetic functions, e.g. AFP, complement (C3a, C5a). albumin.
5. kidney function, e.g. creatinine.
6. cerebral functions, e.g. HE, coma, ICP, $SrjO_2$, PI.
7. systemic metabolism, e.g. pH, lactate and/or pyruvate.
8. systemic circulatory and/or pulmonary functions, e.g. FiO_2, serum Na^+, and
9. perhaps a demographic variable, such as age.

Notes: This list is tentative and variables may be added/subtracted following the resolution of their prognostic value. For an explanation of the meaning of abbreviations please refer to table 6.2.1.

Table 6.2.7 Review of variables that have demonstrated prognostic value in ALF

[1]Study/s	Variables																				
	age	pH	AFP	Alb	Factor V	PT	INR	Serum Bili	Creatinine	Urea	Ascites	HE	Serum- Na	HVPG	FiO_2	FOS	Hb	Ammonia	Lactate	Pyruvate	Ph-alanine
KCC [52,53,260]		✔				✔	✔	✔	✔			✔									
[2]Cliché [55,261]	✔		✔		✔							✔						✔			
MELD+modified [262,263]						✔	✔	✔	✔				✔	✔							
CTP+modified [264,265]				✔		✔		✔			✔	✔									
RFH [266]								✔		✔					✔	✔			✔		
[3]Dabos *et al* [267]																	✔		(✔)	✔	✔
Bernal *et al* [268]																			✔		
[4]Bhatia *et al* [239]	(✔)	(✔)		(✔)		(✔)		(✔)				(✔)						✔			
Clemmesen *et al* [240]																		✔			
[5]Bernal *et al* [241]	(✔)							(✔)					(✔)					✔	(✔)		

Footnotes:

1. The above studies were selected to represent prognostic criteria for all causes of ALF (i.e. mostly paracetamol, viral, cirrhotic). The table is not intended as an exhaustive review, and it does not provide the parameter values used in each system. Sequential organ failure assessment (SOFA) and acute physiology and chronic health evaluation (APACHE) III scoring systems are not included since they were designed with *all*, rather than only liver forms of organ failure in mind.
2. Additional independent predictors of poor prognosis: presence of coma, hepatitis B virus marker (HBsAg)
3. Additional independent predictors of poor prognosis: alanine, acetate, calcium, lactate.
4. Additional independent predictors of poor prognosis: pH, age, HE, cerebral oedema, bilirubin, albumin, PT, bicarbonate.
5. Additional independent predictors of poor prognosis: high MELD score, CVVHF, vasopressors, bicarbonate.

Entries in brackets indicate variables that had prognostic value but were not primarily studied.

6. Abbreviations: KCC = King's College criteria (London), Cliché criteria (France), MELD = Model for end-stage liver disease (US), CTP = Child-Turcotte-Pugh criteria, RFH = Royal Free Hospital criteria, HVPG = hepatic venous pressure gradient, INR = international normalized ratio, AFP = serum α-fetoprotein, ser- = serum, Ph-ala = phenyl alanine, FiO_2 = % inspiratory O_2 concentration, FOS = Failing organ system

One variable of particular interest is arterial ammonia owing to its historic absence in prognostic criteria. It is surprising that despite impressive progress in understanding the central role of ammonia in the pathogenesis of ALF [35-40], studies have only recently undertaken to investigate its importance as a biomarker with prognostic value in ALF [239,241]. Interestingly, Bernal *et al* (2007) [241] found that their uni- and multi-variate models were more accurately predictive of survival when combined with the MELD score, which is itself a multi-systemic prognostic system. In any case, the data of the animal model on which the second of the above animal studies was based (section 5.2) clearly demonstrated a strong correlation between rising arterial ammonia levels and the duration of survival. However, this may be unsurprising in view of the toxicity of the ischemic model.

On-line ICU patient monitoring technologies and time-series data analysis methods have been available for some time [291-295], however, only in recent years has there been any effort to make prognosis scoring systems 'dynamic'. For example, a recent study demonstrated that the prognostic accuracy of sequential organ failure scores (SOFA) of patients in an ICU was significantly improved if the trend or change in the daily evaluations were incorporated into subsequent mortality prediction models, rather than using only the single admission score as has been done to date [296,297]. There seems little doubt that a mortality model's value, both to patient and clinician, will increase with the regularity with which it is updated.

Both the UML and numerical methods employed in this study aimed to model the multi-systemic character of ALF. The UML has repeatedly been indicated as well-suited to data integration in systems biology. To paraphrase Rouquié *et al* [276-278], firstly, 'an entity considered to be a system can be represented as the interface between an internal and external environment on which it is acting and in which it is evolving', and secondly, 'its behaviour is describable as a state trajectory in a time, space and form frame'. The UML is useful as a metamodel in that it can integrate the data of underlying models that may be of such complexity that it is impossible to contain them all in a single model. Take a genomic, proteomic, cellular, organ and metabolic system as a single hierarchical example.

On a minimal level, in this study the UML was useful for specifying a hypothetical ALF-patient-system in terms of the variables (data) composing its organ-system structure, and perhaps more importantly, its functions in terms of a state trajectory in time. Obviously, modeling a complex system such as ALF is error-prone. At this stage a relatively greater value of the proposed model/s lies in their methodological foundation/s rather than the particular clinical instance. In the future it will be desirable to include additional animal and human data.

The numerical approach above resulted in a summed, weighted multivariate combination of absolute-valued data representing the surgical intervention and the rates of change of systemic circulation and biochemical data for which *on-line* detection equipment existed. The variables that were selected had previously established prognostic value in ALF, linearity over time and the availability of *on-line* sensing equipment. The benefits of this approach were:

1. Non-linear analysis methods, such as Kohonen self-organizing maps (SOMs), in the neural network toolbox in Matlab (www.mathworks.com), did not produce useful results on the small data sets.
2. Verification demonstrated that first order (linear appreciation/depreciation with time) assumptions were justified in the employed variables. This meant that based on the duration of the experiments (> 20 hours), the more time-linear and accurate latter part of the numerical model would be more extensively employed than the former.
3. The model satisfied Occam's razor in that a conceptually simple method modeled a process for which no *a priori* descriptive equations existed. The relative ease with which new variables may be incorporated into the numerical model is an attractive part of its design. For example, in future modeling iterations it may be attractive to investigate more biochemically oriented variable sets and to include transcranial doppler (CBF, PI, $SrjO_2$, CMR, CPP), cerebral microdialysis or intracranial pressure (ICP) variables (which are good predictors of HE in ALF [26, 297-299]).

4. The linearization about some point of interest along a non-linear function is a common procedure in bioprocess technology (although the regularity of *on-line* measurements then determines the model's accuracy [11,279-283]).

It was noteworthy that numeric verification using an untrained dataset demonstrated accuracy in the PI model's ability to predict the duration of survival, specifically in the BALSS with-cells group and particularly in view of the numerical method's multi-systemic representation of ALF. However, larger sample sizes would obviously have preferable.

Regarding the biochemical indicator however, although intrinsically possible and even relatively accurate on its training dataset, the BI is understood to be somewhat contrived. Prior studies have found little correlation between independently measured metabolic biomarkers in ALF. For example, only ammonia and bilirubin levels were found to correlate ($p = 0.01$) in a study investigating the prognostic value of arterial ammonia [239]. This is why not all the BI's results were provided and why additional verification was not carried out on the un-trained treatment dataset. It should be recalled that the BI is a 'software sensor' [279,283] that was defined to provide indications of biomarkers in the absence of *on-line* equipment. It is obvious that an *on-line* approach remains the ideal solution.

In terms of system implementation, the proposed numerical model is well suited to application as a 'Kalman filter' (KF). This is a linear state estimator used for calculating the value of bioprocess variables that are normally not measurable *on-line* (e.g. the biomass or product/substrate concentrations in a production bioprocess [11,279-283]). This method involves continuously updating a pre-defined process model with *on-line* sensor measurements for independent variables. An effective KF has two basic requirements:

1. The process model must be accurate and insensitive to measurement errors, and
2. The system and measurement noise should be determinable.

This raises the following points:

The proposed model is unavoidably reliant on the accuracy of sensors for the independent variables. In fact, the variables were chosen owing to the commercial availability of *on-line* sensors. Ensuring measurement accuracy is possible using noise-filtering techniques, such as first or second order filters or a moving average of measurements. A data integration/processing system with a graphical user interface (GUI) would consequently also be necessary. In this respect, an active virtual state estimator, as represented by figure 6.2.2, would be a useful component of a GUI.

Bioprocesses are harsh environments for sensors in that protein fouling of surfaces may cause measurement problems. A solution to this is sample extraction from the process loop with a subsequent buffer-washout phase, as is already used in flow injection systems [270,271]. For example, clinical microdialysis (table 6.2.8) is a technique designed to monitor tissue chemistry (often cerebral) during or after pharmacological, physiological and surgical interventions. Very small diameter sterile catheters are employed; these have semi-permeable membranes to allow the appropriate tissue fluid to pass through. Sample volumes are also kept very small to avoid patient haemodynamic instability.

Table 6.2.8 Examples of commercially available FI systems which are potentially attractive in ALF

Device/s	Primary application	Chemistries	Sample volume	Cost	Reference
YSI7100 MBS	Bioprocess monitoring and control	glucose, lactate, glutamate, glutamine, ammonium, and potassium.	10-15 µl	±R 300 000 incl. initial buffers and calibration fluids	www.YSI.com
CMA600 analyzer	Neuro-microdialysis	glucose, lactate, pyruvate, glutamate, glycerol, and urea.	0.5 µl	±R 500 000 incl. initial buffers and calibration fluids	www.microdialysis.se

Since there are currently no bioprocess monitoring systems designed for ALF, the state estimator in this study was designed for use with equipment normally available in surgical and ICU settings: For example, electrocardiographic (ECG) instruments and arterial blood gas (ABG) technology. In the post-surgical part all but ammonia may be detected using an ABG machine. A variety of sensors for ammonia are commercially available (www.spectronic.co.uk). A sensor for creatinine is not yet commercially available, however, research has been underway to produce one [304]. Perhaps, the most ideal sensors are *biosensors* employing enzymatic amperometric or optical methodologies for detection [305-308].

Assuming the success of modeling ALF in animals, doing so in humans may present more of a challenge. Standardized animal models are 'pure' images of ALF and the interventions are mostly minimized. Interventions in the human scenario tend to be excessive in the hope of saving the patient's life. Linear approaches are therefore likely to be less successful due to these complicating effects. However, extensive clinical 'know-how' exists and this is obviously the basis for successful support of ALF patients. 'Knowledge-based' combined with structured non-linear models may therefore be of value in the human scenario. The UML, as an object oriented meta-modeling method, is likely to continue being useful in integrating these [273,309,310].

6.3 Thoughts and recommendations

In the above two studies, a compartmental pharmacokinetic and an *on-line* prognostic model were investigated. These provide information regarding BAL system performance during treatments, and *on-line* biomarkers and prognosis respectively.

In terms of the former, although the pharmacokinetic modeling approach is a necessary and desirable part of developing a BAL, it provides predictions regarding the clearance or production of only single substances at a time and only after rates of production and or clearance have been measured in *in vitro* and *in vivo* experiments. As has become apparent, the clinical syndrome of ALF is a complex, multisystemic process, which cannot be limited to only individual clearance and/or production variables. The addition of bio-analytical monitoring tools designed to investigate changing clinical variables that participate in known or suspected ways in ALF may help to prevent assumptions regarding pathogenesis and the efficacy of any potential treatment.

Subsequently, a bioprocess state estimator was proposed for a porcine surgical ischemic model of acute liver failure. Its purpose was to create an *on-line* system providing indications of experimental animal prognosis and biochemistry. In the instance described above the model's ease of extension and numerical accuracy would suggest that the diagrammatic and statistical modeling methods were indeed successful. That is, the selected independent variables did accurately determine the particular dependent variables. This also implies that clinical interventions should aim to minimize or reverse changes in these variables to demonstrate the benefit of the treatment. For example, blood sampling should be minimized to prevent haemodynamic instability and the accumulation of ammonia should be minimized using an appropriate means of clearance (e.g. an artificial toxin clearance column and biochemical ammonia minimization strategies). Unlike the pharmacokinetic model, the value of this model resides more in clinical patient management than in BAL design.

The following additional thoughts are relevant:

6.3.1 Refining prognostic models

In view of the fact that studies investigating new variables and those comparing existing systems have continued, one can assume that the final word on prognostic criteria for ALF has not yet been written.

The complexity of ALF will doubtless require several collaborative modeling attempts prior to acceptance as 'complete'. It is therefore sensible, in principle, to proceed with ALF process modeling in animals before attempting application in the human context. Since the outcomes of previous UP-CSIR BALSS trials were apparently affected by the toxicity of the ischemic model (section 5.3) future trials aim to use the anhepatic model [5,220,226,230] to hopefully 'unmask' the benefit/s of the treatment as previously mentioned. As stated, the anhepatic is a type of 'control' for the ischemic, i.e. subtracting the rates of endogenous toxin accumulation will indicate the contribution/extent of hepatic necrosis. This information is useful in the numerical definition of an ALF process model. Additionally, it would be desirable to include several new coagulatory, immunological and cerebral variables (table 6.2.1), in future experiments.

In the human scenario thereafter, spontaneous liver regeneration and clinical interventions aimed at improving prognosis will likely alter biological processes that appeared to linearly appreciate/depreciate with time in the animal scenario/s. Thus, future modeling efforts may benefit from larger sample sizes and non-linear techniques. Pattern recognition and rule-based artificial intelligence systems have successfully been applied to model complex medical problems [291-293]. For this reason, it is probable that a human process model of ALF would benefit from a hybrid *learning and rule-based* design approach [294] which has (apparently) not been attempted before.

6.3.2 Non-linear and multivariate regression experiments

After defining the ALF process model on the 'ischemic-standardization' data, the prospective acquisition of the BALSS treatment data created the possibility of re-examining the new and larger raw dataset with additional analysis and modeling efforts:

The aim was to explore the possibility of there being a prognostic model contained in the data that was composed of variables that were more biochemically-oriented. In particular, variables more similar to those identified in the review of prognostic studies (table 6.2.7) than those defined in the above numerical modeling instance. This effort was in part focused on finding prognostic variables that were preferably not measured by either ABG or ECG instruments since these would in any case be in an ICU.

Kohonen self organizing maps (SOMs in Matlab) were initially re-employed and were once again found to be ineffective, likely due to the still too small sample size. Incidentally, SOMs are a single-layer form of artificial neural networks (ANN [11,311,312-316]) which are useful for indicating multidimensional relationships in an intra-related data space. The problem in this case lay in the biochemical sampling interval: The laboratory variables were sampled 4-hourly to minimize costs and to prevent animal haemodynamic instability (as a result of blood loss). Although the ABG and ECG data was collected on a much higher frequency, including this into the final 'summated dataset' required limiting the sampling interval to the lowest common denominator (i.e. only the data points of all variables on the 4-hourly intervals). SOMs were simply not the appropriate tool for the task.

Subsequently, an un-weighted least squares linear multivariate regression (as is available in SPSS 17.0) was performed on the raw data. Combined as a single set, the following variables were selected: pH, bicarbonate (HCO_3), potassium (K^+), hemoglobin (Hb), lactate, pyruvate, ammonia, bilirubin, creatinine, urea, prothrombin time (PT) and the clotting factors 2,7 and 10. Thereafter, a process of stepwise exclusion of variables not demonstrating significant p-values in the combined-model form was followed to determine the final multivariate model. On completion the following remained, K^+, ammonia, bilirubin, creatinine, PT and urea. The individual p-values were all below 0.05, in fact, the highest was 0.011 for bilirubin. The similarity of this model to the variables identified in the review (table 6.2.7) is indeed noteworthy, particularly to the studies of Dabos *et al* [267], Bhatia *et al* [239] and Bernal *et al* [241].

The difference between this (multi-variate) model and the previous numerical model (state estimator) lies in their derivation methods. The variables in the state estimator were mean rates of change (the gradients) calculated from the first-order relationships of each of the variables of interest in each of the animals, i.e. they related the duration of survival to 'derived' data. The multi-variate model, on the other hand, directly related the raw data to time. The value of this multivariate model lies in demonstrating that the assumption previously made was justified, namely that the rates of change (first derivatives) of the above listed variables are indeed linearly related to the duration of survival. This validates building a dynamic *on-line* prognostic system based on the rates of change of appropriately selected variables. As stated before, such a system will formally require either *on-line* sensors for all of the variables or a process model [300-303] with data inclusion methods for the *off-line* (laboratory) variables.

6.3.3 A UML meta-model to combine the state estimator and the BALSS pharmacokinetic model

A variety of systems have been used to model biological systems, the choice of which is normally determined by the postulated underlying structure of the system, for example, petri nets, boolean switching nets, electronic circuits or ANNs. Each of these systems have advantages and disadvantages determined by the quality and quantity of data, the understood complexity of the system and the degree to which this requires accurate emulation [302,303,315-317].

With this in mind, it is interesting to compare the above state estimator with the pharmacokinetic compartmental model (table 6.3.1). What becomes apparent from the comparison is that the two systems complement each other in that they are designed to examine system pharmacokinetic performance and the patient's prognosis (state trajectory) respectively.

Table 6.3.1 Differences between the state estimator and the compartmental model

Aspect	State estimator	Pharmacokinetic model
Purpose	to create an *on-line* monitoring system that predicts patient prognosis and biochemistry.	*off-line* examination of the impact of system design factors on the efficacy of metabolite production/clearance.
Value	treatment efficacy and financial savings	determining BALSS performance and system design
Assumptions	linearity with time of change in independent variables. No compartmental mass conservation assumption.	conservation of mass of particular metabolite/s in well-stirred compartments.
Types of equations	rates of change of linear functions	ordinary differential equations (ODEs)
Derivation method	empirically derived relationships between *in vivo* survival and biochemistry, and *on-line* biochemistry with *off-line* biochemistry.	*in vitro* measured rate of clearance of metabolite (e.g. ammonia) by bioreactor and *in vivo* measured production by patient
Types of variables	any systemic variables or blood metabolites/biochemicals that may be measured *on-line*.	*off-line* blood metabolites requiring laboratory determinations.
Number of variables	several variables simultaneously.	one variable at a time.
Sensitivity to measurement error	insensitive	sensitive

Combining these two systems might involve their interaction in terms of in and outputs (i.e. output for one may be input for the other). As previously stated, the UML is attractive for combining models of different levels into a meta-model without internal conflict. In this regard, there are convenient extensible markup language (XML) procedures to convert UML diagrams to code.

To achieve this proposed systems integration the following meta-model may be proposed:

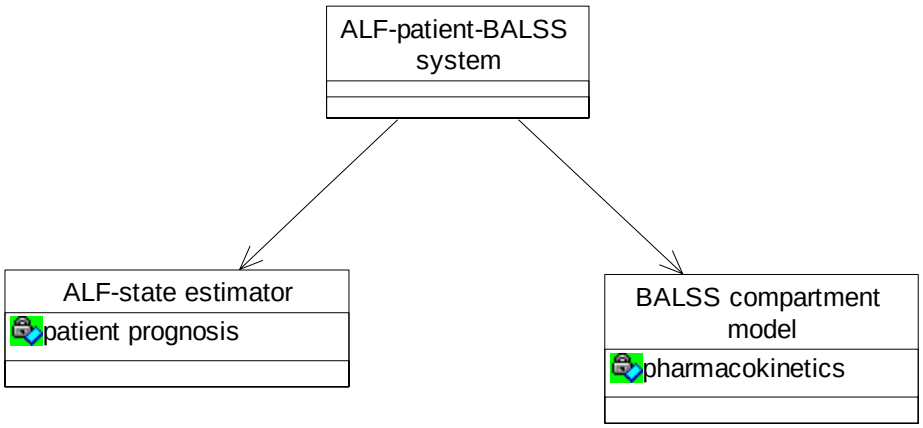

Figure 6.3.1 UML metamodel of the combined ALF-patient-BALSS compartment models. The inheritance of the meta-model includes all the attributes and functionality of the two underlying models.

Obviously certain basic requirements would need to be met in terms of the implementation of such a system. For example, in addition to reaching a more final version of the ALF-patient state estimator, a state trajectory for the compartment model, i.e. the pharmacokinetic dynamics of the BALSS, would also require definition. The result would be a combined ALF-patient-BALSS state model with behaviour inherited from the attributes of the two underlying systems.

In this regard, suitable in and outputs linking the two models would need to be selected. Although the hardware of a bioprocess monitoring system is an independent system (which need not communicate with any particular model), any variables selected to enable communication between the above models would need to match the criteria for inclusion in both i.e.:

1. drugs or metabolites that are alternately cleared and/or produced by the bioreactor and patient respectively,
2. The existence of sensors and equipment for their o*n-line* measurement during experiments
3. As high a correlation, or ‘weight’, with the dependent variable as possible (i.e. a clinical association of relevance in the animal ALF model).
4. As linearly appreciating/depreciating over time (i.e first-order) as possible.

For example, assuming the *on-line* detection of ammonia, potentially in various sites in the system (e.g. arterial in the patient and in the various compartments of the BALSS), the measured data could function as input for both pharmacokinetic and prognosis models. Depending on the use of an animal or human treatment model other variables may also match the above characteristics. In an anhepatic model a variety of plasma proteins (e.g. coagulation factors) and endotoxins may be suitable candidates.

As mentioned previously, it is important to realize that the above models are iterative instances and will benefit from extension in the future. For example, the pharmacokinetic model may additionally include; an artificial toxin clearance device, with known toxin clearance dynamics over time, or the effect of supplementing the patient with blood plasma or albumin. The prognosis model could also be extended to include several of the variables (listed in table 6.2.1) not previously measured. In either case, an appropriate *on-line* monitoring system that is independent of the underlying models will remain a formal requirement.

Finally, assuming both models are well understood, an *in silico* meta-model of the above could be used to simulate the likely behaviour of the combined system. A virtual system such as this would be highly attractive in terms of BALSS system design finalization and therefore time and expense savings prior to proceeding to human clinical trials.

6.3.4 Additional notes on bioprocess monitoring systems

Of the previously mentioned FI systems the CMA system is more attractive than the YSI system for the following reasons:

1. Several input channels are available in the CMA system. Thus, the cerebral biochemical data of several patients along with data from any additional devices may simultaneously be monitored.
2. In clinical, as opposed to laboratory bioprocess systems, feedback control is not required. The CMA device has a data integration software system (ICU Pilot) that is able to simultaneously display trends in several systemic variables (ECG, EEG, ICP, MAP etc) and the measured biochemicals.

3. Since the sampling catheters may be adapted for both cerebral interstitial-fluid and blood plasma, in a BALSS treatment, one catheter could be used to monitor brain chemistry while another monitors plasma chemistry. In this case the sterility issues regarding the *in situ* application of a clinical device have been adequately attended to. This is not so with the YSI machine although a neurological application has not been excluded. In addition, in the ischemic experiments HE, which is a diagnostic characteristic of ALF, could not be diagnosed on the basis of EEG results as these are known to be influenced by sedation, nor by ICP since it was not monitored. Instead, HE was diagnosed via alterations in Fischer's ratio, which relies on after-the-fact biochemical analyses of plasma amino acid ratios. The CMA machine will allow an *on-line* diagnosis of HE via cerebral biochemical indicators potentially integrated with an ICP measurement system. The concentration of the cerebral amino acids may also be compared to the plasma amino acids, as measured in the BALSS-patient circulation loop, and this is likely to provide valuable prognostic information.

Assuming the development of a data inclusion system (Kalman filter) a variety of *off-line*, biochemistry analyzers are ave recently become commercially available that would provide prognostically valuable data for the ALF process model. For example, the Diagostica Stago STA-compact device (www.stago.fr) that measures a variety of coagulatory variables (PT, APTT, fibrinogen, thrombin time, clotting factors and antithrombin) or the large range of Siemens analyzers that perform immuno-assay, chemistry and hematology analyses (www.siemens.com/diagnostics). In addition to the flow injection technology mentioned up to this point, there is also a possibility of incorporating new high-throughput molecular technologies with electronic signal transduction, potentially enabling measurement updates several times a second [2]. The latter will obviously require specification of the correct sensors.

In the course of developing the UP-CSIR BALSS a FI sub-system was designed to take samples from the re-circulating plasma circuit during the course of a treatment (figure 6.3.2). The sampling volume is small, 2 ml, and the sampling interval is programmable: Once every 30 minutes would be sufficient for statistical purposes in an animal model and would also have a minimal haemodynamic impact. Each sampling cycle is followed

by saline washout from an off-line reservoir. However, due to inconvenient electrode sterilization and calibration procedures, the system has not yet been clinically applied. A stand-alone system such as the CMA device, in which all of the problems associated with a clinical application have been solved, remains a more attractive solution.

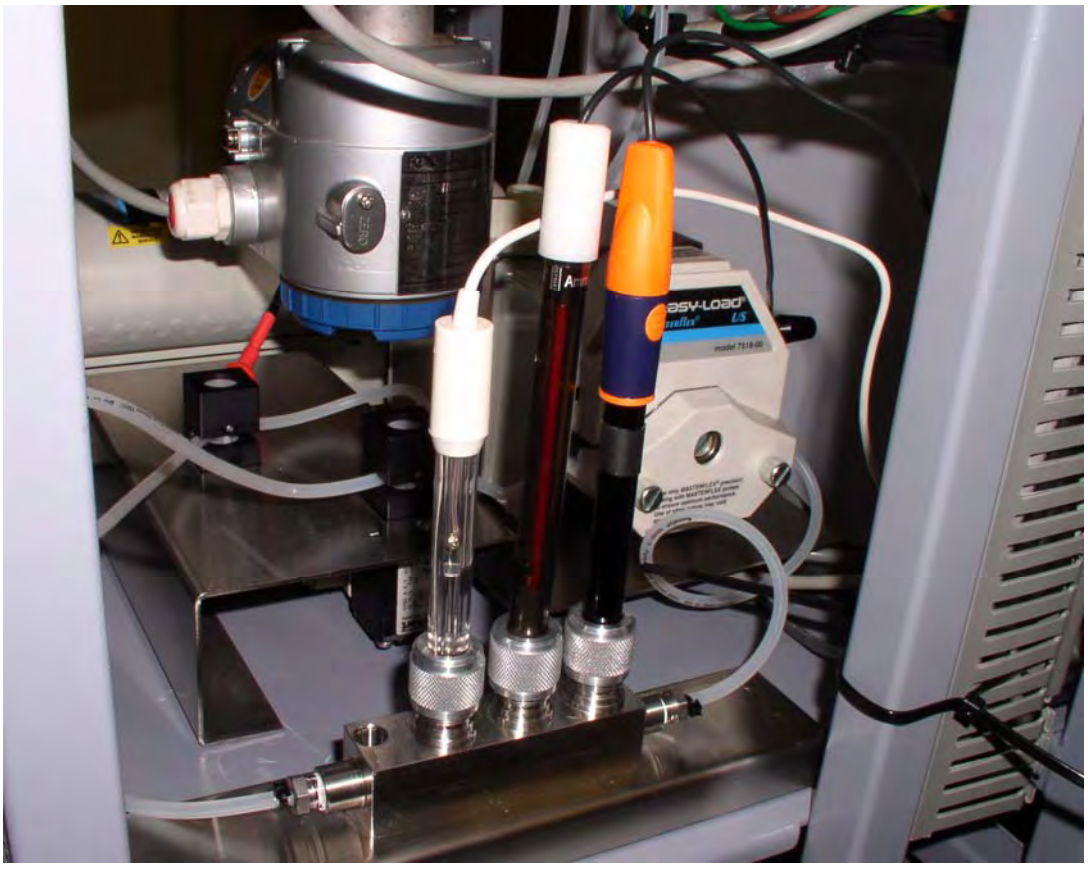

Figure 6.3.2 UP-CSIR BALSS FI sampling manifold with ion-specific electrodes. From left to right carbonate (HCO_3^-), potassium (K^+) and ammonium (NH_4^+) electrodes, with peristaltic pump and controller in the rear.

The considerations in developing a bioprocess monitoring device for a BALSS are likely to be the same as those for renal dialysis technology: The treatments are (and will be) very expensive and one possible way to meet these costs is to improve the diagnostic and treatment competence of the system. A system that integrates the signals of several monitored variables will improve the understanding of the links between haemodynamics, metabolism and physiological regulatory systems and will therefore improve diagnosis and treatment regimens [316].

A monitoring system such as the proposed state estimator could potentially function as a monitoring device in any similar bioprocess. For example, in laboratory toxicological, biotransformation and drug screening research, primary hepatocytes and non-parenchymal co-cultures are a popular *in vitro* model owing to the resemblance of the system to an *in vivo* circumstance [316]. The cost of process development accounts for a large fraction of bringing a drug to market. Thus, there is also a strong economic incentive for improved monitoring tools in the bioprocess engineering market [317]. The critical problem remains a paucity of suitable, affordable sensors and integrated monitoring tools.

7. SUMMARY AND CONCLUSION

"It would be an unsound fancy and self-contradictory to expect that things which have never yet been done can be done except by means which have never yet been tried".

Francis Bacon, Novum Organum VI, *1620*

In evaluating the overall success of this thesis, it is instructive to examine the recommendations for future research made in a recent US-based, acute liver failure workshop, Lee *et al* (2008) [243], paraphrased as follows:

- Continued prospective monitoring to identify epidemiological trends in ALF.
- Use of new molecular methodologies to study ALF (especially 'indeterminate' cause ALF), including, genomics, proteomics, metabolomics etc.
- More basic research into ALF and multiorgan failure pathogenesis.
- Initiation of prospective, well-designed clinical trials for various ALF therapies.
- Improvement in predictive markers, modeling of prognosis and identification of new biomarkers. (This task was also reiterated in a subsequent independent study, Freeman *et al* (2009) [318]).
- More basic research in hepatocyte and stem cell growth and proliferation for the purpose of a therapeutic cell source.
- Continuance of *in vitro* and animal studies for BAL devices, to enable eventual human trials.
- Additional tissue engineering work to develop an effective BAL device for humans.

Importantly, the purpose of this thesis was to present and evaluate a variety of types of models and in this respect the following was done and/or achieved:

- After reviewing the clinical and biological background of acute liver failure and bioartificial liver technology and describing the development of the UP-CSIR BAL,
- Three studies involving *in vitro* lab-scale models of the BAL were presented and evaluated: The first established a sterile, numerically large-scale cell source for

seeding BAL bioreactors. This model remains highly successful, despite its regionally limited application due to the xenogenic primary cell origin. The second study successfully demonstrated bioreactor metabolic function, but also revealed methodological difficulties associated with the use of the perflurocarbon O_2 carrier. In response, the third study employed novel methods such as radio-transparent bioreactor materials and positron emission tomography. In so doing, it demonstrated that the O_2 carrier did indeed benefit bioreactors under hypoxic (ALF-like) treatment conditions. The cost and metabolic appropriateness of transformed cell sources were identified as factors at least partially responsible for preventing BAL-device entry into the commercial arena. New research directions, including genetically engineered transgenic and chimeric animals, were mentioned as promising possibilities.

- Two studies involving *in vivo* animal ALF models were presented: The first successfully demonstrated that IV injected PFC was not toxic in either healthy or liver-injury scenarios, and thus, a potential PFC leakage would not be toxic or hinder the recovery of a severely *liver-compromised* patient undergoing a BAL treatment. The second clinically standardized a large animal surgically-induced ischemic model of ALF in which it was possible to statistically identify prognostically important clinical variables (such as ammonia). However, the unstable and multi-systemic nature of the model was also recognized and this contributed to the inconclusive demonstration of efficacy in the clinical evaluation of the UP-CSIR BALSS subsequently described. Despite this, valuable information resulted, including: parameters for BAL system re-design (such as including an artificial toxin device), the benefit of using alternate animal ALF models and the measurement of additional/new prognostically important clinical variables.
- Two mathematical modeling studies were presented: The first, a mass-balance pharmacokinetic compartmental model using actual *in vitro* and *in vivo* data measured in the studies above, simulated the BAL-patient system in a clinical treatment. Valuable BAL design and operation information resulted, including the minimal requisite cell quantities, exchange and circulation rates and (once again) incorporating an artificial toxin clearance device. The second model was an ALF-

bioprocess state estimator defined using conceptual modeling methods (UML) and a weighted-multivariate numerical approach. This model proved accurate on both 'trained' and prospectively collected 'un-trained' in vivo data in the large animal and BAL clinical experiments described above. However, the benefit of larger sample sizes in future studies was identified. Nonetheless, the model proved in principle that it is possible to create an *on-line* clinical monitoring device with ALF prognostic prediction or 'state estimator' capabilities. The means of implementing such a device, additional non-linear and multivariate statistical experiments conducted on the animal data, along with shortcomings and potential improvements to existing prognostic models were discussed. Based on the complimentarity of the above two models, a method for potentially combining them into a single *in silico* model with the benefits of both was discussed.

On at least a scientific level, it is safe to state that the models defined in this thesis achieved their purpose, specifically to generate information regarding BAL system design and clinical and metabolic performance and thereby to facilitate development in the technology. At least half (particularly the latter half) of the list of Lee *et al* (and Freeman *et al*) above was addressed.

Globally, on the other hand, owing to the many variations in BAL design, the cost and technical challenges associated with the requisite studies, and (perhaps as a result) the fact that the literature is littered with examples of initial enthusiasm followed by disappointing outcomes; It might also be said that additional work is required in all of the segregated sections (*in vitro, in vivo*, and mathematical models), before the technology will proceed beyond a pre-commercial developmental stage. Since this is clearly not a *fait accompli* today, in this thesis thoughts and recommendations regarding research progress were provided per section rather than all being lumped into this conclusion. I hope this has been helpful rather than a hindrance to the reader.

Finally, it seems illogical when considering the extensive previous efforts, that the obstacles remaining in the path to BAL commercialization will be solved using repetitions of historical strategies. In agreement with other authors [1,2,9,17,243], it is

probable that developing a clinically effective device will require ongoing innovations and the integration of the new with existing technologies. In particular, aside from the stated requirement of a cell source that meets the needs of all regulatory-authorities, it is probable that mathematical modeling, (in for example, bioreactor design optimization, BAL system performance, biomarker identification and *on-line* clinical and prognosis monitoring amongst others) will enjoy greater application than has occurred in the past. The expense of clinical trials certainly validates *in silico* modeling.

8. REFERENCES

1. Tzanakis ES, Hess DJ, Sielaff TD, Hu WS. Extracorporeal tissue engineered liver assist devices. *Annu Rev Biomed Eng.* 2000;2:607-32.
2. Nahmias Y, Berthiaume F, Yarmush ML. Integration of technologies for hepatic tissue engineering *Adv Biochem Engin/Biotechnol* 2006;103:309-29.
3. Karp SJ. Clinical implications of advances in the basic science of liver repair and regeneration. *Am J Transplant* 2009;9:1973-80.
4. Michalopoulos GK. Liver regeneration: Alternative epithelial pathways. *Int J Biochem Cell Biol* 2009 doi:10.1016/j.biocel.2009.09.014.
5. Sosef MN, Abrahamse LSL, van de Kerkhove MP, Hartman R, Chamuleau RAFM, van Gulik TM. Assessment of the AMC-Bio-artificial Liver in the Anhepatic Pig. *Transplantation*. 2002;73(2):204-9.
6. Bernal W, Wendon J. Acute liver failure: clinical features and management. *Eur J Gastroenterol Hepatol*. 1999;11:977-82.
7. Bismuth H, Figuero J, Samuel D. What we should expect from a bio-artificial liver in fulminant hepatic failure? *Artif Organs*. 1998;22(1):26-31.
8. Bingaman WE, Frank JI. Malignant cerebral edema and intracranial hypertension. *Clin Neurol* 1995;13:479-509.
9. Matsushita M, Nosé Y. Artificial Liver. *Artif Organs*. 1986;10(5):378-84.
10. Moolman FS, Rolfes H, van der Merwe SW, Focke WW. Optimization of Perfluorocarbon emulsion properties for enhancing oxygen mass transfer in a bio-artificial liver support system. *Biochem Eng J*. 2004;19:237-50.
11. Doran PM editor. Process Modeling. In: Bioprocess engineering principles, London Academic Press, 1995, Chapter 13. p.348-52.
12. Cloete A. A new approach to the adult respiratory distress syndrome. (dissertation) University of Cape Town; 1986.
13. Trey C, Davidson CS. The management of fulminant hepatic failure. In: Popper H, Schaffner F (eds) Progress in liver failure. NY, Grune and Stratton 1970;282-298.
14. Bernau J, Rueff B, Benhamou JP. Fulminant and sub-fulminant hepatic failure: definition and causes. *Semin Liver Dis*. 1986;6:97-106.
15. O'Grady JG. Acute Liver Failure. *Postgrad Med J.* 2005;81:148-54 doi:10.1136/pgmj.2004.026005.
16. Riordan SM, Williams R. Perspectives on liver failure: Past and future. *Semin iv Dis* 2008;28:137-41.
17. Lee WM, Squires RH, Nyberg SL, Doo E, Hoofnagle JH. Acute liver failure: Summary of a workshop. *Hepatology* 2008;47(4):1401-15.
18. Sussman, NL, Kelly, J.H. Extracorporeal Liver Support: Cell-Based Therapy for the Failing Liver. *Am J Kidney Dis.* 1997; 30(5):Suppl.4:S66-71.
19. van der Merwe S.W. Gastroenterologist: Unitas hospital, Pretoria, South Africa 2005. Personal communication.
20. van de Kerkhove MP, Hoekstra R, Chamuleau RAFM, van Gulik TM. Clinical application of bio-artificial liver support systems. *Annals Surg*. 2004;240(2):216-30.
21. United network for organ sharing. Liver transplantation data, available at www.unos.org. accessed 2003-6.

22. Mandala L, Pietrosi G, Gruttadauria S, Vizzini G, Spampinato M, Spada M, Gridelli B. Succesful liver transplant in an HCV-infected haemophiliac patient with fulminant hepatic failure. *Haemophilia* 2007;13(6):767-9.
23. Taliani G, Tozzi A, Fanci R, Biliotti E, Bsi A. Fatal acute hepatitis C virus infection in patients with haematological malignancies. *J Chemother* 2007;18(6):662-4.
24. Gill RQ, Sterling RK. Acute Liver Failure. *J Clin Gastroenterol.* 2001;33(3):191-8.
25. Rahman T, Hodgson H. Clinical management of acute hepatic failure. *Intensive care Med*. 2001;27:467-76.
26. Bernal W, Auzinger G, Sizer E, Wendon J. Review: Intensive care management of acute liver failure. *Semin Liver Dis*. 2008;28(2):188-200.
27. Haussinger D, Schliess F. Pathogenetic mechanisms of hepatic encephalopathy. *Gut* 2008;57:1156-65.
28. Lichter-Konecki U. Profiling of astrocyte properties in the hyperammonemic brain: Shedding new light on the pathophysiology of the brain damage in hyperammonemia. J *Inherit Metab Dis* 2008;31:492-502.
29. Schliess F, Gorg B, Haussinger D. RNA oxidation and zinc in hepatic encephalopathy *Metab Brain Dis* 2009;24:119-34.
30. Stadlbauer V, Wright GAK, Jalan R. Role of artificial liver support in hepatic encephalopathy. *Metab Brain Dis* 2009;24:15-26.
31. Vaquero J, Butterworth RF. Mechanisms of brain edema in acute liver failure and impact of novel therapeutic interventions. *Neurol Res* 2007;29:683-90.
32. Bernal W, Auzinger G, Sizer E, Wendon J. Variation in blood ammonia concentration with site of measurement and evidence of brain and muscle uptake in patients with acute liver failure. Letter to editor. *Liver Int* 2008; 415-7.
33. Clay AS, Hainline BE. Hyperammonemia in the ICU. *Chest* 2007;132:1368-78.
34. Bjerring PN, Hauerberg J, Frederiksen HJ, Jorgensen L, Hansen A, Tofteng F, Larsen FS. Cerebral glutamine concentration and lactate-to-pyruvate ratio in patients with acute liver failure. *Neurocrit Care* 2008;9:3-7.
35. Wright G, Jalan R. Ammonia and inflammation in the pathogenesis of hepatic encephalopathy: Pandora's box?. *Hepatology* 2007;46(2):291-4.
36. Albrecht J, Noreberg MD. Glutamine: A Trojan horse in ammonia toxicity. *Hepatology* 2006;44(4):788-94.
37. Llansola M, Rodrigo R, Monfort P, Montoliu C, Kosenko E, Cauli O, Piedrafita B, Mlili NE, Felipo V. NMDA receptors in hyperammonenia and hepatic encephalopathy. *Metab Brain Dis* 2007;22:321-35.
38. Rodrigo R, Erceg S, Rodriguez-Diaz J, Saez-ValeronJ, Piedrafite B, Suarez I, Felipo V. Glutamte induced activation of nitric oxide synthase is impaired in cerebral cortex in vivo in rats with chronic liver failure. *J Neurochem* 2007;102:51-64.
39. Garcia-Ayllon MS, Cauli O, Silveyra MX, Rodrigo R, Candela A, Compan A, Jover R, Perez-Mateo M, Martinez S, Felipo V, Saez-Valero J. Brain cholinergic impairment in liver failure. *Brain* 2008; sept 4:1-11.
40. Rose C, Felipo V. Limited capacity for ammonia removal by brain in chronic liver failure: potential role of nitric oxide. *Metab Brain Dis* 2005;20(4):275-83.
41. Fischer JE, Baldessarini RJ. Pathogensis and therapy of hepatic coma. In: Progress in Liver disease, Harvard Medical School, 1976 Chapter 23; p.363-397.
42. Vaquiero J, Polson J, Chung C, Helenowski I, Schiodt FV, Reisch J and the US ALF study group. Infection and progression of hepatic encephalopathy in acute liver failure. *Gastroenterol*. 2003;125:755-64.

43. O'Grady JG. Paracetamol hepatotoxicity. *J R Soc Med.* 1997;90:368-70.
44. Donovan JP, Shaw BW, Langnas AN, Sorrell MF. Brain water and ALF: the emerging role of intracranial pressure monitoring. *Hepatology*. 1992;16:267-8.
45. Moore K. Renal failure in acute liver failure. *Eur J Gastroenterol Hepatol*. 1999;11(9):967-75.
46. Gines P, Guevara M, Arroyo V, Rodes J. Hepatorenal syndrome. *Lancet.* 2003;362:1819-27.
47. Wiest R, Groszman RJ. Nitric oxide and portal hypertension: its role in the regulation of intrahepatic and splanchnic vascular resistance. *Semin Liver Dis*. 1999;19:411-26.
48. Barada K. Hepatorenal syndrome: pathogenesis and novel pharmacological targets. *Curr Opin Pharmacol*. 2004;4:189-97.
49. Roland R, Wade J, Davalos M, Nancy R, Jim W, Milagros D. The systemic inflammatory response syndrome in acute liver failure. *Hepatology.* 2000;32:734-9.
50. Goka AKJ, Wendon JA, Willimas R. Fulminant hepatic failure, endogenous endotoxemia, and multiple systems organ failure. In: Matuschack GM, editor. Multiple systems organ failure: hepatic regulation of host defense. New York: Marcel Decker Inc; 1993. p.215-28.
51. Munoz SJ. Difficult management problems in fulminant hepatic failure. *Semin Liver Dis*. 1993;13:395-413.
52. O'Grady JG, Alexander GJM, Mayllar KM, Williams R. Early indicators of prognosis in FHF. *Gastroenterology*. 1989;97:439-45.
53. Anand AC, Nightingale P, Neuberger JM. Early indicators of prognosis in fulminant hepatic failure: an assessment of the King's criteria. *J Hepatol*. 1997;26:62-8.
54. Mitchell I, Bihari D, Chang R. Earlier identification of patients at risk from acetaminophen-induced acute liver failure. *Crit care Med.* 1998;26:279-84.
55. Bernuau J, Goudeau A, Poynard T, Dubois F, Lesage G, Yvonnet B, Degott C, Bezeaud A, Rueff B, Benhamou JP. Multivariate analysis of prognostic factors in fulminant hepatitis B. *Hepatology* 1986;6(4):648-51.
56. Bernau J, Samuel D, Durand Fl. Criteria for emergency liver transplantation with acute viral hepatitis and factor V level 50% of normal: a prospective study [abstract]. *Hepatology*. 1991;14:49A.
57. Lee WM, Galbraith RM, Watt GH. Predicting survival in fulminant hepatic failure using serum-Gc protein concentrations. *Hepatology* 1995;21:101-5.
58. Karvountzis GG, Redecker AG. Relation of alpha-fetoprotein in acute hepatitis to severity of prognosis. *Ann Intern Med*. 1974;80:156-60.
59. Riordan SM, Williams R. Mechanisms of hepatocyte injury, multi-organ failure and prognostic criteria in acute liver failure. *Sem Liver Dis*. 2003;23(3):203-15.
60. Wustrow T, van Hoorn-Hickman R, van Hoorn WA, Fischer A, Terblanche J. Acute hepatic ischemia in the pig: changes in plasma hormones, amino acids and brain biochemistry. *Hepatol Gastroenterol*. 1981;28:143-6.
61. Hazell AS, Butterworth RF. Hepatic encephalopathy: an update of pathophysiologic mechanisms. In: Pathophysiology of Hepatic encephalopathy. *Soc Exp Biol Med*. 1999.222:99-112.
62. Scotto J, Opolon P, Eteve J. Liver biopsy and prognosis in acute liver failure. *Gut*. 1973;14:927-33.
63. Starlz TE, Marchioto T, Kualla K. Homo-transplantation of the liver in humans. *Surg Gynecol Obstet.* 1963;117:659-76.

64. Botha JF, Spearman CW, Millar AJW, Michell L, Gordon P, Lopez T. Ten years of liver transplantation at Grooteschuur hospital. *SAMJ*. 2000;90(9):880-3.
65. Millar AJW, Spearman W, McCullogh M, Goddard E, Raad J, Rode H. Liver transplantation for children: the Red Cross Children's hospital experience. *Pediatr Transplant.* 2004;8:136-44.
66. Sauer IM, Goetz M, Steffen I, Walter G, Kahr DC, Schwartlander R. *In vitro* comparison of the Molecular Adsorbent Recirculation System (MARS) and Single-pass Albumin Dialysis (SPAD). *Hepatology*. 2004;39(5):1408-14.
67. Braun KM, Degen JL, Sandgren EP. Hepatocyte transplantation in a model of toxin-induced liver disease: variable therapeutic effect during replacement of damaged parenchyma by donor cells. *Nature Med*. 2000;6:320-6.
68. Chan C, Berthiaume F, Nath BD, Tilles AW, Toner M, Yarmush ML. Hepatic tissue engineering for adjunct and temporary liver support: critical technologies. *Liver Transplant* 2004;10(11):1331-42.
69. Gerlach JC, Seilinger K, Patzer JF. Bioartificial liver systems: Why, what, whither? *Regen Med* 2008;3(4):575-95.
70. Chamuleau RAFM, Poyck PC, van de Kerkhove MP. Bioartificial liver: Its pros and cons. *Ther Apher Dial* 2006;10(2):168-74.
71. Mc Kenzie TJ, Lillegard JB, Nyberg SL. Artificial and bioartificial liver support. *Semin Liver Dis* 2008;28:210-17.
72. Stadlbauer V, Jalan R. Acute liver failure: liver support therapies Curr *Opin Crit Care* 2007;13:215-21.
73. Gerlach JC, Botsch M, Kardassis D. Experimental evaluation of a cell module for hybrid liver support. *Int J Artif Org*. 2001;24:793-8.
74. Ellis AJ, Hughes RD, Wendon JA. Pilot-controlled trial of the extracorporeal liver assist device in acute liver failure. *Hepatology*. 1996;24:1446-51.
75. Demetriou AA, Brown RS, Busuttil RW, Fair J, McGuire BM, Rosenthal P, Esch JMA, II, Lerut J, Nyberg SL, Salizzoni M, Fagan EA, de Hemptinne B, Broelsch CE, Muraca M, Salmeron JM, Rabkin JM, Metselaar HJ, Pratt D, De La Mata M, McChesney LP, Everson GT, Lavin PT, Stevens AC, Pitkin Z, Solomon BA. Prospective, Randomized, Multicenter, Controlled Trial of a Bioartificial Liver in Treating Acute Liver Failure. *Ann Surg* 2004;239: 660-70.
76. Xue YL, Zhao SF, Luo Y. TECA hybrid artificial liver support system in treatment of acute liver failure. *World J Gastroenterol*. 2001;7:826-9.
77. Mazariegos GV, Kramer DJ, Lopez RC. Safety observations in phase I clinical evaluation of the Excorp Medical Bio-artificial Liver Support System after the first four patients. *ASAIO*. 2001;47:471-5.
78. Morsiani E, Pazzi P, Puviani AC. Early experiences with a porcine hepatocyte-based bio-artificial liver in acute hepatic failure patients. *Int J Artif Org*. 2002;25:192-202.
79. Sauer IM, Zelinger K, Obermayer N. Primary human liver cells as source for modular extracorporeal liver support-a preliminary report. *Int J Artif Org*. 2002;25:1001-5.
80. van de Kerkhove MP, Di Florio E, Scuderi V. Phase I clinical trial with the AMC-bio-artificial liver. *Int J Artif Org*. 2002;25:950-9.
81. Ding YT, Qiu YD, Chen Z. The development of a new bio-artificial liver and its application in 12 acute liver failure patients. *World J Gastroenterol*. 2003;9:829-32.
82. Streetz K, Bioartificial liver devices- tentative but promising progress. *J Hepatol* 2008;48:189-91.

83. Morsiani E, Brogli M, Galavotti D, Pazzi P, Puviani AC, Azzena GF. Biologic liver support: optimal cell source and mass. *Int J Artif Org*. 2002;25(10):985-93.
84. Tsiaoussis J, Newsome PN, Nelson LJ, Hayes PC, Plevris JN. Which hepatocyte will it be? Hepatocyte choice for bio-artificial liver support systems. *Liver Transpl*. 2001;7(1):2-10.
85. Kobayashi N, Okitsu T, Tanaka N. Cell choice for bio-artificial livers. *Keio J Med* 2003;52(3):151-7.
86. Allen JW, Bhatia SN. Improving the next generation of bio-artificial livers. *Cell Develop Biol.*2002;13:447-54.
87. Nieuwoudt MJ, Kreft E, Olivier B, Malfeld S, Vosloo J, Stegman F, van der Merwe SW. A Large Scale Automated Method for Hepatocyte Isolation: effects on Proliferation in Culture. *Cell Transplant.* 2005;14(5):291-9.
88. Nieuwoudt M, Moolman S, Van Wyk AJ, Kreft E, Olivier B, Laurens JB, Stegman F, Vosloo J, Bond R, van der Merwe SW. Hepatocyte Function in a Radial-flow Bioreactor Using a Perfluorocarbon Oxygen Carrier. *Artif Organs* 2005; 29(11): 915-918.
89. Hansen BA, Poulsen HE. The capacity of urea-N synthesis as a quantitative measure of the functional liver mass in rats. *J Hepatol.* 1986;2:468-74.
90. Eguchi S, Lilja H, Hewitt WR, Middleton Y, Demetriou AA, Rozga J. Loss and recovery of liver regeneration in rats with fulminant hepatic failure. *J Surg Res.* 1997;72:112-22.
91. Sussman NL, Kelly JH. Artificial Liver: a forthcoming attraction. *Hepatology.* 1993;17:1163-4.
92. Allen JW, Hassanein T, Bathia SN. Advances in bio-artificial liver devices. *Hepatology.* 2001;34:447-55.
93. Demetriou AA, Reisner A, Sanchez J. New method of hepatocyte transplantation and extracorporeal liver support. *Ann Surg.* 1986;204:259-71.
94. Moolman FS. Oxygen carriers for a novel bio-artificial liver support system. (dissertation) University of Pretoria, 2004, available at http://upetd.up.ac.za #etd-09092004-162043.
95. Rozga J, Morsiani E, Le Page E, Moscioni AD, Giorgio I, Demetriou AA. Isolated hepatocytes in a bio-artificial liver: a single group view and experience. *Biotechnol Bioeng*. 1994;43:645-53.
96. Porter RK, Brand MD. Causes of differences in respiration rate of hepatocytes from mammals of different body mass. *In: Regulatory Integrative Comp Physiol. Am Physiol Soc* 1995;38:R1213-24.
97. Bircher J, Benhamou JP, McIntyre N, Rizzetto M, Rodes J. editors. Physiology of hepatic blood flow. In: Oxford textbook of Clinical Hepatology; 2nd Edition, Oxford University Press: 1999; Chapter 2: p.69-72.
98. McClelland RE, MacDonald J, Coger RN. Modeling O_2 transport within engineered hepatic devices. *Biotechnol Bioeng.* 2003;82(1):12-27.
99. Morsiani E, Galavotti AC, Puviani L, Valieri M, Brogli S, Tosatti S. Radial flow bioreactor outperforms hollow-fiber module as a perfusing culture system for primary porcine hepatocytes. *Transpl Proc.* 2000;32:2715-8.
100. De Bartolo L, Jarosch-Von Schweder G, Haverich A, Bader A. A novel full-scale flat membrane bioreactor utilizing porcine hepatocytes: cell viability and tissue specific functions. *Biotechnol Prog.* 2000;16:102-8.

101. Bader A, De Bartolo L, Haverich A. High level benzodiazepine and ammonia clearance by flat membrane bioreactors with porcine liver cells. *J Biotechnol.* 2000;81:95-105.
102. Morsiani E, Brogli M, Galavotti D, Bellini T, Ricci D, Pazzi P, Puviani AC. Long-term expression of highly differentiated functions by isolated porcine hepatocytes perfused in a radial-flow bioreactor. *Artif Organs.* 2001;25(9):740-8.
103. Yanagi K, Tun T, Taniguchi H, Takada Y, Fukao K, Ohshima N. Development of a packed-bed type bio-artificial liver: metabolic performance of a scaled-up reactor utilizing cultured porcine hepatocytes. *Tissue Eng* 2002:67-73.
104. Flendrig LM, la Soe JW, Jörning GGA, Steenbeck A, Karlsen OT, Bovée WMMJ *et al. In vitro* evaluation of a novel bioreactor based on an integral oxygenator and a spirally wound nonwoven polyester matrix for hepatocyte culture as small aggregates. *J Hepatol.* 1997;26:1379-92.
105. Abrahamse SL, van de Kerkhove MP, Sosef MN, Hartman R, Chamuleau RAFM. Treatment of acute liver failure in pigs reduces hepatocyte function in a bio-artificial liver support system. *Int J Artif Org.* 2002;25:966-74.
106. Gerlach JC. Development of a hybrid liver support system: a review. *Int J Artif Org.* 1996;19:645-54.
107. Hay PD, Veitch AR, Gaylor JDS. Oxygen transfer in a convection enhanced hollow fiber bio-artificial liver. *Artif Organs.* 2001;25(2):119-30.
108. Yana IV. *In vivo* synthesis of tissues and organs. In: R Lanza, R Langer, W Chick, editors. Principles of Tissue Engineering, Austin, TX: Landes & Co. 1997. p.169-178.
109. Allen JW, Bhatia SN. Formation of steady-state oxygen gradients *in vitro*. *Biotechnol Bioeng.* 2003;82(3):253-62.
110. Patent: Van Wyk AJ, Bond RP, Moolman FS, van der Merwe SW. Bioreactor device. PCT aqpplication WO0222775. (Granted NL 1018924C, EA4455, FR2814468).
111. Van Wyk AJ, Malherbe G, Moolman SF, Nieuwoudt M, van der Merwe SW. Design, development and experimental verification of a novel bioartificial liver support system. *SAGES* 2003. poster and oral presentation.
112. Ronné LJT. Design considerations and analysis of a bioreactor for application in a bioartificial liver support system. (MEng dissertation) University of Pretoria 2007.
113. Puviani AC, Ottolenghi C, Tassinari B, Pazzi P, Morsiani E. An update on high-yield isolation methods and on the potential clinical use of isolated liver cells. *Compar Biochem Physio*. 1998;Part A 121:99-109.
114. Sachs DH. The pig as a potential xenograft donor. *Vet Immunol Immunol pathol*. 1994;58:185-91.
115. Gerlach JC, Brombacher J, Kloppel K, Schnoy N, Neuhaus P. Comparison of four methods for mass hepatocyte isolation from pig and human livers. *Transplantation* 1994;57: 1318-22.
116. Gerlach JC, Brombacher J, Smith M, Neuhaus P. High yield isolation from pig livers for investigation of hybrid liver support systems: Influence of collagenase concentration and body weight. *J Surg Re*s 1996;62: 85-9.
117. Seglen, PO. Preparation of rat liver cells. *Methods Cell Biol*. 1976;13:29-34.
118. Morsiani E, Rozga J, Scott HC, Lebow LT, Moscioni AD, Kong LB, Mc Grath MF, Demetriou AA. Automated liver cell processing facilitates large scale isolation and purification of porcine hepatocytes. *ASAIO J*. 1995;41:155-61.

119. Foy BD, Lee J, Morgan J, Toner M, Tompkins RG, Yarmush ML. Optimization of hepatocyte attachment to microcarriers: Importance of oxygen. *Biotech Bioeng* 1993;42:579-88.
120. Nishikawa M, Uchino J, Matsushita M, Takahashi M, Taguchi K, Koike M, Kamachi H, Kon H. Optimal oxygen tension conditions for functioning cultured hepatocytes in vitro. *Artificial Organs*. 1996;20(2):169-77.
121. Rotem A, Toner M, Bhatia S, Foy BD, Tompkins RG, Yarmush ML. Oxygen is a factor determining in vitro tissue assembly: Effects on attachment and spreading of hepatocytes. *Biotech Bioeng*. 1994;43:654-60.
122. Talamini MA, Kappus B, Hubbard A. Repolarization of hepatocytes in culture. *Hepatology*. 1997;25(1):167-72.
123. Falasca L, Michelli A, Sartori E, Tomassini A, Devirgiliis LC. Hepatocytes Entrapped in Alginate Gel Beads and Cultured in Bioreactor: Rapid Repolarization and Reconstitution of Adhesion Areas. *Cells Tissues Organs* 2001;168:126-36.
124. Lecluyse EL, Fix JA, Audus KL, Hochman JH. Regeneration and Maintenance of Bile Canalicular Networks in Collagen-sandwiched Hepatocytes. *Toxicology in Vitro* 2000;14: 117-32.
125. Hoekstra R, Chamuleau RAFM. Recent developments on human cell lines for the bio-artificial liver. *Int J Artif Org.* 2002;25(3):182-91.
126. Smith MD, Smirthwaite AD, Cairns DE, Cousins RB, Gaylor JD. Techniques for measurement of oxygen consumption rates of hepatocytes during attachment and post-attachment. *Int J Artif Org* 1996;19(1):36-44.
127. Sand T, Condie R, Rosenberg A. Metabolic crowding effect in suspension of cultured lymphocytes. *Blood.* 1977;50(2):337-46.
128. Kleiber M. Body size and metabolic rate. *Physiol Rev*. 1947;27:511-41.
129. Wang Z, O'Connor P, Heshka S, Heymsfield SB. The reconstruction of Kleiber's law at the organ-tissue level. *Am Soc Nutrit Sci, Nutritional Methods Res Comm.* 2001:2967-70.
130. Balis UJ, Behnia K, Dwarakanath B, Bhatia SN, Sullivan SJ, Yarmush ML, Toner M. Oxygen consumption characteristics of porcine hepatocytes. *Metabol Eng* 1999;1:49-62.
131. Ju LK, Lee JF, Armiger WB. Enhancing oxygen transfer in bioreactors by perfluorocarbon emulsions. *Biotechnol Prog*. 1991;7:323-9.
132. McMillan JD, Wang DIC. Enhanced oxygen transfer using oil-in-water dispersions. *Ann. New York Acad Sci.* 1987;506:569-82.
133. Elibol M, Mavituna F. Effect of perfluorodecalin as an oxygen carrier on actinorhodin production by Streptomyces coelicor. *Appl Microbiol Biotechnol.* 1995;43:206-10.
134. Arias IM, Boyer JL, Chisary FV, Fausto N, Jakoby WB, Schachter D, Shafritz DA (editors). 2001. The liver: Biology and Pathobiology. NY, Lippincott, Williams and Wilkins, Philadelphia, p 3.
135. Jundermann K, Kietzmann T. Zonation of parenchymal and non-parenchymal metabolism in liver. *Annu Rev Nutr* 1996;16:179-260.
136. Jundermann K, Thurman RG. Hepatocye heterogeneity in the metabolism of carbohydrates. *Enzyme* 1992;46:33-58.
137. Lindros KO. Zonation of cytochrome P450 expression, drug metabolism and toxicity in liver. *Gen Pharmacol* 1997;28:191-6.

138. Runge D, Kohler C, Kostrubsky VE, Jager D, Lehman T, Runge DM, May U. Stolz DB, Strom SC, Fleig WE, Michalopoulos GK. Induction of Cytochrome P450 CYP1A1, CYP1A2, and CYP3A4 but not of CYP2C9, CYP2C19, Multidrug Resistance Associated Protein (MDR-1) by Prototypical Inducers in Human Hepatocytes. *Biochem Biophys Res Comm*. 2000;273:333-41.
139. Wolfe D, Schmidt H, Jungermann K. Short-term modulation of glycogen metabolism, glycolysis and gluconeogenesis by physiological oxygen concentrations in hepatocyte cultures. *Eur J Biochem* 1983;135:405-412.
140. Wolfe D, Jundermann K. Long-term effects of physiological oxygen concentrations on glycolysis and gluconeogenesis in hepatocyte cultures. *Eur J Biochem* 1985;151:299-303.
141. Ohno K, Maier P. Cultured rat hepatocytes adapt their cellular glycolytic activity and adenylate energy status to tissue oxygen tension. *J Cellular Physiol* 1994;160:358-66.
142. Allen JW, Khetani SR, Bhatia SN. In vitro zonation and toxicity in a hepatocyte bioreactor. *Toxicol Sci* 2005;84:110-9.
143. Sivaraman A, Laech JK, Toiwsend S, Iida T, Hogan BJ, Stolz DB, Fry R, Samson LD, Tannenbaum SR, Griffith LG. A microscale in vitro physiological model of the liver: Predictive screesn for drug metabolism and enzyme induction. *Curr Drug Metab* 2005;6:569-91.
144. Riccalton-Banks L, Liew C, Bhandari R, Fry J, Shakesheff K. Long-term culture of functional liver tissue: 3-D coculture of primary hepatocytes and stellate cells. *Tissue engineering* 2003;9(3):401-410.
145. Watanabe T, Shibata N, Westerman KA, Okitsu T, Kobayashi N. Establishment of immortalized human hepatic stellate scavenger cells to develop bioartificial livers. *Transplantation* 2003;75:1873-80.
146. Morin O, Normand C. Long-term maintenance of hepatocyte functional activity in co-culture. *J Cellular Physiol* 1986;129:103-10.
147. Okamoto M, Ishida Y, Keogh A, Strain A. Evaluation of the function of primary human hepatocytes co-cultured with the human hepatic stellate cell (HSC) line L190. *Int J Artif Org* 1998;6:353-9.
148. Lowe KC. Davey MR, Power JB. Perfluorochemicals: their applications and benefits to cell culture. *Tibtech* 1998;16:272-77.
149. King AT, Mulligan BJ, Lowe KC. Review: Perfluorochemicals and cell culture. *Biotechnology* 1989;7:1037-42.
150. Lowe KC, Anthony P, Wardrop J, Davey MR, Power JB. Perfluorochemcals and cell biotechnology. *Art cells, blood subs, immob biotech* 1997;25(3):261-274.
151. Lowe KC. Review. Engineering blood: Synthetic substitutes from fluorinated compounds. *Tissue Engineering* 2003;9(3):389-99.
152. Niu M, Clemens MG, Coger RN. Optimizing normoxic conditions in liver devices using enhanced gel matrices. Biotechnol Bioeng 2007;99(6):1502-12.
153. Khattak SF, Chin K, Bhatia SR, Roberts SC. Enhancing O_2 tension and cellular function in alginate cell encapsulation devices through the use of perfluorocarbons. Biotechnol Bioeng 2007;96(1):156-66.
154. Ju LK, Lee JF, Armiger WB. Enhancing oxygen transfer in bioreactors by perfluorocarbon emulsions. Biotechnol Prog. 1991;7:323-9.
155. Block GD, Locker J, Bowen WC, Petersen BE, Katyal S, Strom SC, Riley T, Howard TA, Michalopolous GK. Population expansion, clonal growth and specific

differentiation patterns in primary cultures induced by HGF/SF, EGF and TDF in a chemically defined (HGM) medium *J Cell Biology* 1996;132(6):1133-49.

156. Runge DM, Runge D, Dorko K, Pisarov LA, Leckel K, Kostrubsky VE, Thomas D, Strom SC, Michalopoulos GK. EGF and HGF activity in serum-free cultures of human hepatocytes. *J Hepatol* 1999;30:265-74.
157. Su T, Waxman D. Impact of DMSO and expression of nuclear receptors and drug-inducible cytochromes P450 in primary rat hepatocytes. *Arch Biochem Biophys* 2004;424:226-234.
158. Powers MJ, Janigian DM, Wack KE, Baker CS, Stolz DB, Griffith LG. Fuctional behaviour of primary rat liver cells in a 3D perfused microarray bioreactor. *Tissue Engineering* 2002;8(3):499-513.
159. Jasmund I, Schwientek S, Acikgoz A, Langsch A, Machens HG, Bader A. The influence of medium composition and matrix on long-term cultivation of primary porcine and human hepatocytes. *Biomolecular Eng* 2007;24:59-69.
160. Niuy M, Clemens MG, Coger RN. Optimizing normoxic conditions in liver devices using enhanced gel matrices. Biotechnol Bioeng 2007;99(6):1502-12.
161. Khattak SF, Chin K, Bhatia SR, Roberts SC. Enhancing O_2 tension and cellular function in alginate cell encapsulation devices through the use of perfluorocarbons. *Biotechnol Bioeng* 2007;96(1):156-66.
162. Sullivan J, Harris DR, Palmer AF. Convection and hemoglobin-based O2 carrier enhanced transport in a HF bioreactor. *Artif Cells, Bl Subs, Biotechnol* 2008;36:386-402.
163. Mareels G, Poyck P, Elloot S, Chamuleau R, Verdonck P. Numerical simulation of fluid flow and oxygen transport in a full scale model of the AMC Bioartificial liver with an in vitro determined hepatocyte distribution. *Ann Biomed Eng*. 2006 34(11):1729-44.
164. Freire MG, Dias AMA, Coutinho JAP, Coelho MAZ, Marrucho IM. Enzymatic method for determining O_2 solubility in perfluorocarbon emulsions. *Fluid Phase Equilibria* 2005;231:109-13.
165. Martin Y, Vermette P. Bioreactors for tissue mass culture: Design, characterisation and recent advances. *Biomaterials* 2005;26:7481-503.
166. Heath CA, Hammer BE, Pimbley JM. Magnetic resonance imaging of flow in HF bioreactors. *AIChE J* 1990;36(4):547-58.
167. Donoghue C, Brideau M, Newcomer P, Pangrle B, DiBasio D, Walsh E, Moore S. Use of MRI to analyse the performance of HF bioreactors. *Ann NY Acad Sci* 1992;665:285-300.
168. Planchamp C, Ivancevic MK, Pastor CM, Valle´e JP, Pochon S, Terrier F, Mayer JM, Reist M. Hollow Fiber Bioreactor: New Development for the Study of Contrast Agent Transport Into Hepatocytes by Magnetic Resonance Imaging. *Biotechnol Bioeng* 2004;85(6):656-65.
169. Ferreira EC, Mota M, Pons MN. Image analysis and multiphase bioreactors Chptr 2 in Multiphase Bioreactor design, JMS Cabral, M Mota, J Tramper (eds) Taylor & Francis, London 25-52, 2001.
170. Kofidis T, Lenz A, Boublik J, Akhyari P, Wachsmann B, Stahl KM, Haverich A, Leyh RG. Bioartificial grafts for transmural myocardial restoration: a new cardiovascular tissue culture concept. *Eur J Cardio-thoracic Surg* 2003;24:906-11.
171. Kofidis T, Lenz A, Boublik J, Akhyari P, Wachsmann B, Stahl KM, Hofmann M, Haverich A. *Biomaterials* 2003;24:5009-14.

172. Walles T, Giere B, Hofmann M, Schanz J, Hofmann F, Mertsching H, Macchiarini P. Experimental generation of a tissue-engineered functional and vascularized trachea. *Gen Thoracic Surg* 2004;129(6):900-6.
173. Phelps ME. Positron emission tomography provides molecular imaging of biological processes. *PNAS* 2000;97(16):9226-33.
174. Mc Kenzie TJ, Lillegard JB, Nyberg SL. Artificial and bioartificial liver support. *Semin Liver Dis* 2008;28:210-17.
175. Fishman JA, Patience C. Xenotransplantation: Infectious risk revisited. *Amer J Transplant* 2004;4:1383-90.
176. Sprangers B, Waer M, Billiau AD. Xenotransplantation: Where are we in 2008? *Kidney International* 2008;74:14-21.
177. Wilhelm M, Fishman JA, Pontikis R, Aubertin AM, Wilhelm FX. Susceptibility of recombinant PERV reverse transcriptase to nucleoside and non nucleoside inhibitors. *Cell Mol Life Sci* 2002;59:2184-90.
178. Ramsoondar J. Conference abstract. *Xenotransplantation* 2007;14:400.
179. Phelps CJ, Koike C, Vaught TD. Production of α1,3 galactosyltransferase deficient pigs. *Science* 2003;299:411-14.
180. Miyagawa S, Nakatsu S, Nakagawa T, Kondo A, Matsunami K, Hazama et al Prevention of PERV infections in pig to human xenostransplantation by the RNA interference silences gene. *J Biochem* 2005;137:503-8.
181. Cooper DKC, Ezzelrahab M, Hara H, Ayares D. Recent advances in pig-to-human organ and cell transplantation. *Expert Opin Biol Ther* 2008;8(1):1-4.
182. Dwyer KM, Robson SC, Nandukar HH. Thromboregulatory manifestations in human CD39 transgenic mice and the implications for thrombotic disease and transplantation *J Clin Invest* 2004;113:1440-6.
183. Chen D, Weber M, McVey JH. Complete inhibition of acute humoral rejection sing regulated expression of membrane-tethered anticoagulants on xenograft endothelium *Am J Transplant* 2004;4:1958-63.
184. Cozzi E, White DJ. The generation of transgenic pigs as potential organ donors for humans. *Nat Med* 1995;1:964-6.
185. Hara H,Long C, Lin YJ, Tai HC, Ezzelrahab M, Ayares D, Cooper DKC. *In vitro* investigation of pig cells for resistance to human antibody-mediated rejection. *Transplant Int* 2008. not yet published. doi:10.1111/j.1432-2277.2008.00736.x
186. Sandgren EP, Palmiter RD, Heckel JL. Complete hepatic regeneration after somatic deletion of an albumin activator transgene *Cell* 1991;66:245-56.
187. Tateno C, Yoshizane Y, Saito N. Near completely humanized liver in mice shows human-type metabolic responses to drugs Am J Pathol 2004;2004:165:901-12.
188. Azuma H, Paulk N, Ranabe A. Robust expansion of human hepatocytes in Fah$^{-/-}$/Rag$^{2-/-}$/Il2rg$^{-/-}$ mice. *Nat Biotechnol* 2007;25:903-10.
189. Bissig KD, Le TT, Woods BN, Verma IM. Repopulation of adult and neonatal mice with human hepatocytes: A chineric animal model *PNAS* 2007;104(51)20507-11.
190. Mavri-Damelin D, Damelin LH, Eaton S, Rees M, Selden C, Hodgson HJF. Cells for bioartificial liver devices: The human hepatoma-derived cell line C3A produces urea but does not detoxify ammonia. *Biotechnol Bioeng* 2007;99(3):644-51.
191. Choi YS, Lee DY, Kim IY, Kang S, Ahn K, Kim HJ. Ammonia removal using hepatoma cells in mammalian cell cultures *Biotechnol Prog* 2000;16(5):760-68.
192. Lorenzini S,Gito S, Grandini E, Andreone P, Bernardi M. Stem cells for end-stage liver disease: How far have we got? *World J Gastroenterol* 2008;14(29):4593-9.

193. Poyck PC, van Wijk ACWA, van der Hoeven TV, de Waart DR, Chamuleau RAFM, van Gulik TM, Oude Elferink RPJ, Hoekstra R. Evaluation of a new immortalized fetal liver cell line (cBAL111) for application in a bioartificial liver. *J Hepatol* 2007; 48(2):266-75.
194. Poyck PC, Hoekstra R, Maas MAW, van Wijk ACWA, van Gulik TM, Chamuleau RAFM. Evaluation of a novel human fetal liver cell line cBAL11 in the AMC-BAL in rats with complete liver ischemia. In Poyck PC PhD thesis: Towards the application of a human liver cell line in the AMC bioartificial liver 2007 ISBN 978-90-9022050-5.
195. Talbot NC, Caperna TJ, Lebow LT, Moscioni D, Pursel VG, Rexroad CE. Ultrastructure, enzymatic and transport properties of the PICM-19 liver cell line. *Exp Cell Res* 1996;225:22-34.
196. Talbot NC, Caperna TJ, Wells KD. The PICM-19 cell line as an in vitro model of liver bile ductules: Effects of cAMP inducers, biopeptides and pH. *Cells, Tissues Organs* 2002;171:99-116.
197. Press release: HepaLife's bioartificial liver exceeds expectations in new tests conducted over prolonged periods of time. May 12, 2008. (www.hepalife.com).
198. Puhl G, Frank J, Muller AR, Steinmuller T, Denner J, Neuhaus P, Gerlach JC. Clinical extracorporeal hybrid liver support- phase I study with primary porcine cells. *Xenotransplantation* 2003;10(5):460-9.
199. Hepalife Inc. Material purchase agreement October 01, 2008 (www.secinfo/d12Pk6.tm8e.htm).
200. Riess JG. Perfluorocarbon-based oxygen delivery. *Artif Cells, Bl subs, Biotechnol* 2006;34:567-80.
201. Krafft MP, Riess JG. Perfluorocarbons: Life Sciences and Medical uses. *J Polym Sci Part A: Polym Chem* 2007;45:1185-98.
202. Spahn DR, Kocian R. The place of artificial oxygen carriers in reducing allogenic blood transfusions and augmenting tissue oxygenation. *Canadian Jnl Anaesthesia* 2003;50(6):41-7.
203. Kim HW, Greenburg AG. Toward 21st century blood component replacement therapeutics: Artificial O_2 carriers *Artif Cells, Bl subs, Biotechnol* 2006;34:537-50.
204. Kuznetsova IN. Perfluorocarbon emulsions: Stability *in vitro* and *in vivo. Pharm Chem Jnl* 2003;37(8):415-20.
205. Ingram DA, Forman MB, Murray JJ. Activation of complement by Fluosol attributable to the pluronic detergent micelle structure. *J Cardiovasc Pharmacol* 1993;22:456-61.
206. Noveck RJ, Shanon EJ, Leese PT et al Randomized safety studies of IV perflubron emulsion. II Effects on Immune Function in healthy volunteers. *Anesth Analg* 2000;91:812-22.
207. Noveck RJ, Shanon EJ, Shor JS et al Randomized safety studies of IV perflubron emulsion. I Effects on Coagulation Function in healthy volunteers. *Anesth Analg* 2000;91:804-11.
208. Burgan AR, Herrick WC, Long DM et al. Acute and subacute toxicity of 100% PFOB emulsion. *Biomat Art Cells Art Org* 1988;16(1-3):681-2.
209. Sedova LA, Kochetygov NI, Berkos MV et al. Side reaction caused by the PFC emulsions in IV infusion to experimental animals. *Art Cells, Blood Subs Immob Biotech* 1998; 26(2):149-57.

210. Sloviter HA, Yamada H, Ogoshi S. Some effects of IV administered dispersed fluorochemicals in animals. *Federation Proceedings* 1970;29(5):1755-7.
211. Mattrey RF, Hilpert PL, Long CD. Hemodynamic effects of IV lecithin-based PFC emulsions in dogs. *Crit care Med* 1989;17(7):652-6.
212. Peck W, Mattrey RF, Slutsky RA. Perfluorooctyl bromide: acute hemodynamic effects in pigs of IV administration compared with standard ionic contrast media. *Investigative Radiology* 1984;2:129-32.
213. Nieuwoudt M, Kunneke R, Smuts M, Becker J, Stegmann GF, Van der Walt C, Neser J, Van der Merwe S. Standardization criteria for an ischemic surgical model of acute hepatic failure in pigs. *Biomaterials* 2006: 27(20);3836-45.
214. Higgins GM, Anderson RM. Experimental pathology of the liver. *Arch Pathol* 1931:12:186-202.
215. Emond J, Capron-Laudereau M, Meriggi F, Bernau J, Reynes M, Houssin D. Extent of hepatectomy in the rat. *Eur Surg Res* 1989;21:251-59.
216. Kubota T, Takabe K, Yang M, Sekido H, Endo I, Ichikawa Y. Minimum sizes for remnant and transplanted livers in rats. *J Hep Bil Pancr Surg* 1997;4:398-404.
217. Topaglu S, Izci E, Ozel H, Topaglu E, Avsar F, Saygun O. Effects of TVE application during 70 % hepatectomy on regeration capacity of rats. *J Surg Res* 2005;124:139-45.
218. Ijichi H, Taketomi A, Yoshizumi T, Uchiyama H, Yonemura Y, Soejima Y. Hyperbaric oxygen induces endothelial growth factor and reduces liver injury in regenerating rat liver after partial hepatectomy. *J Hepatol* 2006;45:28-34.
219. Urakami H, Abe Y, Grisham MB. Role of reactive metabolites of oxygen and nitrogen in partial liver transplantation. *Clin Exp Pharmacol Physiol* 2007;34:912-9.
220. Van de Kerkhove MP, Hoekstra R, van Gulik TM, Chamuleau R. Large animal models of fulminant hepatic failure in artificial and Bioartificial liver support research. *Biomaterials* 2004; 25:1613-25.
221. Seleverstov O, Bader A. Evaluation of liver support systems for preclinical testing by animal trials. *Artificial Organs* 2006;30(10):815-21.
222. Nyberg SL. Galactosamine induced fulminant hepatic failure. *Hepatology.* 1997;26:1367-69.
223. Kalpana K, Ong HS, Soo K.C, Tan SY, Prema Raj J. An improved model of galactosamine induced fulminant hepatic failure in the pig. *J Surg Res.* 1999;82(2):121-130.
224. Grosse H, Ozler Y, Fabre M, Cheruau B, Abbas A, Urbani L. Acetaminophen induced fulminant hepatic failure in pigs: a new model to assess pre-clinical liver assistance (abstract) *Hepatology.* 1996;24:722A.
225. Henne-Bruns D, Artwohl J, Broelsch C, Kremer B. Acetaminophen induced acute hepatic failure in pigs: controversial results to other animals. *Res Exp Med.* (Berlin) 1988;188(6):463-472.
226. Hickman R, Dent DM, Terblanche J. The anhepatic model in a pig. *SAMJ.* 1974;48:263-274.
227. Fourneau I, Pirenne J, Roskams T, Yap SH. An improved model of acute liver failure based on transient ischemia of the liver. *Arch Surg.* 2000;135:1183-9.
228. Flendrig LM, Calise F, Di Florio E, Mancini A, Cerielllo A. Significantly improved survival time in pigs with complete liver ischemia treated with a novel bio-artificial liver. *Int J Artif Org.* 1999;22:701-708.

229. Ytrebo LM, Nedredal GI, Langbakk B, Revhaug A. An experimental large animal model for the assessment of bio-artificial liver support systems in fulminant hepatic failure. *Scand J Gastroenterol*. 2002;9:1077-88.
230. Newsome PN, Plevris JN, Nelson LJ, Hayes PC. Animal models of fulminant hepatic failure: a critical evaluation. *Liver Transpl.* 2000;6(1):21-31.
231. Terblanche J, Hickman R. Animal models of fulminant hepatic failure. *Dig Dis Sci*. 1991;36:770-4.
232. Rahman TM, Hodgson HJF. Animal models of acute hepatic failure. *Int J Exp Path.* 2000;81:145-57.
233. Bhatnagar A, Majumdar S. Animal models of hepatic encephalopathy. *Ind Soc Gastroenterol.* 2003;22:S33-6.
234. Blei AT, Olaffson S, Webster S, Levy R. Complications of intracranial pressure monitoring in fulminant hepatic failure. *Lancet.* 1993;341:157-8.
235. Chem S, Hewitt W, Demetriou A, Rozga J. Prolonged survival in anhepatic pigs treated with a bioartficial liver. *Surg forum Alimentary tract* 1996;161-3.
236. Hickman R, Bracher M, Tyler M, Lotz Z, Fourie J. Effect of total hepatectiomy on coagulation and glucose homeostasis in the pig. *Dig Dis Sci*.1992;37(3):328-34.
237. Vistoli F, Boggi U, Filliponi F, Mosca F. A standardized pig model of total hepatectomy for testing liver support systems. *Transplant proc* 2000;32:2723-5.
238. Engelbrecht G, Hickman R, Kahn D. One-stage total hepatectomy in the rat using microvascular anastmoses. *Microsurgery* 1999; 19:95-7.
239. Bhatia V, Singh R, Acharya SK. Predictive value of arterial ammonia for complications and outcome in acute liver failure. *Gut* 2006;55:98-104.
240. Clemmesen JO, Larsen FS, Kondrup J, Adel Hansen B, Ott P. Cerebral herniation in patients with acute liver failure is correlated with arterial ammonia concentration. *Hepatology* 1999;29:648-53.
241. Bernal W, Hall C, Karvellas CJ, Auzinger G, Sizer E, Wendon J. Arterial ammonia and clinical risk factors for encephalopathy and intracranial hypertension in acute liver failure. *Hepatology* 2007;46(6):1844-52.
242. Sauer IM, Neuhaus P, Gerlach JC. Concept for modular extracorporeal liver support for the treatment of acute hepatic failure. *Metab Brain Dis* 2002;17(4):477-84.
243. Lee W, Squires RH, Nyberg SL, Doo E, Hoofnagle JH. Acute liver failure: Summary of a workshop. Meeting report. *Hepatology* 2008;47(4):1401-15.
244. Cruz D, Bellomo R, Kellum JA, de Cal M, Ronco C. The future of extracorporeal support. *Crit Care Med* 2008;36(4):S243-52.
245. Evenepoel P, Laleman W, Wilmer A, Claes K, Kuypers D, Bammens B, Nevens F, Vanrebterghem Y. Prometheus verus MARS: Comparison of efficiency in two different liver detoxification devices. *Artif Org* 2006;30(4):276-84.
246. Ferenci P, Kramer L. MARS and the failing liver- any help from the outer space? *Hepatology* 2007;46(6):1682-4.
247. Sauer IM, Goetz M, Steffen I, Walter G, Kehr DC, Schwartlander R, Hwang YJ. Pascher A, Gerlach JC. Neuhaus P. In vitro comparison of the MARS and SPAD. *Hepatology* 2004;39:1408-14.
248. Rozga J, Umehara Y, Trofimenko A, Sadahiro T, Demetriou AA. A novel plasma filtration therapy for hepatic failure: preclinical studies. *Ther Apher Dial* 2006;10(2):138-144.
249. Ho DW, Fan ST, To J. Selective plasma filtration for treatment of FHF induced by galactosamine in a pig model. *Gut* 2002; 50:869-76.

250. Rowland M, Tozer TN. Clinical pharmacokinetics concepts and applications. Philadelphia; Lea and Febinger. 1989.
251. Iwata H, Ueda Y. Pharmacokinetic considerations in the development of a bio-artificial liver. *Clin Pharmacokinet.* 2004; 43(4):211-25.
252. Park YG, Iwata H, Ikada Y. Derivation of pharmacokinetics equations for quantitative evaluation of bio-artificial liver functions. *Ann NY Acad Sci.* 2001;944:296-307.
253. Iwata H, Park YG, Ikada Y. Importance of the extracorporeal circulation rate in a bio-artificial liver. *Material Sci Eng.* 1998:C6;235-43.
254. Catapano G, de Bartolo L. Importance of the kinetic characterization of liver cell metabolic reactions to the design of hybrid liver support devices. *Int Jnl Artif Org.* 1996;19(1):670-6.
255. Kanamori T, Yanagi K, Sato T, Shinbo T, Ohshima N. System design of a bio-artificial liver with a high performance hemodialyzer as an immunoisolator using a mathematical kinetic model. *Int J Artif Org*. 2003;26(4):308-18.
256. Ohshima N, Shiota M, Kusano H, Wada G, Tsunetsugu T, Ookawa K, Yanagi K. Kinetic analyses of the performances of a hybrid-type artificial liver support system utilizing isolated hepatocytes. *Material Sci Eng* 1994;C1:79-85.
257. Park YG, Son YS, Ryu HW. Perifusion model for detoxification of drugs in a bio-artificial liver. *Int Jnl Artif Org* 2003:26(5):383-94.
258. Palmes D, Spegel HU. Animal models of liver regeneration. *Biomaterials.* 2004;25:1601-11.
259. Jakubowski A, Ambrose C, Parr M, Lincecum JM, Wand MZ. TWEAK induces liver progenitor cell proliferation. *J Clin Invest*. 2005; 115:2330-40. doi:10.1172/JCI23486.
260. Bailey B, Amre DK, Gaudreault P. Fulminant hepatic failure secondary to acetaminophen poisoning: A systematic review of prognostic criteria. *Crit Care Med* 2003;31(1):299-305.
261. Choi WC, Arnaout WC, Villamil FG, Demetriou AA, Vierling JM. Comparison of the applicability of two prognostic scoring systems in patients with fulminant hepatic failure. *Korean J Int Med* 2007;22:93-100.
262. Kamath PS, Wiesner RH, Malinchoc M, Kremers W, Therneau TM, Kosberg CL, D'Amico G, Dickson ER, Kim WR. A model to predict survival in patients with end-stage liver disease. *Hepatology* 2001;33:464-70.
263. Pelaez-Luna M, Martinex-Salgado J, Olivera-Martinez MA. Utility of the MAYO end-stage liver disease score, King's college criteria and a new in-hospital mortality score in the prognosis of in-hospital mortality in acute liver failure. *Transplant Proc* 2006;38:927-9.
264. Ripoll C, Banares R, Rincon D, Catalina MV, Iacono OL, Salcedo M, Clemente G, Nunez O, Matilla A, Molinero LM. Child, MELD, hyponatremia and now portal pressure. *Hepatology* 2005;42:793-801.
265. Huo TI, Lin HC, Wu JC, Lee FY, Hou MC, Lee PC, Chang FY, Lee SD. Proposal of a modified Child-Turcotte-Pugh scoring system and comparison with the MELD for outcome prediction in patients with cirrhosis. *Liver Transplantation* 2006;12:65-71.
266. Cholongitas E, Senzolo M, Patch D, Kwong K, Nikolopoulou V, Leandro G, Shaw S, Burroughs AK. Risk factors, SOFA and MELD scores for predicting short term mortality in cirrhotic patients admitted to intensive care unit. *Aliment Pharmacol Ther* 2006;23:883-93.

267. Dabos JD, Newsome PN, Parkinson JA, Davidson JS, Sadler IH, Plevris JN, Hayes PC. A biochemical prognostic model of outcome in paracetamol-induced acute liver injury. *Transplantation* 2005;80(12):1712-6.
268. Bernal W, Donaldson N, Wyncoll D, Wendon J. Blood lactate as an early predictor of outcome in paracetamol-induced acute liver failure: a cohort study. *Lancet* 2002;359:558-63.
269. Novelli G, Rossi M, Pugliese F, Poli I, Ruberto E, Martelli S, Nudo F, Morabito V, Mennini G, Berloco PB. Molecular adsorbents recirculating system treatment in acute-on-chronic hepatitis patients on the transplant waiting list improves model for end stage liver disease scores. *Transplant Proc* 2007;39:1864-7.
270. For example see YSI 7100 multi parameter bio-analytical system, www.YSI.com 2007.
271. For example see CMA 600 multi parameter clinical microdialysis system, www.microdialysis.se
272. Booch G, Jacobsen I, Rumbagh J. OMG Unified Modeling Language Specification, available online, www.uml.org, 2008.
273. Aggarwal V. The application of the unified modeling language in object-oriented analysis of healthcare information systems. *J Med Syst*, 2002; 26(5): 383-97.
274. Xiao-Lang X, Wang L, Zhou H. A UML profile for framework modeling. *J Zheijang Univ Sci*, 2004; 5(1): 92-8.
275. Van der Maas AF, ter Hofstede A, ten Hoopen AJ. Requirements for medical modeling languages. *J Am Med Inform Assoc*, 2001; 8: 146-62.
276. Roux-Rouquié M, Caritey N, Gaubert L, Le Grand B, Soto M. Metamodel and modeling language: Towards a unified modeling language (UML) profile for systems biology. *T Comp Sys Biology 2005*; in press.
277. *Roux-Rouquié* M, Soto M. Virtualization in *Systems Biology*: *Metamodels* and modeling languages for semantic integration. T Comp Sys *Biology 2005*;(1):28-43.
278. *Roux-Rouquié,* M., Caritey, N., Gaubert, L. *Using* the Unified Modelling Language (*UML*) to guide the systemic description of biological processes and systems. Biosystems 2004;75:3-14.
279. van der Heijden RTJM, Hellinga C, Lutben K, Honderd G. State estimators (observers) for the on-line estimation of non-measurable process variables. *Tibtech* 1989; 7: 205-9.
280. Leleux DP, Claps R, Chen W, Tottel FK, Harman TL. Applications of Kalman filtering to real-time trace gas concentration measurements. *Appl Phys* 2002;B74:85-93.
281. Simutis R, Havlik I, Lubbert A. A fuzzy-supported extended Kalman filter. *J Biotechnol* 1992;24:211-34
282. Stephanopoulos G, Park S. Bioreactor state estimation. in Biotechnology 2nd edition, Volume 4 Measuring Modeling and Control, VCH Verlagsgeselleschaft mbH, Weinheim Germany 1991.
283. Pelletier F, Fonteix C, da Silva AL, Marc A, Engasser JM. Software sensors for monitoring perfusion cultures: Evaluation of the hybridoma density and the medium composition from glucose concentration measurements. *Cytotechnology* 1994; 15: 291-9.
284. Sprent P. Data-driven statistical modeling. London, Chapman and Hall, Thompson Science, 1998.

285. Myerson RB. Probability Models for Economic Decisions. University of Chicago, Chicago, Thomson/Brooks/Cole, 2005.
286. Hogg RV, Craig AT. Introduction to Mathematical Statistics, 5th ed, New York, Macmillan, 1995.
287. Landau DP, Binder K. A guide to Monte Carlo analysis in statistical physics. 2nd edition, Cambridge University Press. 2005.
288. Wendon J. What to monitor and why? *EASL* congress Copenhagen 2007.
289. Kramer DJ. Prevention and management of infections and MOF. *EASL* congress Copenhagen 2007.
290. Finney RL, Thomas GB editors. Calculus, Reading Massachusetts, Addison-Wesley, 1990, Section 9.7. p.623-44.
291. Hanson CW, Marshall BE. Artificial intelligence applications in the intensive care unit. *Crit Care Med* 2001; 29(2): 427-35.
292. Raghavan SR, Ladik V, Meyer KB. Developing decision support for dialysis treatment of chronic kidney failure. IEEE Trans Inf Tech Biomed 2005; 9(2): 229-38.
293. Jeanpierre L, Charpillet F. Automated medical diagnosis with fuzzy stochastic models: Monitoring chronic diseases. *Acta Biotheoretica* 2004; 52: 291-311.
294. Mahfouf M, Abbod MF, Linkens DA. A survey of fuzzy logic monitoring and control utilization in medicine. *Artif Intell Med* 2001; 21: 27-42.
295. Toma T, Abu-Hanna A, Bosman RJ. Discovery and integration of univariate patterns from daily individual organ-failure scores for intensive care mortality prediction. *Artif Intell Med.* 2008;43(1):47-60.
296. Toma T, Abu-Hanna A, Bosman RJ. Discovery and inclusion of SOFA score episodes in mortality prediction. *J Biomed Inform*. 2007;40(6):649-60.
297. Romsi P, Heikkinen J, Biancari F, Pokela M, Rimpilainen J, Vainionpaa V. Prolonged hypothermia after experimental hypothermic circulatory arrest in a chronic porcine model. *J Thorac Cardiovasc Surg*. 2002;123:724-34.
298. Takada Y, Ishiguro S, Fukunaga K, Gu M, Taniguchi H, Seino K. Increased intracranial pressure in a porcine model of fulminant hepatic failure using amatoxin and endotoxin. *J Hepatol.* 2001;34:825-31.
299. Hanid MA, Mackenzie RL, Jenner RE, Chase RA, Mellon PJ, Trewby PN. Intracranial pressure in pigs with surgically induced acute liver failure. *Gastroenterology* 1979;76(1):123-31.
300. Cimander C, Carlsson M, Mandenius CF. Sensor fusion for *on-line* monitoring of yoghurt fermentations. *J Biotechnol.* 2002;99:237-48.
301. Dowd JE, Weber I, Rodriguez B, Piret JM, Kwok KE. Predictive control of hollow-fiber bioreactors for the production of monoclonal antibodies. *Biotechnol Bioeng* 1999;63(4):484-92.
302. Kovarova-Kova K, Gehlen S, Kunze A, Keller T, von Daniken R, Kolb M, van Loon A. Application of model-predictive control based on artificial neural networks to optimize the fed-batch process for riboflavin production. *J Biotechnol* 2000;78:39-52.
303. Hoffman F, Schmidt M, Rinas U. Simple technique for simultaneous *on-line* estimation of biomass and acetate from base consumption and conductivity measurements in high-cell density cultures of Escherichia coli. *Biotechnol Bioeng* 2000;70:358-61.
304. Erlenkotter A, Fobker M, Chemnitius GC. Biosensors and flow-through system for the determination of creatinine in hemodialysate. *Anal Bioanal Chem* 2002; 372: 284-92.

305. Lindberg LS, Ask P, Fridolin I, Magnusson M, Uhlin F, Ragnemalm B. Sensors for non-invasive regulation of dialysis. Linkopings University, Sweden, available at http://www.imt.liu.se/fmtpa/research/dialysis.html, accessed November 2005.
306. Harms P, Kostov Y, Tao G. Bioprocess monitoring. *Curr Opin Biotechnol*. 2002;13:124-27.
307. Pijanowska DG, Dawgul M, Torbicz W. Comparison of urea determination in biological samples by Enfets on pH and pNH_4 detection. *Sensors.* 2003;3:160-65.
308. Ulber R, Frerichs JG, Beutel S. Optical sensor systems for bioprocess monitoring. *Anal Bioanal Chem*. 2003;376:342-48.
309. Lenz R, Kuhn KA. Towards a continuous evolution and adaptation of information systems in medicine. *Int J Med Informatics.* 2004;73:75-89.
310. Wilcox A, Hripcsak G, Chen C. Creating an environment for linking knowledge-based systems to a clinical database: a suite of tools. *AMIA.*1997:303-7.
311. Schugerl K, Progress in monitoring, modeling and control of bioprocesses during the last 20 years. *J Biotechnol*. 2001;85:149-73.
312. Buntemeyer H, Marzahl Rand J, Lehmanm J, A direct control concept for mammalian cell fermentation processes. *Cytotechnol.* 1994;15:271-9.
313. Roger JM, Sablayrolles JM, Steyer JP, Bellon-Maurel V. Pattern analysis techniques for process fermentation curves. *Biotechnol Bioeng*. 2002;79(7):804-15.
314. Palfreyman N. The construction of meaning in computational and integrative biology. *Jnl Integrative Biol*. 2004;8(2):95-105.
315. Belforte G, Bona B, Milanese M. Advanced modeling and identification techniques for metabolic processes. *Crit Rev Biomed Eng*. 1983;10(4):275-316.
316. Brandon EFA, Raap CD, Meijerman I, Beijnen JH, Schellens JHM. An update on *in vitro* test methods in human hepatic drug biotransformation research: pros and cons. *Toxicol Appl Pharmacol*. 2003;189:233-46.
317. Harms P, Kostov Y, Tao G. Bioprocess monitoring. *Curr Opin Biotechnol*. 2002;13:124-27.
318. Freeman RB, Jamieson N, Schaubel DE, Porte RJ, Villamil FG. Who should get a liver graft? *J Hepatol* 2009;50:664-73.

9. APPENDICES

Appendix A: *In vitro* study methods

A.1 Media and chemicals

Minimum essential medium (MEM), Dulbecco's modified Eagle's medium (DMEM) (both with EBSS and L-glutamine) supplemented with fetal bovine serum (FCS) (10% vol/vol) and pennstrep fungizone 100X (1% vol/vol) were purchased from Bio-Whittaker, Adcock Ingram Scientific, Johannesburg, South Africa. Gentamycin sulphate ((50 mg/ml at 0.1% vol/vol), Phenix, South Africa), insulin ((I2767) 50 mU/L), glucagon ((G664) 16 µg/L), dexamethasone ((D4902) 67 µg/L) and epidermal growth factor (EGF (E9644) 20µg/L); from Sigma-Aldrich, Johannesburg, South Africa, were added to all media. Filter-sterilized collagenase type IV (Sigma (C5138)) was dissolved in MEM (0.68 g/425 ml) with 0.65 g $CaCl_2$, 25 ml of FCS and antibiotics as above. Collagenase solution was prepared fresh on the day of the isolation procedure. Washing buffer at 10-15^oC contained deionised water with 5% FCS, dexamethasone as above, 7.01 g/L NaCl, 0.46 g/L KCl, 0.10 g/L Ca Cl_2 and 2.383 g HEPES. Perfusion buffer at 37 ^oC contained 5% FCS, dexamethasone, 9 g/L NaCl, 0.42 g/L KCl, 2.1 g/L $NaHCO_3$, 0.9 g/L D-Glucose and 4.77 g/L HEPES. For chelation, EDTA (0.58 g/L) was added to Perfusion buffer on the day of the procedure. All buffers were oxygenated with a carbogen gas mixture (5% CO_2 and 90%O_2) during the isolation procedure. Percoll (Sigma (P16440)) was mixed 9:1 with 10X Hank's balanced salt solution (HBSS) (80g/L NaCl, 4g/L KCl, 1/Lg $MgSO_4$, 0.6g/L KH_2PO_4, 0.4g/L Na_2HPO_4 and 10g of Glucose). Solutions used for perfusing the liver during hepatectomy and transport were, firstly, 1L of clinical saline at 5-10^oC, supplemented with 0.58g EDTA, 40mU Insulin, 67 µg/L Dexamethasone and antibiotics, followed by 1L of University of Wisconsin (UW) solution at 5-10 ^oC, with insulin, dexamethasone and antibiotics. The pH of all solutions was adjusted in a sterile manner to between 7.35 and 7.4 using concentrated HCl or NaOH. insulin, glucagon, dexamethasone and EGF were added to media on the day of use.

A.2 Hepatocyte culturing, cell evaluation methods and statistics

The cell suspension received from the Centrifuge and BRAT procedures were evaluated for viability and cell count using the Trypan Blue exclusion test in a Neubauer bright-line hemacytometer. The bowl volume employed in any BRAT procedure was randomly selected. To determine the effect of oxygenating the cells and media during the BRAT procedure, in three pairs of experiments flow cytometry was conducted on hepatocytes received after oxygenation had or had not occurred. After all procedures, media aliquots were tested for pathogens in order to determine the sterility of the procedures. In addition, after both centrifuge and BRAT procedures, aliquots containing 3.5-4 x 10^6 cells were taken for seeding in 75 cm^2 cell culture flasks (Corning, Adcock Ingram, Johannesburg, SA) and subsequent culturing in a humidified CO_2 incubator at 37 degrees Celsius. Culture medium was changed 12 hours after seeding, and every 24 hours thereafter for 7 days. In order to determine the impact on hepatocyte cell cycle, flow cytometry of cells scraped from the cell culture flasks was performed 3 and 7 days after seeding.

Media samples were taken daily prior to changing the medium, to evaluate hepatocyte viability by means of LD and AST leakage and to examine the state of Cellular oxidation and Aerobic metabolism by means of the lactate to pyruvate ratio. Lactate and pyruvate concentrations were measured enzymatically, lactate at 520 nm and pyruvate at 340 nm on the Beckman Synchron LX system (Beckman kit 445875 and Sigma kit 726 respectively). The liver enzymes, lactate dehydrogenase (LD) and aspartate aminotransferase (AST) were also detected enzymatically at 340 nm using the Synchron LX system (Beckman Coulter kits 442655, 442665 respectively).

To allow the cells time to recover after the isolation procedure galactose elimination at Day 2 and urea production at Day 3 were investigated (results not presented in this study). On day 4 after isolation, cytochrome P450 activity was investigated by means of lidocaine clearance, by adding 500 µg/ml lidocaine and sampling once every hour for 3 hours. To measure lidocaine, an aliquot of the sample was spiked with bupivacaine as the internal standard. The proteins were precipitated with 1 M perchloric acid. After centrifugation, the supernatant was decanted and neutralized with 1M NaOH. Two extractions with dichloromethane followed and then the organic layers were combined and dried under a stream of dry nitrogen. The residue was redissolved in dichloromethane and analyzed by gas chromatography mass spectrometry. On completion of the lidocaine study, serum-free MEM replaced that in the flasks, and albumin production was investigated with sampling 24 hours later. Albumin concentration was determined colorimetrically by measuring at 600 nm on a Technikon RA-XT system (Miles Technikon method SM4-0131E94).

The Flow cytometry procedure involved the incubation of 1 ml of propidium iodide solution (Coulter DNA-Prep Reagents Kit) with 100 µL of a 2 x 10^6 cells/ml suspension, in the dark, for 30 minutes at room temperature. The samples were analyzed using a Beckman-Coulter Altra Flow Cytometer. A comparison of forward and side scatter data was used to gate the viable cells, in order to exclude debris from the population of cells present in the samples, while the DNA histograms indicated the relative cell cycle status of the suspension, that is, the proportion of DNA in the G0/G1, S or G2M phases. In order to examine if the cultured hepatocyte populations were proliferating normally and to determine if the isolation procedures had been sterile, daily examination of the culture flasks was performed using an Olympus CKX41 inverted microscope set for phase contrast. Digital micrographs, using an Olympus C4040 camera, were taken at day 3 and day 7 after the seeding of the culture flasks.

Statistical Analyses

GraphPad Prism 2.01 was used as a spreadsheet and Statistix 8 was used for the analysis of all data. Values are presented as the mean $\pm$ the standard deviation. The lidocaine clearance and albumin production trends were calculated as follows: The raw data concentration values were converted to absolute quantities and graphed according to time. Straight lines were fitted to each set of results and the mean and standard deviation of the gradients of these lines were calculated. In the case of the lactate to pyruvate ratios and liver enzyme results, the mean and standard deviations were calculated according to each time interval in each experiment. Flow cytometry results were calculated as above,

and where appropriate, P values ($P<0.05$) were calculated by the 2-tailed Mann-Whitney t-test for possible significant differences.

A.3 Cell culturing, metabolic evaluations and statistics

Daily sampling investigated lactate dehydrogenase (LD), aspartate aminotransferase (AST), glucose, lactate and pyruvate concentrations. These were measured using enzymatic kits. pO_2, pCO_2 and pH were measured on a blood gas machine. The oxygen uptake rate (OUR) was calculated after sampling with the gas supply turned off.

Metabolic clearance/production studies were performed in both dynamic and static configurations as follows: on day 2 D(+)galactose elimination, using gas chromatography mass spectrometry (GC-MS) for detection; on day 3 ammonia detoxification (NH_4Cl) with urea synthesis, using enzymatic methods for detection. On day 4 lidocaine clearance, using LC-MS for detection; and on day 5 albumin production, using a spectrophotometric method. Upon termination on day 7, imaging studies involved either scanning electron microscopy (SEM), to investigate the presence of cells in the foam, or isotopic scanning to examine the seeded-distribution of active hepatocytes in the foam.

For SEM the method was as follows; Circulating medium was replaced with fixative: 2.5% glutaraldehyde in a 0.1 M phosphate buffer (PBS) at pH 7.4. After 30 minutes circulation the foam was removed and sections cut from the inlet, middle and outlet. After washing in PBS buffer these were placed in 1% Osmium tetroxide (OsO_4) for 30 minutes. Following water washes, the samples were dried in ethanol and mounted on aluminium plates. After high pressure CO_2 critical point drying for an hour the samples were gold sputtered and viewed with a JEOL JSM-840 Scanning Electron Microscope.

Radioactive labeling was performed by the active uptake of a 300 μCi dose of ^{99m}Tc-labeled-DISIDA N-(2,6-diisopropylacetanilide)-imino-diacetate which is metabolized only by active hepatocytes. This was injected into the medium and allowed to circulate for 6 minutes. The medium was drained and the circuit washed twice, after which the foam was removed and cut into three radial sections at the inlet, central and outlet portions along the bioreactor axis. These sections were placed on the inverted face of a low energy, high-resolution collimator of an Elscint Apex gamma camera, and scanned for 10 minutes.

Statistics: Microsoft Excel was used for data processing while Statistix 8 was used for analysis. Values are presented as the mean $\pm$ standard deviation. Clearance/production rates were calculated by converting the raw data to absolute quantities and graphing according to time. The gradients of the linear fittings were taken to be the rates. Statistical significance was measured using Student's t test.

Table A.4.1 Modified-HGM cell culture media components

Component	Concentration
Deionized autoclaved H_20	10 L/bottle of DMEM
*Powder DMEM +BSS,glutamine	equivalent for 10 L
$NaHCO_3$	22 g for 10 L equivalent
*Streptomycin-Fungizone	10 ml/L
*Gentamycin sulphate	1 ml/L
*Fetal Calf Serum	100 ml/L
Insulin	mUnits/L
Glucagon	15-20 µg/L
Dexamethazone	67 µg/L
Epidermal Growth factor	20 µg/L
Transferrin (Fe^{2+} saturated)	200 µl/L or 5-6 mg/L
DMSO	1 % v/v
Glucose	2 g/L
Galactose	2 g/L
Nicotinamide	0.610 g/L
Zinc chloride	0.544 mg/L
Zinc sulphate	0.750 mg/L
Cupric sulphate	0.2 mg/L
Manganese sulphate	0.025 mg/L
Sodium selenite	5-6 µg/L

Note: All items except * purchased from Sigma-Aldrich, Johannesburg, South Africa. *'s were purchased from Bio-Whittaker, Adcock Ingram Scientific, Johannesburg, South Africa

Appendix B: *In vivo* study methods

B.1 Anesthesia protocol

Caprofen (Rimadyl ®, 5 mg/kg BW SC) was injected pre-operatively, followed by isoflurane (Safe Line pharmaceuticals) inhalation using a Boyle's isofor inhalation machine with 100 % O_2. Buprenorhine (Temgesic ®, 0.1 ml/100g BW IM) was given at the time of incision. To manage pain post-operatively, carprofen was given once daily with buprenorphine adjusted to 30 % of normal liver weight every 12 hrs. On termination, all animals were euthanased through inhalation of a lethal overdose of isoflurane.

Recovery, pain and toxicity scoring

The National Society for the Protection and Care of Animals (NSPCA) pain and toxicity scoring sheets were completed once daily to assess possible toxicity, pain and humane end-points for the experiments.

Statistics

Microsoft Excel (ver. 2003) was used as a spreadsheet while Statistix (ver. 8, Tallahasee, Fl, USA) was used for data analysis. The mean and standard deviations were calculated for all variables. Non-parametric Wilcoxon rank sum tests, appropriate for small groups, were used to determine the statistical significance of differences between groups.

B.2 Animal preparation

Pathogen-free pigs were purchased from a herd two weeks prior to each experiment to allow for quarantine and acclimatisation. They were housed in environmentally controlled stables (25˚C) with a 12 hr light/dark cycle (University of Pretoria Biomedical Research Centre). Food was composed of a standard pig diet (EPOL) and water until fasting commenced 24 hours prior to each experiment. Energy and electrolytes (Rehidrat, Pfizer) were supplemented during the daytime (08:00-16:00). At 16:00 lorazepam was administered (2 mg IM, Ativan, Aspen) by using a pole-syringe (Dan-Inject) followed by an antibiotic (1g IV, Ceftriaxone, Pharmacare) as intestinal flora prophylaxis. Each pig was hence kept nil per mouth until commencement at 07.00 the following morning.

Anaesthesia protocol

The pigs were immobilized by IM injection of midazolam (0.3 mg/kg, Dormicum, Roche) and ketamine (10 mg/kg, Anaket, Centaur). A 20G IV Teflon catheter (Jelco, Johnson & Johnson) was placed in the ear vein for induction of anesthesia with propofol (3 mg/kg, Diprivan, Astra Zeneca) and intubation with a 7.5 mm endotracheal tube. A nasogastric tube was placed per os to deflate the stomach. After sterile preparation the animal was transferred to the theatre where it was immobilized in the supine position and draped for abdominal surgery. Anaesthesia was maintained with 1.5% isoflurane in an air-oxygen mixture with the aid of a circle rebreathing anaesthetic machine with carbon dioxide absorption (Procare 500, Ohmed, Scientific Group). Fresh gas flow rate was set

at 300 ml/min for oxygen and 600 ml/min for air. Minute volume was maintained with positive pressure ventilation (Ohmeda 7000 Ventilator) to maintain end-tidal carbon dioxide partial pressure in the range of 35-40 mmHg. Intra and postoperative analgesia was supplemented with the lumbar epidural administration of ropivacaine (0.2 ml/kg, Naropin, Astra) and morphine sulphate (0.1 mg/kg, morphine sulphate-Fresenius amps, Fresenius Kabi). Ceftriaxone (1g, Pharmacare) was administered IV as before. Blood volume and blood glucose were maintained with 5% dextrose in a balanced electrolyte solution (Intramed, Ringer Lactate) administered at 10 ml/kg/hr for the duration of anesthesia. All pulse-oximitery (TL-101T, Nihon Kohden, Medical Systems), CO_2 (TG-900P, Nihon Kohden, Medical Systems), electrocardiographic (ECG) (BR-903P, Nihon Kohden, Medical Systems) and electroencephalographic (EEG) electrodes were attached to the animal at this time. Prior to liver devascularization, 500 ml of a gelatin plasma-expander (20 ml/kg IV, gelofusine, B/Braun) was administered IV. This dose was repeated immediately following liver devascularization. Perioperatively, arterial blood pressure was maintained at a mean pressure of between 60-80mmHg (MX 950 Transtar Pressure Transducers, Medex Medical) with the IV infusion of phenylephrine (2-25 µg/kg/min phenylephrine, Covan). Core body temperature was maintained as near as possible to 37.5 degrees C using forced hot air (Bair hugger 505, Augustine Medical).

Catheter placement

Prior to the liver devascularization procedure, an arterial catheter (G16, 115.17 Vigon, Viking Medical) was placed in the common carotid artery for monitoring arterial pressures and blood gases. The external jugular vein was exposed for cannulation with a vascath (CS 15123E, Arrow) and a double lumen venous catheter (CV50688 Fr 7, Arrow) was inserted into the lumen of the internal jugular vein for monitoring central venous pressure (CVP). Positioning was verified after connection of the respective catheters to the monitors. A supra-pubic cystostomy was also performed prior to closing the abdomen using a 10 fg Foleys catheter to monitor urine output

Intensive care

Following surgery the animal was transferred to an intensive care unit (ICU). Continuous ventilation was maintained (40% O_2, tidal volume 10-15 ml/kg) with a post expiratory pressure (PEEP) of 5 mmHg (Ventilator 7200a, Puritan-Bennet). Settings were adjusted hourly according to arterial blood gas (ABG). Sedation was maintained by infusing midazolam (0.3 mg/kg/hr Dormicum, Roche), fentanyl (0.02 mg/kg/hr Fentanyl, Janssen) and pentobarbitone (4 mg/kg/hr Pentobarbitone, 6%, Kyron) with infusion pumps (Modular 3000, Smith's Medical). Boluses of muscular relaxant (0.3 mg/kg/hr Esmeron, Sanofi Synthelabo) were administered IV when necessary. Hemodynamic stability was regulated according to CVP (no less than 14 mmHg) and urine output (2 ml/kg/hr) using fluid boluses including Ringer's lactate (Adcock Ingram) and colloid (Gelofusine, B/Braun). Blood glucose was maintained using 50% glucose (Adcock Ingram) to prevent hypoglycaemia. Dobutamine (2.5-10 µg/kg/min Dobutrex, Eli Lilly) and Phenylephrine (1 µg/kg/min Phenylephrine, Knoll) were titrated to maintain mean arterial blood pressure at a minimum of 60mmHg. Blood potassium (3.4-4.5 mmol/l) and sodium (135-145 mmol/l) concentrations were maintained using Potassium chloride (Adcock Ingram) and Sodium chloride (Adcock Ingram). Heparin was titrated according to activated

clotting time (ACT). Bolus doses (3-5 units/kg) was administered IV until the ACT (as measured by a Hemochron JR, Brittan Health Care) returned to normal (220-250 secs). Body temperature was maintained as above. Intensive care was maintained until the cessation of cardiac function, which was defined as the point of death in this study.

Clinical measurements

Systemic and biochemical indices were measured for the duration of each experiment (table 4.1). Arterial blood pressure and Central venous pressure (CVP) were connected to a calibrated electronic pressure transducer (MX9522, Medex, SSEM). A multiparameter patient monitor (BMM-10-1K, Gambro and BSM 4103K Nihon Kohden) was used to monitor the ECG, pulse rate, CVP, systolic-, diastolic-, mean arterial blood pressure and haemoglobin saturation with the aid of a pulse oximeter probe placed on the tongue. End-tidal CO_2 partial pressure was measured with an in-line sensor placed between the endotracheal tube connection and the breathing circuit. Rectal temperature and ABG measurements were performed hourly while blood biochemical samples were taken four-hourly. Standard [human] laboratory methods were used for these indices. Continuous EEG measurement was performed until termination. A diagrammatic drawing of the brain structure was superimposed on the external bone features and a standardized measuring protocol was adapted from the International 10/20 electrode placement system for humans. Subcutaneous needle electrodes were used for registering activities at the frontal, central, temporal and occipital regions of the brain. A digital recording system was used for EEG monitoring (Medtronic Walter Graphtek PL-EEG, Medtronic) and a software package (Neuro, Galileo NT version 2.31/00, Medtronic) was used for digital spectral Fast Fourier Transform (FFT) analysis. Frequency spectra of 10-second epochs were used in the analysis. In this study we describe only the alpha (8-15 Hz), total delta (0-4 Hz) and relative power values in the frontal and central regions of the brain. All clinical measurements were terminated at death.

Appendix C: The derivation of the compartmental model equations

C.1 System model diagram

The figure below is a simplified representation of the BALSS system connected to a patient, with basic notation and stream (flow-circuit) numbers.

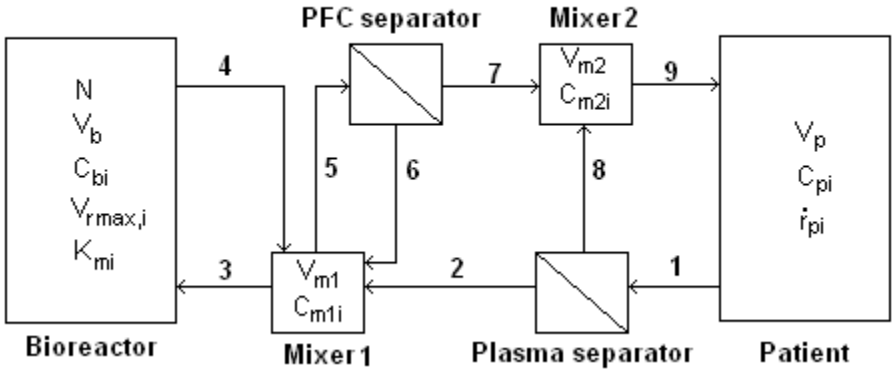

C.2 Model Notation

Symbol	Description	Units
C_{ai}	Concentration of component *i* in stream *a*	mol *i* / m^3
C_{xi}	Concentration of component *i* in compartment *x*	mol *i* / m^3
f_i	Fraction of substrate *i* that is unbound	
g	Ratio of filtrate to feed flow rates for PFC separator	
H_a	Hematocrit in stream *a* = (Volume cellular components)/(Volume plasma + Volume cellular components)	
$K_{m,i}$	Michaelis constant for substrate *i*	mol *i* / m^3
n_{xi}	Number of moles of component *i* in compartment *x*	mol *i*
$\dot{n}_{ai}$	Molar flow rate of component *i* in stream *a*	mol *i* /s
N	Number of hepatocytes in bioreactor	cells
Q_a	Volumetric plasma flow rate of stream *a* (i.e. excluding PFC and cellular blood components)	m^3/s
$Q_{a,pfc}$	Volumetric flow rate of stream *a*, including PFC = $Q_a/(1-\phi_a)$	m^3/s
$Q_{a,ct}$	Volumetric flow rate of stream *a*, including cellular blood components = $Q_a/(1-H_{ct,a})$	m^3/s
r_{xi}	Reaction rate of component *i* in compartment *x*	mol *i* /m^3.s
t	Time	s
$V_{max,i}$	Maximal rate of metabolism for substrate *i*	mol *i* /m^3.s
V_x	Volume of compartment *x*, excluding PFC and cellular blood component volume	m^3
$V_{x,pfc}$	Volume of compartment *x*, including PFC = $V_x/(1-\phi_x)$	m^3
$V_{x,ct}$	Volume of compartment *x*, including cellular blood components = $V_x/(1-H_x)$	m^3

Greek symbols

ϕ_a	Volume fraction of PFC (perfluorocarbon) in stream *a*

General subscripts

0	Value of variable at time zero
a	Stream *a*
b	Bioreactor
ct	Includes cellular blood components
m1	Mixer 1
m2	Mixer 2
p	Patient
pl	Plasma
ι	Constituent / toxin *i*
x	Compartment *x*

C.3 Input parameters (with typical/indicative values for the UP-CSIR BALSS, where available)

Parameter	**Description**	**Typical value**	**Units**
$C_{bi,0}$	Starting concentration of component *i* in bioreactor	0	mol/m^3
$C_{m1i,0}$	Starting concentration of component *i* in mixer *m1*	0	mol/m^3
$C_{m2i,0}$	Starting concentration of component *i* in mixer *m2*	0	mol/m^3
$C_{pi,0}$	Starting concentration of component *i* in patient	0.07	mol/m^3
f_i	Fraction of total substrate *i* that is unbound	1	
g	Filtrate to feed flow rate for PFC separator	0.025	
H_8	Hematocrit of plasma separator concentrate	0.8	
H_p	Hematocrit in patient	0.5	
K_{mi}	Michaelis constant for substrate *i*	20.86	mol *i* / m^3
N	Number of hepatocytes in bioreactor	$1x10^{10}$	cells
$Q_{1,ct}$	Rate of withdrawal of blood from patient	$2x10^{-6}$	m^3/s
$Q_{3,pfc}$	Flow rate of plasma-PFC blend into bioreactor	$8.33x10^{-6}$	m^3/s
r_{pi}	Rate of reaction of component *i* in patient	$3.56x10^{-8}$	mol/m^3.s
$V_{b,pfc}$	Volume of bioreactor	0.0003	m^3
$V_{r\max}$	Maximum metabolic rate of hepatocytes	$3.1x10^{-11}$	mol/s.cell
$V_{m1,pfc}$	Volume of mixer *m1*	0.00065	m^3
$V_{m2,ct}$	Volume of mixer *m2*	0.0001	m^3
$V_{p,ct}$	Volume of blood in patient	0.004	m^3
ϕ_3	Volume fraction PFC in stream 3	0.1	

C.4 Output parameters

$C_{pi}, C_{bi}, C_{m1i}, C_{m2i}$

C.5 Variables that influence the outputs,

g
f_i
N
V_p, V_b, V_{m1}, V_{m2}
$C_{pi,0}$
$V_{\max,i}, K_{mi}, r_{pi}$
$Q_{1,ct}, Q_3$

C.6 Basic assumptions

1. Constituent *i* is well mixed in the bioreactor (*b*), patient (*p*), mixer 1 (*m1*) and mixer 2 (*m2*) (i.e. these vessels are modeled as continuously stirred tank reactors).
2. Both plasma and PFC separators have 100% separation efficiency (i.e. no cellular blood components pass into stream 2, and no PFC (perfluorocarbon) emulsion droplets pass into stream 7).
3. Volumes of lines and separators are negligible.
4. Separators do not differentially separate plasma constituents (i.e. filtrate and concentrate have the same plasma constituent concentrations).
5. Changes in stream volumetric flow rates due to reactions are negligible.
6. PFC does not absorb any plasma components/constituents in significant quantities.
7. Rate of production in patient ($r_{pi}V_p$) is the net rate (i.e. production by body – clearance by body – excretion by body).
8. Bioreactor clearance rates are determined by cell number and by toxin concentration.
9. Mixer 2 is a combination of the two physical reservoirs (the plasma and blood reservoirs).

C.7 Flow rates

The total blood flow rate of stream 1, $Q_{1,ct}$, is an input parameter. The flow rate of stream 8, $Q_{8,ct}$, can be calculated from the known hematocrit (H) levels in streams 1 and 8, where the definition of hematocrit in this document is defined as the volume fraction of cellular components in the total blood stream:

$$Q_{8,ct} = \frac{H_1}{H_8} Q_{1,ct}$$
$$Q_8 = \frac{(1-H_8)}{(1-H_1)} \frac{H_1}{H_8} Q_1 \qquad \text{(C.1)}$$

where $H_1=H_p$

The flow rate of stream 2:

$$Q_2 = Q_1 - Q_8 \tag{C.2}$$

The return flow rate of blood to the patient must be equal to the flow rate of blood extracted from the patient:

$$Q_9 = Q_1 \tag{C.3}$$

The flow rate of stream 7 can now be calculated:

$$Q_7 = Q_9 - Q_8 \tag{C.4}$$

The exit flow rate from the bioreactor must be equal to the inlet flow rate:

$$Q_4 = Q_3 \tag{C.5}$$

The ratio of filtrate flow rate to inlet flow rate for the PFC separator, g, is given by:

$$\begin{aligned} g &= Q_7/Q_5 \\ \therefore Q_5 &= Q_7/g \end{aligned} \tag{C.6}$$

The concentrate flow rate from the PFC separator is now given by:

$$\begin{aligned} Q_6 &= Q_5 - Q_7 \\ Q_6 &= Q_7(1/g - 1) \end{aligned} \tag{C.7}$$

C.8 Concentrations

The number of moles of component i in compartment x is given by:

$$n_{xi} = C_{xi}V_x \tag{C.8}$$

The molar flow rate of component i in stream a is given by:

$$\dot{n}_{ai} = C_{ai}Q_a \tag{C.9}$$

Because of the assumption of good mixing, the concentration of a constituent in the exit streams from any vessel is equal to the concentration of the same constituent in the vessel at any given time:

$$\begin{aligned} C_{1i} &= C_{pi} \\ C_{9i} &= C_{m2i} \\ C_{3i} &= C_{5i} = C_{m1i} \\ C_{4i} &= C_{bi} \end{aligned} \tag{C.10}$$

Because no concentration changes occur in the separators, separator exit concentrations are equal to separator inlet concentrations:

$$\begin{aligned} C_{2i} &= C_{8i} = C_{1i} \\ C_{6i} &= C_{7i} = C_{5i} \end{aligned} \tag{C.11}$$

C.9 Molar balances

Taking a mole balance for component *i* over the patient:

$$\frac{dn_{pi}}{dt} = \text{production - consumption + in - out}$$
$$\frac{d\left(V_p C_{pi}\right)}{dt} = r_{pi}V_p - 0 + C_{9i}Q_9 - C_{1i}Q_1 \tag{C.12}$$

Substituting from equation (C.10), and rearranging:

$$V_p \frac{dC_{pi}}{dt} = r_{pi}V_p + C_{m2i}Q_9 - C_{pi}Q_1$$
$$\frac{dC_{pi}}{dt} = r_{pi} + \frac{Q_9}{V_p}C_{m2i} - \frac{Q_1}{V_p}C_{pi} \tag{C.13}$$

Similarly, taking a mole balance over the bioreactor:

$$\frac{dn_{bi}}{dt} = \text{production - consumption + in - out}$$
$$\frac{d\left(V_b C_{bi}\right)}{dt} = 0 + r_{bi}V_b + C_{3i}Q_3 - C_{4i}Q_4 \tag{C.14}$$

Substituting from equation (C.10) and rearranging:

$$V_b \frac{dC_{bi}}{dt} = r_{bi}V_b + C_{m1i}Q_3 - C_{bi}Q_4$$
$$\frac{dC_{bi}}{dt} = \frac{Q_3}{V_b}C_{m1i} - \frac{Q_4}{V_b}C_{bi} + r_{bi} \tag{C.15}$$

Taking a mole balance over mixer *m1*:

$$\frac{dn_{m1i}}{dt} = \text{production - consumption + in - out}$$
$$\frac{d\left(V_{m1}C_{m1i}\right)}{dt} = 0 - 0 + C_{2i}Q_2 + C_{6i}Q_6 + C_{4i}Q_4 - C_{3i}Q_3 - C_{5i}Q_5 \tag{C.16}$$

Substituting from equations (C.10) and (C.11), and rearranging:

$$V_{m1}\frac{dC_{m1i}}{dt} = C_{pi}Q_2 + C_{m1i}Q_6 + C_{bi}Q_4 - C_{m1i}Q_3 - C_{m1i}Q_5$$
$$\frac{dC_{m1i}}{dt} = \frac{Q_2}{V_{m1}}C_{pi} + \frac{Q_4}{V_{m1}}C_{bi} + \frac{(Q_6 - Q_3 - Q_5)}{V_{m1}}C_{m1i} \tag{C.17}$$

Taking a mole balance over mixer *m2*:

$$\frac{dn_{m2i}}{dt} = \text{production - consumption + in - out}$$
$$\frac{d\left(V_{m2}C_{m2i}\right)}{dt} = 0 - 0 + C_{8i}Q_8 + C_{7i}Q_7 - C_{9i}Q_9 \qquad \text{(C.18)}$$

Substituting from Equations (C10) and (C11), and rearranging:

$$V_{m2}\frac{dC_{m2i}}{dt} = C_{pi}Q_8 + C_{m1i}Q_7 - C_{m2i}Q_9$$
$$\frac{dC_{m2i}}{dt} = \frac{Q_8}{V_{m2}}C_{pi} + \frac{Q_7}{V_{m2}}C_{m1i} - \frac{Q_9}{V_{m2}}C_{m2i} \qquad \text{(C.19)}$$

C.10 Rates of production/clearance

The production rate (r_{pi}) of component i in the patient is assumed to be constant. The rate of clearance/metabolism of component *i* in the bioreactor can be approximated using the Michaelis-Menten relationship [91]:

$$\text{Rate of metabolism} = r_{bi} = \frac{V_{\max,i}C_{bi}f_i}{K_{mi} + C_{bi}f_i} \qquad \text{(C.20)}$$

When $C_{m1i}.fi >> K_{mi}$, then the rate of metabolism = $V_{\max,i}$. When $C_{m1i}.f_i << K_{mi}$, then the rate of metabolism = $V_{\max,i}.f_i.C_{m1i}/K_{mi}$. The Michaelis-Menten parameters ($V_{\max,i}$ and K_{mi}) can be determined from a single compartment bolus experiment by rewriting Equation (A.20), as follows:

$$\frac{dC_i}{dt} = r_i = -\frac{V_{\max,i}C_i f_i}{K_{mi} + C_i f_i}$$
$$-\frac{dt}{dC_i} = -\frac{1}{r_i} = \frac{K_{mi}}{V_{\max,i}C_i f_i} + \frac{1}{V_{\max,i}} \qquad \text{(C.21)}$$

Thus a plot (called a Lineweaver-Burk plot) of $1/r_i$ vs. $1/C_i$ should yield a straight line with y-intercept $1/V_{\max,i}$ and gradient $K_{mi}/V_{\max,i}f_i$.

The $V_{\max}$ value determined from the plot is dependent on enzyme concentration (e.g. if enzyme concentration doubles, $V_{\max}$ doubles), while K_m is not [91]. If one assumes that enzyme concentration is directly proportional to hepatocyte 'concentration' (i.e. hepatocytes per reactor volume), then one can calculate a reduced maximum reaction rate ($V_{r\max}$, with units mol/s.cell) from the experimentally determined $V_{\max}$ value as follows:

$$V_{r\max} = \frac{V_{\max}V_b}{N}$$
$$\text{and } V_{\max} = \frac{V_{r\max}N}{V_b} \qquad \text{(C.22)}$$

This reduced maximum reaction rate can now be used to estimate V_{max} for different reactor sizes and hepatocyte loadings.

Using equation (C.20), equation (C.15), can now be rewritten as:

$$\begin{aligned} V_b \frac{dC_{bi}}{dt} &= r_{bi} V_b + C_{m1i} Q_3 - C_{bi} Q_4 \\ V_b \frac{dC_{bi}}{dt} &= -\frac{V_{\max,i} C_{bi} f_i V_b}{K_{mi} + C_{bi} f_i} + C_{m1i} Q_3 - C_{bi} Q_4 \\ \frac{dC_{bi}}{dt} &= -\frac{V_{\max,i} C_{bi} f_i}{K_{mi} + C_{bi} f_i} + \frac{Q_3}{V_b} C_{m1i} - \frac{Q_4}{V_b} C_{bi} \end{aligned} \tag{C.23}$$

C.11 Summary of equations and parameters

$$\begin{aligned} \frac{dC_{pi}}{dt} &= r_{pi} + \frac{Q_9}{V_p} C_{m2i} - \frac{Q_1}{V_p} C_{pi} \\ \frac{dC_{bi}}{dt} &= -\frac{V_{\max,i} C_{bi} f_i}{K_{mi} + C_{bi} f_i} + \frac{Q_3}{V_b} C_{m1i} - \frac{Q_4}{V_b} C_{bi} \\ \frac{dC_{m1i}}{dt} &= \frac{Q_2}{V_{m1}} C_{pi} + \frac{Q_4}{V_{m1}} C_{bi} + \frac{(Q_6 - Q_3 - Q_5)}{V_{m1}} C_{m1i} \\ \frac{dC_{m2i}}{dt} &= \frac{Q_8}{V_{m2}} C_{pi} + \frac{Q_7}{V_{m2}} C_{m1i} - \frac{Q_9}{V_{m2}} C_{m2i} \end{aligned} \tag{C.24}$$

These equations are supported by the following set of algebraic equations:

$$\begin{aligned} Q_8 &= \frac{(1-H_8)}{(1-H_1)} \frac{H_1}{H_8} Q_1 \\ Q_2 &= Q_1 - Q_8 \\ Q_9 &= Q_1 \\ Q_7 &= Q_9 - Q_8 \\ Q_4 &= Q_3 \\ Q_5 &= Q_7 / g \\ Q_6 &= Q_7 (1/g - 1) \\ C_{1i} &= C_{pi} \\ C_{9i} &= C_{m2i} \\ C_{3i} &= C_{5i} = C_{m1i} \\ C_{4i} &= C_{bi} \\ C_{2i} &= C_{8i} = C_{1i} = C_{pi} \\ C_{6i} &= C_{7i} = C_{5i} = C_{m1i} \end{aligned} \tag{C.25}$$

Calculation of flow rates and volumes from input parameters:

$$\begin{aligned} Q_1 &= Q_{1,ct}\left(1-H_p\right) \\ Q_3 &= Q_{3,pfc}\left(1-\phi_3\right) \\ V_p &= V_{p,ct}\left(1-H_p\right) \\ V_b &= V_{b,pfc}\left(1-\phi_3\right) \\ V_{m1} &= V_{m1,pfc}\left(1-\phi_3\right) \\ V_{m2} &= V_{m2,ct}\left(1-H_{ct,p}\right) \end{aligned} \tag{C.26}$$

Calculation of PFC volume fraction in stream 6:

$$\begin{aligned} &\phi_5 Q_5 = \phi_6 Q_6 + \phi_7 Q_7 \\ &\text{But } \phi_7 = 0 \\ &\therefore \phi_5 Q_5 = \phi_6 Q_6 \\ &\phi_6 = \frac{Q_5}{Q_6}\phi_5 \end{aligned} \tag{C.27}$$

Appendix D: *On line* model sensitivity and verification

Table D.1 Numerical associations in and between classes

Association	Variable 1	Variable 2	Pearson correlation > 0.4	Spearman correlation > 0.3	Comments
	ave_pH	rLactate	-0.71	-0.47	
	ave_pH	ave_pCO_2	-0.67	-0.47	sources of change in pH
	ave_pH	ave_HCO_3	+0.46	+0.58	
	ave_Pulse	rNa+	-0.61	-0.33	electrolyte effect
	rK+	rCreatinine	+0.87	+0.64	kidney indices related
	rCreatinine	Urine_Tot	-0.72	-0.70	
	rBilirubin	rALP	+0.46	+0.59	
	rBilirubin	rALT	+0.73	+0.78	
	rBilirubin	rAST	+0.66	+0.74	
	rBilirubin	rLD	+0.48	+0.73	Liver indices related
Internal	rAmmonia	rBcAA/AroAA	+0.79	-0.39	
	rAmmonia	rAST	+0.53	+0.56	
	rAmmonia	rLD	+0.74	+0.37	
	Fr_a/d_fr	Pw_a/d_fr	-0.47	-0.57	EEG frequency and power
	rPT	rAPTT	-0.49	-0.30	
	rPT	rAntiThrombin	+0.79	+0.68	
	rPT	rFibrinogen	+0.46	+0.31	
	rFibrinogen	rAntiThrombin	+0.81	+0.61	Coagulation indices
	rFactor II	rFactor VII	+0.71	+0.66	
	rFactor VII	rFactor X	+0.69	+0.52	
	rFactor II	rFactor X	+0.44	+0.40	
	rAmmonia	Fr_a/d_fr	-0.79	-0.54	Encephalopathy
	rAmmonia	Fr_a/d_ct	-0.42	-0.36	and the liver
	rAmmonia	Pw_a/d_fr	+0.38	+0.43	
	rBcAA/AroAA	Fr_a/d_fr	+0.90	+0.75	Encephalopathy
	rBcAA/AroAA	Fr_a/d_ct	+0.61	+0.43	and *Fischer's ratio
	rBcAA/AroAA	Pw_a/d_fr	-0.47	-0.43	
	rGlutamine	Fr_a/d_fr	-0.61	-0.46	Encephalopathy
	rGlutamine	Fr_a/d_ct	-0.40	-0.57	and glutamine
	rGlutamine	Pw_a/d_fr	0.92	+0.93	
External	rLactate	Fr_a/d_fr	-0.96	-0.64	Encephalopathy
	rLactate	Fr_a/d_ct	-0.86	-0.89	and lactate
	rLactate	Pw_a/d_fr	+0.47	+0.64	
	rPyr	Fr_a/d_ct	-0.57	-0.39	
	rPyr	Pw_a/d_fr	+0.48	+0.64	
	rCreatinine	rGlutamine	+0.61	+0.43	Kidney function and *AAs
	rCreatinine	rPT	+0.43	+0.72	Coagulopathy
	rCreatinine	rFibrinogen	-0.44	-0.39	and the kidneys
	rCreatinine	rAmmonia	+0.78	+0.35	Liver and kidneys
	Urine_Tot	rHkt	+0.59	+0.53	The effect of fluids
	Fluids_Tot	rHkt	+0.52	+0.46	on hematocrit
	rHb	rHkt	+0.81	+0.68	

Notes: 1. Inclusion in the table required a Pearson coefficient > 0.4 and a Spearman coefficient> 0.3.

2. prefixes: r = rate of change over time, and ave_ = average over time. 3. All variables with Fr_a/d were for indices of electro-encephalograms (EEG), which were measured in the animal experiments, but have shown no prognostic value. BcAA/AroAA = Fischer's ratio, where AAs = amino acids (see section 4.2).

D.2 First-order assumptions

The assumption of the linearity over time of the composing first order equations was investigated by determining the best-fit linear equation for each data for all variables. A mean R^2 value, the numerical square of the Pearson coefficient (and the proportion of the variance in the dependent variable attributable to the variance in each independent variable) was calculated for all variables (figure D.2.1). The majority of the variables had R^2 values above 0.5 (Pearson coefficients > 0.7) which indicated that they mostly linear and justified the numerical design of the model. Of interest was a strong correlation between the variables that exhibited the greatest change, that is, the highest P values (table 4.2.2) and those that were most linear over time. Variables that had R^2 values < 0.5, but which were still felt to possess some prognostic value were weighted to relatively decrease their contribution to the eventual prediction. Specifically, a percentile weight was used related to their linearity. In general, the variables used for prediction during the surgical interval (T<0) had lower R^2 values (were less linear) than those used during the ICU period (T>0). This validated the use of a larger number of variables in the T<0 period, each with relatively less weight than in the T>0 period. It was also expected that the T<0 part would be less accurate than the T>0 part.

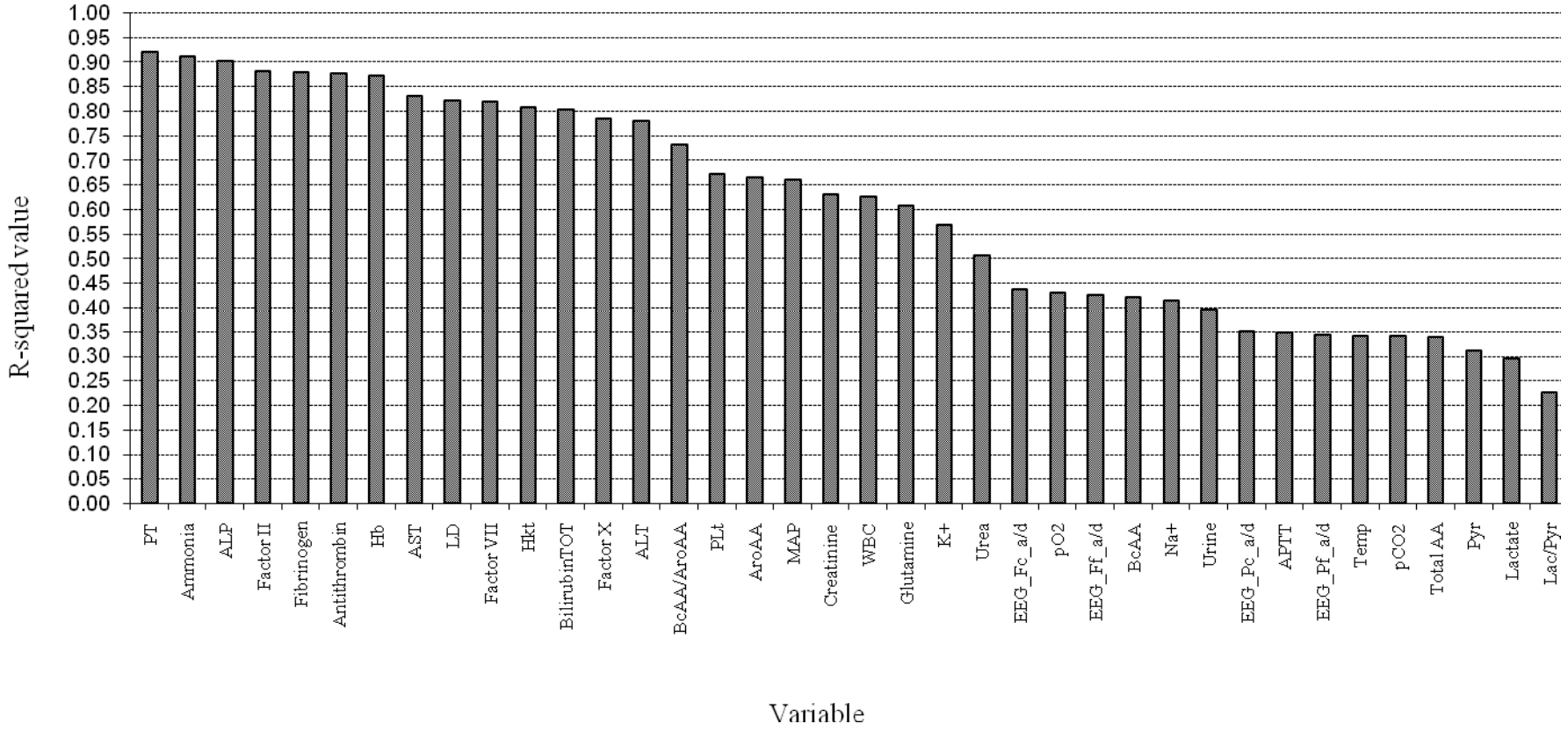

Figure D.2.1 Linearity of variable trends. The majority of measured variables demonstrated an R^2 value above magnitude 0.5.

D.3 Model sensitivity

1. Tornado diagrams [285] function as a macro in Excel and require the specification of a high and low value for each of the input variables of the model. The output is then displayed in terms of each of the composing variables' ranges about the mean predicted value. Thus, the dependence of the model's output on each of the inputs is visible. i.e. the larger the particular input variable's range about the summated mean predicted value, as determined by the weight appropriated to that variable, the greater the influence that variable has on the model's output. The data range used for the diagrams below was that measured in practice (section 5.2). The method assumes the Gaussian normality of the input populations. Only a selection of the BI Tornado diagrams are presented below:

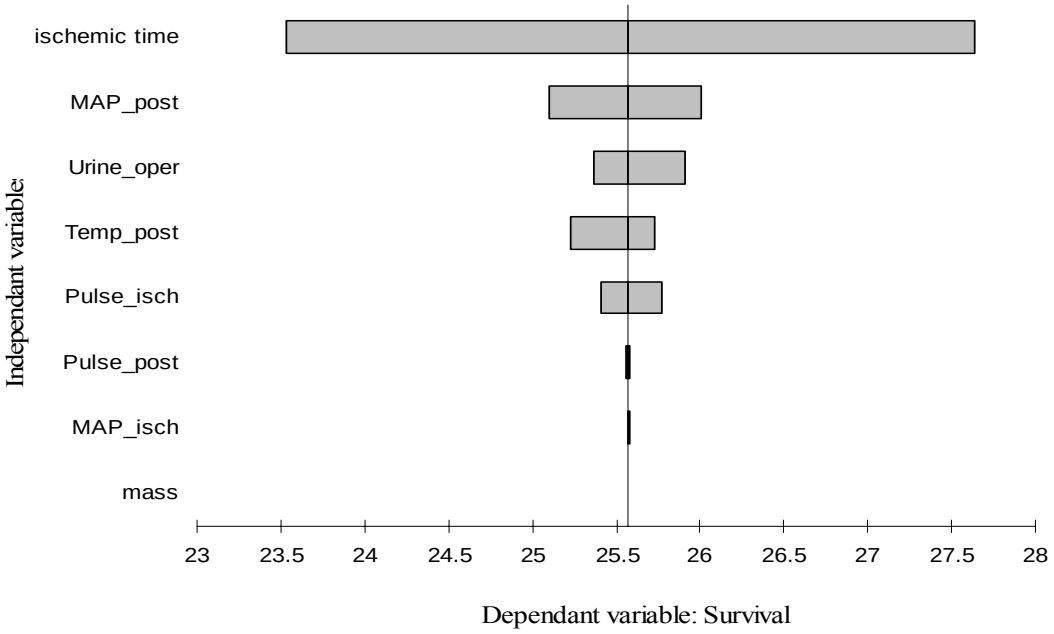

Figure D.3.1 Tornado diagram for PI model (T<0)
Note: The Ischemic time clearly has the greatest impact on Survival during the surgical interval. Output sensitivity is determined by the weight appropriated to each variable.

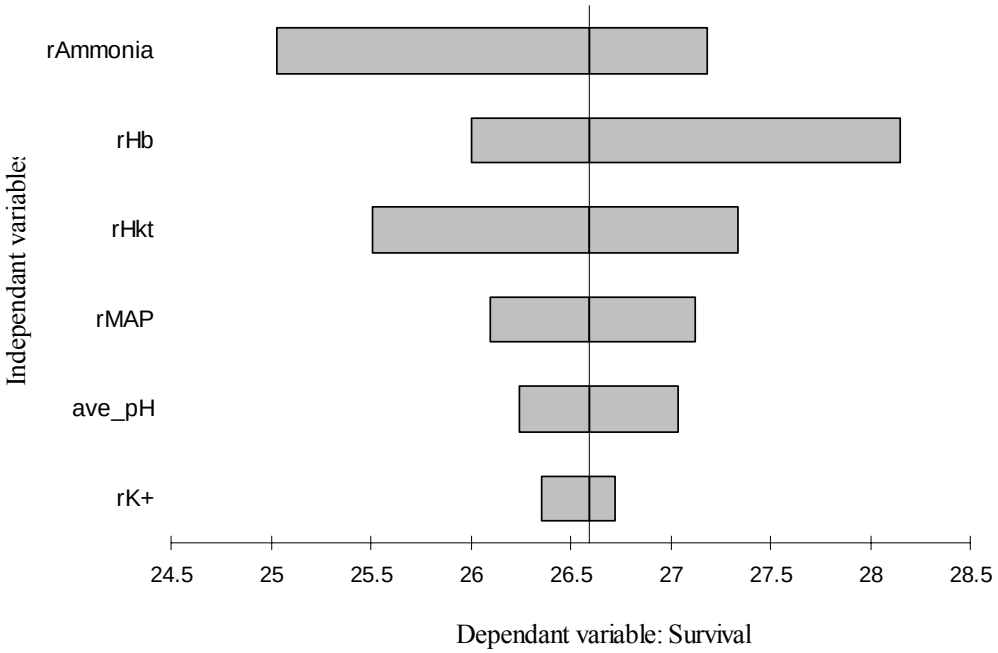

Figure D.3.2 Tornado diagram for PI model (T>0)
Note: The rate of increase of blood Ammonia most strongly impacted Survival after surgery. Output sensitivity is determined by the weight appropriated to each variable.

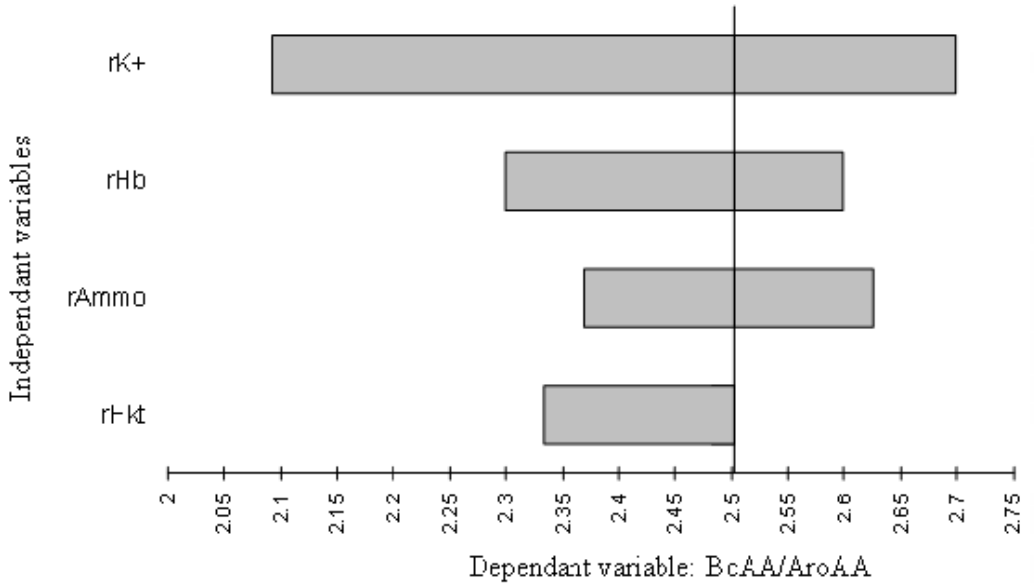

Figure D.3.3 BI Model Sensitivity for BcAA/AroAA (BI) (at 12 hrs)

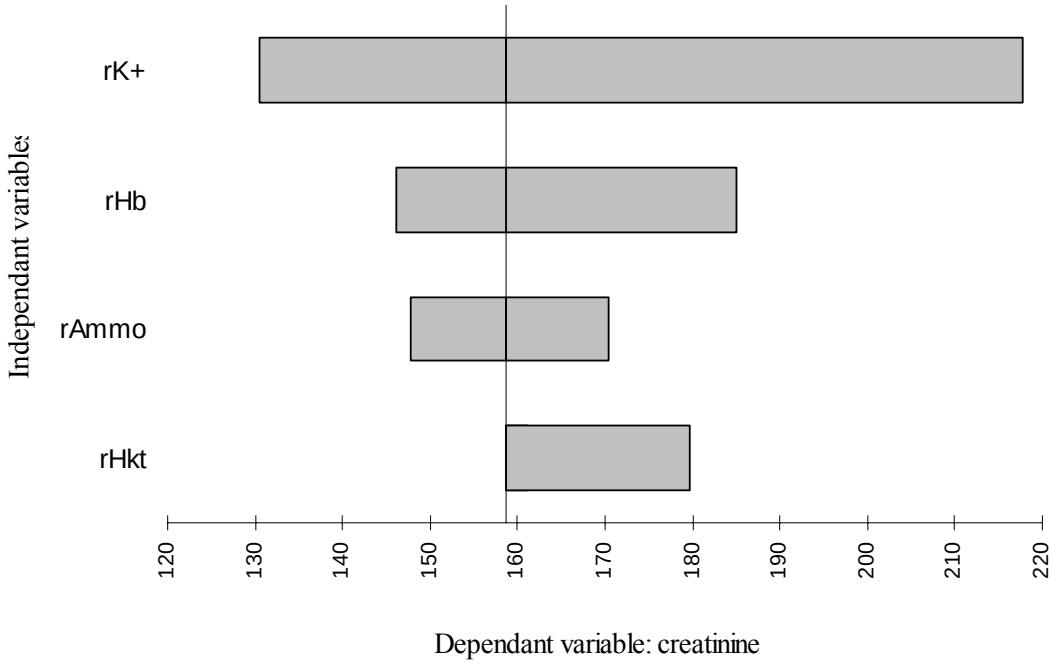

Figure D.3.4 BI Model sensitivity for creatinine (at 12 hrs)

2. Monte Carlo simulation

This procedure [285-287] was used to determine the sensitivity of the model's outputs to generated random numbers as inputs. The model was programmed into an Excel spreadsheet then 1000 random numbers, parameterized about the measured mean and standard deviation for each variable, were generated. This data was used as input to the model. Output sensitivity was determined individually and in combination. i.e. either one variable was randomized independently while retaining all other variables on their mean values, or all variables were randomized simultaneously, followed by the summation of the results. This method of analysis assumes normality in the input data. The latter assumption was also tested by using the same procedure but with uniformly distributed populations of generated numbers. The results were then graphically projected:

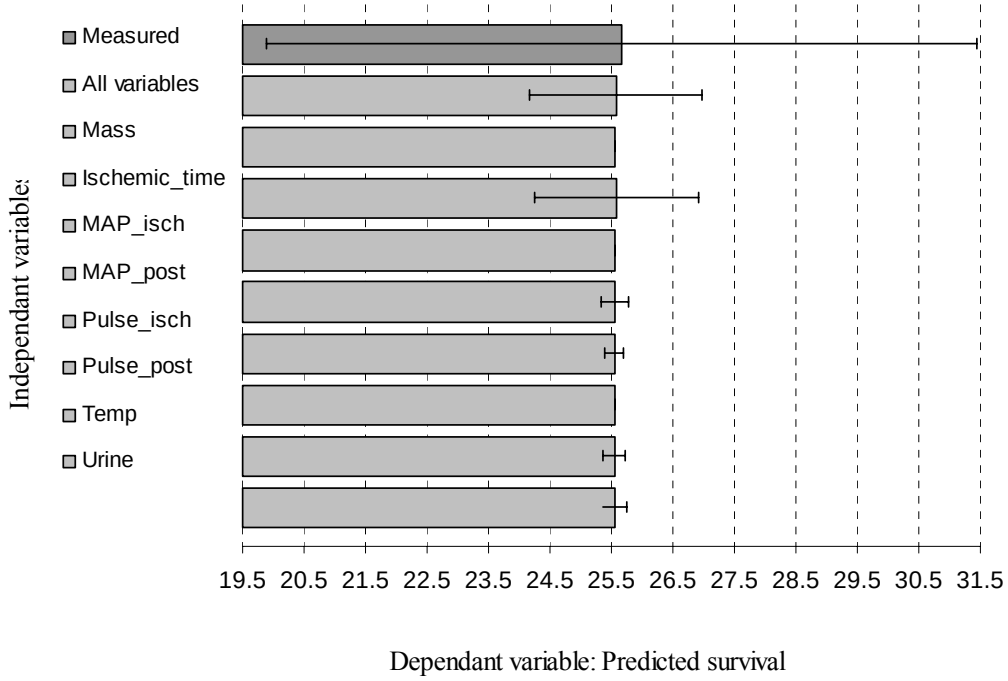

Figure D.3.5 PI Model (T<0) prediction variation using normal distributions (N=1000) of independent variables. The majority of variation in model output originated with the Ischemic_time. All input variables individually very closely approximated the measured mean.

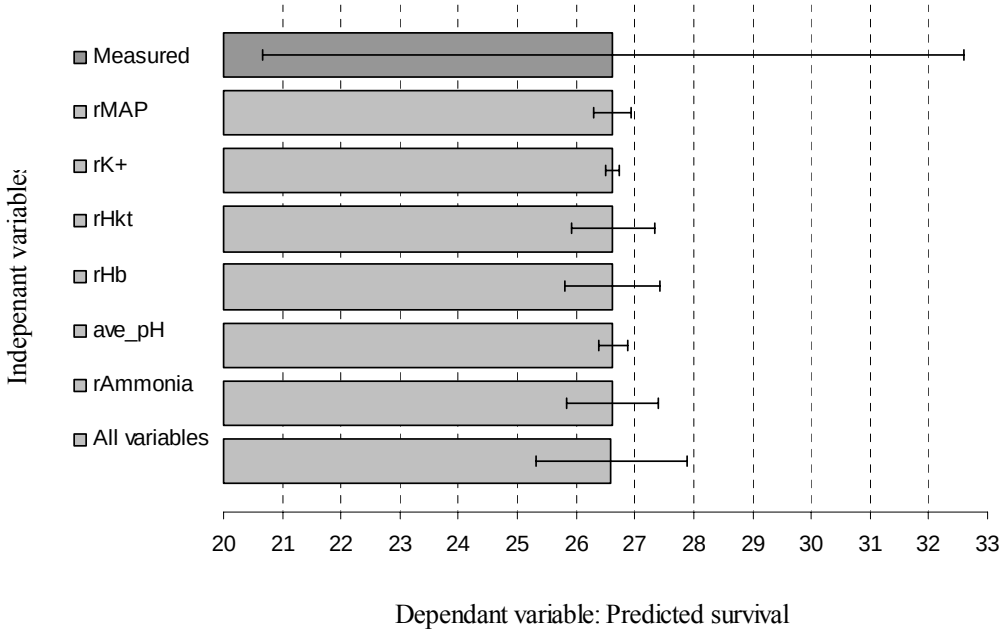

Figure D.3.6 PI Model (T>0) prediction variation using normal distributions [N=1000] of independent variables (T>0). All inputs very closely estimated the measured mean. There was a similar amount of variation in prediction from rAmmonia, rHkt and rHb.

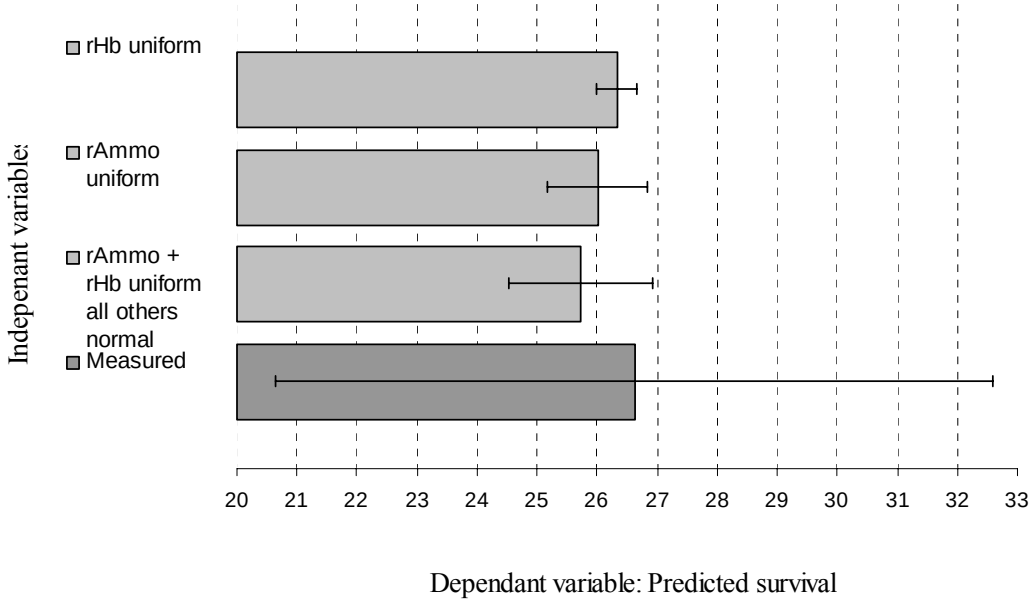

Figure D.3.7 PI Model (T>0) prediction variation using uniform distributions (N=1000) of non-Gaussian variables. Survival was slightly underestimated when the distributions were uniform as opposed to normal.

D.4 Assumptions of normality

The measured raw data for the input variables was tested for normality using Shapiro-Wilk tests with P(W) values as are available in Statistix 8 (table 5.2.7). Despite the small population sizes, it was only in the derived variables rHb and rAmmo (PI model) that normality was excluded in the P(W) values, using the population from which the model's equations had been derived. To examine the effect that non-normal distributions would have on model predictions, the inputs in question were also randomized using uniform distributions. The duration of survival was marginally underestimated in the PI.

Table D.4.1 Normality of independent variables in the PI

Variable	Time period	Shapiro Wilk W-value	P(W) value	Number of cases
Survival		0.8834	0.1705	9
Body weight		0.9485	0.6738	9
Ischemic		0.8502	0.0749	9
time		0.9082	0.3414	8
MAP_isch	**T<0**	0.9767	0.9454	9
MAP_post		0.9191	0.4224	8
Pulse_isch		0.9737	0.9257	8
Pulse_post		0.8442	0.0644	9
Temp_post		0.9063	0.2906	9
Urine_oper				
Survival		0.8925	0.2471	8
rMAP		0.9572	0.9353	8
ave_pH		0.9816	0.9703	8
rK+		0.8727	0.1602	8
rHkt	**T>0**	0.8769	0.1758	8
rHb		0.6765	0.0012	8*
rHb		0.6204	0.0001	12†
rAmmonia		0.7065	0.0027	8*
rAmmonia		0.8200	0.0160	12†

Notes:
1. As the W-value approaches 1, the distribution approaches normality.
If the P(W) value is < 0.05, normality may not be assumed.
2. In the T<0 part of the model all distributions indicated normality.
3. In the T>0 part of the model, only in rHb and rAmmo could normality not be assumed based on the P(W) values in both sets of data.
* Indicates the data sets (N=8) from which the model was initially defined.
† Indicates all the data sets measured (N=12).
4. The effect of non-normal distributions on model prediction variation was tested by means of employing uniform distributions for the above variables (figure 5.2.10).
5. The BI is derived from independent variables present in the T>0 part of the PI. The nature of the distributions of those variables will thus also determine prediction variation in the BI.

Table D.5.1 The number of independent variables used to calculate each biochemical in the BI

	Number of independent variables			
	4	**3**	**2**	**1**
Variable	BcAA/AroAA Fibrinogen Creatinine	ALP	Glutamine Antithrombin LD	Bilirubin PT Factor II, VII, X Factor AST ALT Urea

Notes:
1. The greater the number of weighted input variables the greater the likelihood of prediction accuracy.
2. Due to being determined by only one independent variable, the clotting factors and two of the liver enzymes, are unlikely to be predicted with great accuracy. Unfortunately, at the time of writing, there were no *on-line* sensors for these variables.

D.6 Model Verification methods and results

D.6.1 ANOVA

a. A statistical mean and standard deviation for all measured and predicted values was calculated (columns 4 and 5, table D.6.1). From this a percentage deviation of each predicted mean and standard deviation from each measured mean and standard deviation was calculated (column 6). Bearing in mind the large numerical range of measurement in the biochemical variables it was found that the predicted standard deviations about each mean differed to a greater extent than that in the measured. The greatest error was found in Factor X with a – 4.291 % difference. The percentage error for urea was 280.936%, and those for creatinine and glutamine were also unacceptably large.

b. An ANOVA comparison, using a 'single factor without replication' method on a 0.05 confidence level, was drawn between all predicted and measured populations. The variance in the predicted (above) and measured (below) populations was similar (column 7). In general, the variance in the predicted population was greater than in the measured, with the largest differences in urea, glutamine and creatinine once again. The mean square values (column 8) indicated that sources of variation were less between populations than within them. F-ratios were uniformly smaller than F-crit values, indicating that the differences were best explained by chance. The confidence (P) values (column 10) were mostly above 0.8, with the exception of fibrinogen, AST and LD, whose P values were below 0.55. However, all were far above 0.05, thus, the null hypothesis was rejected. Thus, it was not possible to detect a significant difference between the two populations in any of the parts of the model.

Table D.6.1 ANOVA results for the PI and BI model/s (highlighted variables were discarded)

1. Model Output	2. Pearson Correlation coefficient: predicted to measured	3. Output correction formula	4. Measured: Mean Std dev	5. Predicted: Mean Std dev	6. Percentage deviation of predicted (mean & std dev) from measured	7. Variance: Predicted over Measured.	8. Mean Square (MS): between & within grps.	9. F value & F-crit value.	10. P value (α = 0.05)
Prognosis T<0	0.733	y=0.1913x+20.636	24.88 5.64	25.07 7.69	0.14 4.24	59.08 31.84	0.15 45.46	0.003 4.60	0.956
Prognosis T>0	0.864	y=0.2823x+19.109	26.63 5.98	26.63 6.92	0.001 2.39	47.82 35.70	$5.33x10^{-6}$ 41.76	$1.28x10^{-7}$ 4.60	0.999
BcAA/AroAA	0.811	y=0.6624x+1.3662	1.98 0.75	2.03 0.90	1.27 45.88	0.86 0.57	$1.94x10^{-8}$ 0.72	$2.71x10^{-8}$ 4.03	0.999
BilirubinTOT	0.864	y=1.27x +3.9589	12.41 7.49	13.30 9.24	-0.91 7.28	8.34 56.07	13.74 71.13	0.19 3.98	0.662
Fibrinogen	0.962	y=1.1821x-0.8357	1.96 0.71	1.72 0.74	2.12 27.84	0.55 0.51	0.59 0.53	1.11 4.07	0.297
PT	0.945	y=0.8624x+4.4398	15.39 5.24	16.12 6.57	-0.41 4.31	43.14 27.44	8.82 35.76	0.25 3.99	0.621
AntiThrombin	0.841	y= 0.6329x +28.5	65.98 20.18	65.98 23.99	0.04 1.21	575.56 407.13	$1.11x10^{-4}$ 491.35	$2.26x10^{-7}$ 4.01	0.999
Factor II	0.847	y=0.7741x+8.3169	32.60 13.86	32.60 16.36	-0.03 2.46	267.50 192.09	$1.75x10^{-6}$ 229.8	$7.62x10^{-9}$ 3.99	0.999
Factor VII	0.837	y=0.6739x+14.753	30.35 19.40	30.35 23.18	-0.38 3.83	537.21 376.47	$6.82x10^{-5}$ 456.84	$1.49x10^{-7}$ 3.99	0.999
Factor X	0.786	y=0.6641x+24.718	28.96 27.11	28.96 34.51	-4.29 22.40	$1.19x10^{3}$ 735.03	$3.56x10^{-5}$ 962.96	$3.69x10^{-8}$ 3.99	0.999
ALP	0.747	y=0.4547x+170.63	330.65 260.53	344.56 348.78	-0.10 0.47	$1.22x10^{5}$ $6.79x10^{4}$	$3.39x10^{3}$ $9.56x10^{4}$	0.04 3.98	0.851
AST	0.810	y= 0.763x +1306	1521.16 2025.67	1871.04 2627.43	-0.51 1.13	$6.90x10^{6}$ $4.10x10^{6}$	$2.04x10^{6}$ $5.61x10^{6}$	0.36 3.99	0.549
LD	0.800	y=0.7057x+949.87	1673.18 1545.16	2020.51 2230.23	-0.03 0.11	$4.97x10^{6}$ $2.39x10^{6}$	$2.08x10^{6}$ $3.74x10^{6}$	0.56 3.98	0.459
ALT	0.729	y=0.5878x+88.486	120.0 113.81	126.88 151.95	-0.25 1.69	$2.31x10^{6}$ $1.30x10^{4}$	814.64 $1.83x10^{4}$	0.05 3.98	0.833
Creatinine	0.522	y=0.4318x+82.663	129.55 53.27	129.55 101.95	0.15 1.72	$1.04x10^{4}$ $2.84x10^{3}$	$3.74x10^{-4}$ 6615.82	$5.65x10^{-8}$ 3.99	0.999
Urea	0.164	y= 0.074x +2.391	2.24 0.87	2.31 5.17	-3.66 280.94	26.70 0.75	0.09 13.91	$6.46x10^{-3}$ 13.91	0.936
Glutamine	0.463	y= 0.267x +178.8	207.68 96.39	207.71 207.95	-0.05 1.10	$4.32x10^{4}$ $9.28x10^{3}$	$9.14x10^{-3}$ $2.63x10^{4}$	$3.48x10^{-7}$ 4.01	0.999

D.6.2 Relative error

a. The error of each predicted to corresponding measured value was calculated as a fraction of each measured value. i.e. the deviation at a particular point or *point error*. This was divided by the standard deviation of the measured population and converted to a percentile scale to give the *relative error* for each part of the model. If the *point error* exceeded 100% of the standard deviation of the measured population, then there was a significant difference between the two populations at that point. In general, the closer the mean relative error value to zero, the closer the model has estimated the mean of the measured population, while the standard deviation of the relative error (SD*re*) indicates the predicted population's range of error.

A potential weakness in this method was that when a variable demonstrated a very large numerical range over the course of an experiment, the relative error would tend to be larger in the small range and smaller in the large range of the raw data. i.e. the relative error converged to zero as the measurement range increased. This effect was only noticeable in the liver enzymes in which there were extremely large measurement ranges (from 0-7000 IU/l). These enzymes have no prognostic value in ALF and for this reason the effect could have been ignored. However, for the sake of thoroughness,

b. A quantitative index for comparison was calculated by multiplying the measurement range with the standard deviation of the relative error (SD*re*) (table D.6.2.1). The larger the returned value, the larger the prediction *error region*. This represents a method of indicating the *average relative accuracy* of the various parts of the model. What must be borne in mind, especially in the biochemical variables, is that although the deviation in the relative error may have been small, the measured value range was often very large. In practice the point errors may still have been large.

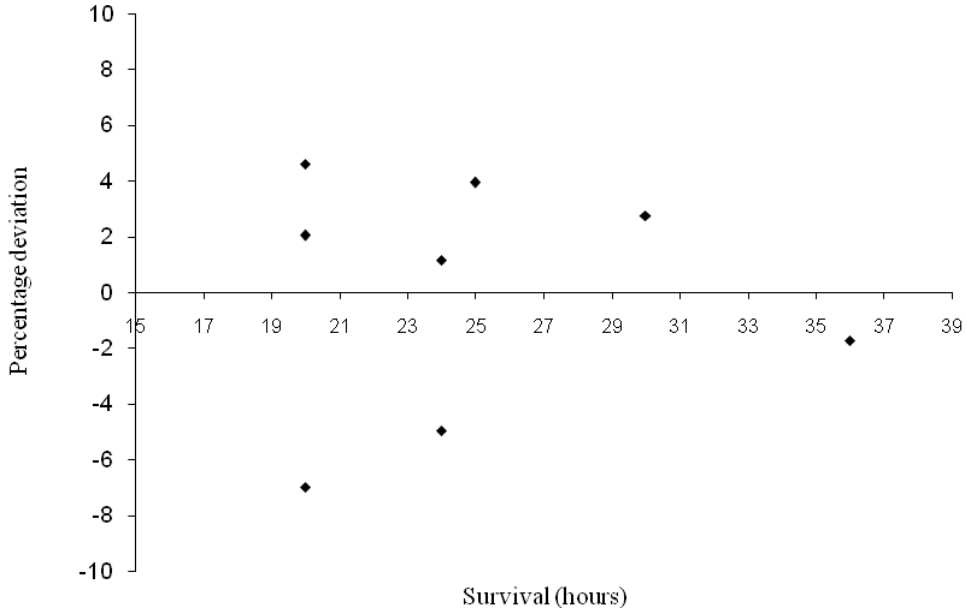

Figure D.6.2.1 Relative prediction error for the PI (T<0)

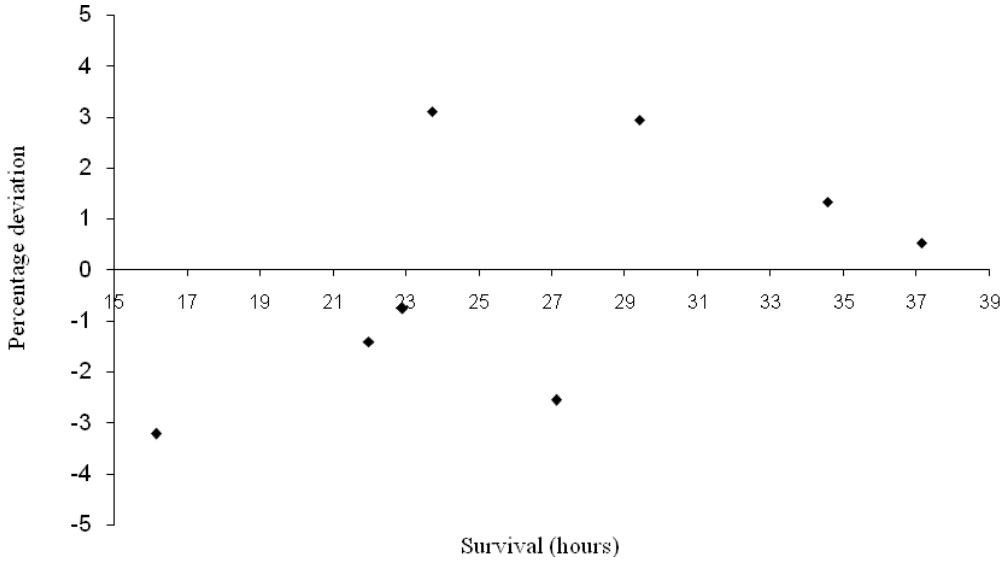

Figure D.6.2.2 Relative error for PI (T>0)

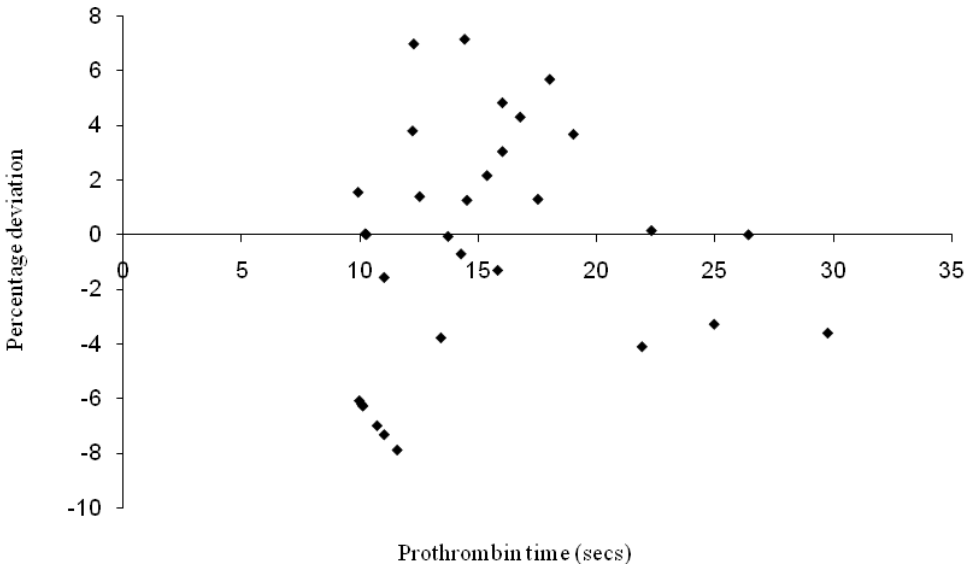

Figure D.6.2.3 Relative error for the BI (Prothrombin time)

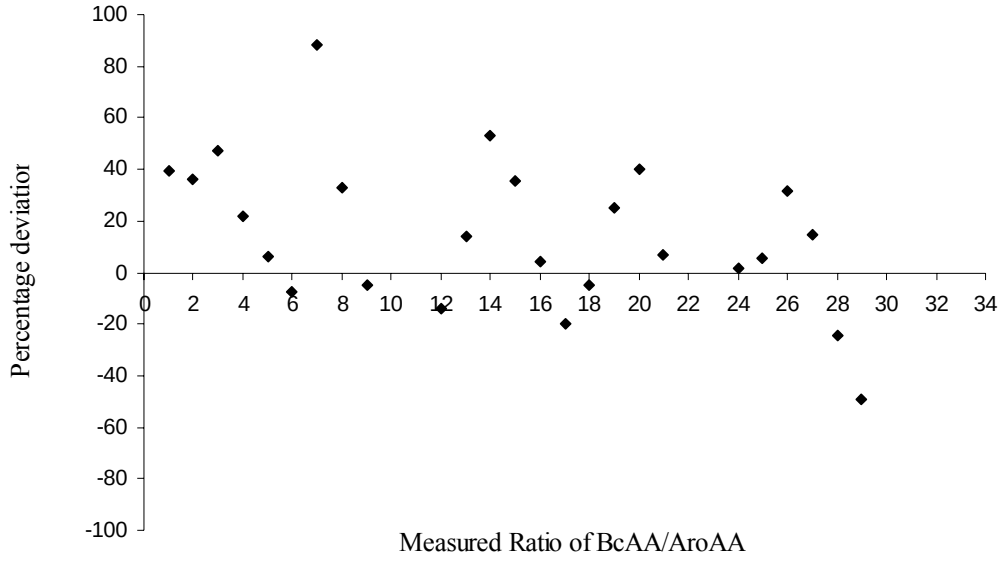

Figure D.6.2.4 Relative error for the BI [BcAA/AroAA]

Table D.6.2.1 Comparative accuracy of the PI and BI models (using 'training' data)

Model	**Measured values**			**Accuracy Index**		
Index	Max	Min	Range	Mean	SD*re*	Range*SD*re*
Prognosis T<0	36	20	16	0.14	4.24	67
Prognosis T>0	36	20	16	0.001	2.39	38
BcAA/AroAA	3.75	1.19	2.55	1.67	29.00	48.43
BilirubinTOT	30.0	1.0	29.0	-0.91	7.28	211.2
Fibrinogen	2.97	0.50	2.47	2.12	27.84	68.76
PT	29.75	9.90	19.85	-0.41	4.31	85.49
AntiThrombin	112.89	14.00	98.89	0.04	1.21	119.44
Factor II	59.65	7.61	52.04	-0.03	2.46	127.87
Factor VII	74.95	6.19	68.76	-0.08	3.28	225.54
Factor X	104.96	1.00	103.96	0.98	3.94	409.93
ALP	1206.0	57.0	1149.0	-0.01	0.32	366.9
AST	6607.0	23.0	6584.0	0.01	0.07	441.1
LD	6161.0	155.0	6006.0	-0.001	0.05	301.2
ALT	377.0	23.0	354.0	0.15	1.15	405.2
Creatinine	284.8	11.5	273.3	0.15	1.72	468.8
Urea	4.6	1.6	3.2	67.71	173.81	556.2
Glutamine	445.0	76.8	368.2	0.63	0.94	344.2

Notes:
1. *SD*re* = Standard deviation of the relative error
2. The closer the mean prediction error to 0, the closer the mean measured value has been estimated.
3. The smaller the Range*SD*re* the smaller the *error region* and the more accurate the predictions.

Acknowledgements

Prof. Schalk W van der Merwe. With your help in these last 8 years I have grown both as a person and in professional capacity as a scientist. Thank you for the opportunity in the first place to participate in this project, without it none of what was subsequently built would have been possible. Thank you for your belief in my abilities, for the positive words to colleagues and for the many times you intervened on my behalf, especially when the resulting outcomes would have been impossible without your help (there are simply too many to list). Thank you for your objective and invariably strategically useful advice, no matter what the subject.

Dr Pierre Cilliers and Prof. JJ Kruger. Thank you for identifying the necessity, your belief in and excellent tutorship for my particular tangent through the sciences. I will certainly try to keep the flame burning. **Prof. P de Vaal.** I realize I was sort of 'forced' on you. Thank you for taking over where the others left off. I hope I am able to do you duty in any future endevours.

Kobus van Wyk, Luke Ronné, Susan Malfeld, Elke Kreft and Elongo Fritz. Thank you for your individual and collective efforts in trying to realize these projects of ours. It is obvious that any success I may have achieved is at least partially dependent on your inputs. In terms of my career, the years we have worked together have been the most enjoyable I have experienced.

Dr Sean Moolman, Kersch Naidoo. Thank you for your always interesting and insightful inputs, especially regarding the commercial side of things. I am grateful for the continued enthusiasm you have displayed for all our projects, our relationship remains productive and pleasurable.

Prof Johan Becker, Dr Scholz Wiggett, Dr Roland Auer and the staff of the UPBRC. Thank you for your help and interest in our projects. Your participation has been critical to our success.

My parents, Ben and Betty Nieuwoudt. Your belief in me kept me going, especially when circumstances were difficult. This thesis is dedicated to you.